



**Evaluation of small extracellular vesicular
microRNAs as biomarkers
for exposure of nicotine and E-liquids
on human lung cells**

by

Sowmya Chinta

**Supervisor: Dr Arijit Mukhopadhyay
Co- Supervisor: Dr Pika Miklavc**

**School of Science, Engineering and Environment
University of Salford, Manchester, UK**

**Submitted for
the Degree of Doctor of Philosophy, 2022**



DECLARATION

I, **Sowmya Chinta**, declare that the thesis entitled “**Evaluation of small extracellular vesicular microRNAs as biomarkers for exposure of nicotine and E-liquids on human lung cells**” and the work presented in the research was carried out at The University of Salford under the guidance of Dr Arijit Mukhopadhyay, Dr Pika Miklavc are my own.

Although most experiments are carried out by myself along with the analysis of this research, some parts of this thesis were carried out in collaboration with other colleagues. Wherever contributions of others are involved, every effort is made to indicate this clearly with due reference to the literature and acknowledgement of collaborative research and discussions. No part of this work has been previously submitted to any institution. I further declare that the materials obtained from other sources have been acknowledged in the thesis.

Sowmya Chinta

2022

CHAPTER 1 : INTRODUCTION.....	20
1.1 MICRORNA (miRNA)	21
1.1.1 BACKGROUND.....	21
1.1.2 miRNA BIOGENESIS	22
1.1.3 MICRORNA ROLE IN CANCERS	23
1.1.4 miRNA CLUSTERS.....	24
1.1.5 GENOMIC DESCRIPTION OF C14MC	26
1.2 THE POTENTIAL OF miRNA AS A BIOMARKER	28
1.3 SMALL EXTRACELLULAR VESICLE (sEVs).....	31
1.3.1 NOMENCLATURE.....	33
1.3.2 BACKGROUND OF sEV	35
1.3.3 BIOGENESIS OF sEV'S	35
1.3.4 SMALL EV COMPOSITION	36
1.3.5 MARKERS OF sEVs	38
1.3.6 HETEROGENEITY OF sEV	39
1.3.7 CHARACTERISATION OF sEVs.....	40
1.3.8 BIOLOGICAL FUNCTION	41
1.3.9 SMALL EVs BASED DATABASES	42
1.3.10 SMALL EV AS BIOMARKER.....	42
1.3.11 SMALL EV- SECRETION AND UPTAKE OF miRNA	43
1.4 SMALL EV DERIVED miRNA AS A BIOMARKER	44

1.5 IMPACT OF NICOTINE INTAKE AND E-LIQUIDS ON LUNG CELLS- A MODEL TO STUDY THE ROLE OF SEV MIRNA FOR BIOMARKER	46
1.5.1 EPIDEMIOLOGY	47
1.5.2 DIAGNOSIS	47
1.6 NICOTINE INTAKE, E-LIQUIDS, AND LUNG CELLS	48
1.6.1 NICOTINE	48
1.6.2 E-LIQUID	49
1.6.3 DIFFERENT TYPES OF E-LIQUIDS	50
1.6.4 DIAGNOSIS AND PATHOGENESIS	51
1.7 APPLICATION OF SEV-DERIVED MIRNA AND LUNG DISEASE CAUSED DUE TO NICOTINE INTAKE AND E-LIQUIDS	52
1.8 AIMS & OBJECTIVES	54
CHAPTER 2 : MATERIALS AND METHODS	55
2.1. CELL-CULTURE.....	56
2.2 TREATMENT WITH NICOTINE, CIGARETTE SMOKE EXTRACT (CSE) AND E-LIQUID	57
2.2.1 NICOTINE TREATMENT OF LUNG CELLS	58
2.2.2 CIGARETTE SMOKE TREATMENT OF LUNG CELLS.....	58
2.2.3 E-LIQUID TREATMENT OF LUNG CELLS	60
2.3 PROLIFERATION ASSAY WITH MTT (3-(4,5-DIMETHYLTHIAZOL-2-YL)-2,5-DIPHENYLTETRAZOLIUM BROMIDE, A TETRAZOLE)	61
2.4 ISOLATION OF SEVs USING CULTURED MEDIA FROM TREATED AND UNTREATED LUNG CELLS	
62	

2.4.1	PRE-CLEANING OF CULTURED MEDIA	62
2.4.2	ISOLATION OF sEVs USING A COMBINATION OF PRECIPITATION AND SIZE EXCLUSION CHROMATOGRAPHY	63
2.5	CHARACTERISATION OF ISOLATED sEVs	65
2.5.1	TRANSMISSION ELECTRONIC MICROSCOPY (TEM).....	65
2.5.2	FLUORESCENT MICROSCOPY FOR EV UPTAKE EXPERIMENT	66
2.5.3	WESTERN BLOT	67
2.5.4	NANOPARTICLE TRACKING ANALYSIS (NTA)	69
2.5.5	FLUORESCENT NANOPARTICLE TRACKING- WITH SPECIFIC ANTIBODY	71
2.6	RNA ISOLATION AND RT-PCR	73
2.6.1	RNA ISOLATION	73
2.6.2	RNA QUANTIFICATION; SYBR GREEN-BASED LIGHT EMISSION	76
2.6.2.1	PRIMER DESIGNING.....	76
2.6.3	REVERSE TRANSCRIPTION.....	77
2.7	NEXT-GENERATION SEQUENCING USING SMALL RNA.....	81
2.7.1	LIBRARY PREPARATION	81
2.7.2	CLUSTER GENERATION AND SEQUENCING.....	86
 CHAPTER 3 : CELLULAR RESPONSE TO TREATMENT, sEV ISOLATION AND CHARACTERIZATION.....		88
 3.1 EFFECT OF NICOTINE, CIGARETTE SMOKE EXTRACT (CSE) AND E-LIQUIDS ON HUMAN LUNG CELLS		89
3.1.1	INTRODUCTION	89

3.1.2	RESULTS	89
3.2	ISOLATION & CHARACTERISATION OF SEVs	99
3.2.1	TRANSMISSION ELECTRONIC MICROSCOPY (TEM).....	99
3.2.2	UPTAKE EXPERIMENT USING FLUORESCENT MICROSCOPY	100
3.2.3	NANOPARTICLE TRACKING ANALYSIS (NTA)	103
3.2.4	FLUORESCENT NANOPARTICLE TRACKING ANALYSIS (F-NTA)	107
3.2.5	WESTERN BLOT SHOWED THE PRESENCE OF CD9 AND C63 TETRASPANINS WERE MOST ABUNDANT IN A549 AND BEAS-2B CELLS.....	114
3.3	DISCUSSION	116

CHAPTER 4: PROFILING OF MICRORNA AS A BIOMARKER IN SEV CARGO124

4.1	COMPARISON OF THE EXPRESSION PROFILE OF DIFFERENT MIRNA PRESENT ON C14MC USING qPCR.....	125
4.1.1	INTRODUCTION	125
4.1.2	DIFFERENTIAL EXPRESSION OF C14MC IN LUNG CELLS AND CARGO OF THESE MIRNAS IN SEV SAMPLES.	125
4.2	SMALL RNA SEQUENCE ANALYSIS USING NGS	146
4.2.1	VARIOUS QUALITY CONTROL CHECKS WERE PERFORMED DURING THE NGS DATA ANALYSIS	146
4.2.2	IDENTIFICATION OF NOVEL BIOMARKERS FROM SEV DERIVED MIRNAS IN LUNG CELLS TREATED WITH NICOTINE COMPARED TO CONTROL.	147
4.2.3	DISCUSSION	153

CHAPTER 5 : GENERAL DISCUSSION AND CONCLUSIONS.....	158
A. APPENDICES.....	164
CHAPTER 6 : REFERENCES.....	175

List of figures

FIGURE 1.1: miRNA BIOGENESIS:	23
FIGURE 1.2: CHROMOSOME 14MC:	27
FIGURE 1.3 : BIOGENESIS OF SEVs;	36
FIGURE 1.4: ORIGIN OF SEVs;	54
FIGURE 2.1: WORKFLOW; A SCHEMATIC REPRESENTATION OF THE FOLLOWED IN THIS STUDY.	56
FIGURE 2.2: EXPERIMENTAL PLAN:	57
FIGURE 2.3: PREPARATION OF CIGARETTE SMOKE EXTRACT:	59
FIGURE 2.4:THE 96-WELL PLATE DESIGN OF MTT ASSAY:	62
FIGURE 2.5: TEMPLATE USED FOR UPTAKE OF SEVs USING FLORESCENT MICROSCOPY:	67
FIGURE 2.6: miRBASE:	77
FIGURE 2.7: SMALL RNA-SEQ LIBRARY GENERATION WORKFLOW:	91
FIGURE 3.2: EFFECT OF NICOTINE, CSE AND E-LIQUID ON A549 AND BEAS-2B CELL LINES;	93
FIGURE 3.3: EFFECT OF DIFFERENT E-LIQUID FLAVOURS (APPLE AND STRAWBERRY – BOTH WITH NICOTINE AND WITHOUT NICOTINE ALONG WITH CONTROL / UNTREATED) ON BEAS-2B CELL LINES;	95
FIGURE 3.4: EFFECT OF DIFFERENT FLAVOURS OF E-LIQUID (APPLE AND STRAWBERRY - NICOTINE/ WITHOUT NICOTINE ALONG WITH CONTROL / UNTREATED) ON A549 CELL LINES;	97
FIGURE 3.5: TEM IMAGES OF SEVs:	99
FIGURE 3.6: TEM IMAGES OF SEVs:	100

FIGURE 3.7: VISUALIZATION OF THE UPTAKE OF SEVs USING FLUORESCENCE MICROSCOPY:
..... 101

FIGURE 3.8: FLUORESCENCE MICROSCOPY IMAGES:..... 102

FIGURE 3.9: MEASURING OF UPTAKE OF SEVs USING FLUORESCENCE MICROSCOPY:..... 103

FIGURE 3.10: ISOLATION AND CHARACTERISATION OF SEVs FROM A549 USING NTA: 104

FIGURE 3.11: ISOLATION AND CHARACTERISATION OF SEVs FROM BEAS-2B USING NTA:.105

**FIGURE 3.12: CONCENTRATION OF NANOPARTICLES IN SCATTER AND FLUORESCENCE MODE
WHEN PBS ONLY VS EV ONLY WAS MEASURED FROM A549 CELLS AND BEAS-2B CELLS..**
..... 108

**FIGURE 3.13: CONCENTRATION OF TOTAL AND FLUORESCENT NANOPARTICLES FROM A549 AND
BEAS-2B CELLS AFTER NP - 40 DETERGENT TREATMENT.** 109

**FIGURE 3.14: CHARACTERIZATION OF TRUE SEVs FROM THE ACTUAL TOTAL PARTICLE COUNT
USING FLUORESCENT NANOPARTICLE TRACKING ANALYSIS (F-NTA) IN A) A549 AND B)
BEAS-2B:.....** 112

**FIGURE 3.15: WESTERN BLOT FOR EV MARKERS FROM A549 CELLS INCLUDING UNTREATED
AND TREATED SAMPLES:.....** 114

**FIGURE 3.16: WESTERN BLOT ANALYSIS OF CD9, CD63, CD81 AND TSG101 EXPRESSION IN
SEVs SAMPLES ISOLATED FROM BEAS-2B CELLS INCUDES BOTH UNTREATED AND
TREATED.** 115

**FIGURE 4.1: DIFFERENTIALLY EXPRESSED MIRNAS IN A549 ENDOGENOUS SAMPLE UPON
NICOTINE TREATMENT:.....** 126

**FIGURE 4.2: DIFFERENTIALLY EXPRESSED MIRNAS IN BEAS-2B ENDOGENOUS SAMPLE UPON
NICOTINE TREATMENT:.....** 127

FIGURE 4.3: DIFFERENTIALLY EXPRESSED MIRNAS IN BEAS-2B ENDOGENOUS SAMPLE UPON E-LIQUID (STRAWBERRY FLAVOUR-WITH NICOTINE) TREATMENT: 128

FIGURE 4.4: HEATMAP FOR A549 AND BEAS-2B UPON NICOTINE TREATMENT COMPARED TO UNTREATED; 130

FIGURE 4.5: HEATMAP FOR BEAS-2B UPON E-LIQUID (STRAWBERRY FLAVOUR WITH NICOTINE) TREATMENT COMPARED TO UNTREATED; 132

FIGURE 4.6: DIFFERENTIALLY EXPRESSED MIRNAS IN A549 sEV SAMPLE UPON NICOTINE TREATMENT: 133

FIGURE 4.7: DIFFERENTIALLY EXPRESSED MIRNAS IN BEAS-2B sEV SAMPLE UPON NICOTINE TREATMENT: 134

FIGURE 4.8: DIFFERENTIALLY EXPRESSED MIRNAS IN A549 sEV SAMPLE UPON E-LIQUID (STRAWBERRY FLAVOUR WITH NICOTINE) TREATMENT: 135

FIGURE 4.9: DIFFERENTIALLY EXPRESSED MIRNAS IN BEAS-2B sEV SAMPLE UPON E-LIQUID (STRAWBERRY FLAVOUR WITH NICOTINE) TREATMENT: 136

FIGURE 4.10: DIFFERENTIALLY EXPRESSED MIRNAS IN A549 sEV SAMPLE UPON E-LIQUID (STRAWBERRY FLAVOUR WITH NO NICOTINE) TREATMENT: 137

FIGURE 4.11: DIFFERENTIALLY EXPRESSED MIRNAS IN BEAS-2B sEV SAMPLE UPON E-LIQUID (STRAWBERRY FLAVOUR WITH NO NICOTINE) TREATMENT: 138

FIGURE 4.12: DIFFERENTIALLY EXPRESSED MIRNAS IN A549 sEV SAMPLE UPON E-LIQUID (APPLE FLAVOUR WITH NICOTINE) TREATMENT: 139

FIGURE 4.13: DIFFERENTIALLY EXPRESSED MIRNAS IN BEAS-2B sEV SAMPLE UPON E-LIQUID (APPLE FLAVOUR WITH NICOTINE) TREATMENT: 140

FIGURE 4.14: DIFFERENTIALLY EXPRESSED MIRNAs IN A549 SEV SAMPLE UPON E-LIQUID (APPLE FLAVOUR WITH NO NICOTINE) TREATMENT: 141

FIGURE 4.15: DIFFERENTIALLY EXPRESSED MIRNAs IN BEAS-2B SEV SAMPLE UPON E-LIQUID (APPLE FLAVOUR WITH NO NICOTINE) TREATMENT: 142

FIGURE 4.16: HEATMAP FOR A549 DERIVED SEV SAMPLES;..... 143

FIGURE 4.17: HEATMAP FOR BEAS-2B DERIVED SEV SAMPLES;..... 145

FIGURE 4.18: MEAN QUALITY SCORE PLOT A) AND SEQUENCE COUNTS PLOT B) OBTAINED FROM NGS DATA ANALYSIS:..... 146

FIGURE 4.19: VOLCANO PLOT OF SEV DERIVED MIRNA FROM A549 AND BEAS-2B TREATED WITH NICOTINE COMPARED TO CONTROL:..... 149

FIGURE 4.20: VOLCANO PLOT OF SEV DERIVED MIRNA FROM A549 AND BEAS-2B TREATED WITH STRAWBERRY FLAVOURED E-LIQUID (WITH NICOTINE) COMPARED TO CONTROL:... 152

List of tables

TABLE 1.1: THE TABLE SUMMARIZES DIFFERENT CIRCULATING BIOMARKERS WITH THEIR REFERENCES IN CANCER.....	30
TABLE 1.2: CATEGORIES OF EV;.....	33
TABLE 2.1: REPRESENTS THE PREPARATION OF 2-FOLD DILUTIONS SERIES USING 100% CSE STOCK SOLUTION.	60
TABLE 2.2: REPRESENTS THE PREPARATION OF DIFFERENT CONCENTRATIONS OF E-LIQUID SOLUTION USING 3.89 MM OF STOCK SOLUTION.	61
TABLE 2.3: CONTENTS OF RESOLVING GELS(I) AND STACKING GELS (II).....	67
TABLE 4.1: LIST OF SIGNIFICANT MIRNAS DETECTED IN SEVs FROM NICOTINE TREATED SAMPLES FROM A549 AND BEAS-2B:.....	150
TABLE 4.2: LIST OF SIGNIFICANT MIRNAS DETECTED IN SEVs FROM E-LIQUID TREATED (STRAWBERRY FLAVOUR-WITH NICOTINE)SAMPLES FROM A549 AND BEAS-2B:	153
TABLE 4.3: DOWNREGULATION OF MIR-382 IN NICOTINE TREATED A549 CELLS SAMPLE USING BOTH QPCR AND NGS TECHNIQUES	155

Acknowledgement

It is said that “For every man’s success, there is a woman behind” but in my case its is the opposite. **”Pappa-Satti Babu Garu”**- The man who dreamt for me and made me dream to reach this path. And then **”My better half- Subash”** who transformed this dream into a reality.

I feel very honoured and proud to have these two people, by their presence in my life and can't stop myself from saying as many thanks as I can!

The story began in 2018, I never thought that I would be all alone “Being married, travelling so far away from my family” to reach my dream. I was introduced to an undergraduate student, who started working with me on the same project during my initial days- **”Thanks to ”Nerea”**-we had a lot of fun time in the lab doing ever new experiments together.

When I think back about my office desk and the lab, the person who comes to my mind is **”Thank you Rumana”**- you will be always remembered as a close friend rather than a lab lead.

Then comes the other two girls **”Thanks to Megan and Kainath”** who were with me in my first-year troubleshooting lab techniques together.

Thinking about the lab times and not remembering my pal **”Toby”** is impossible. Even though he came after me ...we initiated many many experiments together and had exciting times in the lab and in the office sitting opposite to each other. Thanks for your care during my last few days in the lab. I would also like to express my **”Thanks to Oyinda”** as well to take out some time for my experiments during my last days in the lab. As a team- I, Toby and Oyinda had spent so many memorable long day lab experiments together.

”Thank you Camillo” who shared the knowledge of various skilled techniques with me.

”Thank you Nishtha” – I learnt a lot of things from you from the time we were introduced to each other.

”Thank you, Mr. Asgar Hussain Ansari,”- For your help in NGS data analysis and representation.

A special **”Thanks to Dr Lucy”** for providing me with the research cigarettes required for my project.

A special **”Thanks to Prof Ian Goodhead”** for his support.

I would like to express my gratitude to the most influenced female characters in my life from whom I learned to be strong-” **Thank you Amma- Lakshmi”**- you made me strong and daring that I never look back when I faced a real hard time!! **”Thank you, Chinna Amma-Dr Nagamani,”**, we always have had a similar thought process, I saw you growing professionally and in parallel taking care of family with great effort. **”Thank you attaye garu- Swarna Rani”**, - you were always a great support to me, and I admire you.

“Thank you, Chinnu- Durga Prasad,”- being my little brother who has taken care of me like an elder brother of mine. **“Thank you Mavaye garu- Venkateswara Rao Muramalla”** for your belief in me and for your blessing.

A very special **“Thank you Trishika”** for being daughter of mine and **“Thank you Mihira”** to bear with me all the time while I was busy with my studies-Amma loves you. I would also like to express tons of thanks to my near and dear **“Family”** and to all the other people who are directly or indirectly involved in my work.

Finally, I would like to thank my co-supervisor – **Dr Pika Miklavc**. And the whole and sole person whom I like to express my gratefulness is my supervisor **“Dr Arijit Mukhopadhyay”**, without whom I would have never thought to pursue PhD, by travelling so long-distance...far away from my family. You gave me the confidence of building up my dream. I feel privileged to work under you..you have always given me a space to convey my opinions and freedom to my ideas. Thank you for being kind, even when I was going off the path. The point where I stand now is all because of your encouragement. I really appreciate your patience.

List of Abbreviations

EVs	Extracellular Vesicles
sEVs	Small Extracellular Vesicles
CO ₂	Carbon dioxide
C14MC	Chromosome 14 miRNA cluster
A549	Human adenocarcinoma basal epithelial cell
BEAS-2B	Human bronchial epithelial cells
RPMI 1640	Rosewell park memorial institute
FBS	Fetal bovine serum
RNA	Ribose nucleic acid
mRNA	Messenger RNA
miRNA	Micro RNA
CD63, CD9 & CD81	Tetraspanins
PBS	Phosphate buffer saline
BSA	Bovine Serum Albumin
NTA	Nano particle tracking analysis
f-NTA	Fluorescent-Nanoparticle tracking analysis
CAE	Carcinoembryonic antigen
PSA	Prostate-specific antigen
NGS	Next-generation sequencing
CTCs	Circulating tumour cells
cfDNA	Circulating cell-free DNA
gDNA	Genomin DNA
LncRNA	Long non coding RNA
VEGF-A	Vascular endothelial growth factor-A
AGO2	Argonaute 2 protein
MISEV	Minimal information for the studies of extracellular vesicles
ESCRT	Endosomal sorting complex required for transport
GAPDH	Glyceraldehyde-3-phosphate Dehydrogenase

HSP70 and HSP90	Heat shock proteins
MHC	Major histocompatibility complex class-I, and class-II proteins
ELISA	Enzyme-linked immunosorbent assay
FACS	Fluorescence-activated cell sorting
IL4	Interleukin- 4
DHA	Docosahexaenoic acid
nAChR	nicotine acetylcholine receptor
MAPK	Mitogen-activated protein kinase
PG	Propylene glycerol
VG	Vegetable glycerine
MTT	(3-(4,5-dimethylthiazol-2-yl)-2,5-diphenyltetrazolium bromide, a tetrazole)
CDC	Centre for Disease Control and Prevention
RB-ILD	respiratory bronchiolitis interstitial lung disease
LDS	Lithium dodecyl sulphate
CMO	Cell Mask orange
cDNA	Complimentary DNA
Ct	Threshold cycle value
EtOH	Ethanol
qPCR	Quantitative- Polymerase Chain Reaction
RISC complex	RNA-induced silencing complex
PCR	Polymerase Chain reaction
nM	Nano Meter
μ M	Micro Meter/micro molar
μ L	Micro litre
NP-40	Nonyl phenoxy polyethanol
PE dye	Phycoerythrin dye
QC	Quality control
ANOVA	Analysis of variance

DMSO	Dimethyl Sulfoxide
BCA	Bicinchoninic Acid
CSE	Cigarette Smoke extract
MVBs	Multivesicular Bodies
ILVs	Intraluminal Bodies
RIPA	Radioimmunoprecipitation Assay
ncRNA	Non-coding RNA
PET	Positron emission tomography
MRI	Magnetic resonance imaging
NSCLC	Non-small cell lung cancer
HRM	High resolution melting analysis
SEC	Size exclusion chromatography
SDS-PAGE	Polyacrylamide gel electrophoresis
EVALI	E liquid or vaping associated lung injury
TEM	Transmission electronic microscope
(Dlk1)	Delta-like homolog1
(Rtl1)	Retrotransposon-like1
(Dio3)	Type III iodothyronine deiodinase
BALF	Bronchoalveolar lavage fluid
UK	United Kingdom
USA	United States of America
2D	2 dimension
3D	3 Dimension
TAB1	TGF- β -activated kinase 1- binding protein
HMGB3	High mobility group box
THC	Tetrahydrocannabinol

Abstract

Evaluation of small extracellular vesicular microRNAs as biomarkers for exposure of nicotine and E-liquids on human lung cells

Sowmya Chinta

Nicotine intake and E-Cigarette or vaping product use-associated lung injury (EVALI) can cause pulmonary disease with damaging health effects. In this study, we explored miRNAs from small extracellular vesicles (sEVs) for nicotine and E-liquid-associated biomarkers. We investigated miRNAs using NGS and further focused on a large miRNA cluster on C14q32 (C14MC), known to be dysregulated in lung-associated diseases. We asked if E-liquid exposure alters the release of these miRNAs via sEVs, compared to nicotine.

We treated lung epithelial cell lines A549 and BEAS-2B with E-liquid (with and without nicotine) and commercial nicotine (100 μ M) for 72hrs. After treatment, sEVs were isolated using the Size Exclusion Chromatography (SEC) method, followed by total RNA isolation. Isolated sEVs were visualized using Transmission Electron Microscopy (TEM) and uptake was detected using fluorescent microscopy. Characterization of sEVs was performed using nanoparticle tracking analysis (NTA), fluorescent NTA (fNTA) and western blot. MiRNA expression profile for miRNAs from C14MC was measured by qPCR

using the $2^{-\Delta\Delta C_t}$ method. Massively parallel sequencing of small RNA was performed to identify sEV miRNA as novel biomarker.

TEM, NTA, fNTA and western blot – all confirmed the successful isolation and processing of small EVs.

From C14MC, differential expression of sEV miRNA was identified in A549 and BEAS-2B when treated with nicotine, E-liquid (strawberry) and E-liquid (apple). As a representative example, miR-382, which was downregulated with nicotine and apple flavored E-liquid but upregulated with strawberry flavored E-liquid. The downregulation of miR-382 was also confirmed by next generation sequencing approach. From C14MC, other notable miRNAs that showed the potential as biomarkers for E-liquid exposure are, miR-410, miR-541, miR-758 and miR-889. In addition to miR-382, the NGS approach has also identified miR-184, miR-6834 and miR-10b as potential biomarkers which are not within the C14MC region.

Thus, these candidates can potentially serve as non-invasive biomarkers to identify the effect of nicotine and E-liquid exposure on human lung cells.

Keywords: sEVs, E-liquid, EVALI, Nicotine, miRNA, biomarkers

CHAPTER 1 : Introduction

1.1 MicroRNA (miRNA)

MiRNAs are a class of small non-coding RNA molecules with 17-22 nucleotides in size that can regulate mRNA and protein levels by post-transcriptional epigenetic regulation. MiRNAs are found in animals, plants and some viruses regulating gene expression (Bartel, 2004). A single miRNA can target many mRNAs and alter genes' expression and pathways. The first-ever miRNA discovered was *lin-4*, in 1993 in *Caenorhabditis elegans* (Lee et al., 1993). Seven years later, the second miRNA, Let-7, was identified, regulating the developmental timing in *C.elegans* larvae (Roush & Slack, 2008). In humans, Let-7 was the first-ever miRNA discovered in the year 2000. About 2,654 mature human miRNAs have been annotated in the miRbase database (<https://www.mirbase.org>, Release 22.1, 2019), which are involved in many functional and pathogenic pathways including cancer.

1.1.1 Background

Among the two primary nucleic acids (DNA & RNA), RNA is the most ancient and conserved nucleic acid (Šponer et al., 2017). In the transcriptome, different types of RNA are present such as mRNA, rRNA and tRNA, which has a significant function in protein translation. In addition, RNAs can be categorized into coding RNA (cRNA) and non-coding RNA (ncRNA). There are two kinds of ncRNAs, housekeeping ncRNAs (tRNA and rRNA) and regulatory ncRNAs, further divided depending on their size (Li & Liu, 2019). Long ncRNAs (lncRNA) are greater than 200 nucleotides, whereas small ncRNAs have less than 200 nucleotides. Small ncRNAs are subcategorised into microRNA (miRNA), small nucleolar RNA (snoRNA), small nuclear RNA (snRNA), small-interfering RNA (siRNA), and PIWI-interacting RNA (piRNA) (Pasquinelli, 2002).

This study mainly discusses microRNAs and their potential role as a biomarker. MiRNAs can be primarily found inside the cell. In addition, they were also reported outside the cell as vesicle bound miRNA and vesicle free miRNA based on their cargo system. Further, this study focuses on the vesicle bound miRNA, exclusively on small Extracellular Vesicle derived miRNA, as shown in **Figure 1.1**.

1.1.2 miRNA Biogenesis

MiRNAs are a class of small non-coding RNA species that play an essential role in post-translational modification, thereby regulating gene expression. More than 2000 different miRNA species have been identified in humans (Griffiths-Jones et al., 2006).

MiRNAs are known to regulate the translation of mRNA by binding to its 3' untranslated region (3' UTR) (Winter, 2015). Although the whole miRNA sequence can bind to the target sequence, evidence shows that the most crucial target recognition is from the position 2 to 9 nucleotides, known as the "seed region" (Lai, 2002).

These are involved in various critical biological processes necessary for normal physiological development in the human (Fu et al., 2013). miRNAs are transcribed from DNA to a long primary miRNA (pri-miRNAs) sequence, capped and polyadenylated, mediated by RNA polymerase II (Cai et al., 2004). This primary miRNA undergoes two-step processes to form precursor miRNA (pre-miRNAs) and finally mature miRNA (Lee et al., 2002).

While the pri-miRNA is still in the nucleus, a microprocessor complex is formed, including Drosha, DGCR8, and accessory factors producing 70 nucleotides pre- miRNA (Lee et al., 2003). Next, the pre-miRNA is exported into the cytoplasm, where it is cleaved by Dicer to produce a small double-stranded RNA with 18-22 nucleotides in length

(Ketting et al., 2001). One or both strands becomes mature miRNA and gets incorporated into the RISC complex (RNA-induced silencing complex) (Khvorova et al., 2003). The mature miRNA and the RISC complex can target mRNA, resulting in either degradation or repression (Doench et al., 2003).

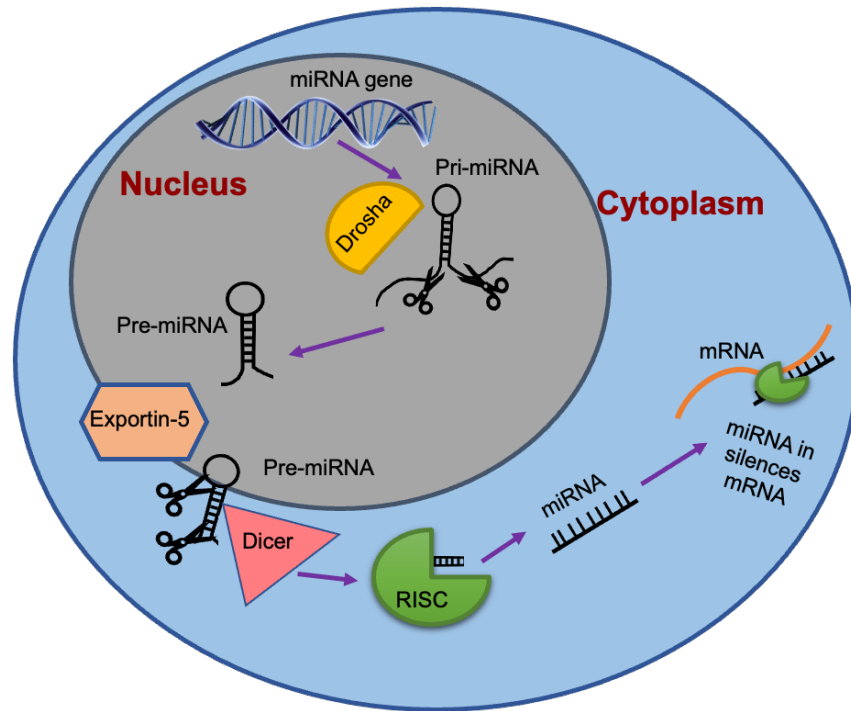


Figure 1.1: miRNA biogenesis: Formation of miRNA, targeting mRNA (Tovar-Camargo et al., 2016).

1.1.3 MicroRNA role in cancers

With the use of various latest technologies like sequencing and high-throughput screening, it has been shown that many miRNAs may be dysregulated in multiple cancers. Studies have shown that about 10% of miRNAs are secreted in extracellular matrix, while the other 90% forms complex with proteins like argonaute 2 and high-density lipoproteins (Arroyo et al., 2011). The miRNAs in circulation may play a crucial role in intercellular communication in the cancer (H. D. Zhang et al., 2018). These miRNAs,

therefore, can be considered as circulating biomarkers for cancer diagnosis and therapeutics (Chen et al., 2014). MiRNA in cancer can either play a role as an oncomiR or a tumour suppressor (Armand-Labit & Pradines, 2017). MiR-155 acts as an oncomiR in the case of lymphoma(Kluiver et al., 2005) and pancreatic cancer (Ryu et al., 2010), whereas the same miRNA acts as a tumour suppressor in the case of ovarian (Qin et al., 2013) and gastric cancer (Li et al., 2012).

There are various reasons for dysregulated expression of miRNA resulting in cancer. Studies showed that about 30% of human genes are regulated by miRNA (Garzon et al., 2006) of which half of the miRNAs are located in fragile loci that are tumour-associated (Calin et al., 2004). One of the reasons could be the function variation of enzymes like Drosha and Dicer, which are associated with miRNA biogenesis (Briers et al., 2015). Studies have shown that a decrease in the levels of these enzymes correlates to bladder (Catto et al., 2009) and ovarian cancer (Merritt et al., 2008). In contrast, increased levels were reported in gastric cancer (Tchernitsa et al., 2010) and cervical squamous cell neoplasms (Muralidhar et al., 2011). Another reason could be altered miRNA in cancer is caused by the transcriptional error of pri-miRNA.

1.1.4 MiRNA clusters

Several miRNAs are seen in clusters, where these miRNAs are produced from a single primary transcript, also known as "polycistronic miRNAs" (Cullen, 2004). Interestingly, about ~30% of miRNAs in the human genome are seen in clusters (Altuvia et al., 2005). These miRNAs are highly conserved across evolution to maintain possible functional consequences.

Based on the number of miRNAs in a group, miRNA clusters can also be classified into three groups (i) large group with more than ten miRNAs, (ii) medium group with 5 - 10 miRNAs and (iii) small group with 2 - 4 miRNAs. Under this classification, there are two large groups, nine medium groups and 142 small groups (Kabekkodu et al., 2018).

Even though these miRNAs within the cluster are highly related, they show different 'seed regions' within the same cluster (Kim & Nam, 2006). As a result, one miRNA can target multiple mRNAs, and single mRNA can be targeted by multiple miRNAs (Wu et al., 2010). MiRNA clusters are seen throughout different regions of the genome and are reported to co-regulate and participate in many cellular, molecular and developmental pathways (Braun & Gautel, 2011).

As per the latest miRbase (version22.1) database, 153 clusters with 1881 precursors miRNAs involving 468 miRNAs are present in the human genome (Kabekkodu et al., 2018). Some of the reported clusters are miR-17/miR-92, miR-106b/miR-25, miR-106b/miR-363 and miR-379/miR-656. These miRNA clusters are seen dysregulated in multiple cancers (Tüfekci et al., 2014), and their dysregulation can result in different disease types like multiple myeloma (Chen et al., 2021; Tüfekci et al., 2014).

1.1.4.1 MiR-17-92 cluster

MiR-17-92 is one of the known and well-studied oncogene clusters responsible for various disease pathogenesis. This cluster influences biological processes like cell proliferation, apoptosis, metastasis, and tumour formation. The upregulation of miR17-92 is studied in ovarian cancer (Hua et al., 2013), lung cancer (X. Zhang et al., 2018), and other cancers. This cluster is located on human chromosome 13 and encodes seven mature miRNAs, miR-17-3p, miR-17-5p, miR-18a, miR-19a, miR19b-1, miR-20a and

miR-92a-1 (Bai et al., 2019). MiR-17-92 cluster is well known for regulating neurological, heart diseases and many other diseases (Bai et al., 2019). Additionally, this cluster member targets tumorigenic pathways like JAK/STAT, PI3K/mTOR and PTEN (Bai et al., 2019).

1.1.4.2 MiR-92a Family

While miR-92a is a part of the miR-17-92 cluster, miR-92a is also a member of the miRNA family with miR-92a-1, miR-92a-2, miR-363 and miR-25. Studies have shown that miR-92a is involved in organ development and tumorigenesis; its overexpression is seen in multiple cancers like colon, prostate, lung, and others (Jiang et al., 2019). Further, this family is reported to be involved in cell proliferation, and apoptosis and its downregulation are studied in breast cancer with increased macrophage infiltration (Nilsson et al., 2012). And its upregulation is correlated with metastasis in the case of colorectal cancer (Shi & Liu, 2020).

1.1.4.3 miR-379/miR-656 cluster

The chromosome 14 miRNA cluster (hereafter C14MC) is one of the largest clusters located within a chromosomal imprinting region in the human genome, with over 50 miRNAs spanning about 40kb (Glazov et al., 2008), as shown in **Figure 1.2**. In humans, the expression of C14MC is limited to the placenta but is also reported in abnormal tissues as a possible tumour suppressor factor in the liver (Yang et al., 2013) and gastric cancer (Guo et al., 2013).

1.1.5 Genomic description of C14MC

C14MC is a eutherian-specific miRNA cluster with an imprinting Dlk1-Dio3 domain, which plays a vital role in prenatal growth, placentation, muscular and brain development (da Rocha et al., 2008). The domain is ~1Mb in size and consists of three paternally

expressed protein-coding genes: Delta-like homolog1 (Dlk1), retrotransposon-like1 (Rtl1), and Type III iodothyronine deiodinase (Dio3) (Seitz et al., 2004).

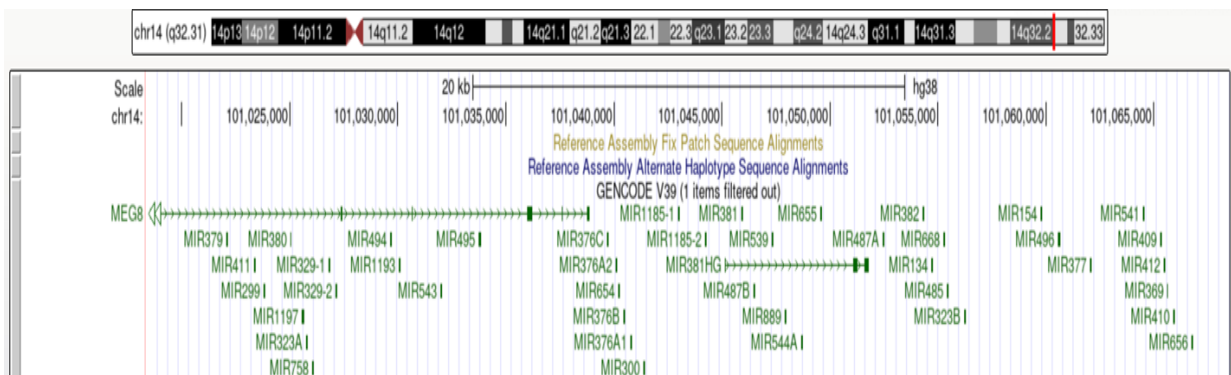


Figure 1.2: Chromosome 14MC: Above is the chromosome ideogram with the red dotted line on the right-side showing cluster miR-379/miR-656 (chr14:101,018,397-101,068,506). Below is the graphic representation of the zoom in the area where the red box shows the whole C14MC cluster. Images adapted from UCSC genome browser (<https://genome.ucsc.edu/>) (Version-GRCh38/hg38).

C14MC also has maternally expressed non-coding RNA transcripts: Meg3, an antisense transcript to Rtl1, as well as small RNAs belonging to C/D small nucleolar RNA (snoRNA) and miRNA families. In humans, the C14MC cluster is divided into two genomic regions: the miR-127/miR136 cluster and the miR-379-miR-410 cluster.

As a region for multiple encoded miRNAs, C14MC shares a common mechanism of regulation. The whole cluster has been reported to be dysregulated in multiple cancers (Laddha et al., 2013). Further, these miRNAs are reported to be dysregulated in the lung cancer (Nadal et al., 2014).

The current study focuses on comparing the miRNA isolated from cultured media from lung cells (A549 & BEAS-2B) treated with nicotine and different flavours of E-liquids from the C14MC cluster.

1.2 The potential of miRNA as a Biomarker

A biomarker is a biological molecule found in blood and other bodily fluids that can indicate physiological conditions within a body (Henry & Hayes, 2012). Any biological molecule such as proteins or RNA detected in various bodily fluids can be considered a biomarker. The best-known protein markers in clinical practice that are measurable in the blood are troponin (Tomásková & Vorel, 2010) for myocardial infarction and carcinoembryonic antigen (CAE) (Hesdorffer et al., 1984) for different cancers, and prostate-specific antigen (PSA) for prostate cancer (Etzioni et al., 2008).

To progress toward personalised and preventive medicine, an accurate and desirable biomarker is a requirement. An ideal biomarker needs to fit specific criteria such as accessibility with a minimally invasive procedure. The other crucial element is the ability to investigate a disease condition ("Biomarkers and surrogate endpoints: preferred definitions and conceptual framework," 2001).

Scientists have discovered the presence of nucleic acids like DNA and RNA in circulation (Kamm & Smith, 1972). In this regard, liquid biopsy is an emerging technology to obtain circulating biomarkers to improve diagnosis and treatment (Freitas et al., 2021). The advantage of using liquid biopsy is that it is minimally invasive, has the scope of repeatability and has improved uptake compared to tissue biopsy.

This technology can detect biomarkers such as circulating tumour cells (CTCs) and circulating cell-free DNA (cfDNA), circulating non-coding RNA (ncRNA) and many, as mentioned in, especially cancer.

Further, considering that miRNAs can be found in bodily fluids like blood, serum saliva and urine, and are resistant to RNase activity and temperature conditions, it has

the potential to be used as biomarkers. MiRNA was first established as a biomarker in 2008 during their examination of diffuse B-cell-lymphoma in the serum samples of patients for cancer (Mitchell et al., 2008).

Table 1.1:The table summarizes different circulating biomarkers with their references in cancer.

Different types of circulating Biomarkers	Disease	References
CTC-Circulating Tumour cells	Cancer	(Ried et al., 2017)
ctDNA-Circulating Tumour DNA	Colorectal cancer	(Gabriel & Bagaria, 2018)
cfDNA Cell-free DNA	Metastatic melanoma	(Valpione et al., 2018)
gDNA via sEV	Cancer	(Kurywchak et al., 2018)
mRNA via sEV	Prostate Cancer	(Souza et al., 2017)
miRNA via sEV	Cancer	(Wang et al., 2018)
lncRNA via sEV	Cancer	(Sun et al., 2018)

Additionally, liquid biopsy can be an ideal technology for miRNA to be used as a biomarker. MiRNA can give the possibility to understand the disease progression and can differentiate different cancer subtypes (Lan et al., 2015).

Studies have shown that miRNAs were involved in the onset and progression of cancer. MiRNAs may act either as tumour suppressor genes or oncogene to regulate cancer-associated genes. miR-34 family with miR-34a and miR-34b/c targets p53, either deleted or down-regulated in cancers like colon and pancreatic cancer. These miRNAs are highly conserved and tissue-specific, wherein miR-34a is highly expressed in the brain, whereas miR-34b/c is expressed in the lungs (Hermeking, 2010). Up-regulated miR-34 inhibits cancer growth by involving cell cycle regulation and apoptosis, whereas its down-regulation causes cell cycle arrest in the G1 phase of senescence. Further, down-regulated miR-34 causes tumour suppression in prostate and breast cancers (Ji et al., 2009).

Additionally, in the case of colorectal cancer, miR-126 is responsible for angiogenesis during tumour progression, where its expression is correlated with the expression of VEGF-A (vascular endothelial growth factor-A). Thus, this miRNA can be used as a prognostic biomarker. miR-31 is also involved in cell proliferation, and its inhibition can enhance drug response in the case of colorectal cancer (Stiegelbauer et al., 2014).

In thyroid cancer, a set of miRNAs such as miR-17-92 cluster, miR-146, miR-221 and miR-222 are up-regulated, resulting in cell proliferation, and blocking cell cycle checkpoints. Other miRNAs like let-7 and miR-30 family can elevate the metastatic potential of the cancer cells. Thus, these all can be potential biomarkers to determine the risk and progression of thyroid cancer (Fuziwara & Kimura, 2014).

MiRNAs let-7b, let-7c, miR-23b, miR-143 and miR-196b are up-regulated in cervical cancer, whereas miR-21 is down-regulated (Granados López & López, 2014). Another set of miRNAs, miR-9 and miR-200a, has been shown to play a vital role in patient survivability in the case of cervical cancer. miR-200a suppression can cause metastasis resulting in over-expression of genes for cell motility, whereas down-regulation of miR-9 can increase tumour cell metabolism (Hu et al., 2010).

1.3 Small Extracellular Vesicle (sEVs)

Apart from being potentially used as a biomarker, miRNA also plays a crucial role in intercellular communication. Although most miRNAs are found inside the cell, a proportion comes out in the body fluids (Weber et al., 2010). As discussed earlier, the miRNA that is in circulation is known as circulating miRNAs. In contrast, the other

miRNAs are vesicle-bound miRNAs such as microvesicles or small extracellular vesicles (sEVs) (Vickers et al., 2011). Studies have shown that about 10% of miRNA are vesicle bound, and the other 90% forms complex with AGO2 and high-density lipids (Arroyo et al., 2011). This kind of packing is necessary to prevent the digestion of miRNA from RNase activity found in body fluids (Weickmann & Glitz, 1982). Further, recent studies show that miRNAs are selective to certain sEVs; the reason could be that the miRNAs found in vesicles could be originated from their origin of cells (Mittelbrunn et al., 2011).

All living cells and organisms maintain dynamic equilibrium under normal/healthy conditions. Equilibrium comprises normal physiological functions such as body temperature, fluid balance, enhanced survivability, and maintaining and regulating homeostasis. In the living system, homeostasis is a state of steady internal and physical conditions. Similarly, in molecular terms, a normal cell state is where all the molecular processes – both intracellular and extracellular, work together to maintain survival and reproductive fitness.

It is much more complex for each cell to maintain homeostasis in a multicellular organism. However, it is vital for cells, various tissues, organs, and the whole organism. These cells, tissues, and other organs would require nutrition, a wide range of proteins, and other vital messages to maintain life. Homeostasis is accomplished by cell-cell communication via extracellular vesicles (EVs), especially small extracellular vesicles (sEVs) (Fu et al., 2016).

EV is a generic term used for the particles released naturally from a cell. EVs do not have a functional nucleus and cannot replicate by themselves. Furthermore, based

on their origin, EVs can be categorized as plasma-membrane derived "ectosome"/microvesicles and endosomal derived sEVs (Théry et al., 2018).

sEVs are proclaimed as a miniature version of their cell of origin, known to be involved in the 'cargo system' for diverse types of biomolecules (Kalluri, 2016). These are abundant in biofluids like plasma, serum, urine, and saliva and are released by all kinds of cells and tissues.

Currently, the major challenge in the field of extracellular vesicles is to differentiate between sEVs and other such small particles like microvesicles (**Table 1.2**).

Table 1.2: Categories of EV; Different types of extracellular vesicles based on their size, functions, markers, and the content they carry within.

CATEGORIES	sEVs	medium/large EVs
Origin	Endosome origin	Plasma membrane
Size	30 <150nm	>200nm
Function	Intercellular communication	Intercellular communication
Surface Markers	CD63, CD81, CD9, flotillin	CD40
Content	Protein & mRNA, miRNA	Protein & mRNA, miRNA

As mentioned before, this research mainly focuses on sEV's and sEV derived miRNA, which may serve as novel non-invasive biomarkers since they are released by different cell types and found abundant in various biofluids in humans.

1.3.1 Nomenclature

EVs released from the plasma membrane are called ectosomes with a size of > 200 nm. Whereas EVs produced within the multivesicular bodies (MVB) inside the cells fuse with the plasma membrane, releasing sEVs with < 200 nm size. sEVs is termed based on their size (<150 nm in diameter) and their content with endosome-associated

proteins. However, the term sEVs is often used in literature for small-sized EVs, with a cut-off filtration pore size of < 200 nm during recovery.

Initially, the term "exosome" was coined in 1987 by (Johnstone et al., 1987) Pan and Johnstone while studying the maturation process of Red Blood Cells. The term exosome in Greek was meant as Exo -outside, and soma – body, was defined as "Outside body ". According to Mitchell et al. in 1997, "exosomes" are soma/body which carry RNA degrading proteins (Mitchell et al., 1997).

Since then and in the following years, with the emerging research work on these exosomes, various terms were used for exosomes like oncosomes, exposomes, etc. (Assinder & Bhoopalan, 2017). Therefore, it was necessary to focus on the appropriate nomenclature and minimal experimental criteria, where various similar-sized biological entities show different functions and origins. As a result, there has been a significant misperception and uncertainty for the scientific community working in this field of extracellular biology. The update and instructions mentioned in the guideline called MISEV (Minimal information for the studies of extracellular vesicles) formed by the International Society for extracellular Vesicles (ISEV) in 2014 have shed some light (Lötvall et al., 2014). The latest set of guidelines was released in 2021 (Witwer et al., 2021) to make precise specifications of these particles.

The latest MISEV 2021 guidelines released includes up-to-date facts and information. According to MISEV 2021, small EVs (hereafter sEV) are a clear and prominent terminology rather than the vague term "exosomes" for better understanding. This categorization was based on their size as “small EVs” (sEVs) - <100 nm or < 200nm

and “medium/large EVs” (m/l EVs) - >200 nm. This study considers sEVs with sizes ranging from 30-150nm in diameter, which fits the MISEV 2021.

1.3.2 Background of sEV

Until 1990s, sEVs were believed to be a disposal process released by the cells after cell death/apoptosis (Johnstone, 1992). Later in the mid-2000s, sEVs were reported to carry diverse cargo like DNA, RNA species, and proteins (H. Valadi et al., 2007). Consequently, because of their small size, attribute in carrying nucleic acids, and mainly due to their bi-layered membrane, these may potentially be used in the drug delivery (Vader et al., 2016).

1.3.3 Biogenesis of sEV's

The mechanism of sEV biogenesis is still not clear. Studies showed that sEVs originated from the endosomal system via multivesicular bodies (MVBs) (Huda et al., 2021). EV biogenesis is involved in multiple regulatory functions (Johnstone et al., 1987). The known conventional process is inward budding like viruses (McDonald & Martin-Serrano, 2009). The process involves the formation of endosomes via inward movement of the endosomal membrane. This membrane moves into cells, forming a ball-like body called intraluminal vesicles (ILVs), which are formed through budding of the multivesicular body (MVBs) (Minciacchi et al., 2015), as shown in **Figure 1.3**. These ILVs are released into the extracellular matrix, where the endosomes fuse with the plasma membrane to become late endosomes referred to as 'sEV'.

It is a continuous process of intercellular communication via sEVs. Studies revealed that ILVs formation needs the endosomal sorting complex required for transport (ESCRT) function which involves protein like Alix, TSG101 and exosome specific surface

markers like CD63 etc, (Villarroya-Beltri et al., 2014). Other available EV specific proteins are fusion proteins (tetraspanins-CD63, CD81 & CD9), cytoplasmic enzymes (GAPDH), and cytoskeletal proteins (Beta-actin) (van Niel et al., 2011).

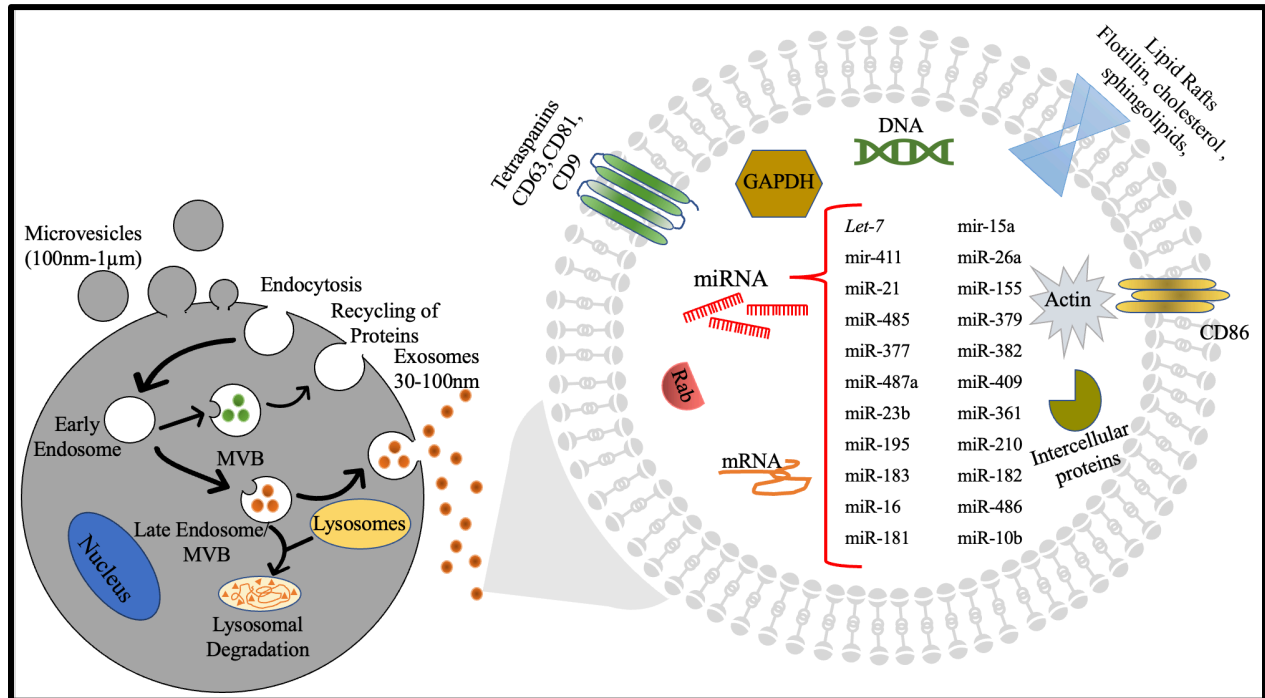


Figure 1.3: Biogenesis of sEVs; The figure represents the origin of sEVs within the cell (in grey, left) and the amplified view within an sEV (right). Different surface markers and internal biomolecules are highlighted. Due to the focus of this study, specific microRNAs altered in human diseases and reported to be released via sEV are indicated. This figure is adapted from (<https://www.novusbio.com/research-areas/cell-biology/Exosome-research-tools>)

1.3.4 Small EV Composition

The main component of sEV is the lipid-bilayer enriched in cholesterol and phospholipids. In this way, sEV acts as a carrier of lipids to carry to recipient cells (M. Record et al., 2014; Michel Record et al., 2014). In addition to lipids, sEV also carries coding RNA molecules, including mRNAs and other non-coding RNAs such as miRNAs (H. Valadi et al., 2007; Hadi Valadi et al., 2007) and lncRNAs (Gezer et al., 2014).

- **Small EV Protein content**

Proteomics studies showed sEV protein content in biological fluids such as plasma, serum, and urine (Guan et al., 2019; Walsh & McGee, 1988), originating from the endocytic pathway. Some of the sEV proteins include annexins and flotillin with membrane transport properties, TSG101 and Alix with biogenesis (van Niel et al., 2018). Other proteins with lipid domain and transport mechanisms (integrins and tetraspanins) and heat shock proteins (HSP70 and HSP90) (Shushkova et al., 2018).

Further studies showed that sEV proteins are involved in intercellular communication, stress response, and lipid metabolism (Lo Cicero et al., 2015). sEV have different lipid profiles, considering: their origin and type of surface protein markers as shown in **Figure 1.3**. Markers such as CD63, CD81, and CD9 are surface markers specific to sEVs. They are used in various experiments to show the presence of sEV's (Smolarz et al., 2019).

- **Small EV RNA content:**

Circulating sEVs and the RNA derived from sEVs, has begun a new area of molecular biology. The most important discovery made in sEVs field was in 2007 when studies showed that these vesicles carried various biological materials such as RNA, miRNA, and proteins showing a novel mechanism of genetic exchange, especially miRNA (H. Valadi et al., 2007). Studies showed that miRNA carried by sEV could suppress protein translation by targeting the entire biological pathway in the recipient cells (Davalos & Esteller, 2010). This mechanism of sEV-derived miRNA sorting and targeting suppression is still under investigation. The latest advance like single cell analysis,

proteomic studies in research might give us a better understanding of the packaging of these miRNAs into sEVs under specific physiological and stress conditions.

A recent study indicates that miRNA cargo into sEV can be complex. The study demonstrates that miRNA possesses a sorting sequence which determines their secretion through sEVs or cellular retention, thereby defining their fate. Thus, the miRNA profile not only suggests vital information between circulating sEV miRNA to the tissue of origin (Garcia-Martin et al., 2022). Therefore, it is necessary to determine if the sEV-derived microRNAs can serve as a reliable marker.

1.3.5 Markers of sEVs

Proteins like flotillin-1, heat-shock 70-kDa proteins (HSC-70), CD63, CD81, CD9, major histocompatibility complex (MHC) class-I, and class-II proteins are often used as markers in literature (van Niel et al., 2018). Improving purification and characterisation methods makes better identification of these proteins possible. Techniques like sucrose gradients differential separation combined with proteomics analysis would suggest the origin of EVs in the cell (Kowal et al., 2016). In contrast, methods that include proteinase K and biotin tagging with the mix of liquid chromatography-tandem mass spectrometry would suggest the orientation and topology of these surface markers (Cvjetkovic et al., 2016).

Additionally, methods like density gradient and immuno-based isolation combined with proteomic analysis would result in a population of sEVs with specific protein markers, including CD63, CD81, and CD9 (Kowal et al., 2016). These membrane-bound classic markers belong to a highly conservative protein family essential for microRNA cargo and cell recognition (Caby et al., 2005). In contrast, other proteins like Hsp-73, Hsp-90, ALIX,

and TSG101 are associated with the endosomal sorting complex necessary for transport and are considered cytosolic proteins involved in sorting cargo (Ostrowski et al., 2010). Several studies have shown the enrichment of these markers to be cell type-dependent.

Taken together, markers such as CD63, CD81, CD9 and TSG101 have commonly used markers indicative of EVs. This study has included these markers to identify and characterise sEVs in experiments such as western blot and fluorescent tagging.

1.3.6 Heterogeneity of sEV

As discussed earlier, cells can release EV subtypes like sEVs, mEVs, IEVs, and microvesicles via endosomal or plasma membrane origin. All these EV populations are alike in their biological and physical characteristics, such as size and density, resulting in the isolation of pure sEVs challenging (Bobrie et al., 2012). Additionally, all these EV subtypes are challenging to validate due to the lack of individual surface-specific markers (Sork et al., 2018). This heterogeneity makes the sEV purity difficult in individual physical characterisation like size and density, which might not correlate with other subpopulations.

All sEVs differ in size, carry different cargoes, and have specific associated membrane proteins. Many studies showed the diverse composition of these sEVs through density gradient isolation and proteomic analysis using LC-MS/MS spectrometry and label-free quantification (Willms et al., 2016). Thus, these are highly multifunctional vesicles and represent a heterogeneity (Poliakov et al., 2009). Although, the identification of sEVs for the tissue-specific origin and separation from subpopulations is still a significant challenge in the field of extracellular vesicle biology. Further, there is a need

for future studies, experimental proofs, and isolation techniques to reduce the complexity of EVs.

1.3.7 Characterisation of sEVs

A single cell can release different sized vesicles as a part of its routine functions from which a few vesicles can be sEV ranging from 30-150 nm in size. Therefore, it is necessary to characterize and distinguish these small EVs from other differently sized particles by techniques.

There are numerous approaches to separate and recover sEV, including high-speed ultra-centrifugation and commercial kits that are comparatively less time-consuming for easy uptake (K. W. Witwer et al., 2013; Kenneth W. Witwer et al., 2013). These kits are mainly based on precipitation, size exclusion, column filtration, Immun isolation methods, etc. For visual characterization, well-known techniques are Transmission electronic microscopy, Fluorescence microscopy, atomic force microscopy, and are in wide spread (Mashouri et al., 2019). In contrast, for detection, techniques like western blot, enzyme-linked immunosorbent assay (ELISA), nanoparticle tracking analyses (NTA), and fluorescence-activated cell sorting (FACS) are in use.

sEV's show specific surface markers are known as CD63, CD81, and CD9, which can distinguish sEV's from m/IEVs extracellular vesicles (Durcin et al., 2017). Considering protein composition, especially on the surface of sEVs like CD9, CD63, and CD81, can be identified using western blots, high-speed flow cytometry (FACS), and mass spectrometry to identify these membrane proteins. This study includes some of these techniques, and the results are mentioned in the results section.

1.3.8 Biological Function

sEVs are membrane-derived nano-sized vesicles of about 30-150 nm released by various cell types such as mast cells, dendritic cells, neuronal cells, and epithelial cells (Théry et al., 2002). These sEVs are involved in cellular interactions such as progression, cell division, and tumorigenesis, serving as multi-purpose carriers (Nieuwland & Sturk, 2010).

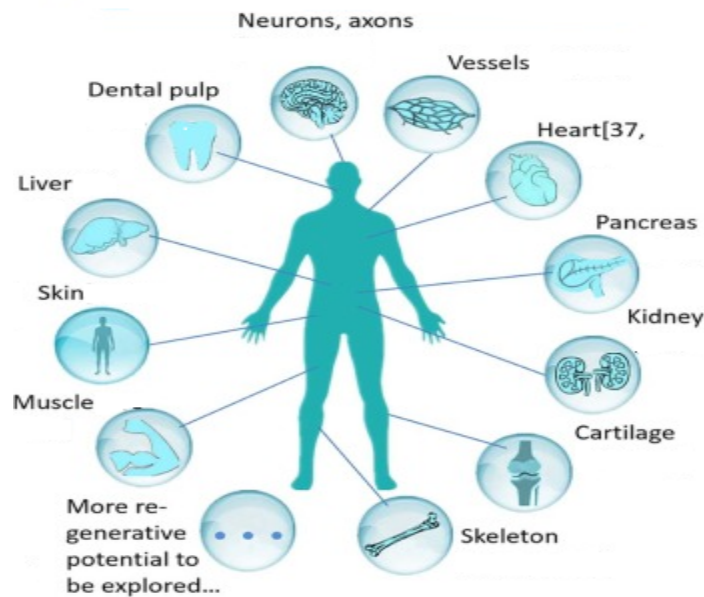


Figure 1.4: Origin of sEV's; A schematic representation of the origin of sEVs from various tissues and organs such as nerves, heart, liver, and kidney and still to be explored, figure adapted from (Jing et al., 2018).

As mentioned earlier, all biofluids such as blood, semen, saliva, plasma, urine, cerebrospinal fluid, amniotic fluid, ascites fluid, synovial fluid, and breast milk can release sEVs (Taylor & Gercel-Taylor, 2008). Even cells such as B cells, dendritic cells, and mast cells of the immune system release sEV's as shown in **Figure 1.4** (Buschow et al., 2009) seen involved in lymphocytic interaction involving B cells and T cells (Muntasell et al., 2007).

Further, sEVs are identified in normal physiological or biological processes such as lactation, inflammation, cell proliferation, immune response, and neuronal function (Simhadri et al., 2008). They are seen in different disease conditions such as thrombosis, diabetes, and atherosclerosis (Azevedo et al., 2007) also progression and development of other diseases like liver diseases (Masyuk et al., 2013), neurodegenerative diseases (Vella et al., 2008) and cancer, etc. Interestingly, it was found that human cancer cells can release a large number of sEVs when compared to normal cells (Jenjaroenpun et al., 2013).

1.3.9 Small EVs based Databases

With all the rising studies on sEVs release and their functional aspect, there is a need to maintain a necessary database for the data collected worldwide. Thus, multiple databases and portals are documenting scientific publications' ongoing research. With the growing interest in EVs, particularly sEV's along with the newest cargo and composition, signalling pathways involved, diseases, target genes, cells, tissues, etc., such as Vesiclepedia (version 4.1) (<http://microvesicles.org/>), Exocarta (3.1.3), (<http://exocarta.org/>), EVSEARCH (<http://evsearch.dk>) and exRNA (<http://exRNA.org>), etc. (de la Torre Gomez et al., 2018).

1.3.10 Small EV as biomarker

As stated above, biomarkers can be acquired easily from all different biofluids, and they can serve as potential biomarkers using liquid biopsy. In biological conditions, sEVs are released by various cell types, including tumour cells (Théry et al., 2002). The other main reason to choose EV as a biomarker is that they are stable, hard to degrade, and their composition reflects its parental origin (Rijavec et al., 2019). Additionally, sEVs are

nano-sized with a diameter of 30-150 nm with a density of 1.13-1.19 g/ml (Taverna et al., 2016). Furthermore, the formation of this sEV is linked to the secretion mechanism. It involves various proteins like heat shock proteins (Hsp70, Hsp80), interactive proteins (Alix) and tetraspanins (CD9, CD81 and CD63), which are known for the characterisation of these sEVs (Yoshioka et al., 2013).

Consequently, studies showed that sEVs could be very useful if combined with technology like “liquid biopsy”, allowing a non-invasive analysis of tumours, which has recently gained a great deal of attention (Rolfo et al., 2014). As a result, focusing on the cargo of EVs will allow us to gain decisive molecular information about the status of the disease.

1.3.11 Small EV- Secretion and uptake of miRNA

MiRNA is found in biological fluids in the extracellular matrix are considered a result of cellular activities such as cell death as a part of the regulatory process (Turchinovich et al., 2012). Secretion of miRNA via sEVs is ceramide dependent, and these secreted miRNAs regulate the growth in the target cells (Kosaka et al., 2010). miRNA secreted via sEV has also been reported to be regulated by signalling molecules such as interleukin-4 (IL4) (Yang et al., 2011) and docosahexaenoic acid (DHA) (Hannafon et al., 2015). Activated IL4 macrophages were found secreting sEVs carrying oncogenic miRNAs, which promotes invasiveness in breast cancer cells (Yang et al., 2011). Whereas DHA, with anti-cancer and anti-angiogenic properties, enhance the release of sEVs with miRNA causing inhibitory effects on tumour angiogenesis (Yang et al., 2011).

Studies have shown that sEVs miRNA acts as intercellular signalling molecules and thereby regulate the activity of recipient cells. A study showed that sEV transferred

miR-105 from breast cancer cells to endothelial cells targets the tight junction protein ZO-1, thereby promoting metastasis (Zhou et al., 2014). Another study showed that sEVs from umbilical cord blood were enriched in miR-21-3p, which accelerated the proliferation and migration of fibroblasts cells, further enhancing the angiogenic properties of endothelial cells, resulting in induced wound healing (Hu et al., 2018).

1.4 Small EV derived miRNA as a biomarker

As mentioned earlier, the miRNA in vesicles/ sEVs can be used as a non-invasive biomarker. Evidence has shown that miRNA associated sEVs may characterise tumours (H. Valadi et al., 2007) and therefore have the efficiency to be diagnostic purposes in the cancers (Calin & Croce, 2006). Tsang et al. showed that sEVs could preferentially take up miRNAs (Tsang et al., 2017). Since miRNAs in sEVs can be detected in different body fluids, including blood, plasma, serum, and amniotic fluid; thus, they can be used as possible non-invasive biomarkers (H. Valadi et al., 2007). Hence, detecting miRNA-associated sEV in biological fluids has opened a new era in clinical biology to explore diagnostic and prognostic markers.

A study by Cazzoli et al. showed the expression of 742 miRNAs in 30 patients, which includes ten lung adenocarcinomas, ten lung granulomas, and ten healthy smokers. They developed a screening panel of six miRNAs (miR-151a-5p, miR-30a-3p, miR-200b-5p and miR-629, miR-100 and miR-154-3p) which can distinguish between lung adenocarcinoma and granulomas (Cazzoli et al., 2013). Another study by Zhou et al. established a panel of six plasma miRNAs (miR-19b-3p, miR-21-5p, miR-221-3p, miR-409-3p, miR-425-5p and miR-584-5p) for the diagnosis of lung adenocarcinoma (Zhou et al., 2017). Among these six miRNAs, miR-19-3p and miR-21-5p were significantly up-

regulated in plasma-derived sEV of patients with lung adenocarcinoma. One more study by Lin et al. showed 27 miRNAs differentially expressed in sEVs isolated from pleural effusion samples between pneumonia and lung cancer patients. Among these, two miRNAs (miR-205-5p and miR-200b) were significantly up-regulated in lung cancer patient samples indicative of these two miRNAs may serve as a biomarker to distinguish between pneumonia and lung cancer (Lin et al., 2016).

Furthermore, studies have shown the significance of using sEV derived miRNA as an early diagnostic marker to reduce lung cancer mortality rate. A recent study by Jin et al. analysed small RNA sequence analysis using sEVs isolated from 46 stages I NSCLC patients and 42 healthy controls for early-stage cancer diagnosis (Jin et al., 2017). Subsequently, using a four-miRNA panel (Let-7b-5p, let-7e-5p, miR-23a-3p and miR-486-5p), they could identify stage I NSCLC with an area under the curve of 0.899 with a sensitivity of 80.25% and specificity of 92.31%.

Due to miRNA being small in size with imperfect base-pairing (in animals), a single miRNA molecule may target hundreds of mRNAs. Expression profiles of miRNAs have been used to differentiate cancer from normal samples and to know the different subtypes since their expression levels can be easily measured using biological samples (Liu et al., 2020).

Additionally, miRNAs are released into the extracellular region via sEVs and thus have been suggested to have the potential to be a biomarker and serve to mediate cell-cell communication (Wang et al., 2016). These miRNAs were found in sEVs protected without getting degradation, which was taken up to the recipient cells and subsequently regulated the distant cells (Chen et al., 2019).

This evidence proposes a potential outcome of utilising sEV derived microRNA as a non-invasive/minimally invasive biomarker for cancer diagnosis. These studies would suggest and support sEVs miRNA as a biomarker in various cancers and be used as a diagnostic /prognostic marker soon.

1.5 Impact of nicotine intake and E-liquids on lung cells- A model to study the role of sEV miRNA for biomarker

Cigarette contains more than 60 different carcinogenic toxic substances (Hecht, 1999). About 72% of lung cancer cases are caused by smoking cigarettes (Brown KF, Rungay H, Dunlop C, et al). The fraction of cancer attributable to known risk factors in England, Wales, Scotland, Northern Ireland, and the UK overall in 2015 (British Journal of Cancer 2018.). Another form of nicotine that began to appear on the market is E-cigarettes, also known as E-pods, vapes and electronic-based nicotine delivery systems. Additionally, E-liquids are available in over 7000 flavours, with other chemical compounds to make up, including some with carcinogenic properties (Goniewicz et al., 2014). This study focuses on the effect of E-liquid forms of nicotine on lung cells.

Lung cancer is a significant health issue in men and women, making up 25% of cancer-related deaths worldwide. Globally, lung cancer is the second most common cancer, with 2.2 million new cases and 1.7 million new deaths in 2020 (Sung et al., 2021). In addition, it is the second leading cause of cancer-related mortality, with 1.80 million deaths estimated in 2020 (Sung et al., 2021).

Early diagnosis is the key to reducing lung cancer. Lung cancer survival rate depends on various factors such as age, sex and the stage at which cancer has been diagnosed. In the UK, the person's survival rate is around 40.6% for at least one year,

16.2% for five years and 9.5% for more than ten years. The lung cancer survival rate continues to fall after 5 yr. diagnosis (Office for National Statistics2019). Therefore, it is essential to develop an early diagnosis to understand the origin and pathology of lung cancer with successful treatment. Thus, it is vital to find out a biomarker for early diagnosis and treatment in the case of lung damage due to nicotine intake and E-liquid exposure.

1.5.1 Epidemiology

Lung cancer is the third most common cancer in the UK, with around 47,838 new cases for persons in 2017, that's about 130 cases every day (Public Health England, November 2019.). About 85,000 people, especially those from the northeast and northwest of England and Scotland, are diagnosed with lung cancer (<https://www.blf.org.uk/>). Therefore, considering the incidence rate, early detection of lung cancer is crucial for lung cancer treatment.

1.5.2 Diagnosis

I. Invasive methods

Tissue biopsy is considered a gold standard for lung cancer diagnosis. Tissue biopsy is an invasive form of test usually recommended when the symptoms are visible and are at a severe/advanced stage. Tissue biopsy is advised to know the patient's functional status. Histological confirmation is a must using tissue biopsy, where an abnormal cell/tissue is collected using a syringe with a needle. These cells/tissues are then examined under a microscope to understand the severity and grade of cancer. This test can be categorised as an invasive form of examination.

II. Non-invasive methods

Currently, various non-invasive tests are available to diagnose lung cancer. Imaging tests like chest X-ray, CT-scan, magnetic resonance imaging (MRI), and positron

emission tomography (PET) are some options for initial evaluation. These tests can reveal an abnormal mass or lesions in the lungs. In contrast, tests like bronchoscopy and endobronchial ultrasound are used to screen the inner lining of the windpipe. These tests involve a long flexible tube with a light and an eyepiece that goes into the lung showing the airway's lining. On the other hand, a cytology test, where a sputum sample can be used to reveal the presence of lung cancer cells under a microscope.

These diagnostic tests are non-invasive and depend on the cancer's stage and spread. Therefore, if the tumour is early, the outcome may lead to misdiagnosis. Thus, the invasive method- tissue biopsy, is considered a gold standard.

1.6 Nicotine intake, E-liquids, and Lung cells

1.6.1 Nicotine

Several studies performed on lung cancer cells and animal models showed nicotine to cause cell proliferation, migration, invasion and promote tumorigenesis (Zou et al., 2013). Nicotine intake is associated with the risk of lung cancer in humans through a gene cluster *CHRNA3/A5/B4*, which binds with nicotine acetylcholine receptor (nAChR) (Changeux, 2010). The nAChR is involved in pathogenesis and promotes the cancer (Singh et al., 2011).

Nicotine is the product of tobacco, which gets metabolised through multiple pathways (Hukkanen et al., 2005). After entering the body, nicotine is rapidly absorbed and distributed. About 70% of the nicotine is converted to cotinine by cytochrome P-450 and excreted as glucuronidated 3-OH cotinine through the urine (Tutka et al., 2005).

Further, nicotine and its metabolites may assist cancer progression with added carcinogens. Nicotine intake in human bronchial epithelial showed the upregulation of

genes associated with mitogen-activated protein kinase (MAPK) (Tsai et al., 2006). Additionally, the effect of nicotine may increase methylation and expression patterns (Soma et al., 2006).

Nicotine can collectively increase cell proliferation by activating MAPK kinase in a nAChR dependent manner. In A549 cells, nicotine increases proliferation, EMT, migration, and invasion (Dasgupta et al., 2009).

1.6.2 E-liquid

Nicotine is an addictive substance that is the major component present in E-liquid vapes, promoting cell proliferation and causing cancer (Davis et al., 2009). E-liquid comprises a mixture of propylene glycerol (PG) and vegetable glycerine (VG) with different flavours, either with nicotine or without nicotine. Additionally, components like diacetyl, benzaldehyde, 2,3-pentanedione and other chemicals present in flavours were known to cause detrimental respiratory outcomes (Allen et al., 2016). Furthermore, metals and metalloids mainly originate from heated coil systems in E-liquid and produce aerosols that can cause adverse health effects, including cancer (Williams et al., 2013).

Moreover, recent reports suggest that using E-liquids can alter innate immunity and airway cytokine expression while increasing the viral infection in primary human airway epithelial cells (Wu et al., 2014) via influencing the co-localisation of bacteria (Hwang et al., 2016). Studies have shown that E-liquids with sweet or fruit flavours can induce more potent oxidisers than tobacco flavours, causing oxidative stress (Lerner, Sundar, Watson, et al., 2015).

However, substantial work to test and interpret the definite quantity of nicotine intake and intake of E-liquid per day was a challenge to capture the health risk of smoking

fully. Conversely, the role of E-liquids on lung damage is unknown and needs to be determined.

1.6.3 Different types of E-liquids

E-liquids are known by many diverse names, such as E-cigarettes, E-pods, vapes and electronic-based nicotine delivery systems (Perrine et al., 2019). E-liquids works on battery operating devices that heat up and produce aerosols that contain nicotine and other additive compounds with different flavours (Grana et al., 2014). These E-liquids are considered safe compared to traditional cigarettes, but they have adverse health effects. This impact can be due to the fine aerosol particles that E-liquid contains, like heavy metals, volatile compounds, and other toxic substances like acetaldehyde, acrolein, and toluene in lower concentrations when compared to cigarettes (Kaur et al., 2018). Further, about 7000 different flavours (Zhu et al., 2014) and other compounds have been identified in making E-liquids, including some compounds with carcinogenic properties (Goniewicz et al., 2014).

Apart from compounds like propylene glycerol (PG) and vegetable glycerine (VG vegetable glycerol, E-liquids have non-nicotine-based smoking options considered to be much safer than cigarettes. Since the launch of electronic-based smoking devices, there has been an assumption that E-liquids can cause lung injury. Later, few lung injury cases were reported in 2012 (Jonas & Raj, 2020; Sommerfeld et al., 2018). This disease was termed “E-liquid or vaping, product use-associated lung injury”/ “EVALI”. Then, in July 2019, the Illinois Department of Public health and Wisconsin Department of Health services began to report the injury caused due to E-liquid. About 142 reported cases were then published in The New England journal of medicine (Layden et al., 2020). Since then,

there has been a rapid increase in cases of this disease. According to the centre for Disease Control and Prevention (CDC), the latest records for 2020 showed 2668 hospitalised cases of EVALI (https://www.cdc.gov/tobacco/basic_information/e-cigarettes/severe-lung-disease.html#latest-information).

1.6.4 Diagnosis and Pathogenesis

The pathological findings of EVALI show a range of variations ranging from fibrinous pneumonitis to pneumonia with diffused alveolar damage-causing lung injury (Butt et al., 2019). With regards to histopathological findings, EVALI cases have been exhibited as acute eosinophilic pneumonia, lipoid pneumonia (Viswam et al., 2018) and respiratory bronchiolitis interstitial lung disease (RB-ILD) (McCauley et al., 2012). At the same time, the radiographic outcome may show the difference due to various factors like specific underlying lung conditions and individual variations of response to an inhaled substance. Thus, it is difficult to understand the condition, and there is no unique aetiology for this disease.

E-liquid can cause changes in lung function showing evidence of peripheral obstructive airway involvement (Meo et al., 2019). E-liquid can also release increased inflammatory and oxidative stress biomarkers causing endothelial dysfunction (Singh et al., 2019). Cigarette smoking can cause increased expression of miRNA in chronic obstructive pulmonary disease and lung cancer (Banerjee & Luetlich, 2012).

Despite identifying EVALI cases, there are many differential diagnoses associated with EVALI and present similar outcomes like eosinophilic pneumonia, lipoid pneumonia (Viswam et al., 2018), and respiratory bronchiolitis interstitial lung disease (RB-ILD) (Butt et al., 2019).

Consequently, EVALI is a severe health condition with public health consequences even though there is enormous popularity with the increased use of E-liquid. Thus, there is a concern with the diagnostic procedure to be more precise. Therefore, considering sEV mediated miRNA as a biomarker to assist in the diagnostic and prognostic process is vital. This study aims to find diagnostic biomarkers that can differentiate nicotine intake among E-liquid users and the difference between those with no-nicotine.

1.7 Application of sEV-derived miRNA and lung disease caused due to nicotine intake and E-liquids

There is an enormous need to understand the prognosis and diagnostics of lung cancer caused to smoking, especially in the case of EVALI. The gold standard technique for diagnosing lung cancer is “Tissue biopsy”. Unfortunately, this technique is not enough to understand the disease state in the case of lung injury due to EVALI. Therefore, it is essential to find a new diagnostic approach to detect early disease.

As mentioned earlier, studies has resulted in a recognized extracellular vesicle, and their properties to load molecular information like RNA and proteins represent their cell of origin to be small Extracellular vesicles (sEVs). Their ubiquitous presence in all kinds of bodily fluids has made them an essential candidate for developing a minimally invasive or non-invasive biomarker. Moreover, many studies consider sEVs derived miRNAs as a diagnostic tool when combined with liquid biopsy for their significance in the lung cancer (Wang et al., 2017).

Further, studies have demonstrated the role of miRNA mediated sEVs as a diagnostic marker. Therefore, liquid biopsy with sEVs is an excellent opportunity for

minimally invasive sampling with repeat evaluation compared with a tissue biopsy, makes it a valuable tool in clinical practice in the case of the lung cancer (Rijavec et al., 2019).

Given the role of sEV mediated miRNA in various biological functions and diseases, this study aims to determine the levels of miRNA expression whether their levels are altered between lung cells exposed to nicotine and E-liquid. Further, to find out the possible in vitro non-invasive biomarker for lung cancer caused due to nicotine intake and use of E-liquid.

This is the first-ever study to shed some light on sEV derived miRNA from conditioned media treated with nicotine and different flavours of E-liquids. Additionally, the current study is to isolate, identify, and characterise sEVs. Subsequently, compare the conditioned media derived sEV miRNA levels with nicotine, different E-liquids, and untreated. Understanding the variation in the conditioned media derived sEV miRNA and their profiles can help develop biomarkers of the disease progression in EVALI.

1.8 Aims & Objectives

This study aims to understand the role of miRNAs derived sEV in the case of lung injury caused by nicotine intake, E-liquids exposure and to find out candidate miRNAs involved, as shown in **Figure 1.5**. The following are the objectives:

1. To analyse the effect of nicotine and different flavours of E-liquid (Strawberry and Apple) with a known concentration on different lung cell types (both cancer and normal cell line) *in vitro*. Further, the characterisation of isolated sEVs using NTA, NTA with fluorescent tagging, TEM, fluorescence microscopy and western blot.
2. To evaluate the expression of candidate miRNAs for nicotine and E-liquid exposure from C14MC using qPCR from sEVs and to identify the candidate miRNAs using high-throughput small RNA next-generation sequencing (NGS) with the potential to be used as a non-invasive biomarker.

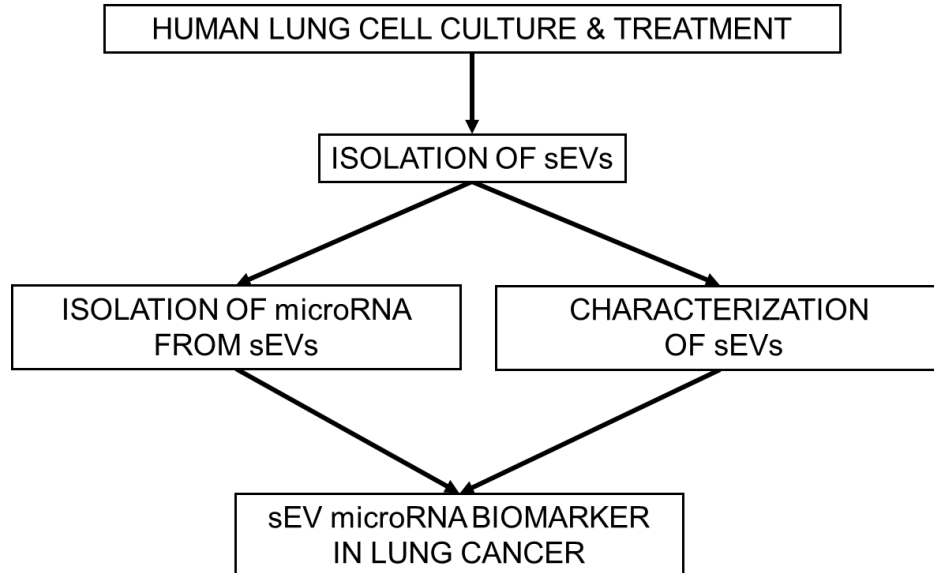


Figure 1.5: Workflow; A schematic representation of the workflow includes cell culture, treatment, and RNA isolation.

CHAPTER 2 : Materials and Methods

2.1. Cell-culture

Two lung cell lines, A549 (cancer - Human adenocarcinoma basal epithelial cells) and Beas-2B (normal - human bronchial epithelial cells), were cultured in T-175 flasks at 37°C in a humidified atmosphere of 5% CO₂. A549 cells were maintained in RPMI 1640 (Roswell Park memorial institute, Labtech, UK) medium supplemented with 10% FBS (Gibco, UK) and 1% penicillin/streptomycin. Beas-2B cells were maintained in RPMI 1640 medium supplemented with 1% FBS (Gibco, UK) and 1% penicillin/streptomycin. These were seeded at a density of 10 million cells/flask and were sub-cultured 72 hrs for the isolation of sEVs when they reached 100% confluency. According to the specific cell line, cells were switched to 10% EV depleted FBS (Thermo Fisher, UK) before 72hrs of sEVs isolation.

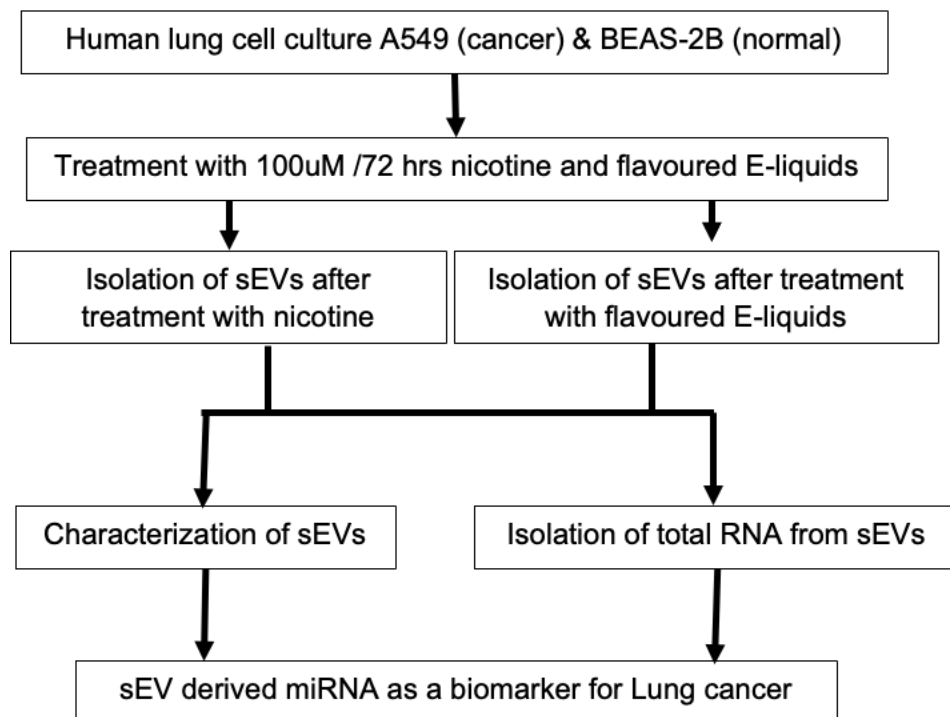


Figure 2.1: Workflow; A schematic representation of the followed in this study.

Three replicates for nicotine and strawberry flavoured E-liquid - with nicotine samples were collected. Three replicates from flavoured E-liquid (strawberry-without nicotine, apple-with nicotine and apple- without nicotine) were collected. These sets were then segregated for different downstream experiments, including characterisation and total RNA isolation for NGS and miRNA expression profiling. The workflow is mentioned in **Figure 2.1** which shows the work plan of this study.

2.2 Treatment with Nicotine, Cigarette smoke extract (CSE) and E-liquid

For the treatment plan with nicotine, CSE and E-liquid, as mentioned earlier, **Figure 2.2** shows that cells were maintained for 72 hrs along with no treatment/ control flask.

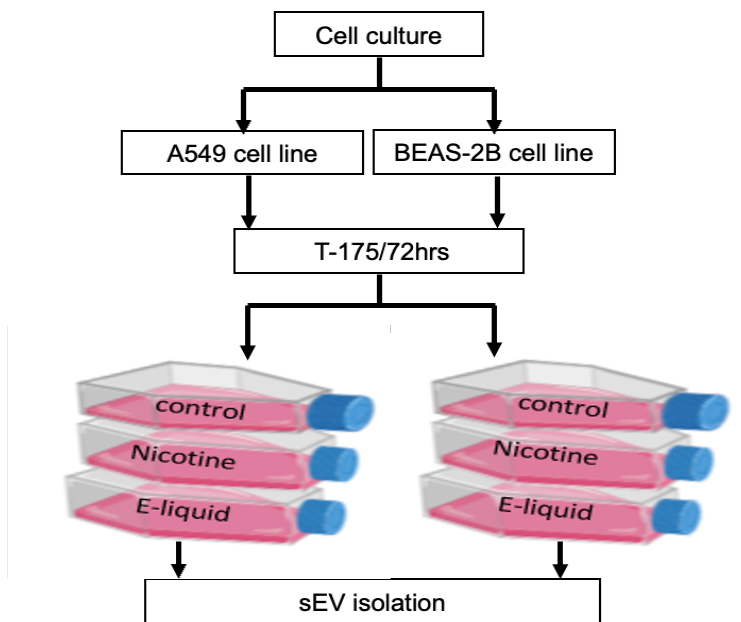


Figure 2.2: Experimental plan: Schematic representation of Cell culture required for sEV characterisation, which includes both A549 and Beas-2B cells in T-175 flasks for 72 hrs with and without (control) treatment for sEV isolation.

At the end of 72 hrs of treatment, the conditioned media was collected and processed for isolation of sEVs. As mentioned earlier, replicates from each cell line, both with and without treatment samples, were used to isolate sEVs for different downstream experiments.

2.2.1 Nicotine treatment of lung cells

Nicotine was purchased from Sigma-Aldrich (Cat no-SML 1236-50MG) and dissolved in plain RPMI media. An average cigarette contains about 10-12mg of nicotine and one can inhale about 1.1 to 1.8 mg on nicotine at the end of each cigarette. When these values are converted into molarity would be 2.3 mM to 3.8 mM. The stock solution was made with a concentration of 2 mM/ ml.

Next, the subsequent dilutions were prepared using the stock solution ranging from 1 mM to 1 μ M concentration. These dilutions were 1 mM, 500 μ M, 100 μ M, 10 μ M, and 1 μ M.

2.2.2 Cigarette smoke treatment of lung cells

3R4F cigarettes, a filtered reference cigarette with a cigarette length of 84mm and a tobacco rod length of 57 mm, were purchased from The University of Kentucky Research and Development centre (University of Kentucky. *3R4F Preliminary Analysis*. <https://ctrp.uky.edu/assets/pdf/webdocs/3R4F%20Preliminary%20Analysis.pdf> . Accessed January 27, 2016). This cigarette has a known nicotine yield of 0.726 mg/cig, mentioned in the MSDS of 3R4F included in the supplementary files.

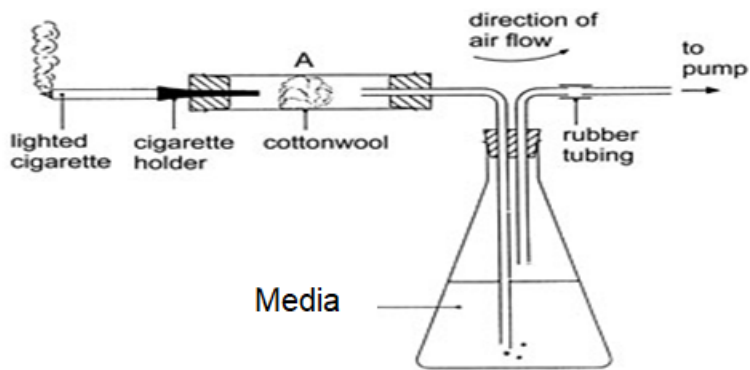


Figure 2.3: Preparation of cigarette smoke extract: A vacuum pump (right) is connected to the flask with media via a rubber tube. On the other side is the cigarette holder (left), where the cigarette fits in and is connected to the flask.

Each cigarette was burnt to a standard length of 1 cm/ 5ml into plain RPMI 1640 media (25ml stock) to get a stock solution of 100% cigarette smoke extract (100% CSE). This was generated using a suction pump with a 10 min/ ml speed, as shown in **Figure 2.3** . After collection, the pH of the CSE media was adjusted to 7.2 - 7.4 using a pH meter. Later, the CSE media was filtered through a 0.22 μM filter. Finally, FBS and penicillin/streptomycin were added to the filtered stock media.

- The calculation for nicotine content in CSE:

The nicotine yield per cigarette was 0.726 mg/cig per the reference cigarette MSDS. This value was used to calculate the concentration equivalent to the commercial nicotine. This was calculated as **157 μM** , which was considered 100% CSE.

Next, considering 100% CSE at 157 μM concentration in 5 ml volume, further dilutions were made by diluting the stock using plain media ranging from 10% to 80% of CSE, as shown in **Table 2.1**.

Table 2.1: Represents the preparation of 2-fold dilutions series using 100% CSE stock solution.

% of CSE	Stock solution needed	Diluent needed	Final conc. of CSE
100% CSE	5ml of 100% CSE	-	157 μM
80% CSE	4 ml of 100% CSE	1ml of plain RPMI media	126.6 μM
60% CSE	3 ml of 100% CSE	2ml of plain RPMI media	94.2 μM
40% CSE	2 ml of 100% CSE	3ml of plain RPMI media	62.8 μM
20% CSE	1 ml of 100% CSE	4ml of plain RPMI media	31.4 μM
10% CSE	500 μ l of 100% CSE	1ml of plain RPMI media	15.7 μM

2.2.3 E-liquid treatment of lung cells

Commercially available flavoured E-liquids were purchased for this study with the brand name; Jucee (<https://vape-jucee.com/product-detail/strawberry-10ml-e-liquid>). These include strawberry, apple and watermelon flavours, with nicotine - 18 mg/ml and without nicotine. Each of them contains vegetable glycerine (VG) and propylene glycol (PG) in a 50:50 (VG/ PG) ratio. This VG / PG is used in E-liquids as a preservative to retain the flavouring in suspension and assists in vaporisation when heated.

The concentration of E-liquid with 18 mg/ ml nicotine was calculated according to the nicotine content which was compared to the commercial nicotine and was calculated as **3.89 mM/ ml**. The same volume of the stock was used in the case of E-liquid without nicotine.

Next, considering E-liquid stock at 3.89 mM concentration in 5 ml volume, further dilutions were made by diluting the stock solution using plain media ranging from 1 mM to 1 μ M of E-liquid as shown in **Table 2.2**.

Table 2.2: Represents the preparation of different concentrations of E-liquid solution using 3.89mM of stock solution.

Different conc.	Stock volume needed	Diluent volume needed	Final conc.
1 mM	1.28 ml of 3.89 mM stock	3.72 ml of plain RPMI media	1 mM
500 μ M	2.5 ml of 1 mM stock	2.5 ml plain RPMI media	500 μM
100 μ M	1 ml of 500 μ M stock	4.0 ml plain RPMI media	100 μM
10 μ M	500 μ l of 100 μ M stock	4.5 ml plain RPMI media	100 μM
1 μ M	500 μ l of 10 μ M stock	4.5 ml plain RPMI media	1 μM

2.3 Proliferation assay with MTT (3-(4,5-dimethylthiazol-2-yl)-2,5-diphenyltetrazolium bromide, a tetrazole)

Cell viability was detected using the MTT assay (MTT(3-(4,5-dimethylthiazol-2-yl)-2,5-diphenyltetrazolium bromide, a tetrazole). Cells from both A549 and Beas-2B were seeded in triplicates in a 96-well plate with a density of 10,000 cells/ well. After 24 hrs of incubation at 37°C and 5% CO₂, cells were treated with nicotine, cigarette smoke extract, and E-liquid with six different concentrations ranging from 1 mM to 1 μ M along with the control/ untreated cells as shown in **Figure 2.4**. Cells were then incubated for 24 hrs, 48 hrs and 72 hrs at 37°C and 5% CO₂ to evaluate the proliferation of cells. The MTT assay was performed by adding 50 μ l Thiazolyl Blue Tetrazolium Bromide to the media in the well.

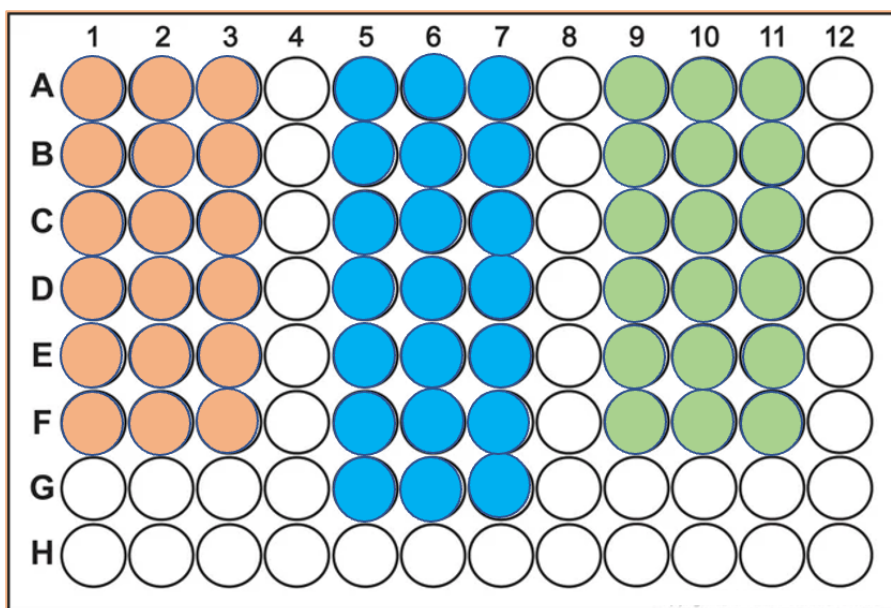


Figure 2.4: The 96-well plate design of MTT assay: Plate design: The orange panel (left) from columns 1 to 3 indicates nicotine treatment where row A was untreated, from row B to F was 2-fold concentration series from 1 mM to 1 μ M in triplicates. The blue panel (middle) from columns 5 to 7 indicates CSE treatment where row A was untreated, and from row B to G was 2-fold concentration series from 100% to 10% in triplicates. The green panel (right) from columns 9 to 11 indicates strawberry flavour E-liquid-with nicotine treatment where row A was untreated, from row B to F was decreasing order of concentrations from 1 mM to 1 μ M in triplicates. This plate was incubated for 24 hrs for proliferation assay. Similar plates were prepared for 48 hrs and 72 hrs incubation.

Following 3 hrs of incubation, the formazan crystals were dissolved by adding 200 μ l of DMSO. Next, the optical density (OD) value was measured using a microplate reader at 540 nm. The results were normalised to the value of the controls / untreated and were represented as mean \pm SD (standard deviation).

2.4 Isolation of sEVs using cultured media from treated and untreated lung cells

2.4.1 Pre-cleaning of cultured media

Isolation of sEVs from cultured media involves an initial pre-cleaning step which removes the cellular debris and aids EV enrichment. Briefly, the cultured media was

collected in a 50 ml tube, and centrifugation was performed at 1000 g for 10 minutes. Next, the supernatant was carefully transferred to a new 50 ml tube avoiding any debris collected at the bottom. Then, another round of centrifugation was carried out at 2000 g for 10 min, and the supernatant was filtered using a 0.22-micron filter and transferred to a fresh tube. Finally, the “cleaned supernatant” was prepared, which can either proceed with sEV isolation or sEV RNA isolation.

2.4.2 Isolation of sEVs using a combination of precipitation and size exclusion chromatography

The isolation and purification of sEVs were based on the principle of a combination of precipitation and size-exclusion chromatography (SEC) technique, resulting in the co-purification of sEVs. An Exo-spin sEV isolation and purification kit (Cell guidance systems, UK) was purchased for conditioned media. SEC technique works on excluding bigger-sized particles with a cut-off pore size 200 nm (nanometer) (Soares Martins et al., 2018). This kit involves four steps, and they are the following:

I. Remove cells and cell debris: As mentioned in step A.

Pre-cleaned supernatant was used for the sEVs isolation.

II. Precipitation of sEV-containing fraction

In brief, 40 ml (2X T175 flask) of the pre-cleaned supernatant was transferred to a 50 ml tube, and centrifugation was performed at 10,000 g for 48 mins. After centrifugation, the supernatant was transferred into a fresh 50 ml tube. Next, the supernatant was transferred into a new 50 ml tube and exo-spin buffer was added in a 2:1 ratio (half the volume of supernatant). Then the solution was mixed by inverting the tube and then the tube was incubated overnight at 4°C. After overnight incubation, the tube was spun at

10,000 g for 96 mins. After centrifugation, the supernatant was aspirated and discarded carefully. Finally, the pellet was resuspended using 100 µl of PBS.

III. SEC column preparation for sEV isolation

The exo-spin column was prepared before the application of the sEV containing pellet. First, the outlet plug of the column was removed, and the column was placed in a waste collection tube. Then, the preservative buffer was aspirated, and the column was equilibrated by adding 250 µl of fresh PBS. Finally, the PBS was allowed to enter the column matrix under gravity so that the preservative buffer flow-through and PBS is filled into the column. Later the flow-through was discarded.

IV. Purifications of sEV

The SEC column was placed in a waste collection tube and 100 µl of the resuspended sEV-containing pellet was applied to the column. The liquid was allowed to enter through the column matrix under gravity until it passed through the flow-through and was discarded behind. Next, the column was placed in a 1.5 ml collection tube. Next, 180 µl of PBS was added to the top of the column matrix and gets eluted. Finally, the column was spun at 100 g for 30 sec and flow-through was collected. The isolated sEVs are now ready for the downstream experiments.

To the sEVs isolates, 2 µl of proteinase inhibitor was added. These were stored at -80°C for downstream experiments and aliquots were to avoid repeat freeze and thaw.

2.2.1.1 Quantification of sEVs using BCA Protein assay

BCA protein assay kit (Thermo Scientific, UK) was used to quantify sEV protein. This technique combines the reduction of cupric ion (Cu^{+2}) to copper ion (Cu^{+1}). This reduction was detected using a highly sensitive colourimetric cuprous cation (Cu^{+1}) called

the bicinchoninic acid (BCA). The reaction results in a purple colour product due to the formation of chelation of two molecules of BCA with one cuprous ion. This complex exhibits an absorbance at 562 nm that was linear to the amount of protein concentration with a range of 20-2000 µg/ ml. The reference standard used in this assay was Bovine Serum Albumin (BSA).

A standard curve ranging from 0-2000 µg/ml was derived using nine serial dilution points with BSA. All the samples and the standards were in triplicates. The samples (25 µl) were mixed with (175 µl) working reagent and incubated at 37°C for 30 min. After incubation, absorbance for standard and samples were recorded at 562 nm.

Next, a standard curve was obtained using each of these absorbance differences, subtracted by the averaged blank absorbance, measured using a plate reader. Finally, the differences in absorbance were converted to µg/µl compared to the standard curve.

BCA assay was performed on sEV standards from A549 and samples, which include cell lysate and sEV isolates from A549, BEAS-2B with and without treatments.

2.5 Characterisation of isolated sEVs

2.5.1 Transmission electronic microscopy (TEM)

sEVs were visualized using transmission electronic microscopy (TEM). Briefly, 10µl of sEVs were pipetted onto a parafilm. A glow discharged grid was placed onto the sample and incubated at RT for 10 mins. The grid was washed twice with 100µl of PBS. Next, the grid was fixed on 1% glutaraldehyde for 5mins. After 5 mins, the grid was washed twice with 100µl of ddH₂O. Again, the grid was incubated on 1% aqueous UA for 30 – 90. Next, the grid was incubated on 4%UA/2% Methyl Cellulose (UA/MC) at a 1:9 ratio on ice for 10mins. After incubation, the grid was picked up from UA/MC using a 5

mm wire loop, and the excess solution was drained using a filter paper by dragging the loop at an angle of 45°. The grid was then left to dry for 20 mins. Imaging was performed at 120KV on an FEI Tecnai G² Spirit with Gatan RIO16 digital camera. TEM was performed on sEVs isolated from A549 and BEAS-2B cells, including untreated and treated with E-liquids sEVs.

2.5.2 Fluorescent microscopy for EV uptake experiment

sEVs were isolated from untreated A549 and BEAS-2B cells using size exclusion chromatography (SEC). 10mM concentration of sytoRNA dye was prepared as per the manufacturer's instruction. This dye was used to resuspend isolated sEVs where high concentration was with 5mM stained sEVs and low concentration was with 0.5mM stained sEVs. The experimental template is shown in **Figure 2.5**.

Further, on day 1, A549 and BEAS-2B cells were seeded in the 8-chambered plate at 80,000 cells/well and left for 24hrs. Then on day 2, cells were treated with labelled sEVs and incubated for the next 24 hrs. On day 3 the supernatant was removed and washed with PBS. Later, the plate was used to capture images for uptake of sEVs under fluorescent confocal microscopy and analysed using image J software.

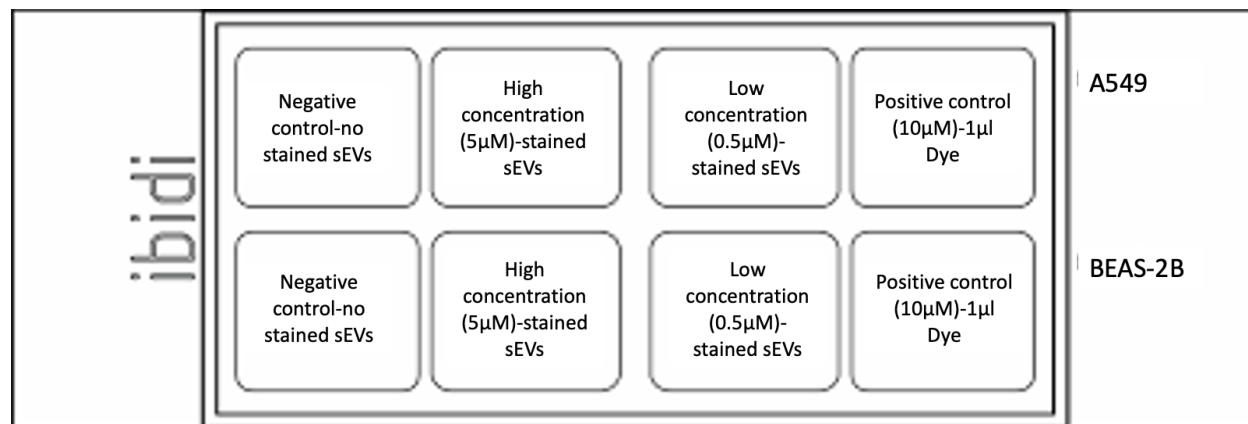


Figure 2.5: Template used for uptake of sEVs using Florescent microscopy: Different concentrations of stained sEV and controls were included in the experimental plan.

2.5.3 Western Blot

I. SDS-PAGE and Transfer

- Preparation of Hand-cast gel

The 1.5 mm glass plates (Bio-rad, UK) were assembled, and the resolving gel was made as follows.

i. Resolving Gel

Table 2.3: Contents of resolving gels(i) and stacking gels (ii). Samples were resuspended in LDS sample buffer (lithium dodecyl sulfate) and denatured by heating at 70°C for 10 minutes. Then, electrophoresis was carried out in a Bio-Rad mini-protean II equipment using an SDS-PAGE running buffer. The run was for approximately 2 hrs at 90 Volts or until the dye reached the bottom of the gel.

Resolving Gel	12% (10ml)
ddH2O	3.3 ml
Acrylamide 30%	4.00 ml
Tris-HCL [1.5M] p ^H 8.8	2.34 ml
SDS [10%]	100 µl
APS [10%]	100 µl
TEMED	4 µl

Once the resolving gel gets solidified, stacking gel was poured on the top of resolving gel in the glass plates.

ii. Stacking gel

Stacking Gel	4 ml
ddH2O	2.7 ml
Acrylamide 30%	670 ml
Tris-HCL [1.5M] p ^H 6.8	500 ml
SDS [10%]	40 µl
APS [10%]	40 µl
TEMED	4 µl

- Sample preparation for SDS-PAGE - Cell lysate and sEV isolate fractions

i. Preparation of cell lysate

Both A549 and Beas-B cells (1 million) were trypsinised and centrifuged at 239 g for 5 mins and then washed twice with 100 µl of PBS. Next, cells were centrifuged, and PBS was removed. Later, 100 µl of RIPA (Sigma-Aldrich) was added to the cells for lysis, and the tube was vortexed. Next, the tube was incubated for 30 mins at 4°C. Debris was removed by centrifugation at 13000 g for 15 mins at 4°C. Finally, the supernatant was collected, called “Clarified cell lysate”, and stored at -20°C or -80°C.

ii. Preparation of sEV fraction

One aliquot of isolated sEVs from the set of replicates from each cell line, including both with and without treatment, was used to perform the experiment. About 40 µg of protein extract were prepared using sEV isolates from A549, and Beas-2b, both with and without treatment, mixed with LDS (lithium dodecyl sulphate) sample buffer (Thermo Fisher, UK) denatured at 70 °C for 10 min. Cell lysate (Amount-20 µg) from the same cell lines was used as a positive control.

Once the SDS-PAGE run was finished, the glass plates with gel were cracked open, and the gel was separated from the plates. Next, the gel was then transferred onto a membrane using a transfer tank with a transfer buffer at 0.4 Ampere for 90 minutes. This was performed at 2°C - 4°C and was covered with ice to maintain the temperature.

II. Immunoblotting

After transfer, the transfer efficiency of the membrane was determined using Ponceau Red (Sigma-Aldrich) staining for 5 mins and then the membrane was washed with distilled water at room temperature. Next, the nitrocellulose membrane was blocked

using 5% BSA (Bovine serum albumin, Sigma-Aldrich, UK) mixed in PBS containing 0.1% Tween 20. Blocking was carried out on a shaker for approximately 2 hrs at a speed of 35 rpm. Next, primary antibodies such as CD63, CD9, CD81, TSG101 and Calnexin (Fisher Scientific) were diluted in 5 mL of 2.5% BSA and PBS containing 0.1% Tween 20 in a 50 mL falcon tube. Later, the membrane was incubated overnight at 4°C in the 50 mL falcon tube which was then placed on a roller at 35 rpm speed.

III. Detection and Imaging

The membrane was washed three times using PBS containing 0.1% Tween 20/ wash buffer for 10 mins intervals. Next, approximately 1.0 µl anti-mouse secondary antibody (Cell signalling, UK) was diluted (1:5000) in 5 mL of 2.5% BSA and PBS containing 0.1% Tween 20 in a 50 mL falcon tube. The membrane was incubated in this tube for 2 hrs at room temperature on a roller with 35 rpm speed. After incubation, the membrane was rewashed three times using PBS containing 0.1% Tween 20/ wash buffer for 10 mins intervals. Finally, the protein was detected using the super signal west Fempto PLUS chemiluminescent substrate method (Thermo Fischer). This chemiluminescence technique involved mixing approximately 1 mL of enhancer/luminol solution with 1 mL of stable peroxide solution, and the membrane was incubated for 1 min. Excess fluid was then absorbed with tissue. Finally, Antibody binding was then visualised using Gbox (Syngene), and the images/ signal were captured.

2.5.4 Nanoparticle Tracking Analysis (NTA)

2.5.4.1 Mycoplasma detection

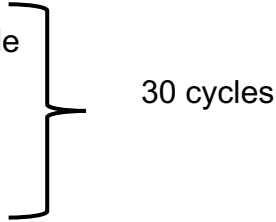
Regular check for mycoplasma is necessary. Mycoplasma infection may not only change the cellular response, but these species can also release EVs, which may interfere with the target EVs. Mycoplasma contamination can cause artefacts during NTA

analysis. Therefore, the samples were tested for mycoplasma using the Mycoplasma PCR detection kit (Applied biological materials Inc., Canada).

For this experiment sample was collected directly from the culture which were maintained atleast for 48 – 72 hrs and were 80% confluent. Next, individual components were mixed and the assesmbled reaction was placed on ice.

- 2X PCR Master mix -12.5 μ l
- Primer Mix – 1 μ l
- Test Sample, positive control , NTC (negative template control- ddH₂ O) – 2.5 μ l
- Nuclease – Free H₂ O – 25 μ l

Further, the reaction mixture was gently mixed and was spun Next, standard thermocycling PCR was performed with the following conditions:

- Enzyme Activation at 95 °C / 3 mins – 1 cycle
 - Denaturation at 95 °C / 15 secs – 1 cycle
 - Annealing at 55 °C / 15 secs
 - Extension at 72 °C / 15 secs
 - Final extension at 72 °C / 1 min – 1 cycle
 - Holding at 4 °C .
- 

After PCR, the amplified product was analyzed using agarose gel electrophoresis and the gel was visualized for amplified product. If the PCR product was ~500bp/ 370- 550 bp in length then the sample was positive for mycoplasma/ mycoplasma strains.

2.5.4.2 Nanoparticle Tracking Analysis (NTA)

Nanoparticle tracking analysis was performed using “ZetaView” (Particle Matrix, Germany). NTA technique measures the size and number of particles based on their

random movement called “Brownian motion” in a solution. Each aliquot of isolated sEVs from the set of six replicates from each cell line sample was checked for concentration and size distribution of sEVs. Briefly, samples were diluted using PBS in 1:1000 dilution factor, and then the suspension was illuminated by a laser beam. The scattered light from the particles was measured by the microscope objective lens and recorded at the video frame rates. This movement can be visualised, recorded, analyzed, or saved in real-time using ZetaView software. Raw data were collected and analysed for size distribution and concentration.

2.5.5 Fluorescent Nanoparticle tracking- with specific antibody

Fluorescent nanoparticle tracking was performed using “ZetaView- single laser” (Particle matrix, Germany). Fluorescent NTA techniques identify and differentiate EVs and sEVs based on their tetraspanins contents – CD9, CD63 and CD81. The instrument works on the principle of scanning technology and the use of a single laser at a wavelength of 520 nm with a 550 nm long-wave pass filter.

One aliquot of isolated sEVs from the set of six replicates from each cell line was used to perform the experiment. Further, sample dilution was calculated in a way that the particle count should be in the range of 150-200 particles/frame. Next, lipophilic membrane dye “Cell Mask orange” (CMO, Cat no- 10093243, Invitrogen, UK) were pre-diluted in a 1:250 ratio using PBS. Fluorescently labelled antibodies conjugated against human CD9 (PE/Dazzle™ 594 Antibody), CD81 (PE/Dazzle™ 594 Antibody) and CD63 (PE/Dazzle™ 594 Antibody) were purchased from Biolegend (BioLegend UK Ltd) and diluted in 1:2.5 ratio using PBS.

Next, the sample was prepared using 1 µl of stain mixture of CMO dye/ Fluorescent antibody to 9 µl of each of the samples and incubated in the dark for 30°C at room temperature for 1 hr. After incubation, the sample was diluted in dilution ratio to achieve 150-200 particles/frames.

Further, to evaluate the total particle count and the overall size of the stained samples were measured in scatter mode using a 520 nm filter. After that, the specific measurement for anti- tetraspanins was carried out using the “ZetaView- single laser” in fluorescence mode with standard fluorescent settings. The resulting outcome was analyzed with ZetaView software.

The sample purity was calculated according to the following relationship:

$$\text{Sample Purity} = \frac{\text{conc. fluorescence mode CMO}}{\text{conc. scatter mode}}$$

The ratios of CD9, CD81 and CD63 positive EVs were calculated with the following formulas:

$$\% \text{ CD9 positive} = \frac{\text{conc. fluorescence 520 nm}}{\text{conc. scatter mode}} * 100\%$$

$$\% \text{ CD81 positive} = \frac{\text{conc. fluorescence 520nm}}{\text{conc. scatter mode}} * 100\%$$

$$\% \text{ CD63 positive} = \frac{\text{conc. fluorescence 520 nm}}{\text{conc. scatter mode}} * 100\%$$

2.6 RNA isolation and RT-PCR

2.6.1 RNA Isolation

2.6.1.1 Endogenous RNA Isolation from cultured cells

The endogenous RNA was isolated from the cultured cells using a combination of phenol-chloroform based method and Trizol lysis buffer (Thermo Scientific, UK). In this study, we used 1 million cells for the isolation of total RNA. The cells were washed with PBS, and the tube was placed on ice. Cells were pelleted down, and 500 µl of lysis solution was added to the tube and briefly vortexed. Next, a 50 µl miRNA homogenate additive was added to the lysate and mixed by inverting the tube several times. Further, the tube was left on ice for 10 mins.

Next, 500 µl of Phenol-chloroform was added and vortexed for 30-60 sec. After vortex, centrifugation was performed at 10,000 g for 5 mins at room temperature. After centrifugation, the upper aqueous layer was carefully separated, and 1.25 volume of 100% ethanol was added. Later, 700 µl aqueous layer/ ethanol was pipetted into the filter cartridge, and centrifugation was performed at 10,000 g for 15 sec each time until the aqueous layer/ethanol was passed through the filter. Each time the flow-through was discarded. Next, 700 µl of miRNA wash solution I was added to the filter, and centrifugation was performed for 5-10 sec, and the flow-through was discarded. After centrifugation, 500 µl of wash solution 2/3 was added to the filter, and centrifugation was performed for 5-10sec. The flow-through was discarded. Next, the filter was placed into a new collection tube, and 100 µl of pre-heated (95°C) nuclease-free water was added at the centre of the filter. The tube was spun at maximum speed for 20-30 sec to recover RNA.

Isolated total RNA was quantified for miRNA as mentioned and stored at -20°C for downstream processes.

2.6.1.2 sEV RNA Isolation from cultured media

The isolation of sEV RNA includes cultured media from 2 x T175 flask with and without treatment. The initial step involves pre-cleaning the cultured media. Briefly, the isolation of RNA from sEV was performed using a combination of two principles as mentioned in the below section:

i. sEV Purification

In the first step, sEVs were isolated from both the cell lines - A549 and Beas-2B, which includes with and without treatment conditions. Then, cultured media was collected, and the pre-cleaning step was performed. Next, we used a combination of precipitation and SEC based kit – “Exo-spin columns” for sEV isolation. In the end, 200 µl sEVs were eluted in a tube. Further, to isolate RNA from sEV, the tube with sEVs was pretreated with proteinase K and RNase A. This step was performed to eliminate the residual protein and RNA outside the vesicles / sEVs.

ii. Proteinase K and RNase A Treatment on sEV isolates

Firstly, 50 µl of sEVs was collected in an eppendorf. Then to the eppendorf, 1 µl of Proteinase K (20 µg/ mL) was added by pipetting up and down. The mixture was then incubated at 37°C for 30 mins. Next to this tube, 0.5 µl of a protease inhibitor (Halt 100X) was added and was incubated on ice for 10 mins. Later, 1 µl of RNase A was added to the tube and incubated at 37°C for 30 mins. After this incubation, 700µl of Trizol/ QIAzol (Qiagen) was added immediately to stop the RNase A action, and the tube was vortexed. Later the tube was left for 20 mins on the bench.

iii. RNA isolation from sEV

In the second step, the RNeasy MinElute spin column was used to recover EV RNA. This method is based on a combination of trizol-based lysis and silica-membrane-based total RNA purification.

The tube with lysate at the end of section ii was collected and incubated at room temperature for 5 mins. After incubation, 90 μ l of chloroform was added to the tube, and the tube vigorously shaken for 5 secs. Next, the tube was incubated for 2 - 3 mins at room temperature, and centrifugation was performed at 12,000 g at 4°C. After centrifugation, the upper aqueous layer was carefully transferred to a new tube, and 2 volumes of 100% ethanol were added by pipetting. Next, the 700 μ l of the aqueous layer/ethanol was pipetted into the RNeasy MinElute spin column, and centrifugation was performed at 8000 g for 15 secs at room temperature. The flow-through was discarded, the left-over aqueous layer/ethanol was added to the spin column, and the centrifugation step was repeated. Next, 700 μ l of RWT buffer was added to the spin column, and centrifugation was performed at 8000 g for 15 sec at room temperature. Flow-through was discarded, 500 μ l of RPE buffer was added to the spin column, and centrifugation was performed at 8000 g for 15 secs at room temperature. Flow-through was discarded, and the RNeasy MinElute spin column was placed in a new collection tube. The column with an open lid was spun at full speed to dry the membrane, and the flow-through was discarded. RNeasy MinElute spin column was placed in a new collection tube, and 14 μ l of RNase-free water was added to the centre of the tube. Centrifugation was performed at full speed for 1min to elute total RNA.

Isolated total RNA was quantified for miRNA and stored for downstream processes.

2.6.2 RNA quantification; SYBR Green-based light emission

Quantification of miRNA was performed based on the principle of light emitted by SYBR green. The quantification of miRNA was performed using a Qubit assay (Thermo Fisher Scientific, UK). The protocol involves the preparation of master mix which includes a buffer (200X concentrate of DMSO) and light-sensitive fluorescent dye (SYBR green).

The master mix calculation should include two standards plus the number of samples to be tested. Standard 1 has a 0 ng/ μ l concentration, and standard 2 has a 10 ng/ μ l of concentration. Briefly, standard tubes one and two were added with 190 μ l of master mix/ fluorescent dye with 10 μ l of standard one and standard two solutions, respectively in each tube. Further, sample tubes were added with 198 μ l of master mix/ fluorescent dye with 2 μ l of each sample. The final volume in each tube was made to 200 μ l. Then, all the tubes were vortexed for 30 sec and incubated at room temperature for 2 min. Finally, the reading was measured using Fluorometer 3.0.

Isolated RNA from the cells and cultured media were stored at -80°C in RNase-free water for downstream processes. Once the RNA samples get converted to cDNA, they were stored at -20°C.

2.6.2.1 Primer Designing:

The primers were designed as per project needs. The miRNA primers were typically 19-24 nucleotides in size. The entire mature miRNA was used as a forward primer. The sequence was obtained using the site <http://www.mirbase.org/> as shown in **Figure 2.6**.

The list of miRNAs with their primer sequence are included in the appendices (page-183).

Mature sequence hsa-miR-134-5p	
Accession	MIMAT0000447
Sequence	8 - ugugacugguugaccagagggg - 29 Get sequence
Deep sequencing	54980 reads, 129 experiments
Evidence	experimental; cloned [2-4], Illumina [5]
Database links	RNAcentral: URS0000272A92_9606
Predicted targets	TargetScanVert: hsa-miR-134-5p miRDB: hsa-miR-134-5p microrna.org: hsa-miR-134-5p

Figure 2.6: miRbase: The screenshot taken from the miRbase website represents the sequence of miR-134-5p of Homo sapiens.

2.6.3 Reverse Transcription

2.6.3.1 Amount of RNA for cDNA

In this study, a starting amount of 3 ng total RNA was converted to cDNA for sEV derived RNA, whereas a starting amount of 50 ng of total RNA was converted to cDNA for endogenous RNA. Additionally, to this amount of total RNA, 1.5 µl of spike-in Cel-miR-39 was added as a internal control just before converting sEV derived RNA to cDNA, making up a final volume of 5 µl using RNase free water. Next, the expression levels of the spike-in were detected at the qPCR step using a Cel-miR-39 specific primer.

I. Preparation of Spike-in control

The spike-in/mimic control *C.elegans* miR-39 was purchased from Qiagen with no human homolog. It was supplied lyophilised at 10 pmol in a tube and was used as a control spike-in for sEV derived miRNA expression. The tube was reconstituted by adding 100 µl of RNase-free water, resulting in 2×10^{10} copies/ µl stock. The stock was aliquoted and stored at -80°C.

A diluted solution of stock was prepared using 4 μl of 2×10^{10} copies/ μl stock to 16 μl of RNase-free water, which resulted in 4×10^9 copies/ μl dilution. Further, for the working solution and to use the spike-in at the cDNA step, 2 μl of 4×10^9 copies/ μl was added to 48 μl of RNase-free water, which resulted in 1.6×10^8 copies/ μl . Finally, 1.5 μl (2.4×10^8 copies) of the working solution was added at the cDNA conversion step.

2.6.3.2 cDNA conversion

The total RNA was quantified using Qubit assay (specific for microRNA) and was utilised for cDNA synthesis using QuantiMir kit (System Biosciences), which comprises poly-A tailing and anchor dT adaptor. Briefly, the process includes 3-steps, namely: a) PolyA tail, b) Anneal anchor dT adaptor, and c) Synthesise cDNAs. The reaction requires 10 pg -10 μg of total RNA with 5 μl of the final volume. All these steps were carried out on the ice.

In the first step, 5 μl of total RNA was mixed with the reagents – 2 μl of 5x ployA buffer, 1 μl of 25 mM MnCl_2 , 1.5 μl of 5 mM ATP, 0.5 μl of polyA polymerase. Then, the mixture with a final volume of 10 μl in the tube was incubated for 30 min at 37°C .

In the second step, 5 μl of Oligo dT Adaptor was added to the tube. Then, the tube was heated for 5 mins at 60°C and cooled to room temperature for 2 mins.

Finally, in the third step, 4 μl of 5x RT buffer, 2 μl of dNTP mix, 1.5 μl of 0.1M DTT, 1.5 μl of RNase-free H_2O , 1 μl of reverse transcriptase were added to the tube. The tube with a final volume of the 20.5 μl mixture was incubated for 60 mins at 42°C . Next, the tube was heated for 10 mins at 95°C . Finally, converted cDNA was stored at -20°C until further use.

2.6.3.3 Real-time PCR (RT-PCR)

Primers for microRNA used in this study were obtained from Eurofins Genomics and were ordered based on the miRbase database. In addition, 2x SYBR green master mix was purchased from Bio-line. To determine the expression profile of various microRNAs included in this study were mixed with the following reagents per reaction:

Reagents	Initial concentration	Volume
SYBR Green qPCR master mix	2X	15 μ l
User-designed forward primer	10 μ M	1 μ l
Universal Reverse primer	10 μ M	0.5 μ l
Diluted QuantiMir cDNA	20X	1 μ l
RNase-free water	-	12.5 μ l
Total volume/well		30 μl

PCR amplification was performed in Rotor-Gene Q (Qiagen) thermal cyclers using

the following program:

- STEP I- 50°C for 2min.
 - STEP-II- 95°C for 10min.
 - STEP III- 95°C for 15sec
 - STEP IV- 60°C for 1min
- } 40 cycles of step III and IV.

Data was read at 60°C for 15 sec, followed by melt curve analysis. All the test samples were run in duplicates along with negative template control (NTC).

I. Real-time PCR data analysis

The relative quantification of expression profiles of microRNAs was determined using Ct values by the $2^{\Delta\Delta Ct}$ calculation method. Briefly, the amplification of target microRNA and the internal controls were monitored based on the High-resolution melting analysis (HRM). HRM characterizes intercalating SYBR Green dye, which binds to the

double-stranded PCR products. The software records the excitation/detection wavelength of SYBR green dye with the combination of dissociation/melting conditions of a double-stranded PCR product.

The resulting amplification plots were used to determine the threshold cycle (Ct) value, defined as the number of cycles taken for fluorescence intensity, using the Rotor-Q software. The Ct values were inversely proportional to the amount of transcript produced. Finally, the Ct values of target microRNAs were normalised to the internal control. Internal control used in this study were U6 for endogenous RNA and Cel-39 primer (Qiagen) for sEV derived RNA.

2.7 Next-Generation sequencing using small RNA

One aliquot of isolated sEVs from the set of replicates from, Human adenocarcinoma basal epithelial cells - A549 (cancer) and human bronchial epithelial cells Beas-2B (normal) with E-liquid and nicotine treatment along with control/without treatment in duplicates were used to perform this experiment.

sEV derived RNA were treated with proteinase K and RNase A to eliminate any residual outside these vesicles/ sEVs. This step was to ensure that the small RNA was isolated from inside the vesicles.

For library preparation, a starting amount of 6 ng of total RNA was used to prepare libraries. All the samples were prepared accordingly.

2.7.1 Library preparation

Isolated sEV RNA from all the samples was used to generate small RNA libraries using a small RNA-Seq library prep kit for Illumina (Lexogen, Austria). This kit includes two main steps, which are:

2.7.1.1 Library Generation

The first step was to heat RNA samples and 3' Adaptors to resolve secondary structures before the ligation was performed. 6 μ l (6 ng total RNA diluted with H₂O) of the RNA sample was mixed with 1 μ l of 3' Adaptors in a tube. Next, the mixture was incubated for 2 mins at 70°C in a pre-heated thermocycler. The tube was then placed on ice and spun before opening the tube. Next, master mix one containing 12 μ l ligation mix one and 1 μ l enzyme mix one was prepared. The tube was mixed well and spun down. Add 13 μ l of this master mix one to the denatured RNA and mix well. The tube was spun and incubated in a thermocycler for 1 hr at 28°C.

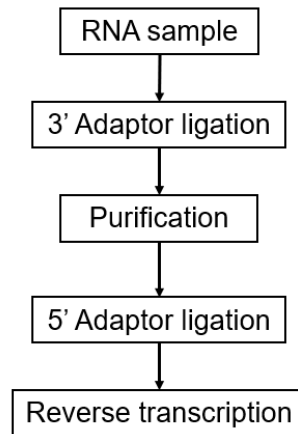


Figure 2.7: Small RNA-seq library generation workflow: Schematic representation of Small RNA-seq library generation workflow

The second step was to remove the excess 3' adaptor/ purification. The tube with 20 μ l of the ligation reaction was transferred into a 1.5 ml tube. To this tube, 300 μ l of column binding buffer was added and mix well by pipetting. Next, 50 μ l of 100% EtOH was added to the reaction and mix well. The tube was then centrifuged at 3,500 g at 18°C, and the flow-through was discarded. Next, 600 μ l of column wash buffer was applied to the column and spun for 1 min at 14,000 g at 18°C. Again, Flow-through was discarded, and the tube was spun for 2 mins at 14,000 g at 18°C to dry the column. Next, the column was transferred to a new 1.5 ml tube, and 12 μ l of elution buffer was applied. Centrifugation was carried out for 1 min at 200 g and 2 mins at 14,000 g at 18°C to elute the 3' adapter-ligated RNA. The eluate was transferred into an RNase-free PCR tube.

The third step was to ligate a 5' adapter to the RNA. Before ligation, the 5' adapter was denatured. This 1 μ l of 5' adapter was denatured for 2 mins at 70°C in a thermocycler and placed in ice. The master mix two with 1 μ l denatured 5' adapter, and 11 μ l ligation with 1 μ l of enzyme mix/reaction mix was prepared. The master mix was mixed well and

spun down. 13 μ l of master mix two was added and mixed with the eluate obtained from the second step. This reaction mixture was incubated in a thermocycler at 28°C for 1 hr.

The last step was to convert the 3' and 5' ligated RNA into cDNA using a reverse transcription primer. For cDNA conversion, 1 μ l of Reverse Transcription primer was added to the product of step three. The reaction was mixed well and spun down. The tube was incubated for 2 mins at 70°C in a pre-heated thermocycler. This tube was on ice and was spun before opening. Again, master mix three with 8 μ l first-strand cDNA synthesis mix and 1 μ l of enzyme mix/reaction mix was prepared. The master mix was mixed well and spun down. Add 9 μ l of the master mix three to each to the reaction tube and mix well. Incubate the reaction in a pre-heated thermocycler for 1 hr at 50°C. Again, the tube was spun before opening.

2.7.1.2 Library Amplification

In this step, Illumina P5 and P7 adapter sequences were added to enable Illumina sequencing. This kit includes unique Small RNA i7 Index primers (Sri7001-Sri7008), respectively. For this, master mix four with 50 μ l PCR mix, 3 μ l P5 primer and 11 μ l of PCR grade H₂O was prepared. The master mix was mixed well and spun down. Now, to the tube with ~ 33 μ l cDNA, add 64 μ l of master mix four and add 3 μ l of respective Small RNA i7 Index primer/ sample. Again, the tube was mixed well and spun down. 12-22 cycles of thermocycling was performed with the following program:

- STEP I- 98°C for 30sec.
- STEP-II-22 cycles of 98°C for 10secs.
- STEP III- 60°C for 30secs
- STEP IV- 72°C for 15secs

- Final extension at 72°C for 10 mins, hold at 10°C.

The final step was to purify these amplified libraries to remove PCR components that can interfere with the quantification and other downstream processes.

For this, the finished PCR reaction (~100 µl) was transferred into a fresh 1.5 ml tube, and 300 µl of column binding buffer was added and mixed by pipetting. Next, 50 µl of 100 µl of EtOH was added to the reaction and mixed well. This solution was transferred onto a purification column placed in a 2 ml collection tube. The tube was centrifuged at 3,500 g at 18°C, and the flow-through was discarded. Next, 600 µl of column buffer was applied to the column. This column was centrifuged for 1 min at 14,000 g at 18°C, and the flow-through was discarded. This step was repeated twice, and the flow-through was discarded. Next, centrifuge the column for 2 min at 14,000 g at 18°C to dry the column. Now, the column was transferred to a 1.5 ml tube, and 20 µl of elution buffer was applied. The tube was centrifuged for 1 min at 200 g and 2 mins at 14,000 g at 18°C To elute the library.

Finally, the Small RNA-Seq library was prepared and stored at -20°C.

2.7.1.3 Library quantification and quality control

Potential contaminants in RNA samples such as salts, metal ions and phenol may have caused a negative impact on the efficiency of the NGS protocol. Therefore, Small RNA-seq library quantification was performed as a part of quality control. This quantification includes the analysis of the concentration, size distribution, and banding pattern of the amplified products. The concentration of the RNA sample was verified using capillary electrophoresis (such as Agilent Bioanalyzer, Agilent screen tape) and the fragment length was quantified using qPCR.

I. Library Quantification for fragment length

The Small RNA-seq library was quantified for fragment length using high sensitivity screen tape system (Agilent D1000). The ladder used for the quantification has a size ranging from 35 -1000 bp.

Briefly, 2 µl of High Sensitivity D1000 sample buffer was mixed with 2 µl of High Sensitivity D1000 Ladder was prepared. Next, samples were prepared by mixing 2 µl High Sensitivity D1000 sample buffer with 2 µl of DNA sample. Spin down the tube with a ladder and samples. Samples were loaded into a 2200 tape station instrument for sample analysis.

Finally, each sample was analysed using tape station controller software, and the whole file with all the sample details, including fragment length, was saved.

II. Library Quantification for concentration

The Small RNA-seq library was quantified for concentration using the NGSBIO library quant kit (PCR biosciences, UK). This qPCR method was used to measure molecules used as templates for library amplification and cluster generation.

Before starting, briefly vortex and spin down the 2x qPCR BIO SyGreen mix, DNA standards, and 10x Illumina primers. Next, the dilution buffer was prepared by diluting 1 part of 10x dilution buffer with nine parts of water and mixed thoroughly. Then, dilution buffer was mixed to dilute the libraries by $\times 10^6$. Next, a master mix was prepared for three replicates of each standard and each library sample. The master mix was prepared by adding 10 µl of 2x qPCR BIO SyGreen mix, 2.0 µl of 10x Illumina primers, 4.0 µl of the diluted sample or DNA standard and 4.0 µl of PCR grade dH₂O. Next, qPCR was performed with the following steps as mentioned below.

- One cycle at 95°C for 1 min – Polymerase activation
- 40 cycles at 95°C for 15 secs- Denaturation
- and 45°C for 45 secs- Annealing/ extension
- Melt profile analysis

Finally, the data were analysed by creating a standard curve using the Ct values of DNA standards and the efficiency was calculated. The standards range from 2 pM to 0.2 fM, where the samples were in this range were quantified. The concentration was calculated for the diluted sample and the size adjustment.

library concentration

$$= \text{reaction concentration} \times \text{dilution factor} \times \frac{452}{\text{average fragment length}}$$

2.7.2 Cluster generation and Sequencing

Eight pM (picomolar) library was used for cluster generation in MiSeq v3 flow cell followed by sequencing on Illumina MiSeq using standard Illumina standard workflow. Four samples were loaded into each flow cell, and sequencing was performed.

2.7.2.1 Denature and Dilution of library

Library concentration was made to four nM (nano Molar) and was denatured using freshly prepared 0.2 N NaOH. After denaturation, the resulting library concentration was 20 pM. Next, the library was diluted to reach a concentration of eight pM using HT1-hybridization buffer. To the eight pM library, PhiX control library with a final concentration of 12.5 pM was added. 6µl of PhiX (1% spike-in) was added to the denatured and diluted

library. The combined mixture of library and PhiX was loaded onto the reagent cartridge. Sequencing was performed on MiSeq.

2.7.2.2 Data Analysis

Once the sequencing is finished, the data was obtained in the form of FASTQ file. Next, various quality control (QC) checks were performed on the data. This QC includes Per base N content, Mean quality score, Per sequence GC content, Sequence length distribution, sequence count and per sequence quality.

Overall, 29043632 single-end reads were sequenced using Illumina MiSeq. Raw sequencing reads quality was checked using FastQC (v0.11.9). Further, miRDeep2 (v0.1.2) package was used for 3' adaptors removal, length-based filtering (minimum 16 nucleotides). Followed by sequencing, reads alignment (bowtie1.0.0) against Human reference genome (hg19) and miRBase (v22) was performed. Differential expression analysis of miRNAs between control and treated samples was performed using edgeR (v3.36.0) with a likelihood ratio test. Visualization of differentially expressed miRNAs was performed using a Bioconductor package Enhanced Volcano¹ (v1.12.0) with a minimum threshold of log₂ fold change more than and equal to 1.

¹ Data analysis for small RNA sequencing and the volcano plots presentation was done by Mr. Asgar Hussain Ansari, IGIB Delhi.

CHAPTER 3 : Cellular response to treatment, sEV isolation and characterization

3.1 Effect of nicotine, cigarette smoke extract (CSE) and E-liquids on human lung cells

3.1.1 Introduction

This chapter includes the treatment of lung cells with nicotine, cigarette smoke and E-liquid and their effect. Further, as mentioned earlier in the methods section, after treatment, EVs were isolated and characterized from the cultured media.

3.1.2 Results

3.1.2.1 Effect of nicotine, cigarette smoke extract (CSE) and E-liquid- strawberry flavour (with nicotine) on A549 and BEAS-2B cells

Earlier, many studies have shown that other sources of nicotine, such as cigarette smoke and E-liquid, may cause toxicity at higher concentrations regardless of normal /cancer cell line (Rowell et al., 2017). One can inhale 1.1 mg to 1.8 mg of nicotine per cigarette in physiological conditions.

To evaluate the effect of nicotine, and other sources of nicotine like CSE and E-liquid on lung cells, MTT assay was performed. In the MTT assay, A549 and BEAS-2B were tested against different concentrations of nicotine, CSE and E-liquid (with nicotine) compared to the control.

Results showed a difference in the percentage of proliferating cells. After 48hrs of treatment, CSE showed the highest significant change in the proliferation of cells among the three toxicants, next was E-liquid and the least was nicotine.

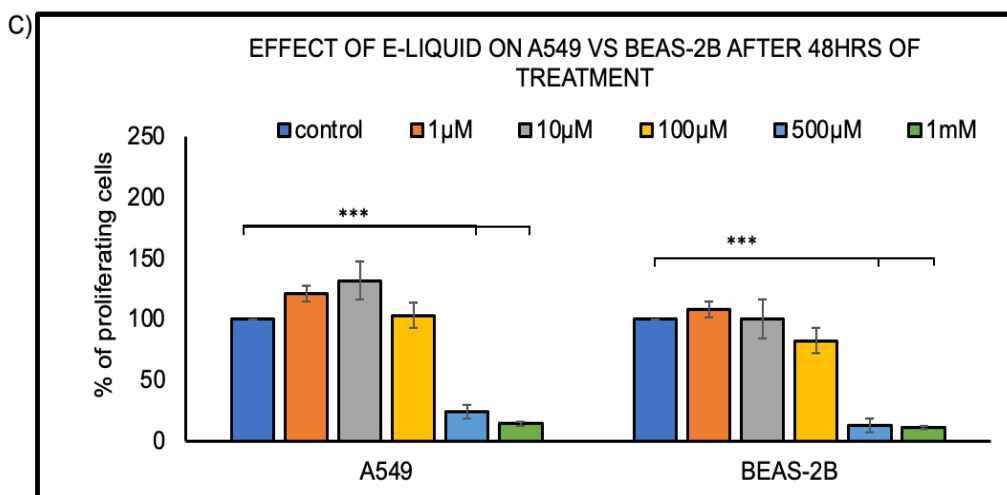
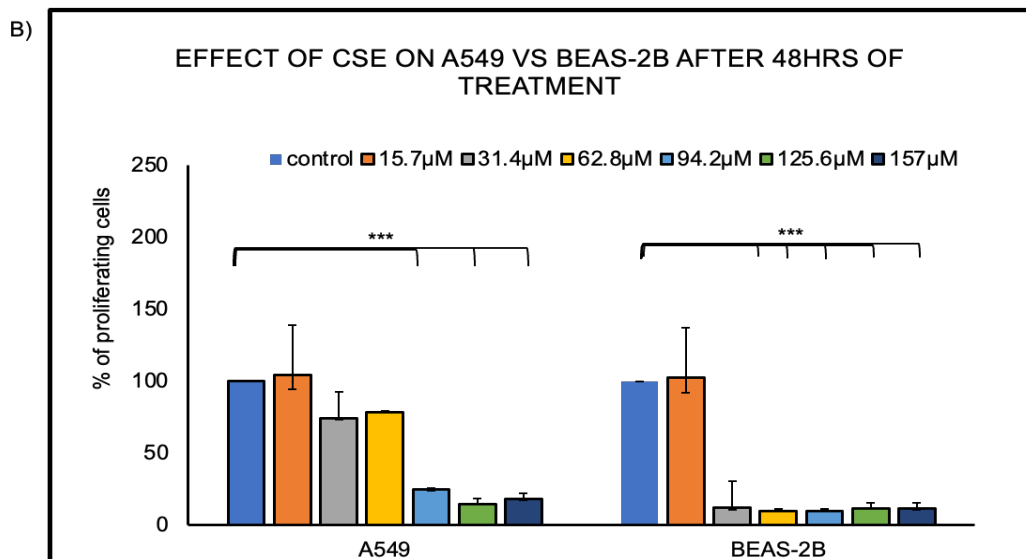
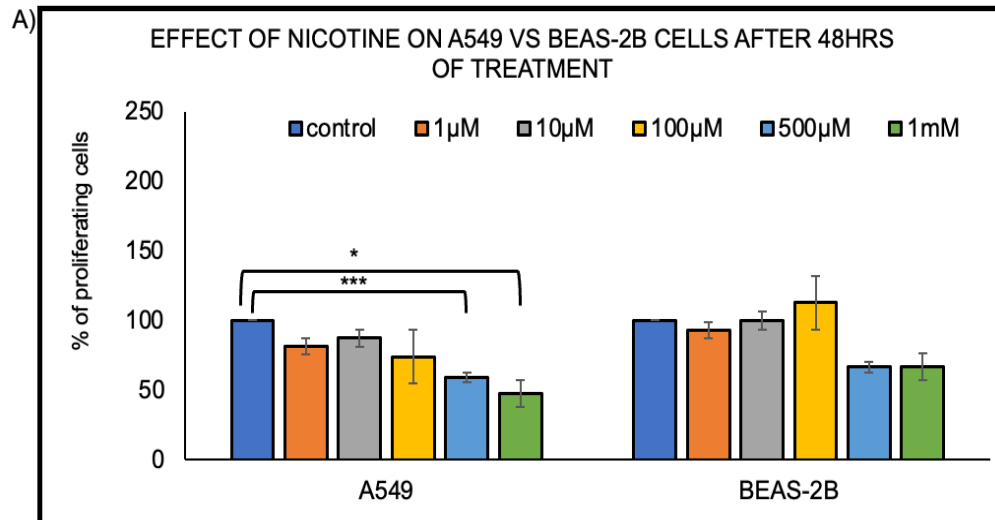


Figure 3.1: Effect of nicotine, CSE and E-liquid on A549 and BEAS-2B cell lines; Cells were treated with A) nicotine, B) CSE (percentage of CSE was converted into concentration and represented in μM units), and C) E-liquid (strawberry flavour-with nicotine) for 48hrs. Cell proliferation was determined using an MTT assay at an absorbance of 540nm. Results are expressed as a percentage of proliferating cells. Each bar represents the mean \pm SEM of technical - triplicates. Data was analysed using t-test (p-value <0.05 and $*** <0.001$ respectively).

When A549 were treated with nicotine, after 48hrs, 500 μM and 1mM concentrations showed significantly reduced of proliferating cells with a p-value <0.001 and p-value <0.05 , respectively. However, with BEAS-2B, there was no significant change in the percentage of proliferating cells, as shown in **Figure 3.1 A**).

Further, when A549 was treated with CSE, after 48 hrs, there was a decline in the percentation of proliferating cells from 62.8 μM (40% CSE) to 157 μM (100% CSE). Whereas in BEAS-2B, the decline in proliferating cells was observed from 31.4 μM (20% CSE) to 157 μM (100% CSE) with a p-value <0.001 , as shown in **Figure 3.1 B**). The results showed that BEAS-2B was much more sensitive to CSE when compared to A549.

With E-liquid (strawberry flavour-with nicotine), after 48 hrs, A549 showed a significant decrease in proliferation of cells with 500 μM and 1 mM concentrations with a $p < 0.001$. A similar outcome was observed in BEAS-2B as well, with a significant value of $p < 0.001$, as shown in **Figure 3.1 C**).

The result indicated that after 48 hrs, BEAS-2B showed altered proliferation of cells to a greater extent when compared to A549 with all the three toxicants when compared to control/ untreated.

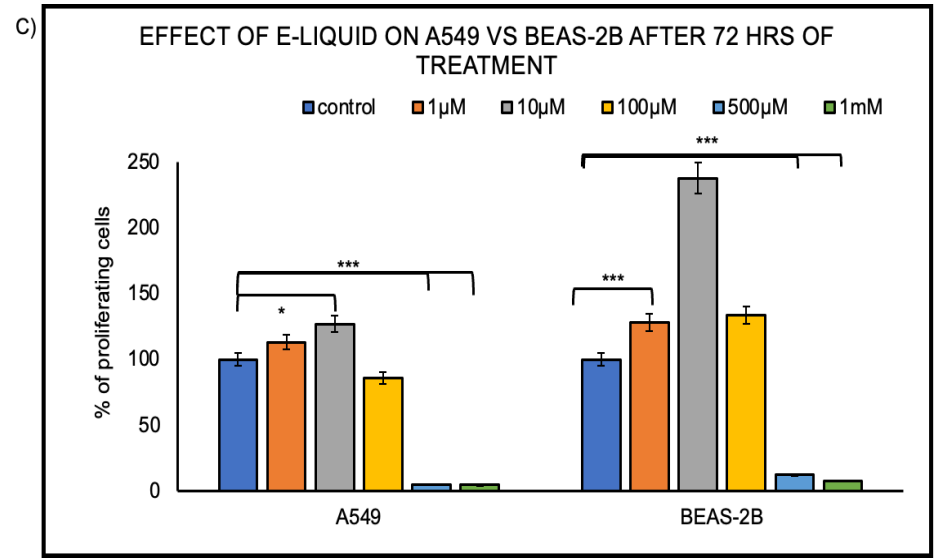
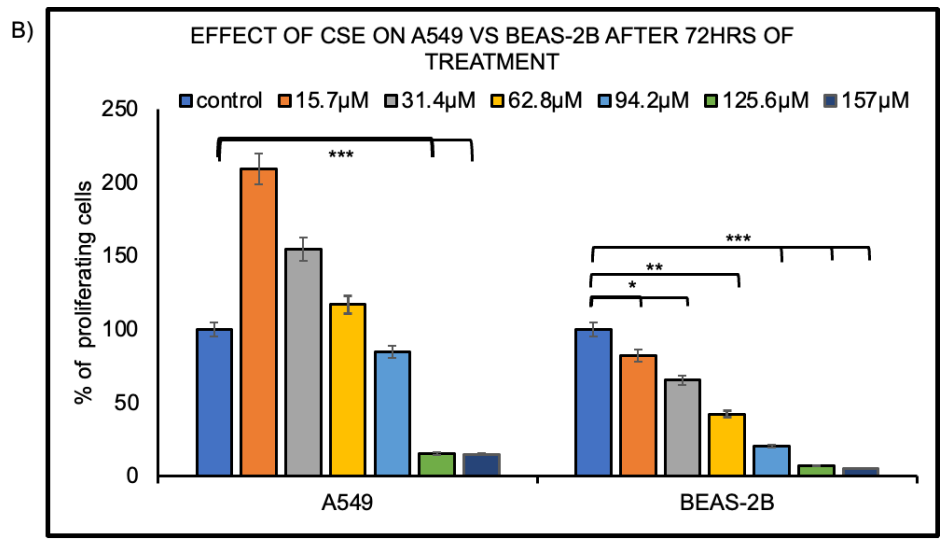
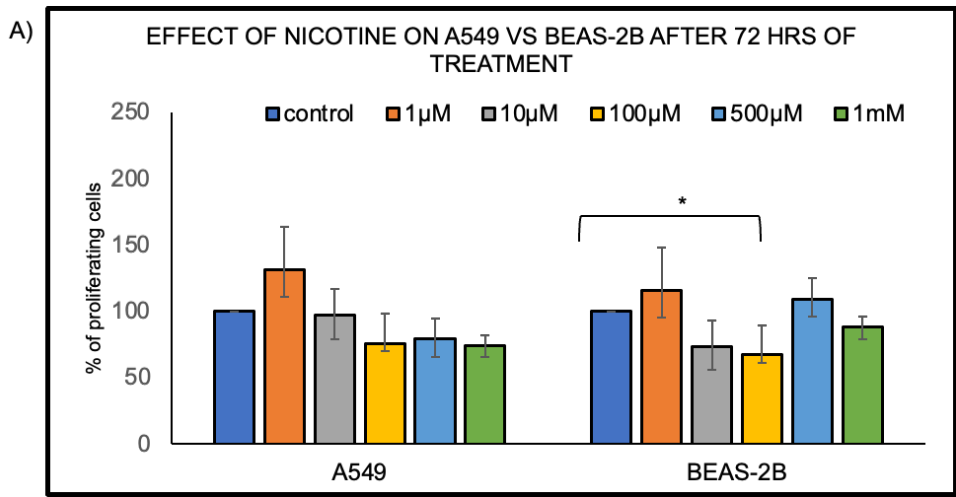


Figure 3.2: Effect of nicotine, CSE and E-liquid on A549 and BEAS-2B cell lines; Cells were treated with A) nicotine, B) CSE (percentage of CSE was converted into concentration and represented in μM units) and C) E-liquid (strawberry flavour-with nicotine) for 72 hrs. Cell proliferation was determined using an MTT assay at an absorbance of 540nm. Results are expressed as a percentage of proliferating cells. Each bar represents the mean \pm SEM of technical - triplicates. Data was analysed using t-test (p-value * <0.05 , ** <0.01 and *** <0.001 respectively).

When treated with nicotine for 72 hrs, A549 showed a change in the percentage of proliferating cells when compared to control/ untreated. In BEAS-2B, at 100 μM concentration, a significant ($p<0.05$) change in proliferating cells was observed when compared to the control, as shown in **Figure 3.2 A**).

After 72 hrs of CSE treatment on A549, there was a significant ($p<0.001$) drop in proliferating cells at 125.6 μM (60% CSE) and 157 μM (100% CSE) compared to control/ untreated. However, in BEAS-2B, a significant decline in the proliferation of cells was observed from the lowest concentration of 15.7 μM (10% CSE) up to the highest concentration of 157 μM (100 % CSE), as shown in **Figure 3.2 B**).

Further, 72 hrs of E-liquid (strawberry flavour - with nicotine) treatment indicated a significant decrease in proliferation of A549 cells at 10 μM , 500 μM and 1 mM concentrations with a significant change ($p< 0.05$ and $p<0.001$). In BEAS-2B, after 72hrs of treatment, a significant increase at 1 μM ($p<0.001$) and a significant decrease at 500 μM and 1 mM concentrations ($p<0.001$), as shown in **Figure 3.2 C**).

Overall, considering 48hrs and 72hrs treatment, the result indicates that all the three components, commercial nicotine, CSE and E-liquid (strawberry flavour - with nicotine) had effect regardless of the type of cell line.

The present study explored the possible effects of nicotine, CSE and E-liquid treatments at specific concentrations in an *in-vitro* assay. Previously, several

experimental evidence showed that cell death/apoptosis and stress could cause the release of sEVs. These reasons may interfere with the reproducibility of miRNAs as biomarkers. Since MTT results showed cell death at higher concentrations, it was necessary to isolate sEVs from actively dividing cells. Due to this reason, a precise concentration was essential where cells were stable and alive even after treatment.

Taking these results together, considering the literature (Du et al., 2018) and downstream experimental conditions, we decided to use a 100µM concentration for further experiments.

3.1.2.2 Effect of flavoured E-liquids (with and without nicotine) on BEAS-2B and A549 cells

As mentioned earlier, E-liquids can cause the condition called EVALI. There is a need to evaluate the causative factors involved in this condition. Therefore, this part of the study includes the effect of two flavoured E-liquid – Apple (with and without nicotine) and strawberry (with and without nicotine) on the A549 and BEAS-2B. Studies have shown that there has been an unknown risk with the usage of E-liquids regardless of whether it is with nicotine or without nicotine (Schweitzer et al., 2015) . The significant components in E-liquids are propylene glycol, polycyclic aromatic hydrocarbons, nitrosamines, volatile organic chemicals, glycerine, and organic chemicals apart from nicotine (Schweitzer et al., 2015)

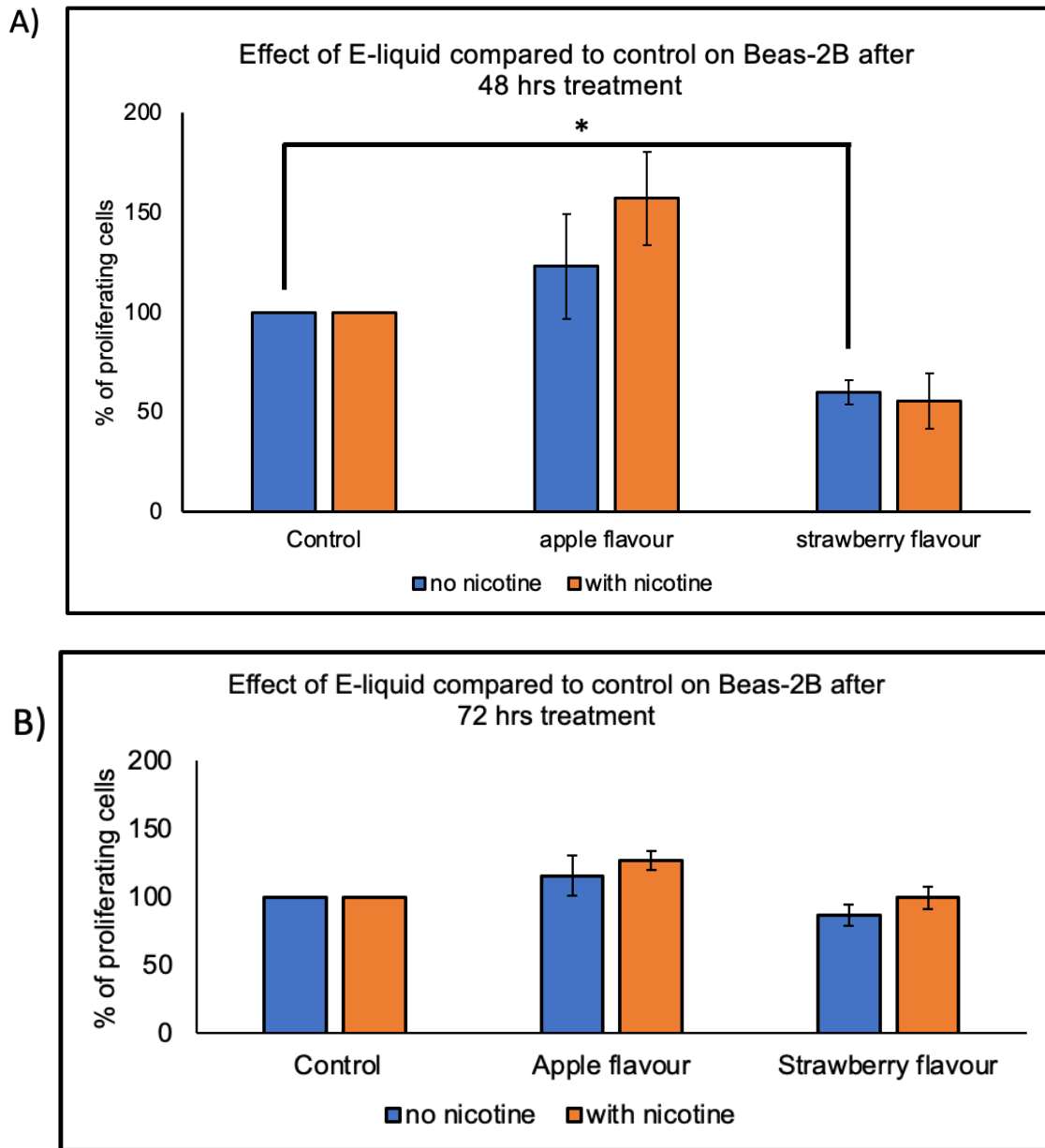


Figure 3.3: Effect of different E-liquid flavours (apple and strawberry – both with nicotine and without nicotine along with control / untreated) on BEAS-2B cell lines; Cells were exposed for A) 48 hrs and B) 72hrs with 100µM of nicotine/ without nicotine. Cell proliferation was determined using an MTT assay at an absorbance of 540nm. Results are expressed as a percentage of proliferating cells. Each bar represents the mean ± SEM of technical - triplicates. Data were analysed using a t-test (p-value <0.05).

In BEAS-2B, there was a slight increase in proliferating cells with apple flavour E-liquid (with and without nicotine) after 48 hrs and 72 hrs. But a significantly reduced proliferation of cells was observed after 48 hrs with strawberry flavour E-liquid - without nicotine upon treatment with a p-value of <math><0.05</math>. Whereas this significant change was not seen after 72 hrs of treatment with strawberry flavour E-liquid - without nicotine as shown in **Figure 3.3 A)** and **Figure 3.3 B)**.

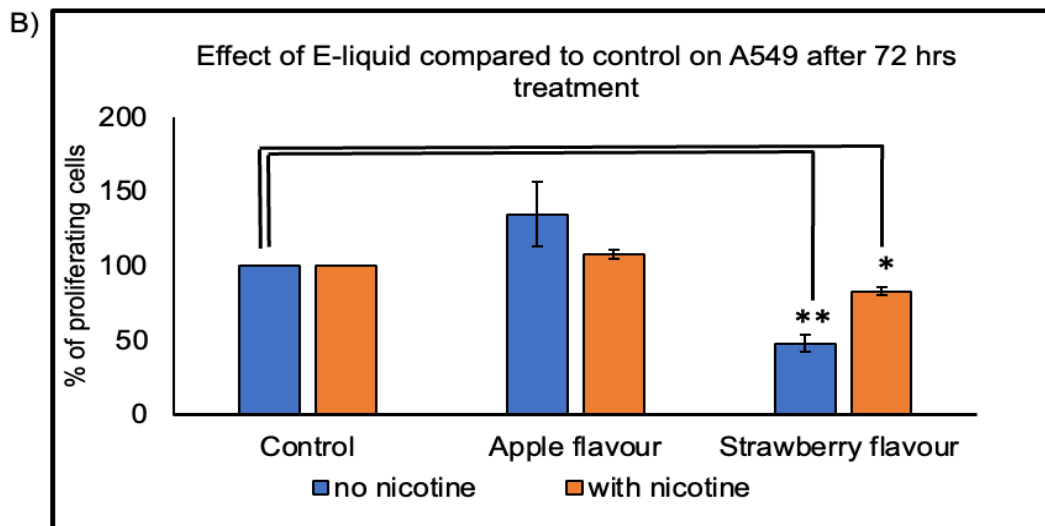
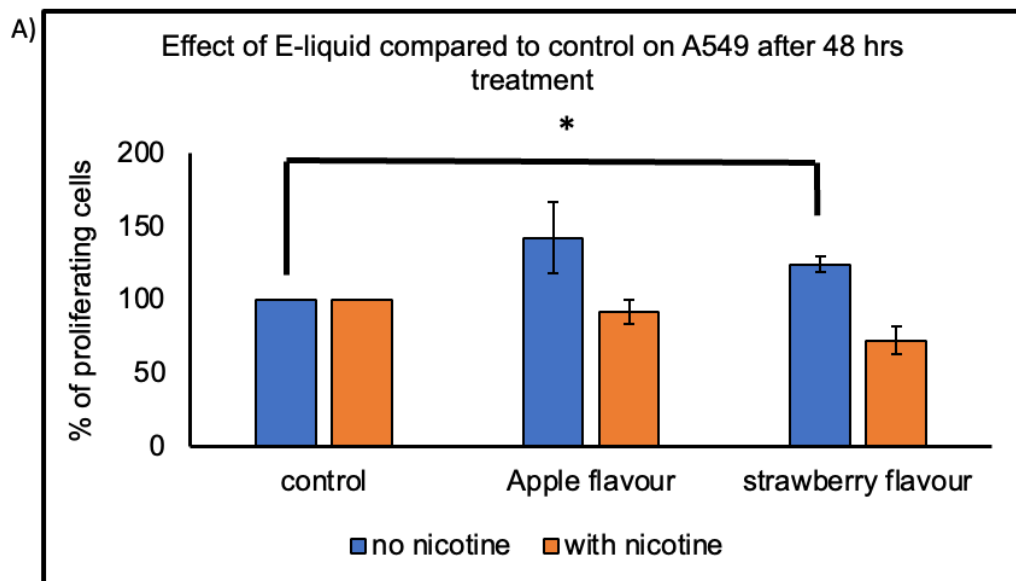


Figure 3.4: Effect of different flavours of E-liquid (apple and strawberry - nicotine/ without nicotine along with control / untreated) on A549 cell lines; Cells were exposed for A) 48 hrs and B) 72hrs with 100µM of nicotine/ without nicotine. Cell proliferation was determined using an MTT assay at an absorbance of 540nm. Results are expressed as a percentage of proliferating cells. Each bar represents the mean ± SEM of technical- triplicates. Data was analysed using T-test (p-value * <0.05 and ** <0.01).

In A549, among the two flavours, apple flavour E-liquid (with and without nicotine) showed a change in proliferating cells after 48 hrs and 72 hrs of treatment. With strawberry flavour, E-liquid (without nicotine) showed a significant change in the proliferation of cells after 48 hrs with a $p < 0.05$. This change was continued even after 72 hrs with a significant value of $p < 0.01$. Whereas strawberry flavour, E-liquid (with nicotine) showed a significant change after 72 hrs with a $p < 0.05$ compared to control as shown in **Figure 3.4 A)** and **Figure 3.4 B)**.

Another observation was that apple flavour E-liquid showed increased proliferation of cells compared to control and strawberry flavour. This was observed in both the cell lines.

Collectively, MTT assay with flavoured E-liquids – apple and strawberry flavour (nicotine and without nicotine) showed that strawberry flavour had a more substantial impact overall. Of the two strawberry flavours, E-liquid's - without nicotine led to reduced proliferation of cells, which could be due to components like propylene glycol, glycerine, and vitamin E acetate, but not just nicotine alone. These results indicated that nicotine alone is not the only risk factor, but some other causative components could have enhanced the effect resulting in reduced proliferation. At this point, it was unclear which specific component was influencing these results, and thus further investigation would be required.

Next sEVs collected from these treatment conditions were characterised by TEM, NTA and western blot.

3.2 Isolation & characterisation of sEVs

3.2.1 Transmission electronic microscopy (TEM)

The morphology and the size of isolated sEVs were visualized using TEM. The membrane integrity was maintained using SEC-based isolation of sEVs so that the spherical structure remains intact.

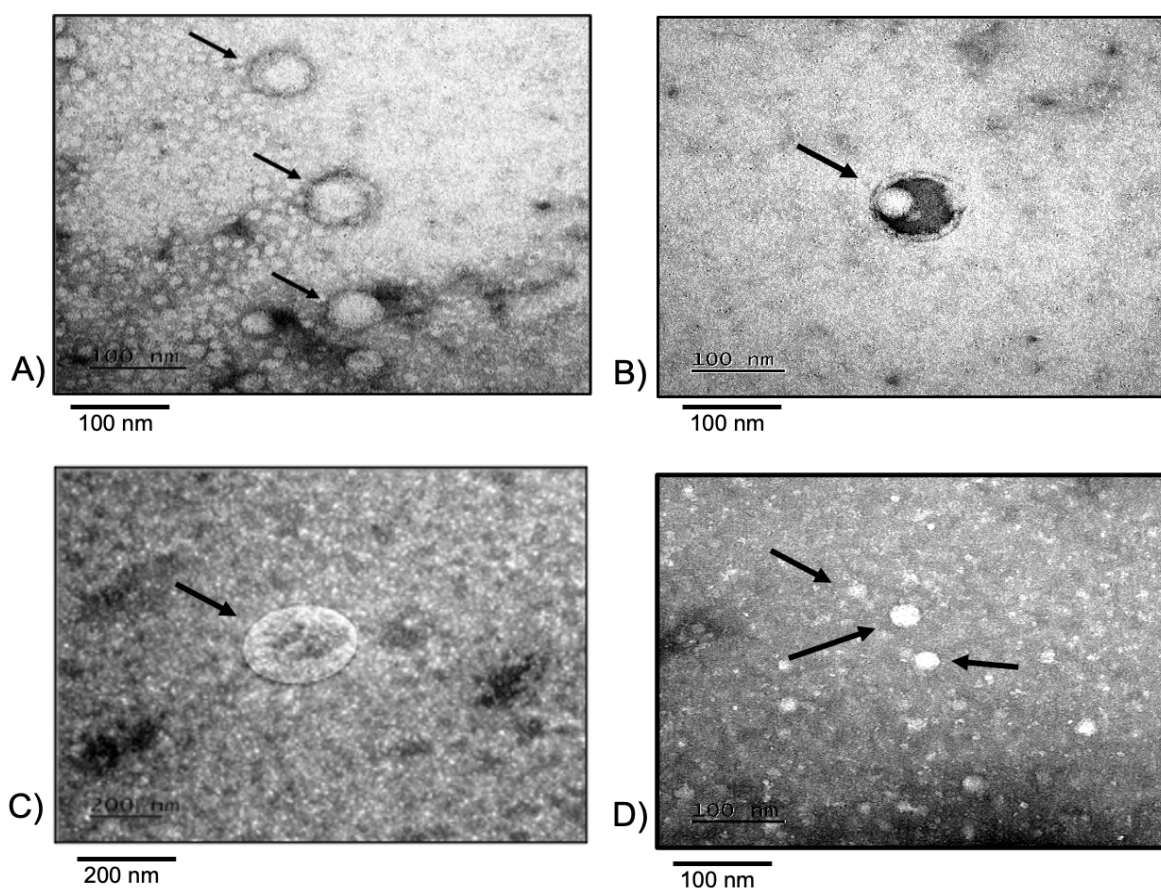


Figure 3.5: TEM images of sEVs: Representative transmission electronic microscopy (TEM) images of isolated sEVs using SEC method where A, and B were isolated from untreated A549. C, D were isolated from strawberry flavour E-liquid (with nicotine) treated A549. Membrane-bound consistent with sEVs are indicated with black arrows were within the range of 30-150nm.

Images were captured from sEVs secreted from A549 cells as shown in **Figure 3.5** and BEAS-2B cells as shown in **Figure 3.6** on both untreated and treated with E-

liquid samples. The images confirm that the particles were cup-shaped sEVs within the expected size range of 30-150nm.

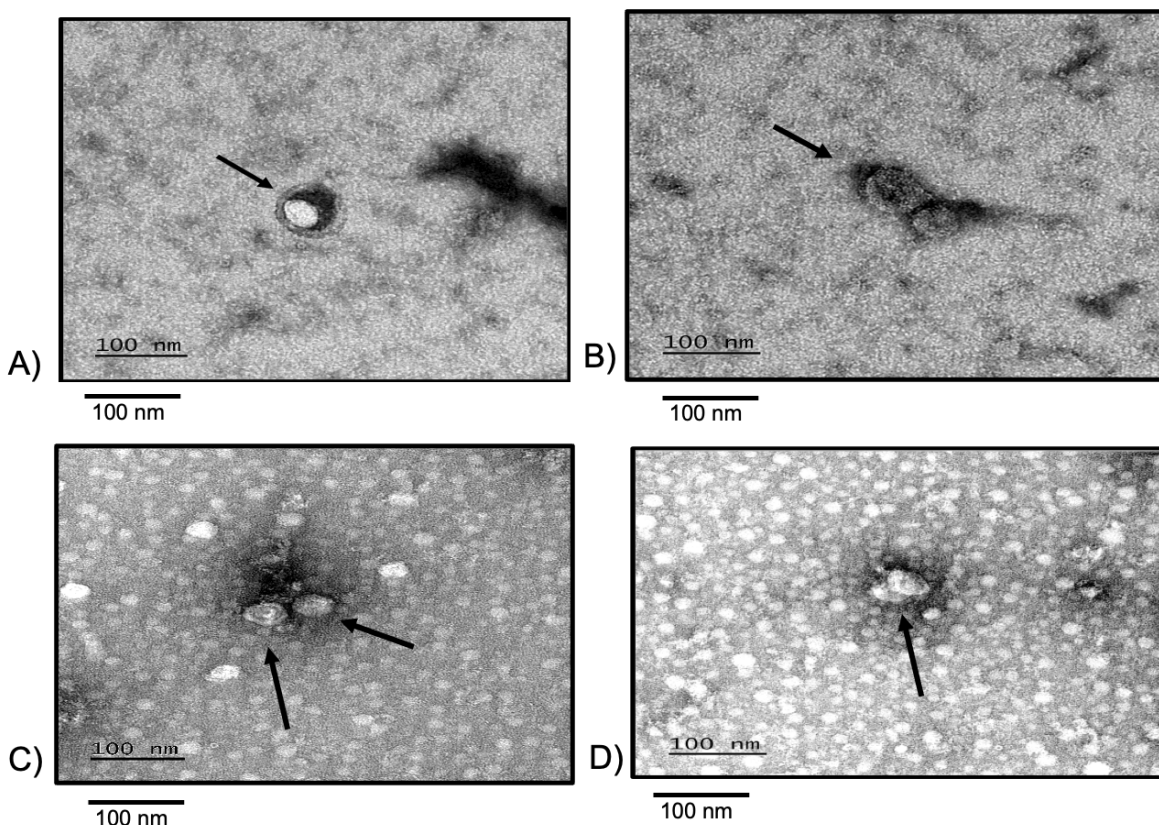


Figure 3.6: TEM images of sEVs: Representative transmission electronic microscopy (TEM) images of isolated sEVs using SEC method (scale bar-100nm) where A, B were isolated from untreated BEAS-2B and C, D were isolated strawberry flavour E-liquid (with nicotine) treated BEAS-2B. Membrane-bound consistent with sEVs are indicated with black arrows were within the range of 30-150nm.

3.2.2 Uptake experiment using fluorescent microscopy

Isolated sEVs from untreated cells from A549 and BEAS-2B were used for labelling using sytoRNA dye. Labelled sEVs were added to both the cells to verify the uptake of sEVs by human adenocarcinoma cells in culture. Fluorescently labelled sEVs were

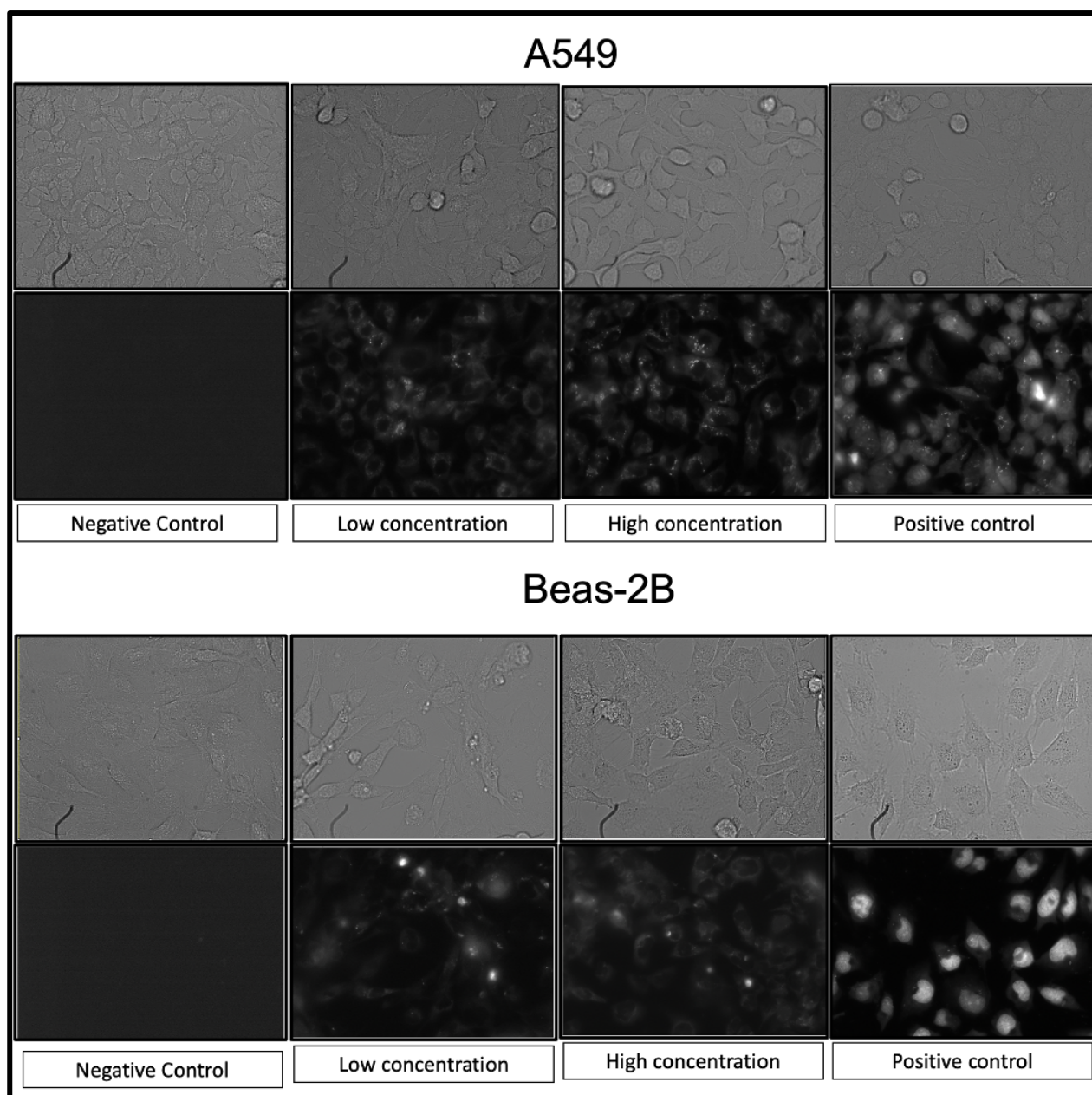


Figure 3.7: Visualization of the uptake of sEVs using fluorescence microscopy: The images are captured in bright field mode and fluorescent mode to visualize the sytoRNA stained sEVs on A549 and BEAS-2B cells with a scale bar of $20\mu\text{M}$ for all the images. The experiment includes negative control-not treated with stained sEVs, high concentration- $5\mu\text{M}$ stained sEVs, low concentration- $0.5\mu\text{M}$ stained sEVs and positive control- $1\mu\text{l}$ dye with $10\mu\text{M}$ concentration.

identified within the cells, suggesting uptake of sEVs. Live confocal microscopy images were obtained from different regions of both A549 and BEAS-2B after 24-h post-treatment with labelled sEVs which are shown in **Figure 3.7**.

As shown in **Figure 3.8**, A549 and BEAS-2B cells were positive for uptake of labelled sEVs.

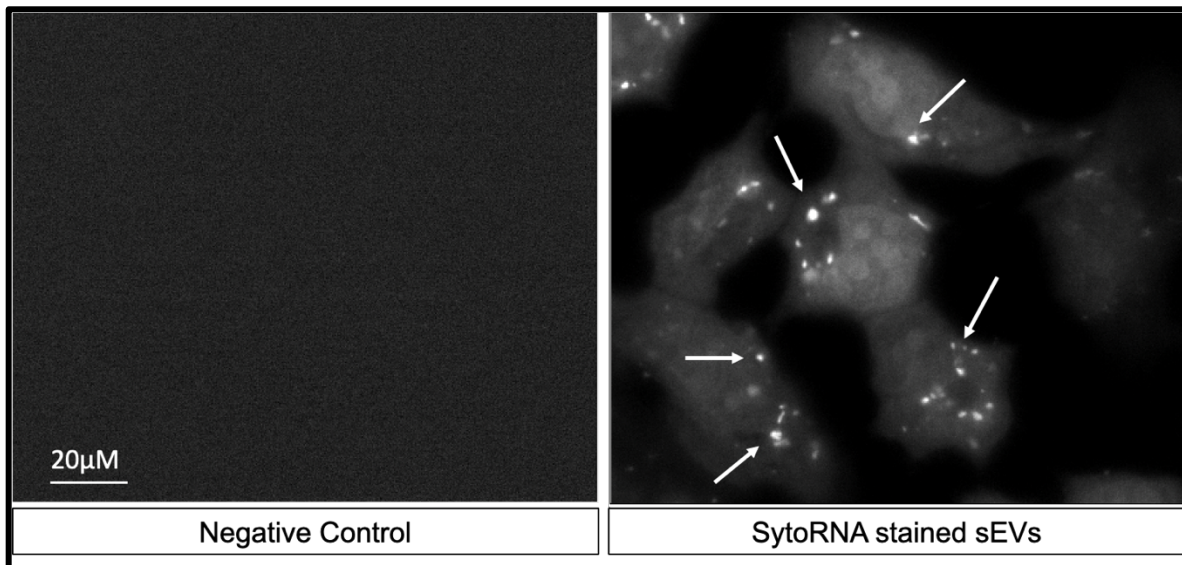


Figure 3.8: Fluorescence microscopy images: Cells show the uptake of SytoRNA-stained sEVs which were added to the cells and the image was captured after 24 hrs of incubation. On the left is the image captured from the negative control and on the right is the image captured from the well with a high concentration of SytoRNA-stained sEVs. Stained sEVs are indicated with a white arrow.

The fluorescence intensity was measured against negative control from each well with a high, low concentration of stained EVs and positive control. As shown in **Figure 3.9 A)**, A549 cells showed a significant difference in the intensity between negative control and high concentration of stained sEVs suggesting the uptake of an elevated amount of stained sEVs with $p < 0.001$.

In BEAS-2B, the fluorescence intensity between negative and low concentration was different with $p < 0.05$ and was much high when compared with positive control with a $p < 0.001$ shown in **Figure 3.9 B**).

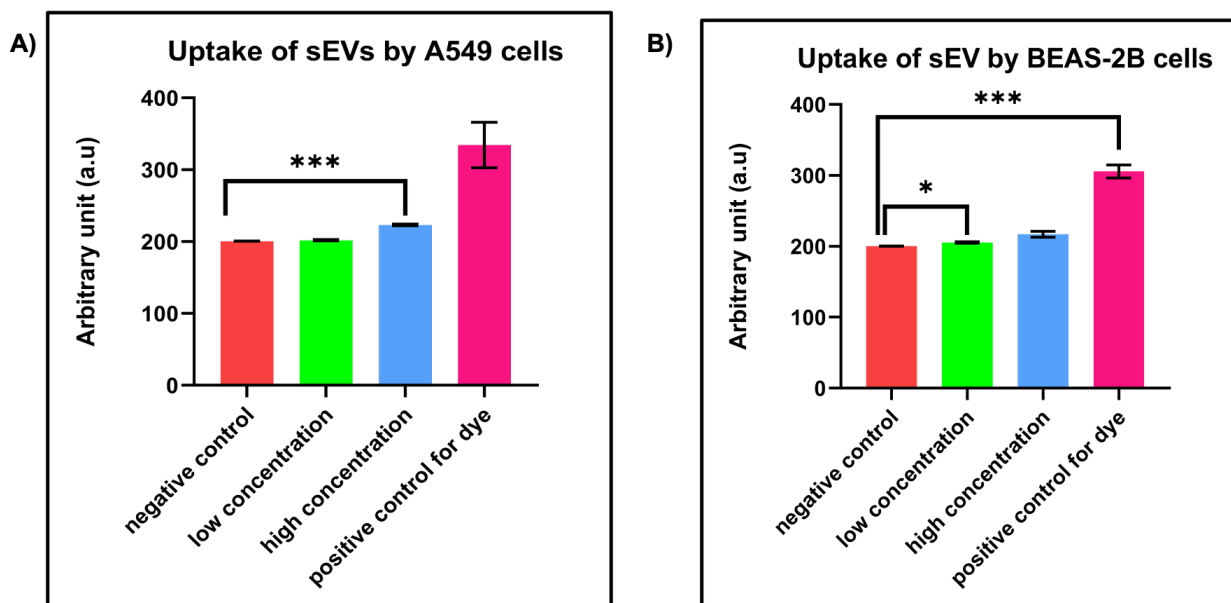


Figure 3.9: Measuring of Uptake of sEVs using fluorescence microscopy: A) A549 showed a significant difference between the fluorescence intensity of negative control and high concentration of sEV with SytoRNA. B) BEAS-2B showed a significant difference between the fluorescence intensity of negative control to low concentration of sEV with SytoRNA and positive control with SytoRNA. Each bar represents the mean \pm SD of replicates ($n=2$). The experiment includes negative control-not treated with stained sEVs, high concentration- $5 \mu\text{M}$ stained sEVs, low concentration- $0.5 \mu\text{M}$ stained sEVs and positive control- $1 \mu\text{l}$ of dye with $10 \mu\text{M}$ concentration added directly to cells. Data were analysed using an unpaired student t-test with an adjusted p-value using Holm Sidak correction method for multiple comparisons ($* < 0.05$, $*** p < 0.001$) with Graph pad prism version 9.

3.2.3 Nanoparticle tracking analysis (NTA)

Small EVs were isolated from A549 and BEAS-2B using size exclusion chromatography (SEC), and the NTA measurements were taken on the same day after isolation.

In A549, the mean concentration of the samples was, untreated sample 7.6×10^9 particles/mL, nicotine treated 1.6×10^{10} particles/mL and E-liquid treated (strawberry flavour- with nicotine) 1.18×10^{10} particles/mL, E-liquid treated (strawberry flavour - no nicotine) 2.2×10^{10} particles/mL, apple flavour E-liquid (with nicotine) treated 2.2×10^{10} particles/mL and apple flavour E-liquid (no nicotine) treated 2.6×10^{10} particles/mL was shown in **Figure 3.10**.

In A549, a significant difference was observed between nicotine treated and E-liquid treated-Apple flavour – no nicotine, when compared to untreated with a $p < 0.01$ and $p < 0.001$. And there was no significance between the other samples compared to the untreated sample.

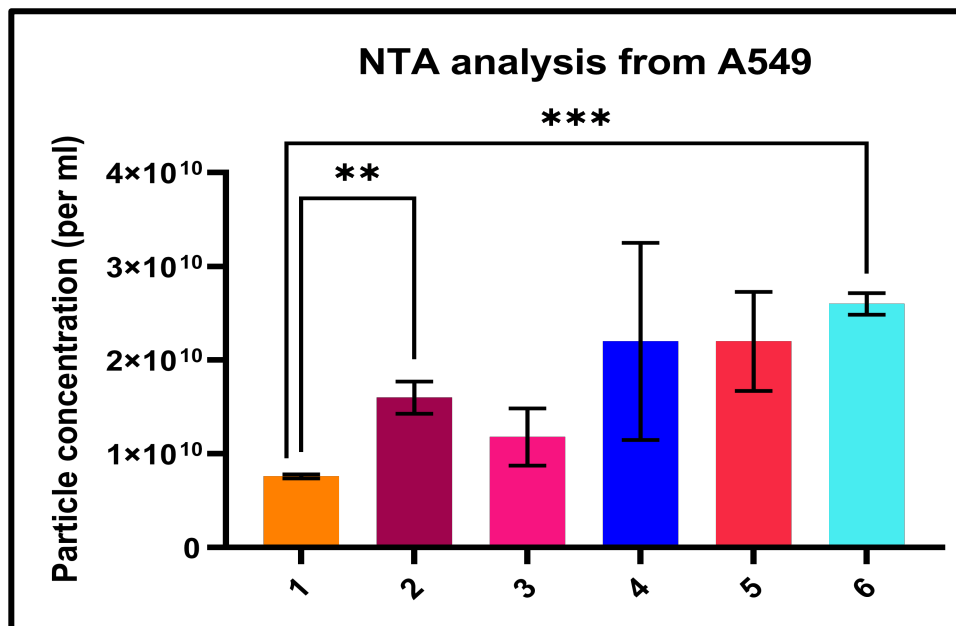


Figure 3.10: Isolation and characterisation of sEVs from A549 using NTA: Particle concentration depicted as the mean of particle concentration were estimated using Zeta view particle matrix (biological replicates, $n=3$.) These sEV samples were isolated from 1- untreated, 2- nicotine treated, 3- E-liquid treated (strawberry flavour-with nicotine), 4- strawberry flavour-no nicotine, 5- apple flavour- with nicotine and 6- apple flavour-no nicotine from A549. Results are expressed as particles/ml. Each bar represents the mean \pm SEM of three replicates using student *t*-test. All these replicates represent biological replicates. Data were analysed using Graph pad prism version 9.

In BEAS-2B, the mean concentration of the samples was, untreated sample - 6.4×10^{10} particles/mL, nicotine treated - 1.56×10^{10} particles/mL strawberry flavour E-liquid (with nicotine) treated - 1.17×10^{10} particles/mL, strawberry flavour E-liquid (no nicotine) treated - 2.95×10^{10} particles/mL, apple flavour E-liquid (with nicotine) treated - 2.6×10^{10} particles/mL and apple flavour E-liquid (no nicotine) treated - 3.5×10^{10} particles/mL measured by NTA was shown in **Figure 3.11**. There was no statistical difference between the samples when compared to the untreated sample.

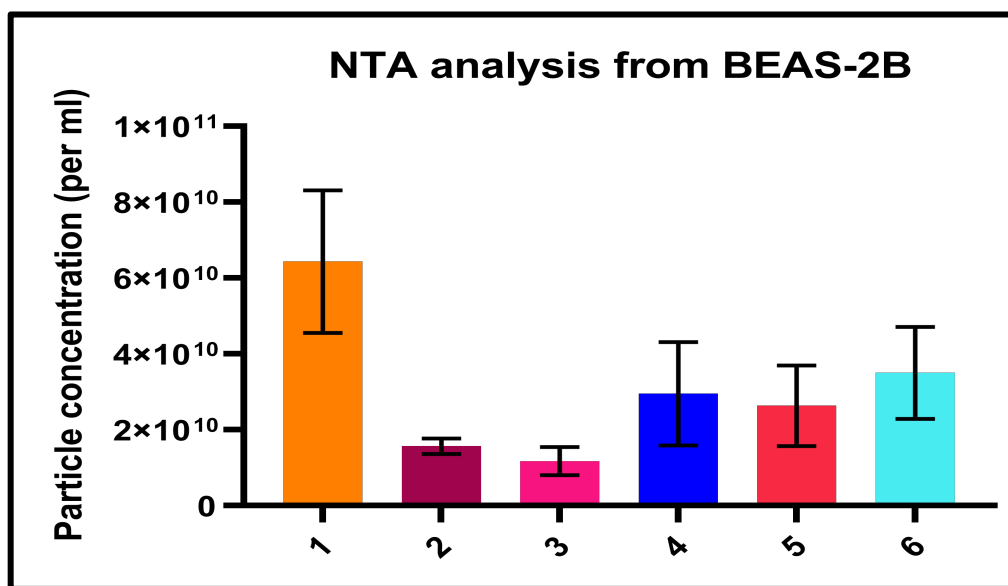


Figure 3.11: Isolation and characterisation of sEVs from BEAS-2B using NTA: Particle concentration depicted as the mean of particle concentration were taken using Zeta view particle matrix (biological replicates, $n=3$). These sEV samples were isolated from 1- untreated, 2- nicotine treated, 3- E-liquid treated (strawberry flavour-with nicotine), 4-strawberry flavour-no nicotine, 5- apple flavour- with nicotine and 6- apple flavour-no nicotine from BEAS-2B. Results are expressed as particles/ml. Each bar represents the mean \pm SEM of three replicates using student *t*-test. All these replicates represent biological replicates. Data were analysed using Graph pad prism version 9.

Across the board, all the samples showed particle size within the size range of sEVs (30-200 nm). However, larger-sized particles were also observed which are suggestive of aggregate formation.

Further, the interesting observation was that in both A549 and BEAS-2B, strawberry flavour E-liquid – with no nicotine showed the least mean particle concentration.

3.2.4 Fluorescent nanoparticle tracking analysis (f-NTA)

To estimate the proportion of sEVs from the population of total nanoparticles, f-NTA was performed using Zeta View with a single laser at 520 nm and 550 LWP (long-wave pass) filter. Following fluorescence labelling, samples were analysed in both in scatter mode and fluorescence mode. sEVs were isolated from both A549 and BEAS-2B cell lines, with treatment conditions, as described earlier.

Here, we have also investigated two different conditions which can affect the f-NTA measurement. The two conditions were i) Use of PBS as a diluent for EV samples, ii) Use of 0.5% non-ionic detergent NP – 40 to check for membrane-bound protein proportion with CMO (Cell mask orange) dye. These two conditions are considered as control experiments in the context of the use of the f-NTA technique for the characterization of sEVs.

3.2.4.1 Phosphate buffer saline (PBS) does not cause any unwanted background for EV sample measurement and analysis

To evaluate whether PBS/diluent has any background effect while analyzing the result for particle concentration of EV measurement using Zeta View, a control experiment was performed. Two factors - the particle/ frame and the concentration of CMO dye were kept constant.

The particle concentration of “PBS only” was 1.4×10^9 particles / mL, whereas PBS with CMO dye in scatter mode was 5.83×10^9 particles / mL. In the fluorescence mode, the measurement was below the detection limit (detection limit- $> 1 \times 10^6$ particles/ml).

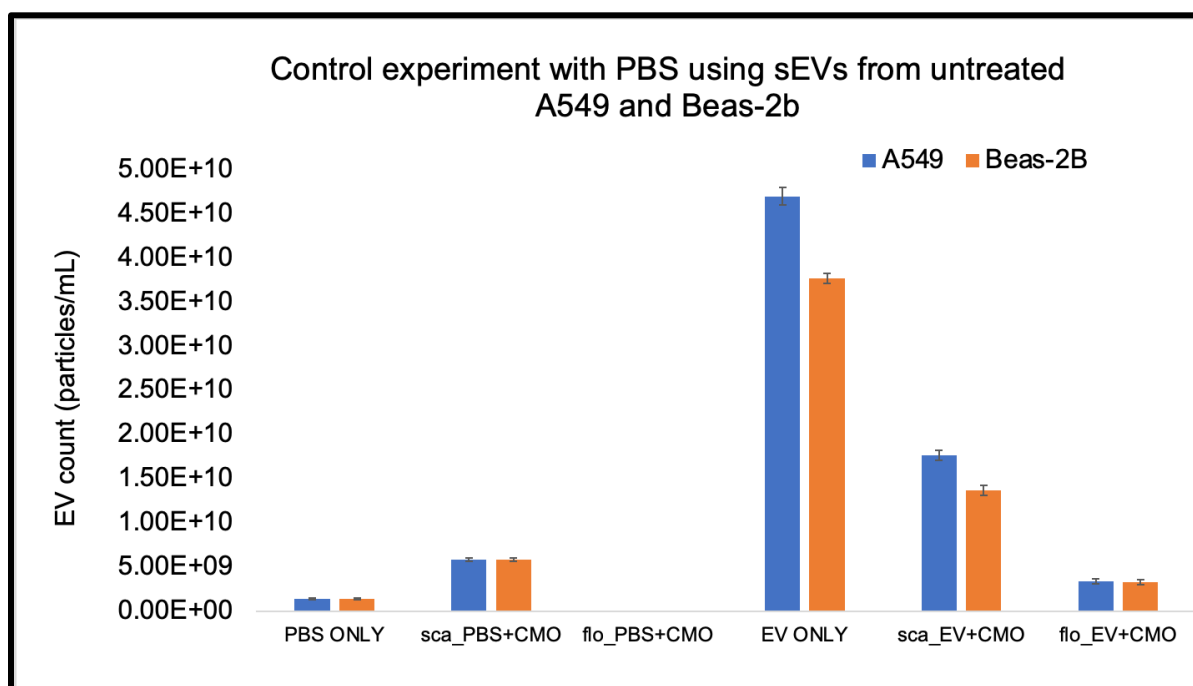


Figure 3.12: Concentration of nanoparticles in scatter and fluorescence mode when PBS only vs EV only was measured from A549 cells and BEAS-2B cells. Samples include (from left) PBS only (NTA), PBS with Cell mask orange (CMO) measured in scatter mode, PBS with Cell mask orange (CMO) measured in fluorescence mode, EV only (NTA), EV with Cell mask orange (CMO) measured in scatter mode, EV with Cell mask orange (CMO) measured in fluorescence mode. The experiment was performed on the same day with three readings, and the error bars were represented in mean \pm SEM ($n=3$).

The next sample measured was “EV only” isolated from A549 cells, and BEAS-2B cells showed NTA measurements as A549 - 4.7×10^{10} particles/ mL and BEAS-2B - 3.77×10^{10} particles /mL.

The next sample “EV with CMO”, in scatter mode measured A549 - 1.77×10^{10} particles /mL and BEAS-2B - 1.37×10^{10} particle/ mL, whereas in fluorescent mode, the measurements were A549 - 3.4×10^{10} particles/ mL and BEAS-2B - 3.27×10^{10} particles /mL.

As shown in **Figure 3.12**, sEV samples from both the cell lines showed similar outcomes suggestive of no background deviation due to the use of PBS in measuring the true EV concentration during sample preparation and measurement.

3.2.4.2 f- NTA captures the true EVs which has tetraspanin surface markers and disruption of EVs with NP- 40 detergent will results in null reading

To confirm that the markers detected were surrounded by the lipid membrane, EVs were treated with a non-ionic 0.5% NP-40 detergent to disrupt the lipid membrane.

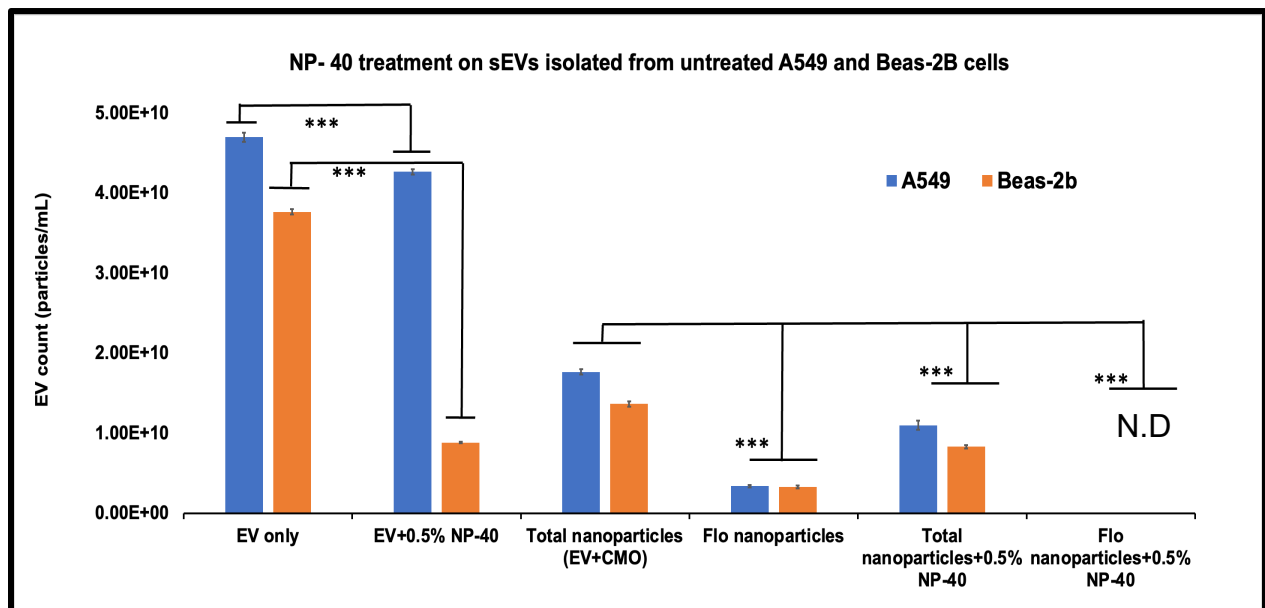


Figure 3.13: Concentration of total and fluorescent nanoparticles from A549 and BEAS-2B cells after NP - 40 detergent treatment. Samples include (from left) EV only with NTA, EVs after 0.5% of NP- 40 treatment with NTA, EVs with CMO in scatter mode, EVs with CMO in fluorescence mode, EVs after 0.5% of NP- 40 treatment with CMO in scatter mode, EVs after 0.5% of NP- 40 treatment with CMO in fluorescence mode. EVs with or without CMO dye were treated with 0.5% of NP - 40, and their respective concentration was measured. The concentration of EVs from both A549 and BEAS-2B cells before and after 0.5% of NP- 40 treatment was significantly different ($p \leq 0.001$), which was marked with *** asterisk symbol. EVs with CMO were measured for concentration with both scatter, and the fluorescence mode of NTA before and after 0.5% of NP- 40 treatment were significantly different ($p \leq 0.001$). The experiment was performed on the same day with three readings, and the error bars were represented in mean \pm SEM ($n=3$) and N.D refers to not detected.

EVs only for NTA concentration (4.7×10^{10} particles/ mL and 3.77×10^{10} particles/ mL) and with 0.5% of NP- 40 detergent treatment (4.27×10^{10} particles/ mL and 8.83×10^9 particles/ mL) showed significant difference in concentration of sEVs from A549 and BEAS-2B cells with a $p \leq 0.001$.

Following the addition of CMO dye to EVs and with 0.5% of NP- 40 detergent treatment, the samples showed a significant difference in concentration of sEVs from A549 and BEAS-2B cells in both scatter mode without / with treatment (without - 1.77×10^{10} particles/ mL , 1.37×10^{10} particles/ mL and with - 1.10×10^{10} particles/ mL and 8.3×10^9 particles/ mL) and fluorescent mode (without - 3.4×10^9 particles/ mL, 3.27×10^9 particles/ mL and with treatment – under the minimum detection limit (limit - $>1 \times 10^6$ particles/ mL) with a $p \leq 0.001$.

As shown in **Figure 3.13**, the result indicates that there is complete disruption of EV membrane upon 0.5% of NP- 40 detergent treatment. This results in null measurement by Zeta View assuring that f-NTA techniques work on the key point of labelled surface markers. And if the surface gets disrupted, f-NTA techniques will not work.

3.2.4.3 Characterisation of sEV from A549 for tetraspanin markers using fluorescent nanoparticle tracking analysis (f-NTA)

To identify the EV specific tetraspanin CD9, CD81 and CD63 using f-NTA, EVs were measured and compared between untreated, treated with nicotine and different flavours of E-liquids (with and without nicotine) samples isolated from A549.

f-NTA determined the percentage of nanoparticles with positive markers- CD9, CD81 and CD63, which can differentiate particles from true EVs. The samples were normalized against CMO (cell mask orange), a lipid-bound membrane dye during

fluorescence mode. All the samples were found to be positive for EV specific markers CD9, CD81 and CD63.

In A549 sEVs, the untreated sample showed 66.81 % CD9 positive particles, and the treated sample showed a range of 19.35 % - 15.94 % CD9 positive particles. With CD81, 73.17 % of untreated and 22.39 % - 12.8 % treated samples were positive particles. For CD63, 52.01 % of untreated whereas 17.21 % - 9.07 % of treated samples were positive, as shown in **Figure 3.14 A**).

These markers were PE-conjugated with higher brightness; however, the fluorescence gets bleached. Also, these tetraspanin markers proportion were seen to vary between untreated versus treated samples and across the EV batches. Overall, 50% of the particles were positive for EVs in the untreated sample, whereas about 20 % - 25 % were positive for tetraspanin markers across the treated samples out of all nanoparticles detected.

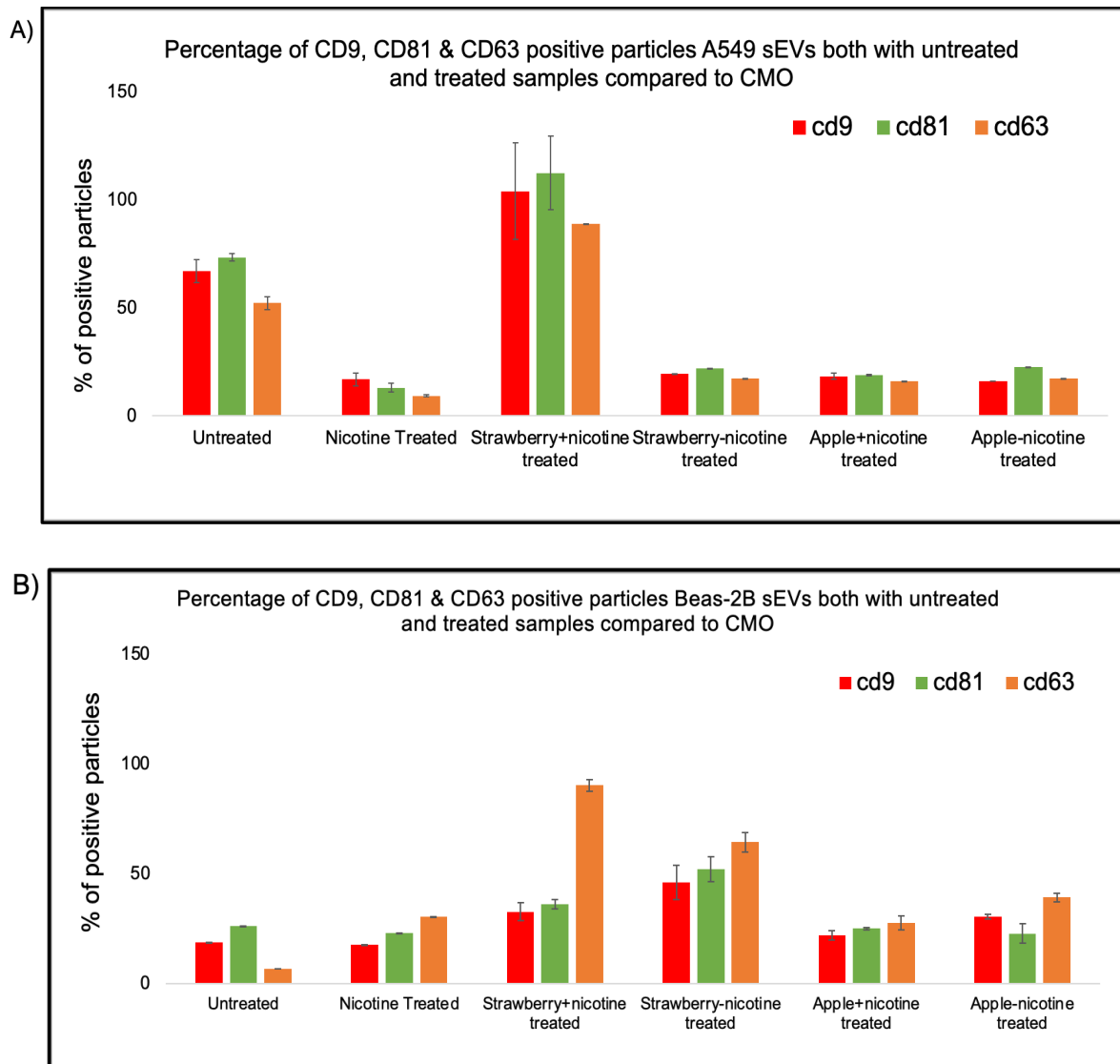


Figure 3.14: Characterization of true sEVs from the actual total particle count using fluorescent nanoparticle tracking analysis (f-NTA) in A) A549 and B) BEAS-2B: Examination of an extracellular vesicle preparation from both cell lines, including untreated and treated samples. Treated samples were (from left) nicotine treated, strawberry flavour with 100 μ M nicotine treated-(strawberry+nicotine), strawberry flavour with no nicotine treated (strawberry-nicotine), apple flavour with 100 μ M nicotine treated - (apple+nicotine), and apple flavour no nicotine treated- (Apple-nicotine). Comparison between the overall biological vesicle count (grey; 100%) to the actual CD9 positives (red), CD81 positives (orange) and CD63 positives (green) vesicles. Each bar includes the three measurements and the error bars represented in mean \pm SEM(n=3).

In BEAS-2B sEVs, the untreated sample showed 18.75 % of CD9 positive particles whereas treated samples showed a range of 17.42 % - 46.00 % of CD9 positive particles

Next, CD81 positive particles in untreated samples were 26.12 % and in treated samples, the range was 22.88 % - 51.90. Further, for CD63 in untreated samples was 6.71 and in treated samples, 27.56 % - 90.18 % of CD63 positive particles were observed in the **Figure 3.14 B**).

f-NTA measurements were normalized to the percentage of lipid-bound membrane dye – CMO in fluorescence mode. All the samples were positive for EV specific markers CD9, CD81 and CD63.

In this study were the abundance of CD63 in BEAS-2B, untreated sample, compared to treated samples. CD63 positive particles were 6.71%. However, in treated samples, the range of CD63 positive particles was 27.56 % - 90.18 %. This was suggestive of an increase in the % of CD63 positive particles upon different treatments. Further, in A549, CD63 positive particles were abundant in untreated, and the treated samples showed decreased CD63 positive particles except in the case of strawberry flavour E-liquid sample with nicotine. Moreover, biological repeats might suggest if this change is reproducible.

These tetraspanin markers were seen to vary between untreated versus treated samples and across the EV batches. Overall, < 50% of the particles were positive for EVs in the untreated sample, whereas about < 25 % of the particles were positive for tetraspanin markers across the treated samples out of 100 % nanoparticles detected.

3.2.5 Western Blot showed the presence of CD9 and C63 tetraspanins were most abundant in A549 and BEAS-2B cells

EVs were further confirmed using western blot with EV specific markers CD9, CD63, CD81 and TSG101 and negative marker - Calnexin. The experiment includes cell lysate from both the cell lines A549 - cancer and BEAS-2B – normal as a positive control and EV samples with untreated, treated with nicotine and flavoured E-liquid.

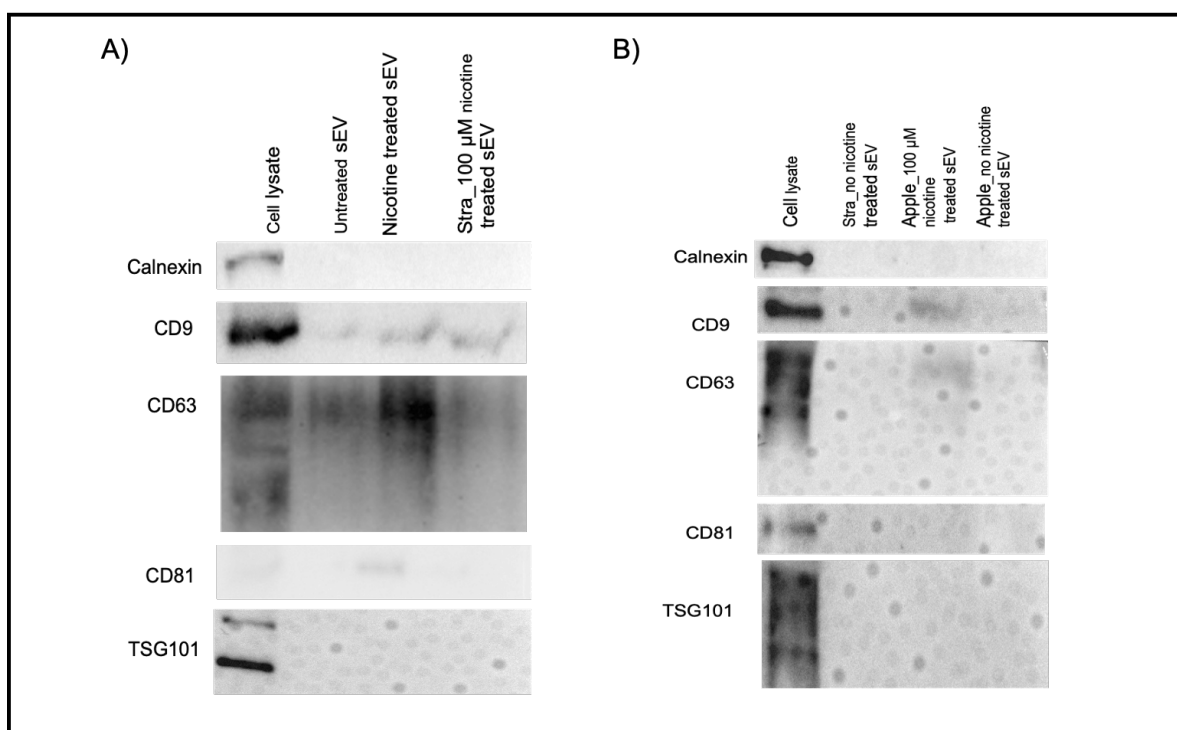


Figure 3.15: Western blot for EV markers from A549 cells including untreated and treated samples: CD9, CD63, CD81 and TSG101 expression was detected in samples that includes A) (from left) lane 1 is cell lysate (A549- 20 μg protein), lane 2 is untreated sEVs from A549 (40 μg protein), lane 3 - 100 μM nicotine treated and lane 4 - treated with strawberry flavour E-liquid with 100 μM nicotine. B) Treated samples include (from left) lane 1- cell lysate (A549- 20 μg protein), lane 2-treated with strawberry flavour without nicotine, lane 3- treated with apple flavour 100 μM nicotine, lane 4 - treated with apple flavour without nicotine. Image of Calnexin is a representative. However, each blot was tested for calnexin and that was negative for all the EVs samples.

In the samples from A549, CD9 and CD63 markers were positive, whereas CD81 was lowly expressed and TSG101 was negative. The negative marker, calnexin (a marker for endoplasmic reticulum), was detected in cell lysate but not in the EV sample. This

confirms that EVs were pure and not contaminated with cellular bodies which were shown in **Figure 3.15** A) and B).

In flavoured E-liquid samples, CD9 and CD63 were partially positive, whereas CD81 and TSG101 were low in amount. Calnexin was negative for all the EVs samples and positive for cell lysate, suggesting that these samples were not contaminated with cellular content.

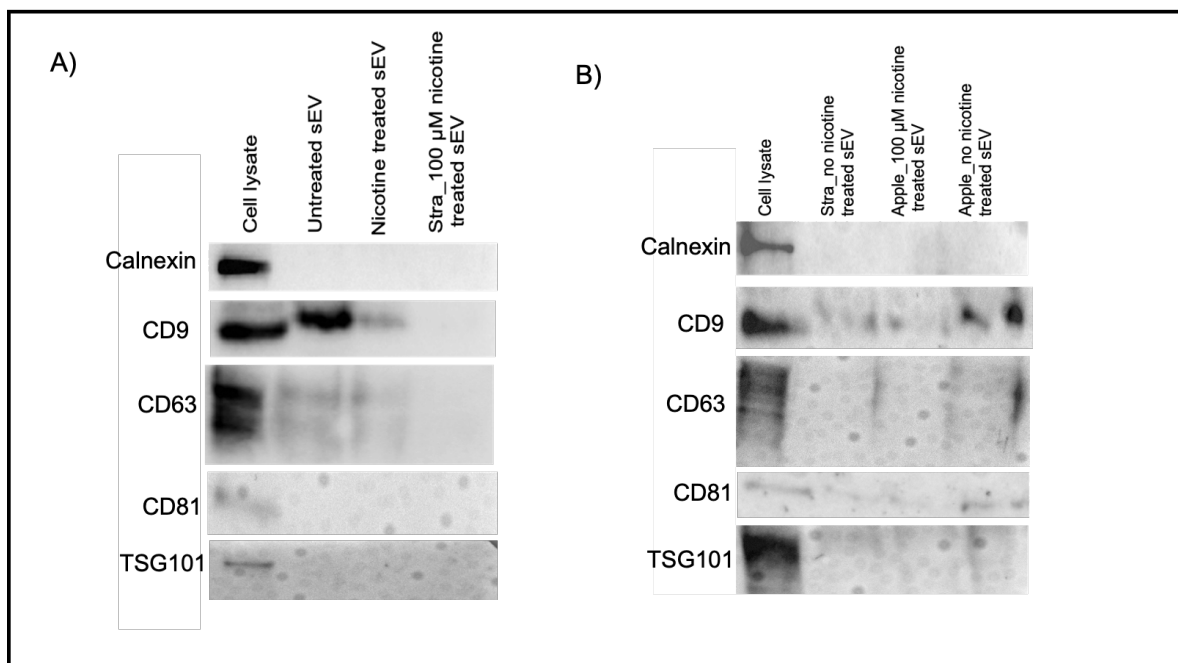


Figure 3.16: Western blot analysis of CD9, CD63, CD81 and TSG101 expression in sEVs samples isolated from BEAS-2B cells includes both untreated and treated. Treated samples include (from left) strawberry flavour without nicotine treated, apple flavour 100 µM nicotine treated, apple flavour without nicotine treated. Expression of EV specific markers was determined where lane 1 is cell lysate (BEAS-2B - 20 µg protein), lane 2 is sEVs from BEAS-2B (40 µg protein) treated with strawberry flavour no nicotine, lane 3 is sEVs from BEAS-2B treated with apple flavour 100 µM nicotine (40 µg- protein), lane 4 is sEVs from BEAS-2B treated with apple flavour no nicotine (40 µg- protein) A) expression of CD9 B) expression of CD63 C) expression of CD81 and D) expression of TSG101.

In the EV samples isolated from BEAS-2B, both CD9 and CD63 were positive for the samples, including untreated, treated with nicotine and partially positive

for treated with strawberry flavoured 100µM E-liquid. Whereas for CD81 and TSG101, these samples were low in amount shown in **Figure 3.16** A) and B). However, all these samples were negative for calnexin and positive for cell lysate, indicating that these samples were not contaminated with cellular content.

Further, samples isolated from flavoured E-liquid, again CD9 and CD63, were positive and negative for calnexin. CD81 and TSG101 were partially expressed in low amounts in these samples. All these samples were negative for calnexin and positive in the case of cell lysate.

Altogether, both the cell line showed that CD9 and CD63 were abundant proteins in all the EV samples. Whereas CD81 and TSG 101 were lowly expressed. This experiment confirms that all the samples were proven for EVs and that there was no contamination of cellular content due to the absence of calnexin.

3.3 Discussion

In the present study, we identified that the impact of nicotine, CSE and E-liquids on human lung cells showed a change in the percentage of proliferating cells with few significant aspects. A cellular model with A549 and BEAS-2B was used to evaluate the effect of nicotine, CSE and E-liquid on proliferating cells. The finding shows a significant effect of CSE among the three toxicants on both cancer and normal cells. However, the results showed that the BEAS-2B was much more susceptible to these treatments when compared to A549 (Ji et al., 2017). Nicotine is one of the major components present in CSE and flavours E-liquids which can affect the proliferation of cells (Silva et al., 2012). Studies have shown that nicotine can promote growth and induce metastasis (Ye et al.,

2004) which is reflected in the results showing both A549 and BEAS-2B with change in proliferation of cells.

When studying the effects of CSE and E-liquid on the cells, the primary concern was to identify the physiologically relevant range of concentration for these components. CSE was prepared from the research cigarette 3R4F, which was smoked into the media. In comparison, different flavours of E-liquid were bought from the market with a known nicotine concentration. In the present study, we used commercial nicotine as a reference to define the concentration of CSE and E-liquids.

On average, a smoker can inhale about 1.1mg to 1.8 mg of nicotine per cigarette, making 22mg to 36 mg of nicotine per pack.

(https://sntc.medicine.ufl.edu/Content/Webinars/SupportingDocs/3031-Essenmacher_-_Handout_1.pdf). Further, the other limitation was the administration of E-liquid to the cells. We were unable to produce vapes and thus mixed the E-liquid in the culture medium for exposure.

This study reveals a significant drop in cell proliferation in the case of cells treated with higher concentrations like 500 μ M and 1mM. Whereas 100 μ M and lower concentrations, were indicating healthy cell proliferation. This was suggestive that 100 μ M can be used to test for different experiments like sEV release and miRNA expression assay (Du et al., 2018). Further, all the experiments are performed considering concentrations of nicotine at 100 μ M for 72hrs (Zanetti et al., 2019).

Further, this is the only study where an MTT assay was performed to study the effect of flavoured E-liquids using lung cells. This study has also included the investigation the effect of two flavours of E-liquids. E-liquids contain various chemical components that can

cause adverse health effects with lung injury in the case of EVALI (Floyd et al., 2018). Among these two flavours, strawberry flavour (no nicotine) showed significant cell viability reduction, suggesting that non-nicotine elements can also cause detrimental effects on lung tissue (Chivers et al., 2019). Known ingredients in nicotine-based E-liquids include propylene glycol and glycerine in addition to nicotine (Burstyn, 2014). Flavouring components like diacetyl and 2,3 – pentanedione were also identified (Allen et al., 2016). The causative elements which can show side effects could be THC - tetrahydrocannabinol and vitamin E acetate along with nicotine (Layden et al., 2020).

Studies have shown an increased risk associated with THC in E-liquids (Ghinai et al., 2019). The elements used as thickeners, diluents and flavourings are considered safe because of their accepted safety limits; however, their long-term consequences with minimal inhaling are not yet clear (Erythropel et al., 2019). These can cause injury to lung tissue (Thiri6n-Romero et al., 2019). They can limit the oxygen, disrupt the cell membrane, cause inflammation to the inner lining of the lung and mucosa, and cause pneumonia (Muthumalage et al., 2020). Accumulated findings showed that E-liquids could cause inflammation and reduce cell integrity with the presence of different flavours and other elements of E-liquids (Bengalli et al., 2017).

All these studies suggest that along with nicotine, there are other components in E-liquid which can enhance the effect of exposure. It is possible that more than one component may cause this lung injury condition but not just nicotine alone. Although there are many studies on the mechanism of nicotine tumorigenesis and the effect of nicotine on lung cells. However, there are limited studies on lung injury caused by E-liquid.

Further, the limitation of this study is the laboratory-based 2D submerged cell culture which does not match the human physiological nor the exact E-liquid exposure (Polosa et al., 2019). The use of human samples with a smoking and vaping habits could have closely mimicked the in vivo conditions. Thus, there is a need to investigate the causative agents and to compare the impact of nicotine and E-liquid on human health.

EVs are secreted by all kinds of tissues and cells. In this study, we used a 2D cell culture where lung cells were grown to isolate EVs and were isolated cultured medium. This study involves an investigation of the presence of EVs from the samples isolated from A549 and BEAS-2B culture media. The characterisation of EVs includes techniques like TEM, fluorescence microscopy, NTA, f-NTA and western blot.

TEM results revealed the size of EVs, which indicated that the particles were within the desired size range of less than 200 nm (Rikkert et al., 2019). TEM was performed to assess the presence of EVs, their quality, morphology, and the sample's purity.

EVs are known for their function in cell-to-cell communication (Becker et al., 2016). The uptake experiment revealed that the EVs were up taken by the recipient cells from the extracellular space. This is indicative of EV acting as a vehicle and the ability to deliver messages from one cell to another (Chiozzini et al., 2022).

Nevertheless, EVs can be easily misperceived with similar-sized nanoparticles. Thus, it is vital to have various techniques that comprise control experiments for a rigorous and informative analysis. Nanoparticle Tracking Analysis (NTA) was performed to measure the size distribution and concentration of the EV samples. NTA showed an any significant difference in concentration of sEVs samples between nicotine treated and

apple flavour E-liquid-no nicotine treated samples when compared to untreated/ control. However, there was no significance observed in other samples of A549. In BEAS-2B there was no significant difference observed across all the samples. EV samples from A549 and BEAS-2B showed heterogeneity and particles were within the expected range of EVs. Bigger sized particles >200 nm were also observed, those were suspected to be the aggregates. However, it is essential to keep in mind that these instruments work on the principle of light scatter and Brownian motion; there is a need to focus on the following standardised protocol and specifications like camera setting and sensitivity (Defante et al., 2018). Variable handling may cause an overestimation of concentration measurement.

Considering the reason, we additionally performed fluorescence Nanoparticle Tracking Analysis (f-NTA) to confirm the presence of EV tetraspanin surface markers. Simultaneously performed f-NTA revealed the presence of tetraspanins CD9, CD81 and CD63 in all the EV samples from both the cell lines (Andreu & Yáñez-Mó, 2014). The result showed that all the three tetraspanins were detected in lower concentrations in all the samples. These were suggestive of the presence of true EVs in the sample, which was less than 50% of the total nano-sized particles. The reason could be that the bigger non-EV nano-sized particle impurities could be nano-bubbles, inorganic salt precipitates, and protein aggregates (Webber & Clayton, 2013). EV samples showed varying percentages of tetraspanin marker, which gives the confidence of the presence of pure EVs. With f-NTA, in A549, the most abundantly seen tetraspanin markers were CD9 and CD63, which was also reflected in western blot results. Whereas BEAS-2B was rich in

CD63 in the E-liquid treated- strawberry flavour with and without nicotine samples, which was slightly exhibited in western blots.

Variation in each sample with regards to each of the markers in all the samples was observed. Despite the brightest available dyes, sometimes f-NTA can underestimate the actual stained particles, especially with PE dye, due to its fast bleaching. This could explain the lower labelled percentage of detectable stained antibodies during the experiment. Even then, f-NTA provides consistent results between samples, revealing a trend in the expression of tetraspanin markers. Given that this study uses f-NTA with single laser settings where each sample was measured for different markers using different fractions from the same vial. The other reason was that each marker was captured individually, and thus there was a variation in scatter mode reading (Fortunato et al., 2021). To overcome all these issues, we performed control experiments to show the impact of diluent (PBS) used to dilute the EV samples. Further, the use of CMO dye (cell mask orange) shows that the dye binds to the surface and that if the surface of EVs were disrupted, the instrument would show a null value (Midekessa et al., 2021). This is indicative that f-NTA captured all the surface tetraspanins present in the sample.

sEV were further characterized using the western blot technique. The western blot showed EV markers CD9, and CD63, which are indicative of small EVs (Mathieu et al., 2021), where EVs were lysed using RIPA buffer. However, CD81 and TSG 101 have a low amount of expression in some EV samples. Additionally, all the EV samples were negative for calnexin (a marker for endoplasmic reticulum), reassuring that the EVs are not contaminated with cellular material (Kowal et al., 2016). EV samples were

characterised according to the MISEV guidelines 2018 (Théry et al., 2018) and MISEV 2021 (Witwer et al., 2021).

However, in both f-NTA and western blot, the outcome was not equivalent, which could be due to the difference in sample preparation and the type of detection of the position of the EV marker. f-NTA can measure the surface markers with a smaller sample volume, whereas western blot demands huge sample volume with lysed EVs to get a detectable lysed protein load. The other fact that needs to be considered is that f-NTA works on laser power, the strength of the light source, and the number of fluorophores associated per frame, which directly correlates with the scattered light and results in the number of detectable nanoparticles (Fortunato et al., 2021).

The other fact that needs to be considered is the effect of the sample's freeze and thaw conditions, which can also impact the particle size, concentration, and presence of surface markers on the EVs (Gelibter et al., 2022).

Nevertheless, EV detection is challenging because of its size and heterogeneity in size and morphology. In this study, we presented five different techniques which can give explicit knowledge about the morphology, size, concentration, and presence of EV markers to enumerate EVs, which provides the necessary information on the true sEVs from the actual non-EV population within a size range of less than 200 nm. Each technique has its strengths and limitations, but efforts were made to calibrate the instrument and used standardised protocols for EV isolation, characterization and sample preparation were maintained to obtain results.

In conclusion, CSE detrimental effect among all the three toxicants mentioned earlier. Further, strawberry flavour E-liquid-without nicotine showed a significant change

in cell survivability among the two flavours included in this study. After treatment, sEVs were characterized by experiments like TEM, fluorescent microscopy, NTA, f-NTA and western blot. Next, we performed the isolation of miRNA from sEVs for miRNA profiling and small RNA sequencing to evaluate novel biomarkers.

CHAPTER 4 : Profiling of microRNA as a biomarker in sEV cargo

4.1 Comparison of the expression profile of different miRNA present on C14MC using qPCR.

4.1.1 Introduction

This chapter comprises of expression of miRNA from C14MC using qPCR and small RNA sequencing using NGS from sEV samples. sEV samples were isolated from A549 and BEAS-2B cell cultured media which includes nicotine and flavoured E-liquids along with control.

4.1.2 Differential expression of C14MC in lung cells and cargo of these miRNAs in sEV samples.

4.1.2.1 MiR-487b was significantly upregulated upon nicotine treatment in A549 cells

miRNA expression profiling was performed on 15 miRNAs from C14 (arranged as per order on chromosome 14) for miRNA expression of samples from endogenous and sEV (control, nicotine treated) from A549, as shown in **Figure 4.1**. Further, four non-cluster miRNAs (miR-17, miR-21 let-7a and miR-155) were also included where two miRNAs (miR-17 and let-7a) were downregulated when compared to control, and miR-21 was upregulated. Interestingly, all C14 miRNAs were downregulated when compared to control, among these only miR-487b was seen as significantly less- down regulated with a p-value of <0.001.

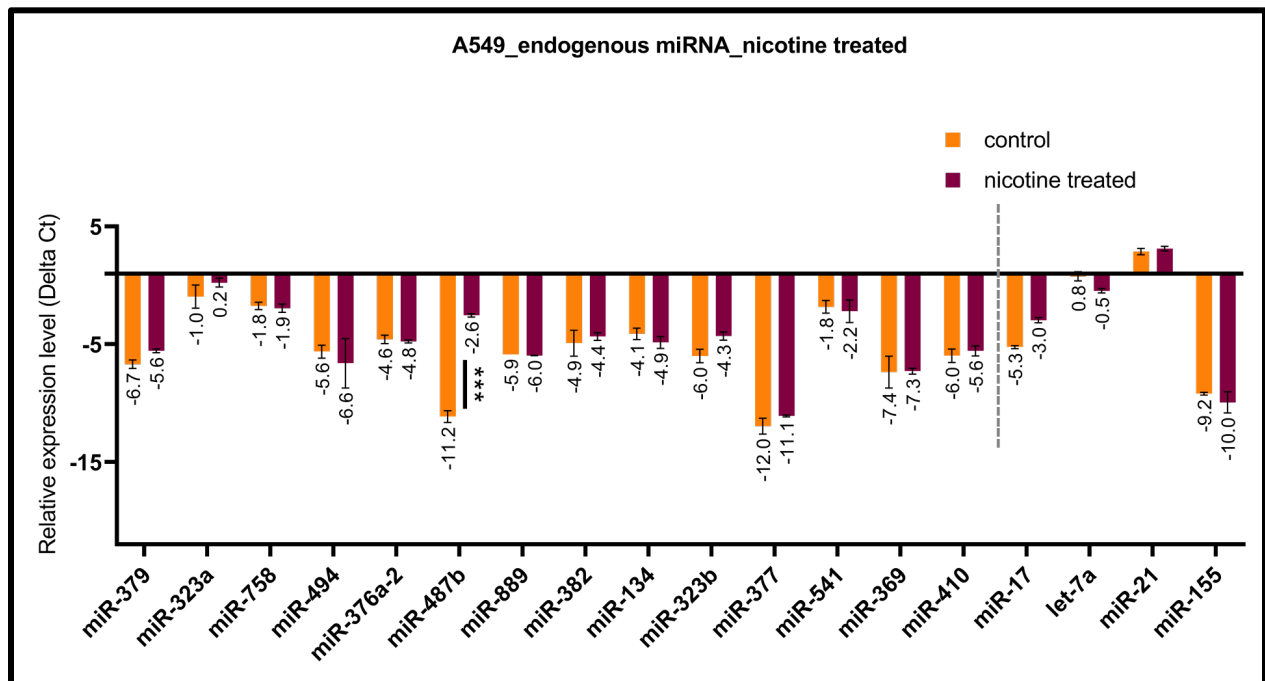


Figure 4.1: Differentially expressed miRNAs in A549 endogenous sample upon nicotine treatment: Endogenously isolated miRNAs from control and nicotine treated samples to perform miRNA expression profile (Relative expression) of C14MC miRNAs in A549 cells. The relative expression was normalised with U6. The dotted grey line represents the separation of C14MC and non-cluster miRNAs. The experiment was performed in duplicates, and miR-17 was considered a positive control. P-value was calculated by performing an unpaired student t-test with an adjusted p-value using Holm Sidak correction method for multiple comparisons (***) $p < 0.001$.

In BEAS-2B, 13 miRNAs were tested for differential expression from C14. Five miRNAs (miR-376c, miR-487b, miR-541, miR-758 and miR-889) were upregulated, whereas three miRNAs were downregulated (miR-323b, miR-369, miR-381) and five miRNAs (miR-323a, miR-376a-2, miR-382, miR-410 and miR-494) showed an opposite trend between control and nicotine samples as shown in **Figure 4.2**. Among non-cluster miRNAs, miR-17 was upregulated, and let-7a showed the opposite trend. None of these miRNAs was significantly expressed.

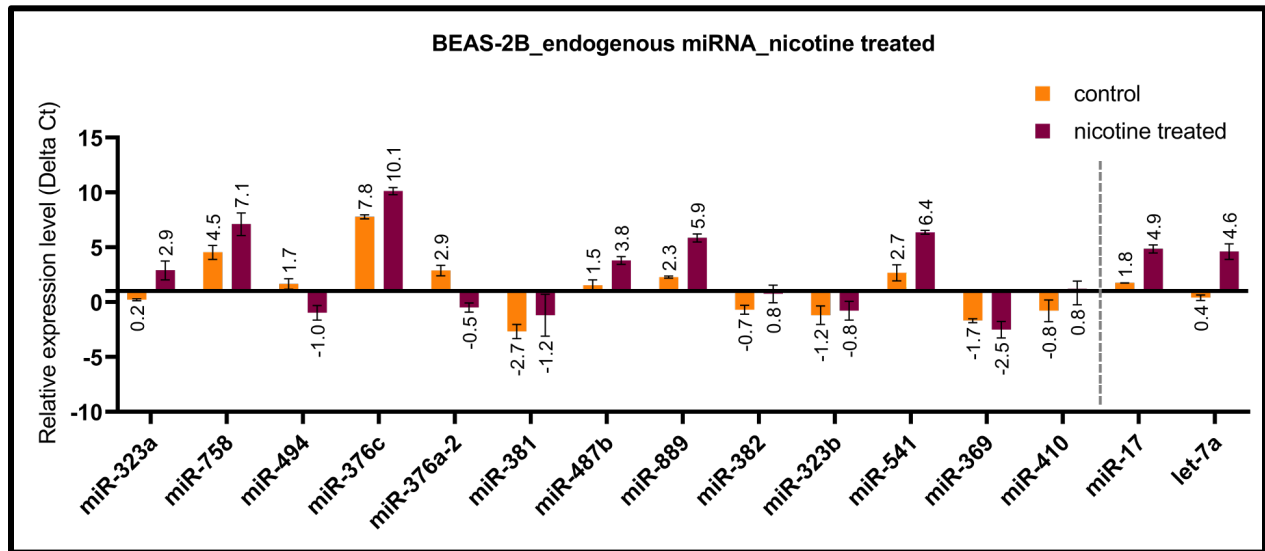


Figure 4.2: Differentially expressed miRNAs in BEAS-2B endogenous sample upon nicotine treatment: Endogenously isolated miRNAs from control and nicotine treated samples to perform miRNA expression profile (relative expression) of C14MC miRNAs in BEAS-2B cells. The relative expression was normalised with U6. The dotted grey line represents the separation of C14MC and non-cluster miRNAs. The experiment was performed in duplicates, and miR-17 was considered a positive control. P-value was calculated by performing an unpaired student t-test with an adjusted p-value using Holm Sidak correction method for multiple comparisons.

4.1.2.2 Differentially expressed miRNAs between control and E-liquid (strawberry flavour with nicotine) in BEAS-2B cells

In BEAS-2B, 11 miRNAs from C14MC were tested for differential expression. Among these, four miRNAs (miR-376a-2, miR-376c, miR-494, miR-381 and miR-541) were upregulated shown in **Figure 4.3**.

Three miRNAs (miR-323a, miR-410 and miR-889) were expressed in opposite trends. None of these miRNAs was significant except miR-21 which is a non-cluster miRNA. miR-21 was significantly upregulated compared to control.

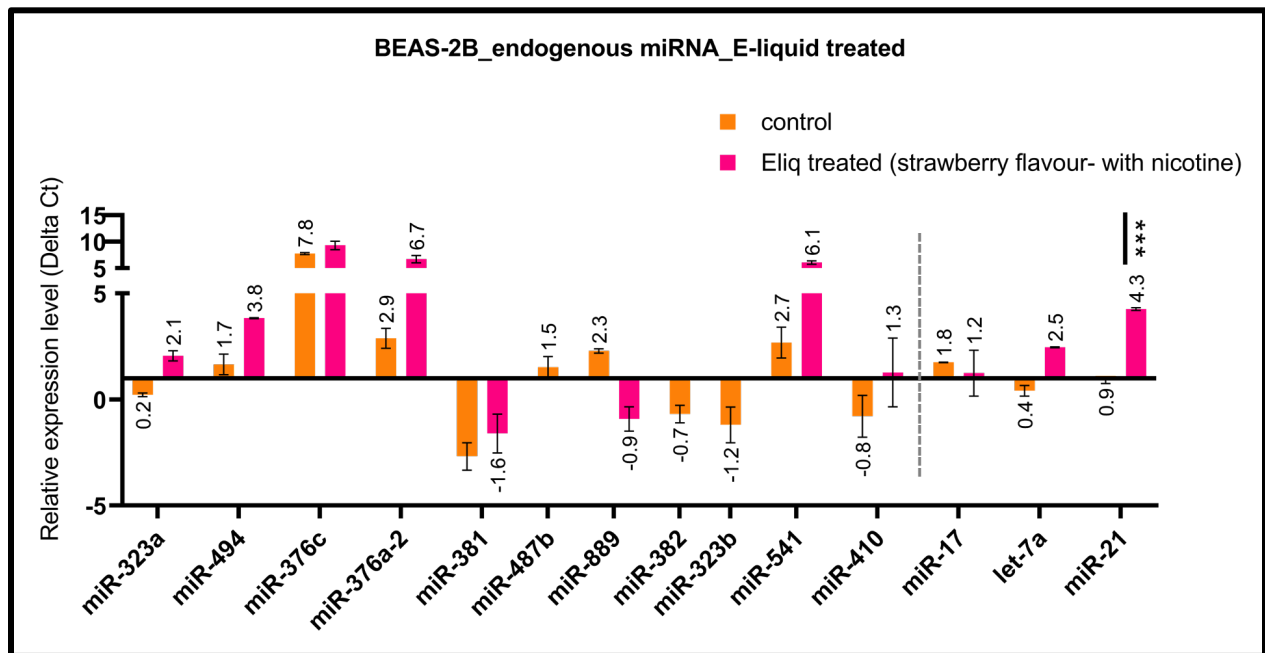


Figure 4.3: Differentially expressed miRNAs in BEAS-2B endogenous sample upon E-liquid (strawberry flavour-with nicotine) treatment: Endogenously isolated miRNAs from control and E-liquid treated samples to perform miRNA expression profile (relative expression) of C14MC miRNAs in BEAS-2B cells. The relative expression was normalised with U6. The dotted grey line represents the separation of C14MC and non-cluster miRNAs. The experiment was performed in duplicates, and miR-17 was considered a positive control. P-value was calculated by performing an unpaired student t-test with an adjusted p-value using Holm Sidak correction method for multiple comparisons.

Interestingly, three miRNAs (miR-323b, miR-382 and miR-487b) were not seen expressed in E-liquid treated sample. However, it would be interesting to study these three miRNAs which didn't express upon E-liquid treatment. The three miRNAs may be used as biomarkers to differentiate between untreated, and E-liquid treated samples.

4.1.2.3 sEV derived miRNA expression profiling was compared to endogenous miRNA in lung cells upon nicotine treatment

C14MC miRNAs expression was tested in A549 and BEAS-2B cells and sEV samples using qPCR.

In A549, 15 miRNAs from C14MC were tested for expression profiling, out of which only 11 miRNAs were found in sEVs. In endogenous conditions, six miRNAs were upregulated (miR-323a, miR-323b, miR-487b, miR-377 and miR-379). Whereas two miRNAs were found to be downregulated (miR-494 and miR-134).

Along with C14MC, four non- cluster miRNAs, which were known as candidate miRNAs in the case of lung cancer, were also tested, of which miR-17 was considered a positive miRNA in this study. Let-7a was tested and found downregulated whereas miR-21 showed no change. In the sEV samples, out of eleven miRNAs, one miRNA (miR-410) was upregulated, and the rest of the ten miRNAs were found downregulated. Three miRNA (miR-17, miR-21 and let-7a) were also found to be downregulated. Interestingly, miR-155 was not found in sEVs.

Additionally, three miRNAs (miR-369, miR-377 and miR-379) were not found in the sEV samples, as shown in **Figure 4.4 A**). miR-323a, miR-323b and miR-487b were found upregulated in the endogenous sample but were seen downregulated in sEV samples. Whereas miR-410, which was not changed upon nicotine treatment in the endogenous sample, was found upregulated in the sEV sample.

A549 Nicotine treated		
miRNAs	Endogenous	sEV
C14MC		
miR-379	2.19	
miR-323a	2.27	0.01
miR-758	0.88	0.03
miR-494	0.51	0.04
miR-376a-2	0.88	0.01
miR-487b	>100	0.02
miR-889	0.88	0.01
miR-382	1.37	0.01
miR-134	0.6	0.06
miR-323b	3.25	0.03
miR-377	1.82	
miR-541	0.77	0.01
miR-369	1.06	
miR-410	1.33	4.58
Non-cluster miRNAs		
miR-17	4.89	0.01
Let-7a	0.43	0.12
miR-21	1.19	0.01
miR-155	0.59	

BEAS-2B Nicotine treated		
miRNAs	Endogenous	sEV
C14MC		
miR-379		
miR-323a	6.41	1.06
miR-494	0.16	4.69
miR-487b	4.86	0.8
miR-889	11.84	0.29
miR-382	2.72	0.94
miR-323b	1.33	3.04
miR-377		
miR-541	12.82	0.76
miR-410	3.11	0.05
Non-cluster miRNAs		
miR-17	8.6	2.26
Let-7a	18.51	1.74
miR-155		

Figure 4.4: Heatmap for A549 and Beas-2B upon nicotine treatment compared to untreated; showing differential expression (fold change) of C14MC miRNAs in A) A549 and B) BEAS-2B cell treated with nicotine for 72hrs of incubation. The fold change was calculated against untreated/control samples and normalised with U6 for endogenous samples and with cel-39 for the sEV sample. The experiment was performed in duplicates, and miR-17 was considered a positive control. Any fold change greater than 100 was represented as >100. (Red indicates upregulation ≥ 1.5 , green indicates downregulation ≤ 0.6 , black-not differential ranging 0.6-1.5, light blue indicates no expression). The relative expression levels of miRNAs from sEV mentioned in this heatmap map can be seen in the following **Figure 4.6** and **Figure 4.7** individually.

In BEAS-2B, 11 miRNAs were tested for expression profile, out of which only eight miRNAs were found in the sEV fraction. Of these 11, six miRNAs (miR-323a, miR-382, miR-410, miR-487b, miR-541, and miR-889) were found to be upregulated, one miRNA (miR-494) was downregulated, and one miRNA (miR-323b) showed no change. Whereas in the sEV fraction, out of eight miRNAs, two miRNAs (miR-323b and miR-494) were upregulated, two miRNAs (miR-410 and miR-889) were downregulated, and the rest of four miRNAs (miR-323a, miR-382, miR-487b and miR-541) showed no change in their expression as shown in **Figure 4.4 B**).

Interestingly, three miRNAs (miR-155, miR-377 and miR-379) from the non-cluster and C14MC group were not expressed in both endogenous and sEV fractions.

MiRNAs like miR-410 and miR-889 were found to be upregulated in endogenous conditions but were found to be downregulated in sEV samples. In non-cluster miRNAs, miR-17 and let-7a were also tested and found to be upregulated in both endogenous and sEV samples.

4.1.2.4 miRNA expression profiling of lung cells upon E-liquid (strawberry flavour-with nicotine) treatment

C14MC miRNAs were tested for expression in BEAS-2B and A549 cells. However, the internal control U6 was not expressed in A549 endogenous samples treated with E-liquid. Due to this reason, the data analysis was not performed. The reason could be E-liquid which was purchased commercially and was not a lab-graded chemical.

We tested 15 miRNAs from C14MC and four miRNAs from outside the cluster (miR-17, miR-21, Let-7a and miR-155) for expression profile. Out of these 15, nine miRNAs (miR-323a, miR-323b, miR-376a-2, miR-376c, miR-410, miR-487b, miR-494, miR-758 and miR-889) were seen to expressed in endogenous sample. Five miRNAs (miR-369, miR-381, miR-134, miR-377 and miR-379) did not showed expression. From non-cluster miRNAs, only one miRNA (miR-17) showed expression, whereas the other two miRNAs (miR-21, let-7a) did not show expression, and only miR-155 did not expressed in both the fractions as shown in **Figure 4.5**.

BEAS-2B-Eliquid treated		
miRNAs	Eliq treated(stra+nic)-Endogenous	Eliq treated(stra+nic)-sEVs
C14MC		
miR-379		
miR-494	4.53	5.12
miR-376c	0	
miR-889	0.53	5.33
miR-377		
miR-541	10.59	>100
miR-410	4.18	2.63
Non-cluster miRNAs		
miR-17	2.37	
Let-7a	5.52	
miR-21	10.27	3.05
miR-155		

Figure 4.5: Heatmap for Beas-2B upon E-liquid (strawberry flavour with nicotine) treatment compared to untreated; showing differential expression (fold change) of C14MC miRNAs in BEAS-2B cell treated with E-liquid (strawberry flavour with nicotine) for 72hrs of incubation. The fold change was calculated against untreated/control samples and normalised with U6 for endogenous samples and with cel-39 for the sEV sample. The experiment was performed in duplicates, and miR-17 was considered a positive control. Any fold change greater than 100 was represented as >100. (Red indicates upregulation ≥ 1.5 , green indicates downregulation ≤ 0.6 , black-not differential ranging 0.6-1.5, light blue indicates no expression). The relative expression levels of miRNAs from sEV mentioned in this heatmap map can be seen in the following **Figure 4.9** individually.

In BEAS-2B, ten miRNAs were tested for expression profiling along with three non-cluster miRNAs. Of these ten miRNAs, eight miRNAs (miR-323a, miR-323b, miR-376a-2, miR-410, miR-487b, miR-494, miR-758 and miR-889) were found in the endogenous samples. Interestingly, six out of seven miRNAs were found upregulated except miR-889, which was downregulated, whereas miR-376c did not show any change. Two miRNAs (miR-377 and miR-379) were not expressed. The three non-cluster miRNAs (miR-17, miR-21 and let-7a) were also upregulated whereas miR-155 did not show expression.

Further, out of these ten miRNAs, only five miRNAs (miR-323a, miR-410, miR-494, miR-541 and miR-889) were seen upregulated in sEV samples. Whereas four miRNAs (miR-376a-2, miR-376c, miR-377 and miR-379) were not seen expressed in sEV samples. From non-cluster miRNAs, only one miRNA (miR-21) was seen upregulated, while the other three miRNAs (miR-17, let-7a and miR-155) did not express.

Interestingly, miR-889 was the only miRNA which was seen downregulated among all the miRNAs and between endogenous and sEV samples. MiR-889 was found upregulated in sEV samples. Therefore, it can be a remarkable miRNA to consider as a biomarker.

4.1.2.5 Both A549 and BEAS-2B cells showed downregulated miRNA, and eight miRNAs from C14MC showed significant downregulation in sEVs upon nicotine treatment in A549 cells

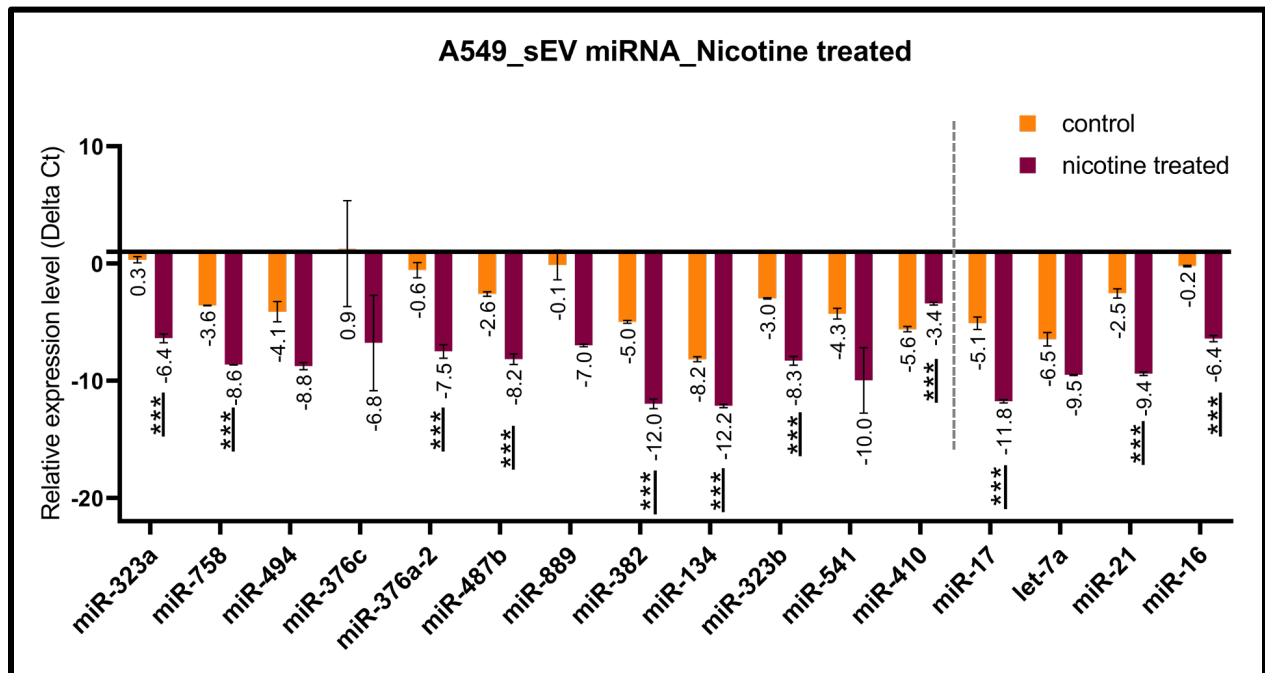


Figure 4.6: Differentially expressed miRNAs in A549 sEV sample upon nicotine treatment: sEV isolated miRNAs from control and nicotine treated samples to perform miRNA expression profile (relative expression) of C14MC miRNAs in A549 cells. The relative expression was normalised with Cel-39. The dotted grey line represents the separation of C14MC and non-cluster miRNAs. The experiment was performed in

duplicates, and miR-17 was considered a positive control. P-value was calculated by performing an unpaired student t-test with an adjusted p-value using Holm Sidak correction method for multiple comparisons (***) $p < 0.001$.

In A549, eight out of 12 miRNAs were found significant when treated with nicotine. All the 12 miRNAs were downregulated. All these miRNAs were found in sEV and were seen downregulated as shown in **Figure 4.6**.

From non-cluster miRNAs, three miRNAs (miR-17, miR-16 and miR-21) were significantly downregulated and Let-7a was downregulated but not significant.

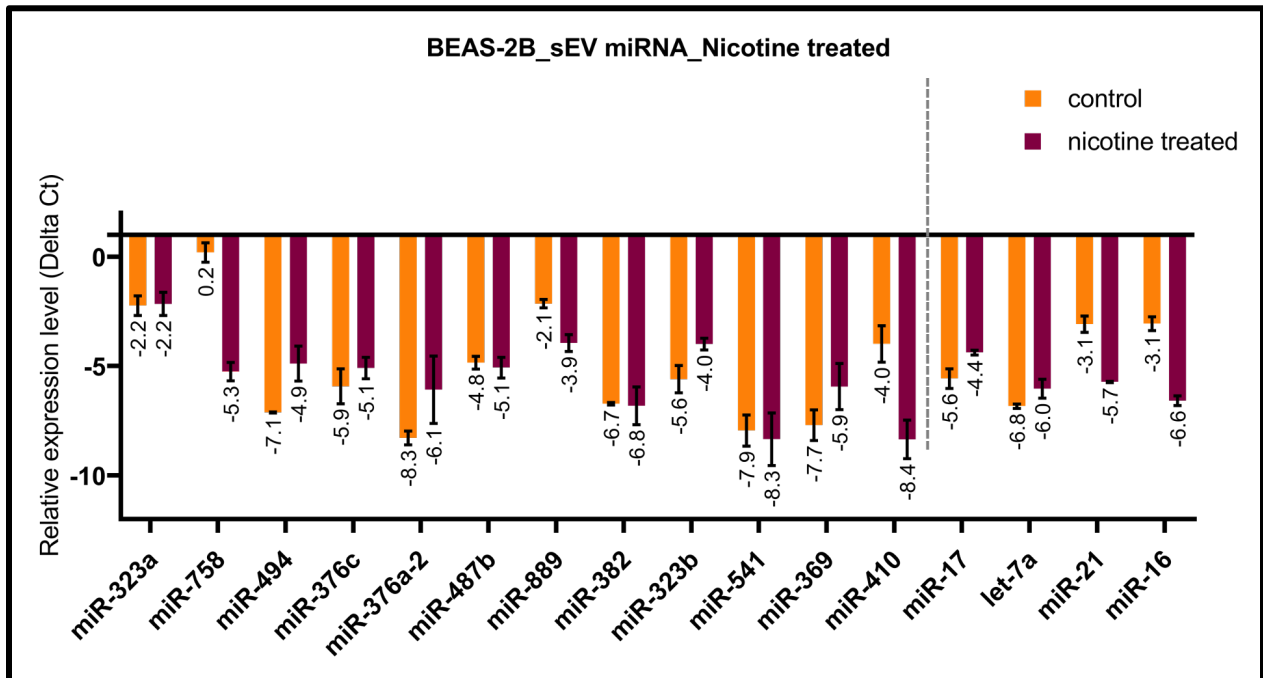


Figure 4.7: Differentially expressed miRNAs in BEAS-2B sEV sample upon nicotine treatment: sEV isolated miRNAs from control and nicotine treated samples to perform miRNA expression profile (relative expression) of C14MC miRNAs in BEAS-2B cells. The relative expression was normalised with Cel-39. The dotted grey line represents the separation of C14MC and non-cluster miRNAs. The experiment was performed in duplicates, and miR-17 was considered a positive control. P-value was calculated by performing an unpaired student t-test with an adjusted p-value using Holm Sidak correction method for multiple comparisons.

In BEAS-2B, 12 miRNAs were tested for miRNA expression profiling. Five miRNAs (miR-494, miR-376c, miR-376a-2, miR-323b and miR-369) were upregulated and the six miRNAs (miR-323a, miR-758, miR-487b, miR-323b, miR-382 and miR-410) were found downregulated in sEV sample. However, none of the miRNAs was significant, as shown in **Figure 4.7**.

4.1.2.6 Lung cells showed downregulated miRNAs when treated with strawberry flavour E-liquid containing nicotine

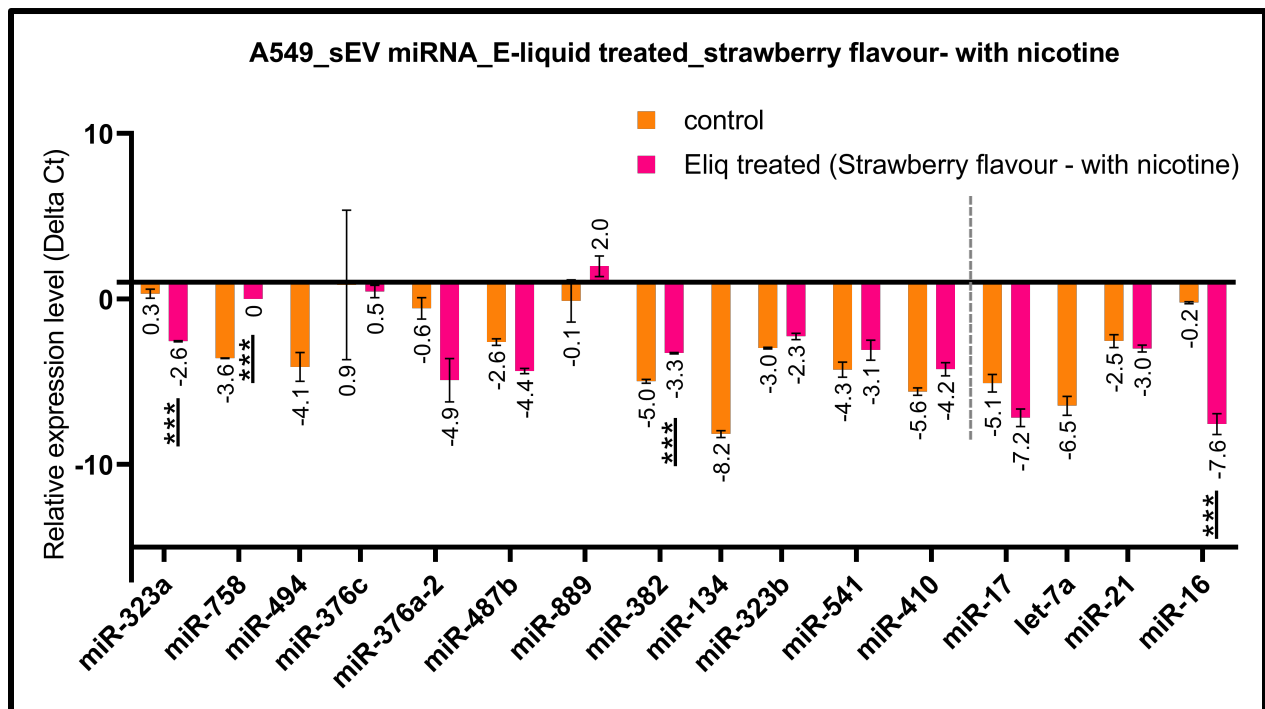


Figure 4.8: Differentially expressed miRNAs in A549 sEV sample upon E-liquid (strawberry flavour with nicotine) treatment: sEV isolated miRNAs from control and strawberry flavoured E-liquid with nicotine treated samples to perform miRNA expression profile (*relative expression*) of C14MC miRNAs in A549 cells. The *relative expression* was normalised with Cel-39. The dotted grey line represents the separation of C14MC and non-cluster miRNAs. The experiment was performed in duplicates, and miR-17 was considered a positive control. P-value was calculated by performing an unpaired student *t*-test with an adjusted *p*-value using Holm Sidak correction method for multiple comparisons (***) $p < 0.001$.

In A549, three (miR-323a, miR-382 and miR-758) out of 12 miRNAs were significantly dysregulated when treated with strawberry E-liquid containing nicotine. Of these miR-323a was downregulated whereas miR-382 and miR-758 were upregulated when compared to control.

All the 11 miRNAs were downregulated, whereas miR-889 showed the opposite trend when compared to control. miR-376c was expressed in the control sample only, as shown in **Figure 4.8**.

In BEAS-2B, 12 miRNAs were present in sEV samples. All these 12 miRNAs were downregulated upon treatment with strawberry flavour E-liquid containing nicotine. However, none of these miRNAs was significant, as shown in **Figure 4.9**.

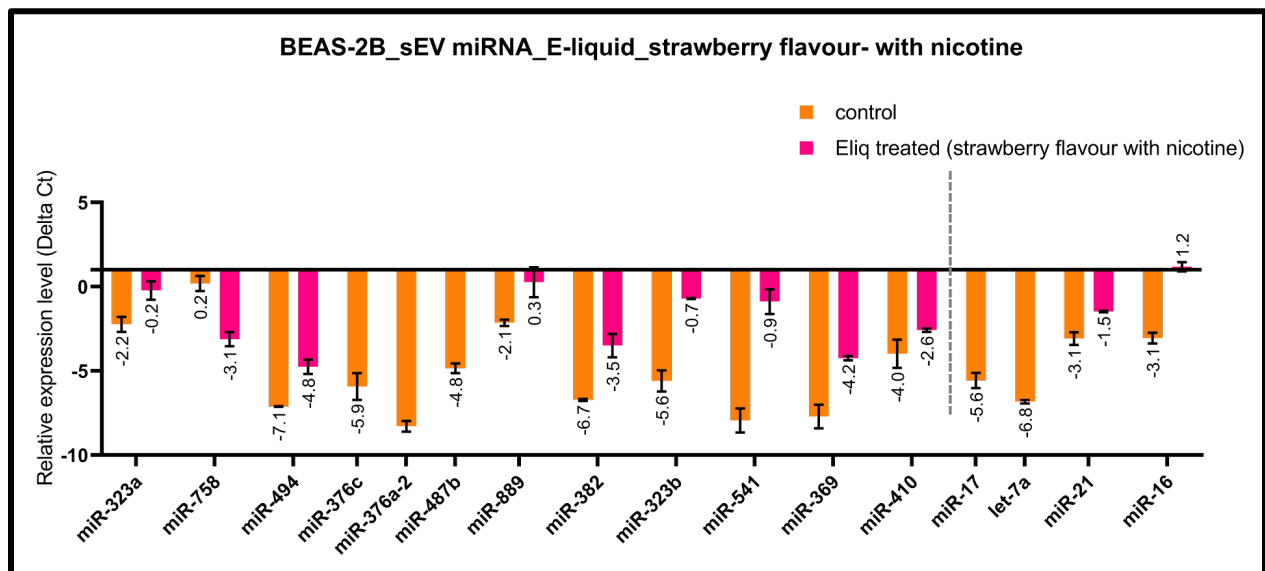


Figure 4.9: Differentially expressed miRNAs in BEAS-2B sEV sample upon E-liquid (strawberry flavour with nicotine) treatment: sEV isolated miRNAs from control and strawberry flavoured E-liquid with nicotine treated samples to perform miRNA expression profile (relative expression) of C14MC miRNAs in BEAS-2B cells. The relative expression was normalised with Cel-39. The dotted grey line represents the separation of C14MC and non-cluster miRNAs. The experiment was performed in duplicates, and miR-17 was considered a positive control. P-value was calculated by performing an unpaired student t-test with an adjusted p-value using Holm Sidak correction method for multiple comparisons (***) $p < 0.001$.

4.1.2.7 miR-758 was significantly downregulated upon treatment with strawberry-flavoured E-liquid with no nicotine in lung cells

In A549, 12 miRNAs from C14MC were tested for expression profile. All 12 miRNAs were found downregulated in sEV samples. However, two miRNAs (miR-323a and miR-758) were found to be significantly downregulated whereas miR-382 was significantly upregulated. miR-376c was only found in control samples and was not seen expressed in E-liquid treated sample as shown in **Figure 4.10**.

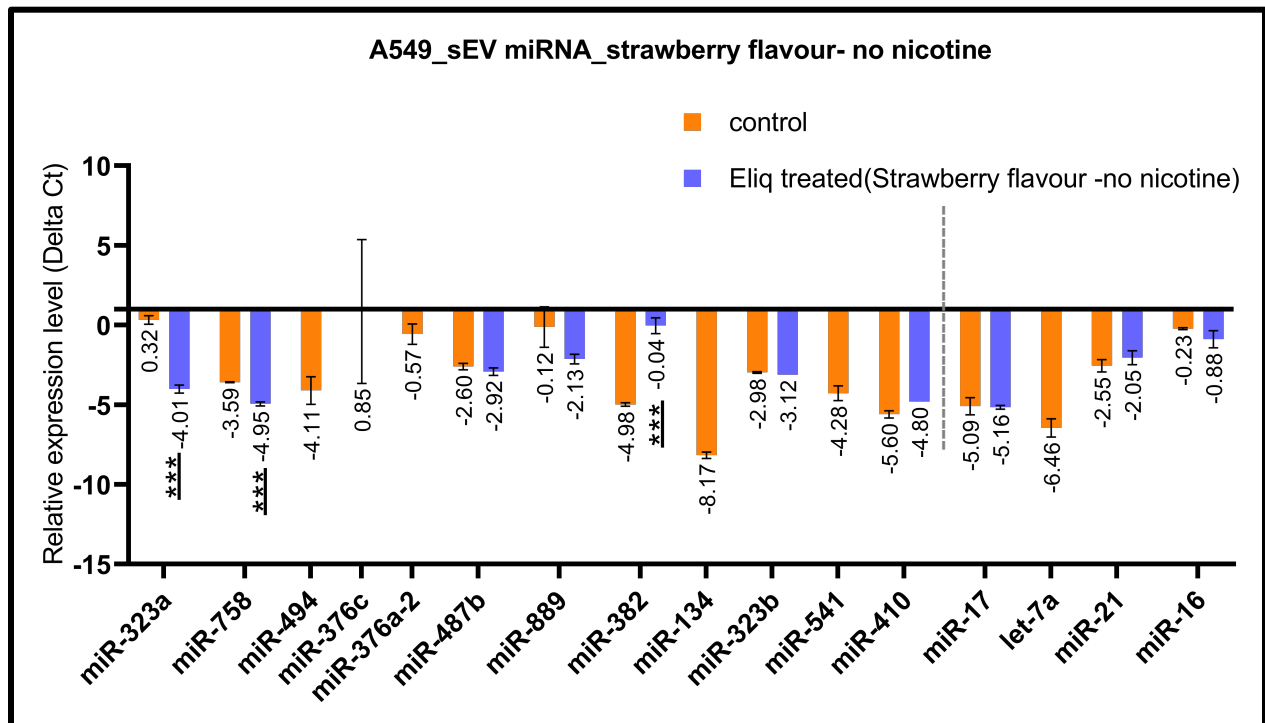


Figure 4.10: Differentially expressed miRNAs in A549 sEV sample upon E-liquid (strawberry flavour with no nicotine) treatment: sEV isolated miRNAs from control and strawberry flavoured E-liquid with no nicotine treated samples to perform miRNA expression profile (relative expression) of C14MC miRNAs in A549 cells. The relative expression was normalised with *Cel-39*. The dotted grey line represents the separation of C14MC and non-cluster miRNAs. The experiment was performed in duplicates, and miR-17 was considered a positive control. P-value was calculated by performing an unpaired student t-test with an adjusted p-value using Holm Sidak correction method for multiple comparisons (***) $p < 0.001$.

In BEAS-2B, 12 miRNAs were seen in sEV samples, and among these, two miRNAs (miR-541 and miR-758) were significantly downregulated. All these miRNAs were downregulated except miR-541, which was expressed in the opposite direction when compared to control, as shown in **Figure 4.11**.

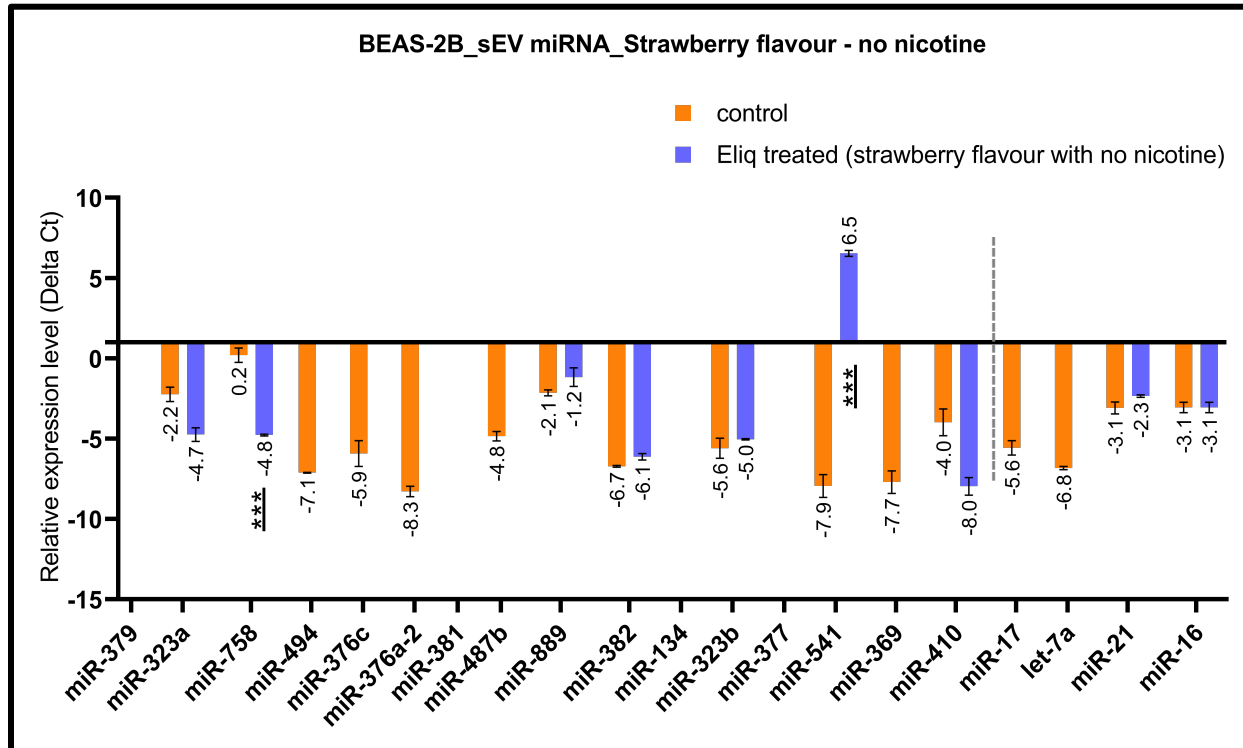


Figure 4.11: Differentially expressed miRNAs in BEAS-2B sEV sample upon E-liquid (strawberry flavour with no nicotine) treatment: sEV isolated miRNAs from control and strawberry flavoured E-liquid with no nicotine treated samples to perform miRNA expression profile (relative expression) of C14MC miRNAs in BEAS-2B cells. The relative expression was normalised with Cel-39. The dotted grey line represents the separation of C14MC and non-cluster miRNAs. The experiment was performed in duplicates, and miR-17 was considered a positive control. P-value was calculated by performing an unpaired student t-test with an adjusted p-value using Holm Sidak correction method for multiple comparisons (***) $p < 0.001$.

4.1.2.8 miR-541 and miR-758 showed similar significant expression upon E-liquid (apple flavour with nicotine) treatment in lung cells

In A549, 12 miRNAs from C14MC were found in sEV upon E-liquid (apple flavour with nicotine) treatment. Two miRNAs (miR541 and miR-758) were found significant with

a p-value of <0.001, where miR-758 was downregulated, and miR-541 was found in the opposite trend when compared to control. Except for miR-541, all the other miRNAs were downregulated. However, miR-376c and miR-134 were not found in the treated sample, as shown in **Figure 4.12**.

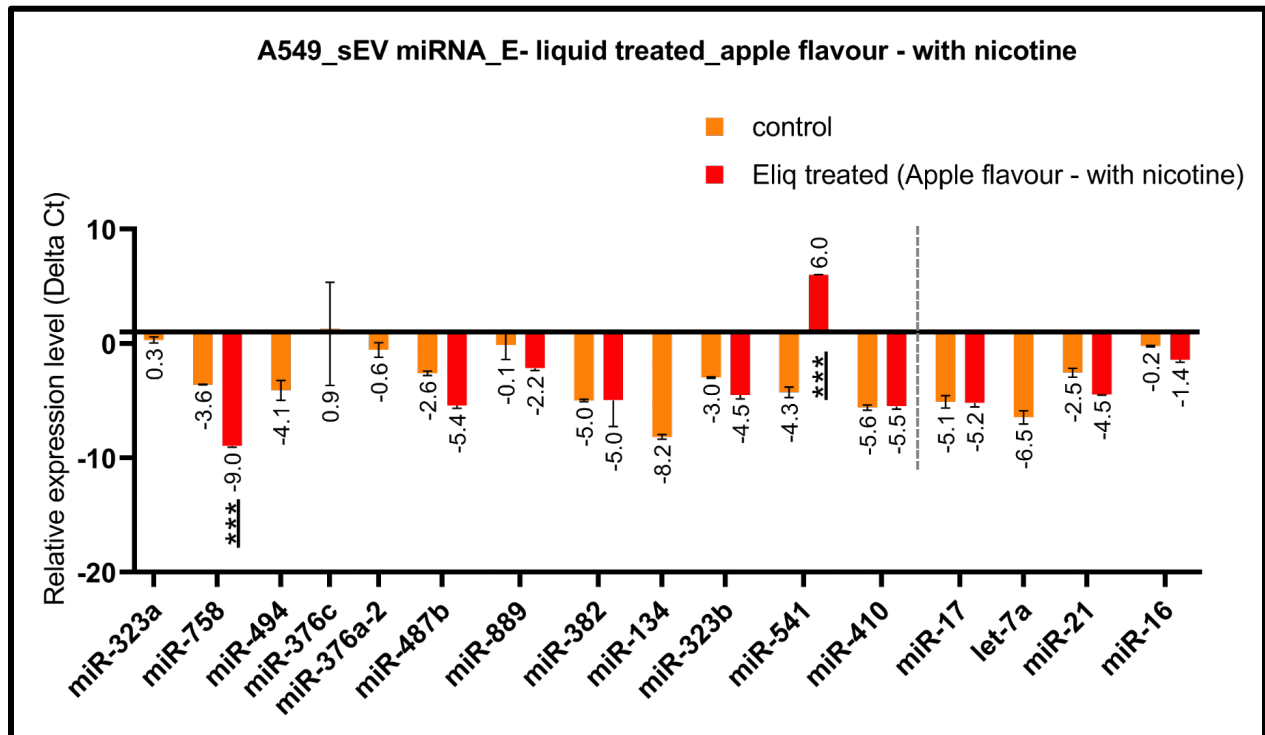


Figure 4.12: Differentially expressed miRNAs in A549 sEV sample upon E-liquid (apple flavour with nicotine) treatment: sEV isolated miRNAs from control and apple flavoured E-liquid with nicotine treated samples to perform miRNA expression profile (relative expression) of C14MC miRNAs in A549 cells. The relative expression was normalised with Cel-39. The dotted grey line represents the separation of C14MC and non-cluster miRNAs. The experiment was performed in duplicates, and miR-17 was considered a positive control. P-value was calculated by performing an unpaired student t-test with an adjusted p-value using Holm Sidak correction method for multiple comparisons (***) $p < 0.001$.

In BEAS-2B, four (miR-323a, miR-494, miR-541 and miR-758) out of 12 miRNAs were found significant upon E-liquid (apple flavour with nicotine) treatment. Of these four, two miRNAs (miR-541 and miR-758) were commonly significant in A549 and BEAS-2B cell lines. Interestingly, both these miRNAs showed similar expression upon E-liquid

treatment. Whereas five miRNAs (miR-323b, miR-369, miR-376a-2, miR-376c and miR-382) did not express in the treated sample, as shown in **Figure 4.13**.

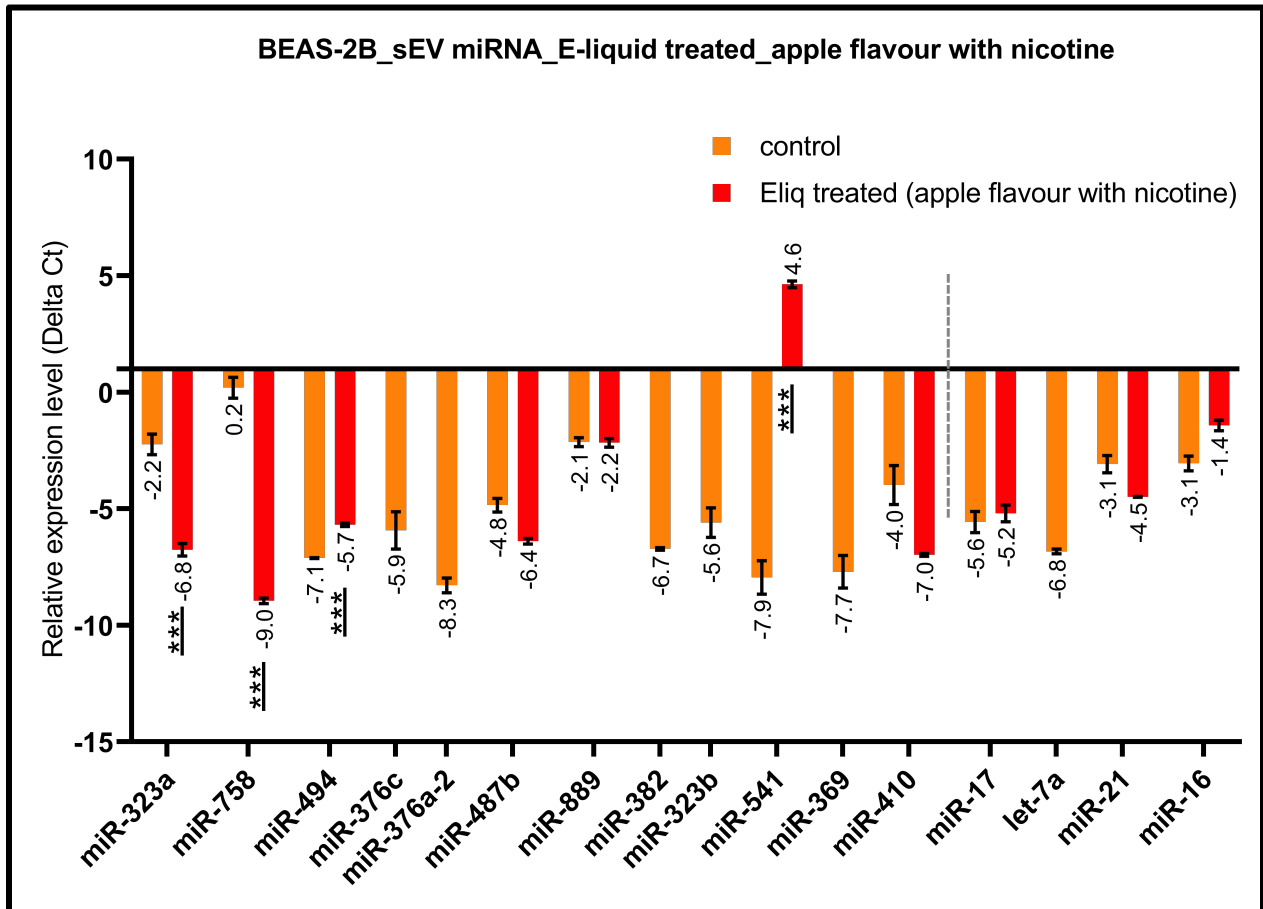


Figure 4.13: Differentially expressed miRNAs in BEAS-2B sEV sample upon E-liquid (apple flavour with nicotine) treatment: sEV isolated miRNAs from control and apple flavoured E-liquid with nicotine treated samples to perform miRNA expression profile (relative expression) of C14MC miRNAs in BEAS-2B cells. The relative expression was normalised with Cel-39. The dotted grey line represents the separation of C14MC and non-cluster miRNAs. The experiment was performed in duplicates, and miR-17 was considered a positive control. P-value was calculated by performing an unpaired student t-test with an adjusted p-value using Holm Sidak correction method for multiple comparisons (***) $p < 0.001$.

4.1.2.9 miR-758 was significantly downregulated upon treatment with apple flavour E-liquid - with no nicotine in lung cells

In A549, 12 miRNAs from C14MC were found expressed in sEVs when treated with apple flavour E-liquid with no nicotine. Among these, four miRNAs (miR-323a, miR-487b, miR-541 and miR-758) were found to be significant.

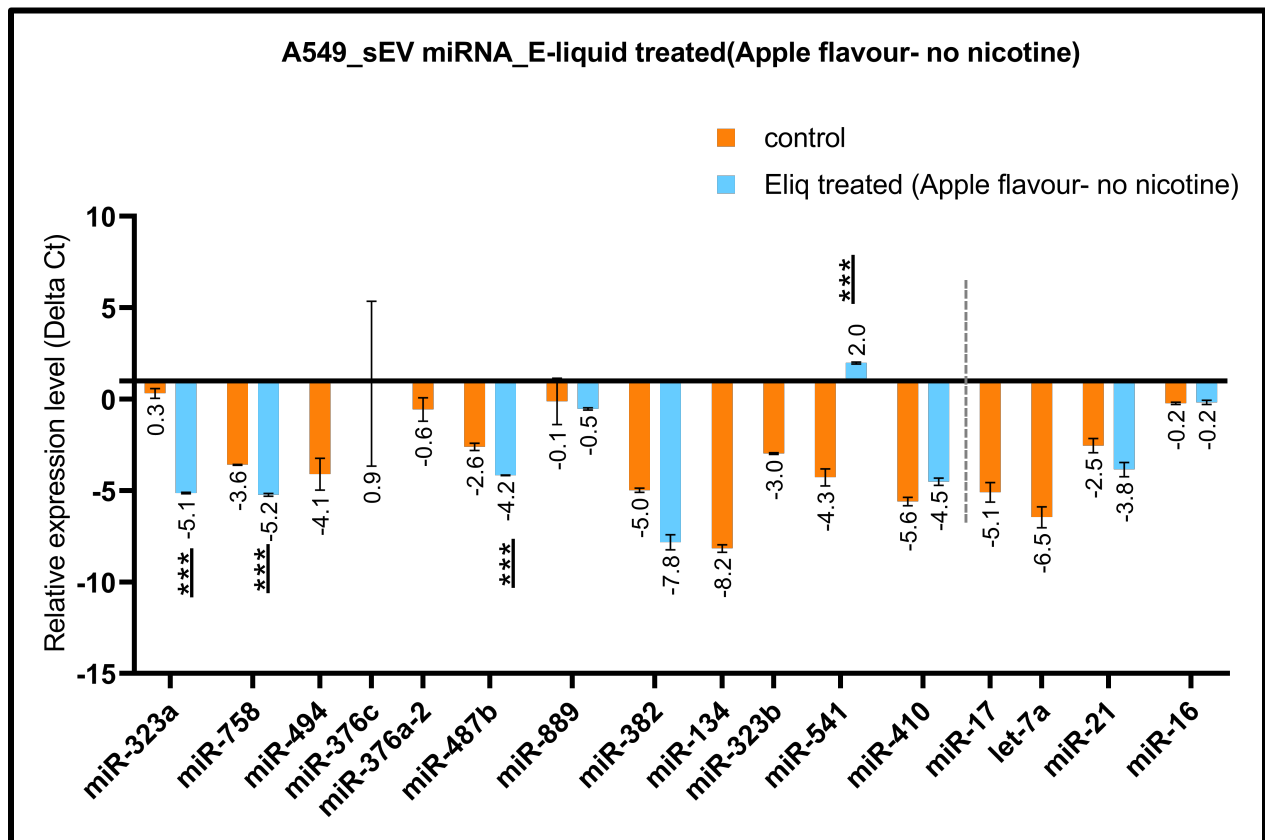


Figure 4.14: Differentially expressed miRNAs in A549 sEV sample upon E-liquid (apple flavour with no nicotine) treatment: sEV isolated miRNAs from control and apple flavoured E-liquid with no nicotine treated samples to perform miRNA expression profile (relative expression) of C14MC miRNAs in A549 cells. The relative expression was normalised with Cel-39. The dotted grey line represents the separation of C14MC and non-cluster miRNAs. The experiment was performed in duplicates, and miR-17 was considered a positive control. P-value was calculated by performing an unpaired student t-test with an adjusted p-value using Holm Sidak correction method for multiple comparisons (***) $p < 0.001$.

Of these four, three miRNAs (miR-323a, miR-487b and miR-758) were downregulated, whereas miR-541 showed the opposite trend when compared to control, as shown in **Figure 4.14**.

Further, miR-323b, miR-376a-2, miR-376c, miR-494 and miR-134 were not expressed in the treated sample. However, all the miRNA expressed were found to be downregulated except miR-541.

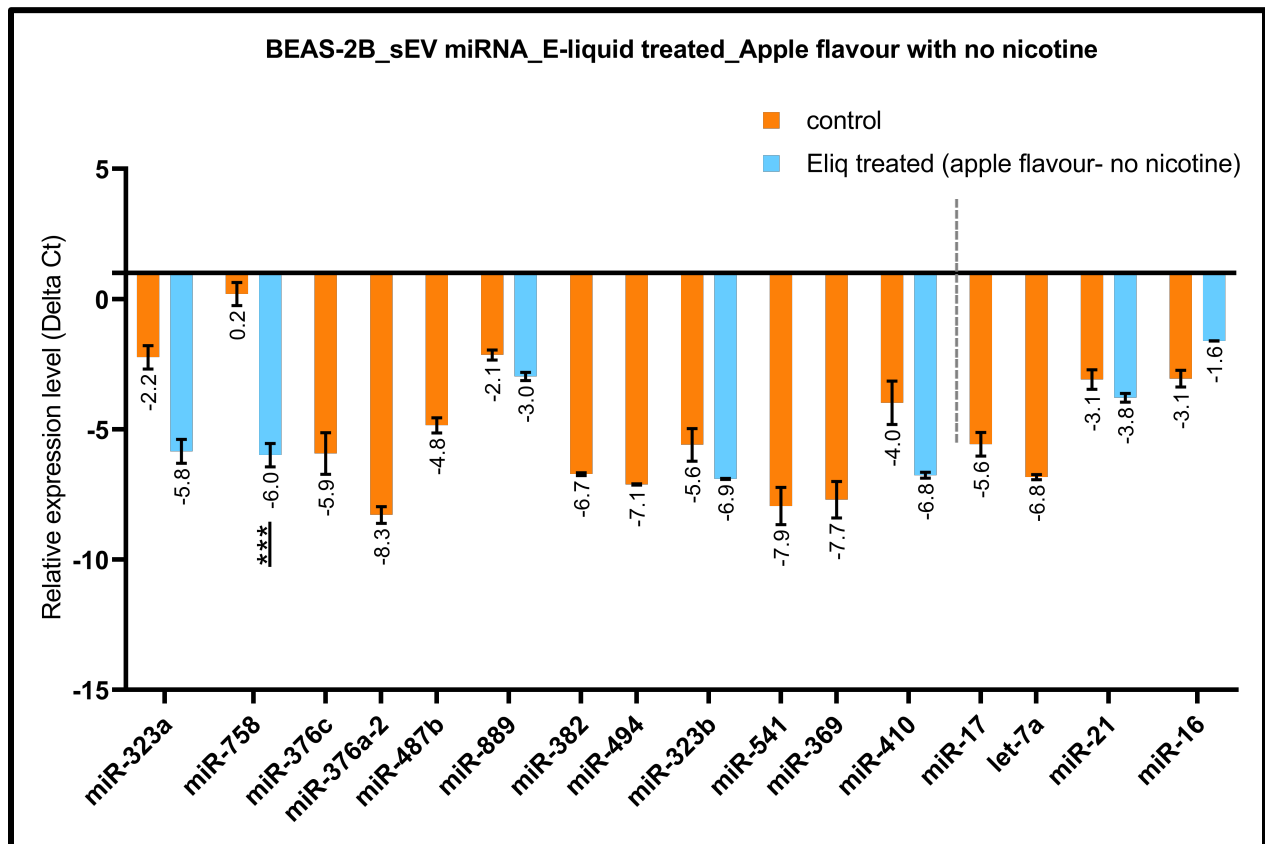


Figure 4.15: Differentially expressed miRNAs in BEAS-2B sEV sample upon E-liquid (apple flavour with no nicotine) treatment: sEV isolated miRNAs from control and apple flavoured E-liquid with no nicotine treated samples to perform miRNA expression profile (relative expression) of C14MC miRNAs in BEAS-2B cells. The relative expression was normalised with Cel-39. The dotted grey line represents the separation of C14MC and non-cluster miRNAs. The experiment was performed in duplicates, and miR-17 was considered a positive control. P-value was calculated by performing an unpaired student t-test with an adjusted p-value using the Holm Sidak correction method for multiple comparisons (***) $p < 0.001$.

In BEAS-2B, 12 miRNAs were found in sEV samples when treated with apple flavour E-liquid (with no nicotine). All these 12 miRNAs were downregulated. miR-758 was found to be significantly downregulated with a $p < 0.05$. Seven miRNAs (miR-369, miR-376a-2, miR-376c, miR-382, miR-487b, miR-494 and mir-541) were not expressed in treated samples, as shown in **Figure 4.15**.

4.1.2.10 Differential expression of C14MC miRNAs among sEV derived miRNAs from nicotine treated and flavoured E-liquid (strawberry and apple- with and without nicotine) when compared to control in lung cells

A549- sEV fraction					
miRNA	Nic treated	Eliq-stra+nic	Eliq-stra-nic	Eliq-App+nic	Eliq-App-nic
C14MC					
miR-379					
miR-323a	0.01	0.14	0.05		0.02
miR-758	0.03	12	0.39	0.02	0.32
miR-376a-2	0.01				
miR-487b	0.02	0.3	0.8	0.14	0.34
miR-889	0.01	4.29	0.25	0.24	0.75
miR-382	0.01	3.26	30.8	0.35	0.14
miR-323b	0.03	1.64	1.13	0.35	
miR-377					
miR-541	0.01	2.27		>100	76.34
miR-410	4.58	2.58	1.76	1.09	2.14
Non-cluster miRNAs					
miR-17	0.01	0	0	0	
Let-7a	0.01	0.73	1.41	0.26	0.41
hsa-miR-16	0.01	0.01	0.64	0.44	1.04
miR-155					

Figure 4.16: Heatmap for A549 derived sEV samples; showing differential expression (Fold change) of C14 miRNAs in A549 cell treated with nicotine, strawberry flavour E-liquid with nicotine (Eliq-stra+nic), strawberry flavour E-liquid without nicotine (Eliq-stra-nic), apple flavour E-liquid with nicotine (Eliq-app+nic) and apple flavour E-liquid without nicotine (Eliq-app-nic) for 72hrs of incubation. The fold change was calculated against the untreated/control sample and normalised with cel-39. The experiment was performed in duplicates, and miR-17 was considered a positive control. Any fold change greater than 100 was represented as >100. (Red indicates upregulation ≥ 1.5 , green indicates downregulation ≤ 0.6 , black-not differential ranging 0.6-1.5, light blue indicates no expression).

In A549, 12 miRNAs from C14MC were tested for expression profiles across the board. Three miRNAs (miR-155, miR-377 and miR-379) were not found in sEV samples, as shown in **Figure 4.16**.

As mentioned earlier, many miRNAs did not express in E-liquid samples. Further, only five miRNAs (miR-382, miR-410, miR-487b, miR-758 and miR-889) were seen expressed in all the samples. Additionally, two miRNAs (miR-410 and miR-541) were found upregulated in at least three out of five samples. Simultaneously, three miRNAs (miR-323a, miR-487b and miR-758) were found downregulated in four out of five samples. And two miRNAs (miR-382 and miR-889) showed downregulation in at least three out of five samples. Therefore, the expression of all these miRNAs may be used to differentiate the effect of different nicotine-containing toxicants.

In BEAS-2B, 11 miRNAs were tested for miRNA profiling. Three miRNAs (miR-155, miR-377 and miR-379) were not found in sEV samples. Three miRNAs (miR-410, miR-758 and miR-889) were found across all the samples.

BEAS-2B-sEV fraction					
miRNAs	Nic treated	Eliq(Str+nic)	Eliq(Str+nic)	Eliq(App+nic)	Eliq(App+nic)
C14MC					
miR-379					
miR-758	0.02	0.1	0.03	0.97	0.01
miR-494	4.69	5.12		2.69	
miR-487b	0.8			0.34	
miR-889	0.29	5.33	1.97	0.42	0.56
miR-382	0.94	9.32	1.51	0.35	
miR-323b	3.04	29.65	1.47		0.4
miR-377					
miR-541	0.76	>100	>100	>100	
miR-410	0.05	2.63	0.06	2.08	0.15
Non-cluster miRNAs					
miR-17	2.26		1.57		
Let-7a	1.74				
miR-21	0.16	3.05	1.67	0.26	0.61
miR-16	0.09	18.9	0.69	0.12	2.73
miR-155					

Figure 4.17: Heatmap for BEAS-2B derived sEV samples; showing differential expression (Fold change) of C14 miRNAs in BEAS-2B cell treated with nicotine, strawberry flavour E-liquid with nicotine (Eliq-stra+nic), strawberry flavour E-liquid without nicotine (Eliq-stra-nic), apple flavour E-liquid with nicotine (Eliq-app+nic) and apple flavour E-liquid without nicotine (Eliq-app-nic) for 72hrs of incubation. The fold change was calculated against the untreated/control sample and normalised with cel-39. The experiment was performed in duplicates, and miR-17 was considered a positive control. Any fold change greater than 100 was represented as >100. (Red indicates upregulation ≥ 1.5 , green indicates downregulation ≤ 0.6 , black-not differential ranging 0.6-1.5, light blue indicates no expression).

Two miRNAs (miR-494 and miR-541) were found upregulated in three of the five samples, and two miRNAs (miR-323b, miR-382, miR-410 and miR-889) were upregulated in two out of five samples. miR-758 was found to be downregulated in four of the five samples, as shown in **Figure 4.17**. Taken together, most of the samples showed upregulated miRNAs.

4.2 Small RNA sequence analysis using NGS

4.2.1 Various quality control checks were performed during the NGS data analysis

In this study, various QC steps were performed for NGS. The first one was the Mean quality score. The mean quality score is interpreted in the Phred-scale score. A Phred score of 20 or above is acceptable, because it qualifies 99% accuracy, with a 1% chance of error. Usually, a sequence of data should have a Phred score of >Q30. This gives confidence that all the data obtained are accurate, supported by the per base N content plot in **appendices- Figure A.2**, which showed bases at each position with no rise in the curve.

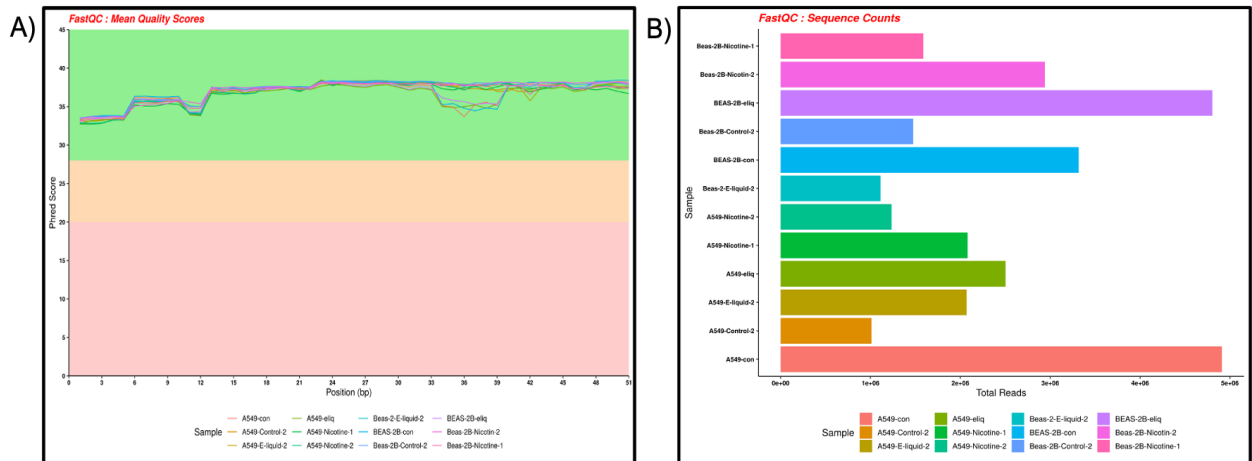


Figure 4.18: Mean Quality score plot A) and Sequence Counts plot B) obtained from NGS data analysis: The plot A) with mean score showed a range of 30-40 Phred score. Plot B) showed a total read count with a range from ~ 1 million to ~ 5 million reads.

The mean quality score shown in the plot showed a Phred score in the range of 30-40, which is an acceptable range with 99.99% accuracy as shown in **Figure 4.18 A)**. The sequence count plot showed that there are a total of 12 samples in total. All the

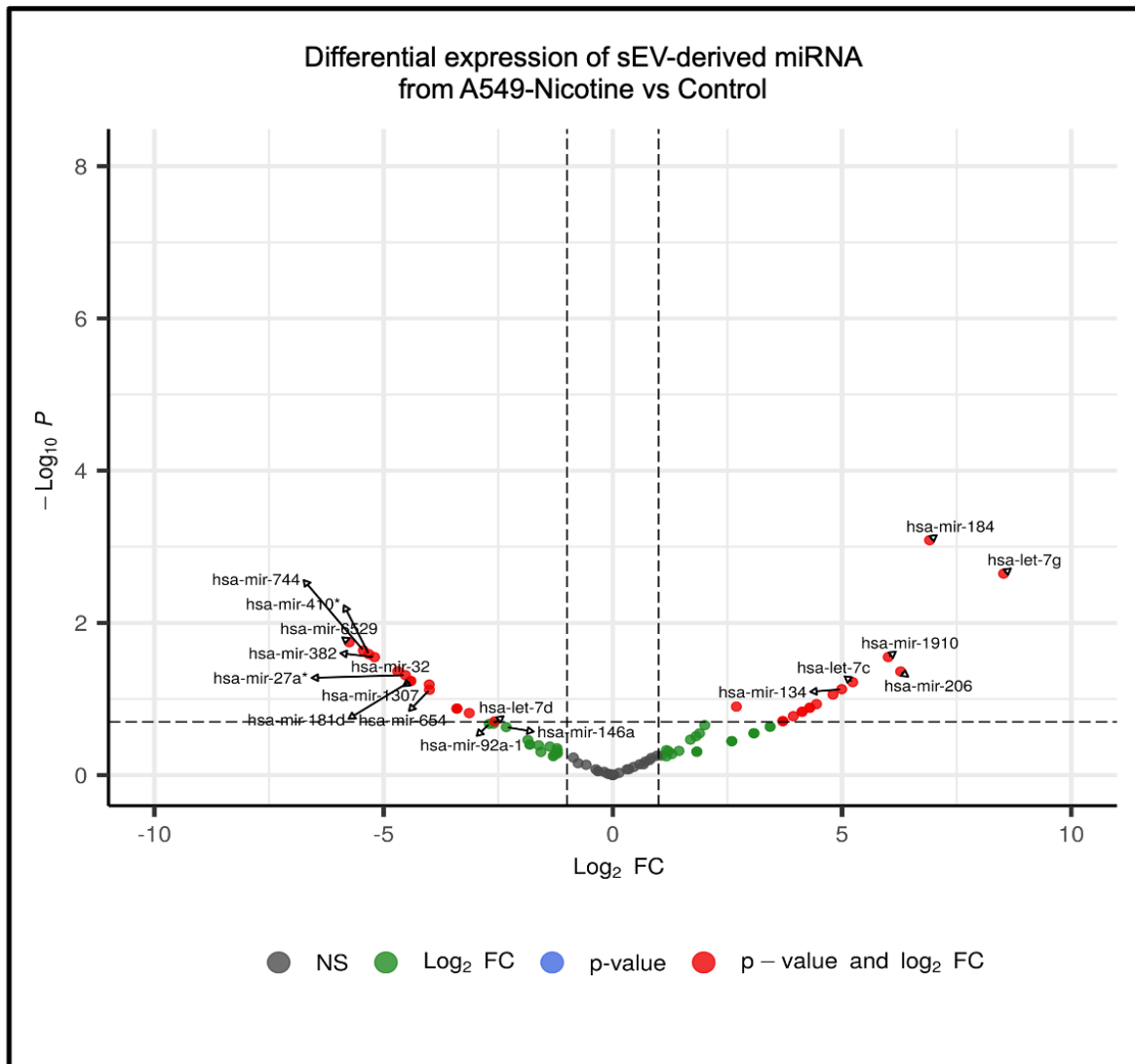
samples produced a total read count with a minimum of ~1 million to ~5 million reads as shown in **Figure 4.18 B**).

4.2.2 Identification of novel biomarkers from sEV derived miRNAs in lung cells treated with nicotine compared to control.

In this study, small RNA next-generation sequencing (small RNA-seq) was performed to compare the sEV derived miRNA isolated from control and nicotine treated lung cells. A total of 3823 miRNAs were detected in isolated sEV derived miRNAs. A change in the expression of miRNA with more than two-fold increase or decrease with a p-value <0.05, miRNAs were considered significant.

In A549 as shown in **Figure 4.19 A**), the volcano plot revealed that the expression of 10 miRNAs was significant in nicotine treated samples when compared to control. Four miRNAs (Let-7g, miR-184, miR-1910, miR-206) showed significant upregulation. Whereas six miRNAs (miR-27a*, miR-32, miR-382, miR-410*, miR-6529 and miR-744) showed significant downregulation.

A)



B)

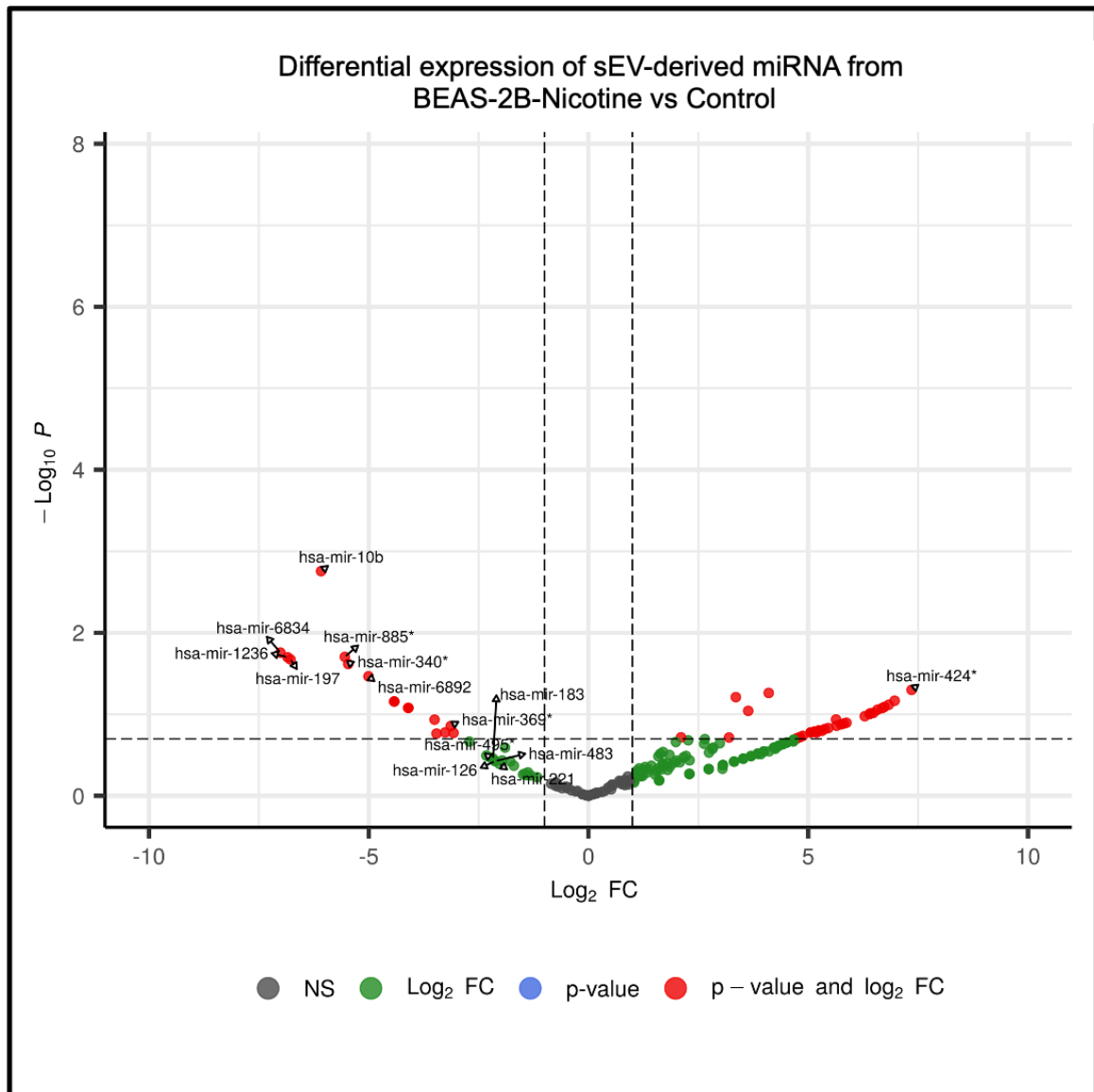


Figure 4.19: Volcano plot of sEV derived miRNA from A549 and BEAS-2B treated with nicotine compared to control: The volcano plot was constructed using fold-change values, P values, and differentially expressed miRNAs. The plot shows the intensity of miRNA expressed between sEV derived miRNA from control and nicotine treated A) A549 and B) BEAS-2B cells. The horizontal axis presents the log₂ ratio and the vertical axis represents -log₁₀ (ANOVA, P-value). The red colour indicates that the expression of sEV derived miRNAs was significant. The left side of the plot shows upregulated miRNAs, and the right side of the plot indicates downregulated miRNAs in the nicotine treated group compared to the control.

In BEAS-2B, eight miRNAs (miR-10b, miR-1236, miR-197, miR-340*, miR-6834, miR-6892 and miR-885*) were found to be significant upon nicotine treatment when

compared to control. All the eight samples were significantly downregulated with a fold change of greater than -5 as shown in **Figure 4.19 B**).

The fold change is mentioned in **Table 4.1**

Table 4.1: List of significant miRNAs detected in sEVs from nicotine treated samples from A549 and BEAS-2B: were A) miRNAs detected in A549 treated with nicotine Log Fold change and P-value, B) miRNAs detected in BEAS-2B treated with nicotine Log Fold change and P-value. These miRNAs were identified based on one-way ANOVA.

A)

A549-Nicotine treated vs control		
miRNA	Log FC	Pvalue
hsa-let-7g	8.52	0.00
hsa-mir-184	6.91	0.00
hsa-mir-1910	6.01	0.03
hsa-mir-206	6.28	0.04
hsa-mir-27a*	-4.53	0.05
hsa-mir-32	-4.69	0.04
hsa-mir-382	-5.20	0.03
hsa-mir-410*	-5.32	0.03
hsa-mir-6529	-5.75	0.02
hsa-mir-744	-5.44	0.02

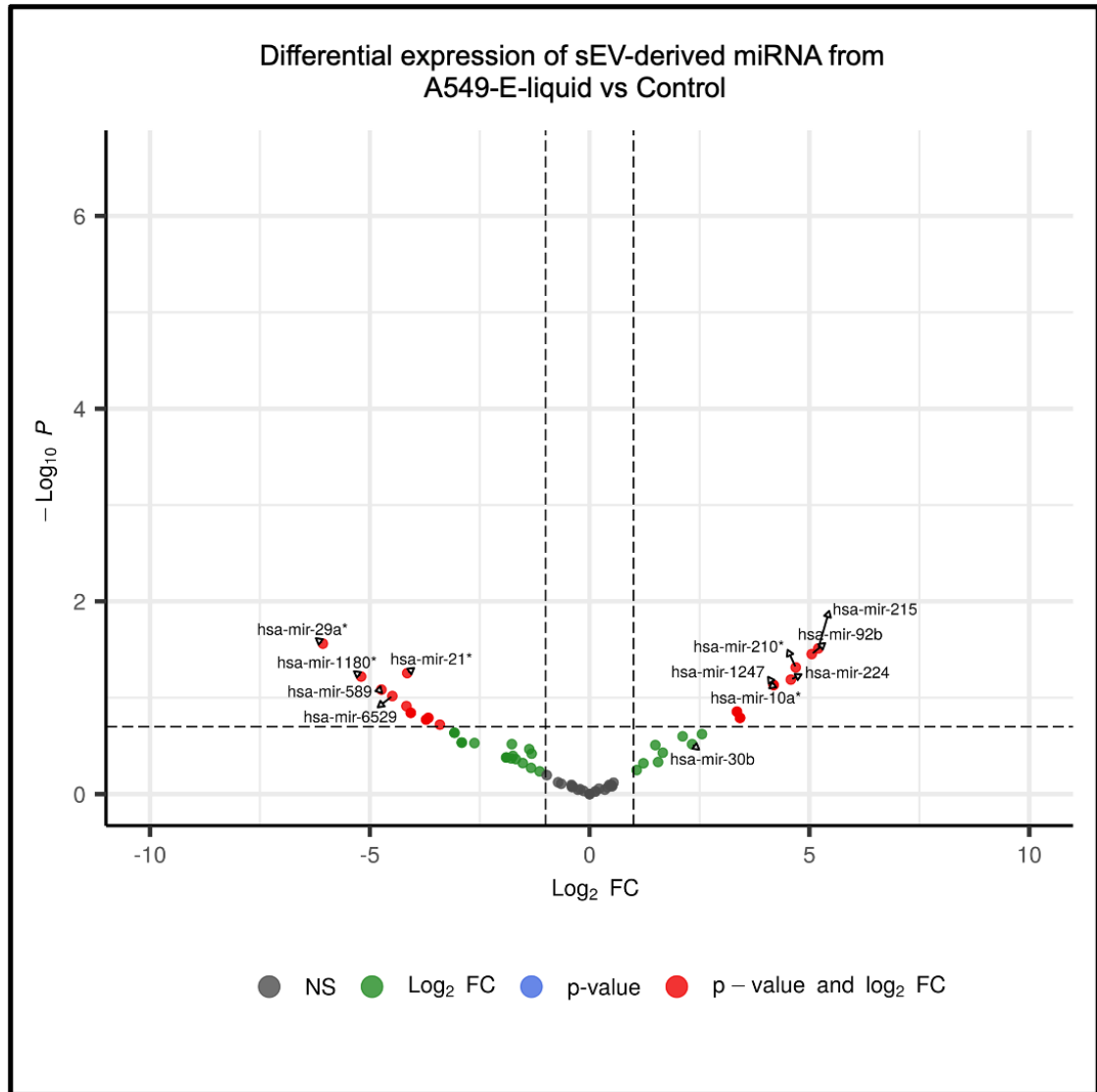
B)

Beas-2B-Nicotine treated vs control		
miRNA	logFC	PValue
hsa-mir-10b	-6.08	0.00
hsa-mir-1236	-6.84	0.02
hsa-mir-197	-6.78	0.02
hsa-mir-340*	-5.47	0.02
hsa-mir-6834	-7.01	0.02
hsa-mir-6892	-5.01	0.03
hsa-mir-885*	-5.54	0.02

4.1.1.1 Identification of novel biomarkers from sEV derived miRNAs in lung cells treated with strawberry flavour E-liquid - with nicotine compared to control.

As mentioned earlier, a total of 3823 miRNAs were detected from the samples treated with strawberry flavour E-liquid (with nicotine) compared to control. And a change in the expression of miRNA with more than two-fold increase or decrease with a p-value of <0.05, miRNAs were considered significant.

A)



B)

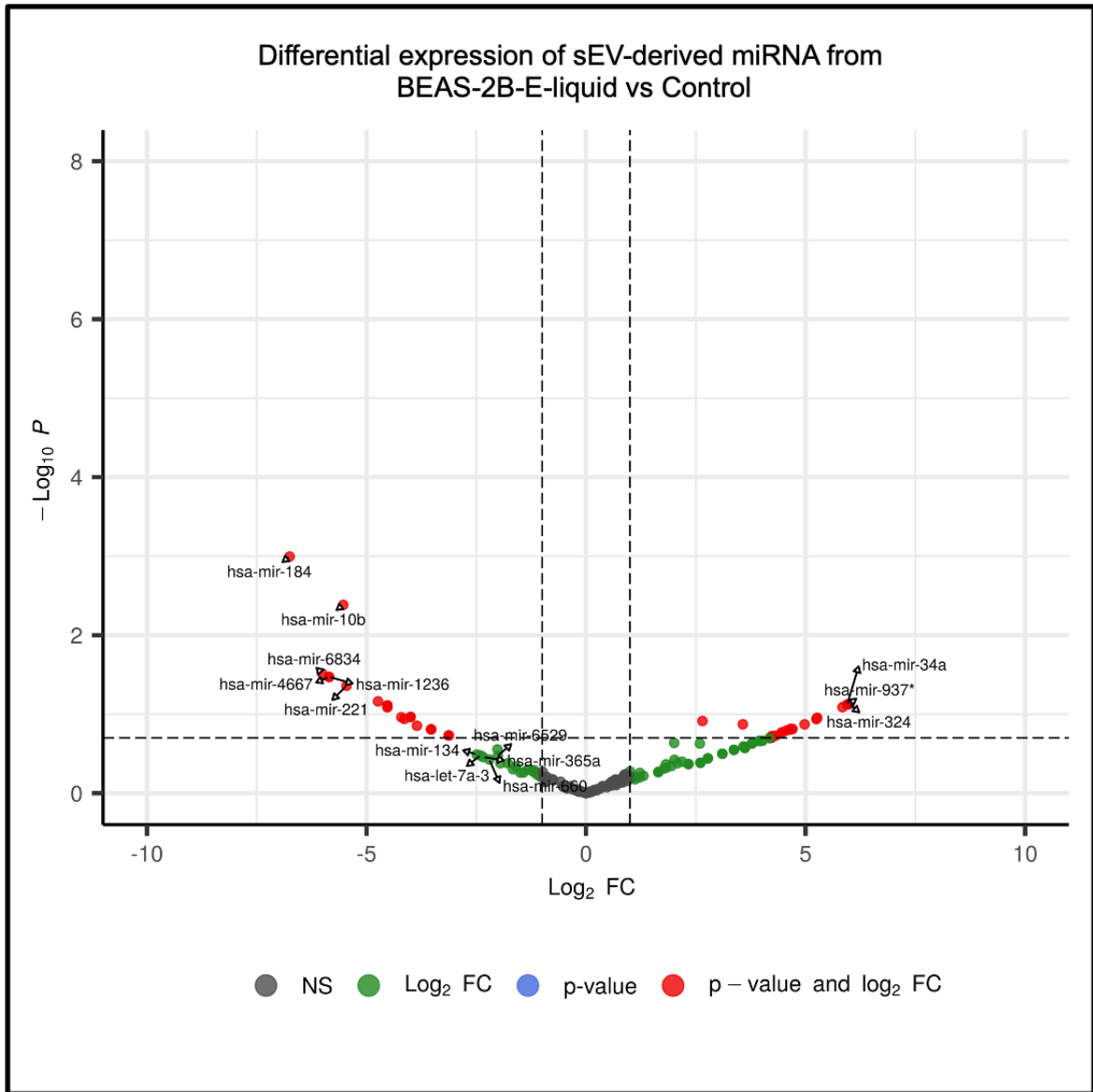


Figure 4.20: Volcano plot of sEV derived miRNA from A549 and BEAS-2B treated with strawberry flavoured E-liquid (with nicotine) compared to control: The volcano plot was constructed using fold-change values, P values, and differentially expressed miRNAs. The plot shows the intensity of miRNA expressed between sEV derived miRNA from control and strawberry flavoured E-liquid (with nicotine) treated A) A549 and B) BEAS-2B cells. The horizontal axis presents the log_2 ratio and the vertical axis represents $-\text{log}_{10}$ (ANOVA, P-value). The red colour indicates that the expression of sEV derived miRNAs was significant. The left side of the plot shows upregulated miRNAs, and the right side of the plot indicates downregulated miRNAs in the nicotine treated group compared to the control.

In A549, four miRNAs (miR-210*, miR-215, miR-29a* and miR-92b) were significant and in BEAS-2B, six miRNAs (miR-10b, miR-1236, miR-184, miR-221, miR-4667 and miR-6834) were found significant upon E-liquid treatment. In A549, three miRNAs (miR-210* miR-215 and miR-92b) were upregulated with a fold change of greater than 4-fold and miR-29a* was downregulated with - 6-fold as shown in **Figure 4.20 A**). Whereas in BEAS-2B, all these miRNAs were significantly downregulated with a fold change of ≥ 5 as shown in **Figure 4.20 B**).

Taken all the data together three miRNAs (miR-10b, miR-1236 and miR-6834) were commonly detected in the BEAS-2B cell line with nicotine and E-liquid treatments. These three miRNAs were significantly downregulated with the treatment and were showing a similar downtrend. Whereas miR-184 was detected in nicotine treated A549 and E-liquid treated BEAS-2B.

The fold change is mentioned in **Table 4.2**

Table 4.2: List of significant miRNAs detected in sEVs from E-liquid treated (strawberry flavour-with nicotine)samples from A549 and BEAS-2B: were A) miRNAs detected in A549 treated with nicotine Log Fold change and P-value, B) miRNAs detected in BEAS-2B treated with nicotine Log Fold change and P-value. These miRNAs were identified based on one-way ANOVA.

A)

A549-E-liquid treated vs control		
miRNA	logFC	PValue
hsa-mir-210*	4.69	0.05
hsa-mir-215	5.20	0.03
hsa-mir-29a*	-6.07	0.03
hsa-mir-92b	5.05	0.04

B)

Beas-2B-E-liquid treated vs control		
miRNA	logFC	PValue
hsa-mir-10b	-5.53	0.00
hsa-mir-1236	-5.85	0.03
hsa-mir-184	-6.75	0.00
hsa-mir-221	-5.46	0.04
hsa-mir-4667	-5.85	0.03
hsa-mir-6834	-6.01	0.03

4.2.3 Discussion

In this study A549 and BEAS-2B treated with nicotine, and different flavours of E-liquid (with and without nicotine) for 72 hours. Small EVs were isolated from cultured

media to evaluate the miRNA expression using qPCR. As mentioned in the earlier section **4.1.2.2**, there was no endogenous expression of U6 in A549 treated with E-liquid. U6 expression values were needed to normalise the data. Therefore, A549 with E-liquid treated endogenous miRNA data were not analysed.

We chose 15 miRNAs from C14MC which are known to be dysregulated in lung disease and four non-cluster miRNAs based on previous literature (Nadal et al., 2014). Seven out of 15 miRNAs from C14MC and three out of four non-cluster miRNAs were significantly dysregulated in nicotine treated samples compared to control. The remaining miRNAs did not show a significant change in their expression levels among these samples.

Similarly, five out of 15 from C14MC and one of four non-cluster miRNA were significantly dysregulated in strawberry flavour E-liquid treated sample, and seven out of 15 miRNAs from C14MC were significantly dysregulated in apple flavour E-liquid treated samples compared to control. The qPCR analysis did not show significant changes in the remaining miRNAs. However, most of the sEV miRNAs showed a trend of downregulation in nicotine treated sample (miR-323a, miR-382, miR-487b, miR-541 and miR-758) and upregulation in E-liquid treated samples. Our data on cell viability assay showed significant cell death which can suggest the enrichment of sEV-mediated miRNAs from E-liquid treated samples (**Figure 3.1** and **Figure 3.2**).

Interestingly, in A549, miR-376a-2 showed significant downregulation in nicotine treated sample. However, there was no expression in E-liquid samples. In BEAS-2B, miR-541 showed no change in expression but showed upregulation in E-liquid samples.

Another key finding in this study was the differential expression of miR-758, which was significant across all the samples.

Some of the miRNA, which was found significant were miR-382, miR-541, miR-410, miR-889 and miR-758.

We performed small RNA-sequence analysis in duplicates and combined the data to interpret the differential expression of all miRNAs. We found 16 novel miRNAs from nicotine treated samples and 10 miRNAs from E-liquid samples. The key miRNA was miR-382 which was significant in nicotine treated sample. The downregulation of miR-382 in nicotine treated A549 cells sample was observed in qPCR which was also confirmed in small RNA sequence data. The fold change can be seen in **Table 4.3**.

Table 4.3: Downregulation of miR-382 in nicotine treated A549 cells sample using both qPCR and NGS techniques

miRNA	qPCR	NGS
hsa-miR-382	0.01	-5.20

miR-382 shows tumour-suppressive functions have been reported in colorectal cancer by targeting SP1 gene (Ren et al., 2018) and NR2F2 gene (Zhou et al., 2016). miR-382 is seen upregulated in gastric adenocarcinoma tissues (Seo et al., 2019) and in breast cancer (Ho et al., 2017). Additionally, sEV miR-382 has been reported in NSCLC where its downregulation is shown associated with poor overall survivability (Luo et al., 2021).

Further, miR-541 was found to be overexpressed in lung fibroblasts which may inhibit mortality of human lung fibroblasts thereby regulating lung fibrosis by targeting

cyclic nucleotide phosphodiesterase 1A (Ren et al., 2017). However, there were no studies found with the reference to sEV miR-541 as of present times.

Studies showed that miR-410 affects the proliferation and apoptosis of A549 cells by regulating SOCS3/JAK-STAT signalling pathway (Li et al., 2020). Another study showed that miR-410 induces epithelial-mesenchymal transition and radioresistance by activating PI3K/mTOR pathway in NSCLC (Yuan et al., 2020). Additionally, increased levels of miR-410 can induce stem cell markers like Sox2, Oct4, Nanog, CXCR4 as well as stem cell surface markers CD44 and CD166 in NSCLC (Ke et al., 2017). miR-410 thereby acts as an oncogene in NSCLC by downregulating SLC34A2 activating Wnt/ β -catenin pathway (Zhang et al., 2016). Further, it targets BRD7 promoting cell proliferation in NSCLC (Li et al., 2015). However, there are no studies found with a reference to sEV miR-410 of present times.

Previous studies showed that miR-889 targets TAB1 (TGF- β -activated kinase 1-binding protein) and these are inversely correlated. The study showed that expression of miR-889 is low in NSCLC tissues and cell lines and can be associated with tumour, node and metastasis stages of NSCLC patients. Thus, miR-889 inhibits NSCLC by targeting TAB1 mRNA causing the progression of the NSCLC (Dong et al., 2019). Another study reported that miR-889 was increased in NSCLC cancer tissues compared to adjacent tissues. The potential target of miR-889 was KLF9. Additionally, the upregulation of miR-889 was enhancing tumorigenesis in vitro and KLF9 was reduced. Thus, showed miR-889 to have a potential therapeutic role in NSCLC (Han et al., 2019). However, there were no studies found with the reference to sEV miR-889 as of current times.

Furthermore, miR-758 targets HMGB3 (high mobility group box) which inhibits proliferation, invasion, migration and increased apoptosis in NSCLC cells thereby may provide a target for the treatment (Zhou et al., 2019). However, there are no studies with reference to sEV miR-758 as of the current times.

Dysregulation of miRNA is seen in many disease conditions, including cancer. MiRNA contributes to cancer progression by targeting genes that are involved in cell proliferation, migration, invasion and angiogenesis (Hanahan & Weinberg, 2011). This study investigates microRNAs with the potential to be used as biomarkers in the case of lung injury. Investigation of miRNA expression may provide diagnostic and prognostic markers, which may have the potential to be used as a non-invasive biomarker in associated lung diseases. Further studies will be required to understand the effect of such EV mediated miRNAs on biological pathways impacting cellular phenotype.

In order to explore whether EV miRNA could have the potential to be used as a biomarker and to compare the effect of nicotine and E-liquids, we used 2D cell culture as a model to mimic the physiological condition of exposure to these toxicants.

This is the only study in our knowledge where nicotine and flavoured E-liquids were compared to find candidate miRNA in the case of E-liquid associated lung injury, especially sEV derived miRNA as a non-invasive biomarker. The drawback of this study is that it is difficult to mimic the normal human physiological conditions; thus as a future plan, these miRNAs need to be validated using human samples with a history of smoking or vaping.

CHAPTER 5 : General discussion and conclusions

E-liquid or vaping associated lung injury (EVALI) is a recently reported condition where patients required critical care (Hayes et al., 2022). Due to the recent surge and popularity of E-liquid use, there are not many studies yet to identify biomarkers for the diagnosis and monitoring of E-VALI. Samples like bronchoalveolar lavage fluid (BALF) have been shown to be used for EVALI specific biomarkers (Blount et al., 2020). However, obtaining BALF is an invasive procedure and is painful. The current study focuses on identifying sEV derived miRNA as a source of non-invasive circulating biomarkers (Fan et al., 2018). We focused on a specific cluster of microRNAs on chromosome 14 (C14MC) for its known involvement in human cancers (Laddha et al., 2013). A recent study on lung cancer showed that C14MC members are preferentially loaded into sEVs and were not correlated with their expression levels within the cells (Tsang et al., 2017). Another study showed that the sequence context of the 3' end of mature microRNAs determines their potential to be loaded as cargo in sEVs (Garcia-Martin et al., 2022). It remains to be seen if the preferential loading of C14MC members in sEV can be explained by their sequence context.

We observed, that in BEAS-2B cells, miR-494 was endogenously downregulated but was upregulated in sEV upon nicotine treatment. Similarly, miR-889 showed that same pattern upon E-liquid treatment as shown in **Figure 4.4 B**) and **Figure 4.5**. This apparent mismatch of differential expression between endogenous and sEV miRNA has been also reported earlier (Garcia-Martin et al., 2022) (Tsang et al., 2017).

We also observed scenarios where the sEV miRNA expression change upon treatment matched with the change in the endogenous fraction. For example, miR-382 was downregulated both endogenously and in sEVs, which was also confirmed by both

NGS and qPCR experiments (**Table 4.3**). Additionally, miR-376a-2a from A549 and Let-7a from BEAS-2B were observed to be expressed only in nicotine treated sEVs and not expressed in sEV from E-liquid samples (**Figure 4.16** and **Figure 4.17**). Furthermore, in BEAS-2B, miR-541 showed downregulation in sEV from nicotine treated samples whereas it was upregulated in sEVs from E-liquid treated samples in lung cells (**Figure 4.17**). All these miRNAs are potential biomarkers which can distinguish nicotine exposure from E-liquid exposure in human lung cells.

In conclusion, this study showed that even nicotine-free e-liquids are detrimental to human lung cells, at similar levels of cigarette smoke, and sometimes worse. Our quantitative expression data, partially supported by massive parallel high throughput sequencing, identified five specific microRNAs from C14MC, which can be potential biomarkers specific for E-VALI. There are, miR-382, miR-494, miR-541, miR-376a-2 and miR-889. Further research will be needed where a panel of these non-invasive biomarkers can be validated in the body fluids of smokers and users of E-liquid.

E-liquids have gained a lot of popularity as an alternative to traditional smoking known for the last 10 years (Peck et al., 2018). Studies are ongoing to understand the toxicity of E-liquid in the human health (McDonough et al., 2021). There are pieces of evidence that E-liquid vapour exposure can induce toxicity, oxidative stress and inflammatory responses in lung epithelial cells (Lerner, Sundar, Yao, et al., 2015) which is also reflected in the cell survival assay presented in this thesis (**Figure 3.1** and **Figure 3.2**). The toxicity may be due to the flavourings of E-liquid and not just due to nicotine (Rowell et al., 2017). This was seen in our data where strawberry flavoured E-liquid (without nicotine) has the biggest negative impact on cell survival (**Figure 3.3** and

Figure 3.4).

E-liquid is mainly composed of propylene glycol (PG) mainly used as a solvent and vegetable glycerine to generate vapours which carry the nicotine and other flavours. Once heated, chemicals used for flavouring might create toxic vapours, compromising the health and safety aspect of e-liquids (Ween et al., 2020). Leaching of metalloids from the heating devices can further aggravate the toxic effects of vaping on human lungs (Zhao et al., 2020).

Scientific evidence are now accumulating about the harmful effects of E-liquids and vaping on human cells. In parallel, public health professionals and policymakers are encouraging long term smokers to switch to vaping in an effort to reduce the carcinogenic effects of traditional cigarettes.

There are debates on the safety of E-liquid use and a global campaign from the scientific community to ban these products whereas government-oriented healthcare professionals want to release the distraction of E-liquid usage (Hajek et al., 2019). Moreover, there is a varying legal status for the purchase of electronic cigarettes worldwide. There is no restriction on E-liquids in countries like Canada (Raymond et al., 2018) and the USA to date, however, the USA has recently announced a cap on nicotine amount in E-liquids of 20 mg/ml (Raymond et al., 2018). Countries like Australia have prohibited nicotine-containing products and India (Relita Mendonca et al., 2019) recently banned the sales. On the other hand, in countries like the UK and New Zealand government agencies, charities and healthcare sectors are promoting E-liquid as a life-saving option (Erku et al., 2020). There is an increase in marketing from quitting traditional cigarettes and promoting E-liquid as a safer alternative.

Taking all this together this study suggests that all these factors contribute to the use of E-liquid, impacting the general population and propose to revisit the government policies of suggesting E-liquid as 95% safer than smoking and an option for cigarette cessation (Kmietowicz, 2018). There is a need for greater regulation of E-liquid products with a focus on banning flavourings (Drazen et al., 2019). Strong communication in marketing on the availability of E-liquids and related products is required with the support of the scientific community and policymakers to prevent further loss of life.

Limitations

A major limitation of this study is the way to administrate E-liquid to match the physiological exposure. In this study, E-liquid was added as a solution to the growing cells. This project involves 2D cell culture which might not give a similar outcome to match the normal physiological condition. It would be interesting to expand this project on 3D culture, and organoids and include human samples for validation. Further, this study focuses only on the biomarker aspect of E-liquid after 72 hrs of exposure however it would be interesting to see the long-term exposure and to understand the role of E-liquids in the development and progression of the disease. Moreover, the other limitation of sEVs is that EVs are still not known for their tissue specific aspect. Thus, it will be difficult to differentiate the EVs based on their tissue specific origin irrespective of the source of EVs like blood, urine and serum etc. Another limitation could be the potential dilution effect of EVs from the source of EVs for it to be used as a marker. Additionally, its expected reference range, which has not yet set will also be an limitation.

Future plan

To understand the health risks of E-liquid it is essential to evaluate the long-term exposure studies to the growing concerns about the role and impact of E-liquid on the development and progression of the disease. As a future plan, this project should be extended by adding 3D culture, organoids, animal models and human samples to validate the suggested microRNA panel. Additionally, this study would require further confirmation by including additional cell lines which might show a similar outcome. Further, to spread awareness about the message - “Do not vape Thinking it to be safe”, It is essential to utilise the marketing strategy to convey to reach the common man. Globally, tighter rules and regulations on these vaping products should be incorporated with the help of the collaboration of the scientific community and policymakers to prevent further loss.

A. Appendices

Figure A.1: 3R4F Research grade cigarette



3R4F Preliminary Analysis

Cigarette Design Criteria

Cigarette Length	84 mm
Tobacco Rod Circumference	24.8 mm
Tobacco rod Length	57 mm
Filter Length	27 mm
Total Resistance to Draw (RTD)	128 mm H ₂ O
"Tar"	9.5 mg/cigt

Cigarette Rod		Cigarette Filter	
Filter	3R4F Blend	Tow	Cellulose Acetate 2.9/41,000
Cuts per Inch	30	Plasticizer	9% Triacetin
Paper Permeability	24 CORESTA units	4-up Resistance to Draw	115 mm H ₂ O
Paper Citrate	0.60 %	Circumference	24.45 mm
Tobacco Weight (13% OV)	0.783 mg	Length	27 mm
Length	57 mm		

Target Total Cigarette

Tipping Paper Length	32 mm, white
Dilution	30 +/- 5%
Circumference	24.8 mm
Length	84 mm
Resistance to Draw	128 mm H ₂ O
Weight	1.06 g
Pack Moisture	13% Oven Volatiles

Final Total Cigarette Measurements (n = 11)

Dilution	29 (4.2) %
Circumference	24.9 (0.07) mm
Total Resistance to Draw	133.5 (4.45) mm H ₂ O
Cigarette Weight	1.05 (0.002) g
Tobacco Weight	0.775 (0.001) g
Pack Moisture	12.9 (0.33)% Oven Volatiles
Firmness	2.43 (0.113) mm

Preliminary FTC Smoking Results Average

Butt Length	35 mm
Puff Count	9.0 (0.112)
Total Particulate Matter, TPM	10.9 (0.168) mg/cigt
"Tar"	9.4 (0.142) mg/cigt
Nicotine	0.726 (0.009) mg/cigt
Carbon Monoxide	11.9 (0.208) mg/cigt

Final FTC Smoking Results Average (n=12)

Puff Count	9.0 (0.15)
Total Particulate Matter, TPM	11.0 (0.33) mg/cigt
"Tar"	9.4 (0.30) mg/cigt
Nicotine	0.73 (0.013) mg/cigt
Carbon Monoxide	12.0 (0.48) mg/cigt

Preliminary Filler Analysis

Total Alkaloids	1.98 % (.04) at 13% Oven Volatiles
Reducing Sugars	8.4 % (0.4) at 13% Oven Volatiles
Glycerin	2.7 % (0.1) at 13% Oven Volatiles

Final Filler Analysis (n=23)

Total Alkaloids (as-is)	2.05 % (0.04) at 11.6% Oven Volatiles
Reducing Sugars (as-is)	8.7% (0.3) at 11.6% Oven Volatiles
Glycerin (as-is)	2.36 % (0.05) at 11.6% Oven Volatiles

Blend Summary	2R4F	3RF4
Flue Cured	32.51 %	35.41%
Burley	19.94 %	21.62%
Maryland	1.24 %	1.35%
Oriental	11.08 %	12.07%
Reconstituted (Schweitzer Process)	27.13 %	29.55%
Glycerin (dry-weight basis @ 11.6% OV)	2.80 %	2.67%
Isosweet (Sugar)	5.30 %	6.41%

S. no	miRNA	Primer sequence
Internal controls		
1	Human U6	CTCGCTTCGGCAGCACA
2	Cel- 39-3p	TCACCGGGTGTAATCAGCTTG
C14MC		
1	hsa-miR-379-5p	TGGTAGACTATGGAACGTAGG
2	hsa-miR-323a-5p	AGGTGGTCCGTGGCGCGTTTCGC
3	hsa-miR-758-5p	GATGGTTGACCAGAGAGCACAC
4	hsa-miR-494-5p	AGGTTGTCCGTGTTGTCTTCTCT
5	hsa-miR-376a-2-5p	GGTAGATTTTCCTTCTATGGT
6	hsa-miR-487b-5p	GTGGTTATCCCTGTCCTGTTTCG
7	hsa-miR-889-5p	AATGGCTGTCCGTAGTATGGTC
8	hsa-miR-382-5p	GAAGTTGTTTCGTGGTGGATTTCG
9	hsa-miR-134-5p	TGTGACTGGTTGACCAGAGGGG
10	hsa-miR-323b-5p	AGGTTGTCCGTGGTGGAGTTTCGCA
11	hsa-miR-377-5p	AGAGGTTGCCCTTGGTGAATTC
12	hsa-miR-541-5p	AAAGGATTCTGCTGTCGGTCCCCT
13	hsa-miR-369-5p	AGATCGACCGTGTTATATTCGC
14	hsa-miR-410-5p	AGGTTGTCTGTGATGAGTTTCG
Non- cluster miRNAs		
1	hsa-miR-17-5p	CAAAGTGCTTACAGTGCAGGTAG
2	hsa-Let-7a	TGAGGTAGTAGGTTGTATAGTT
3	hsa-miR-21-5p	TAGCTTATCAGACTGATGTTGA
4	hsa-miR-155-5p	TTAATGCTAATCGTGATAGGGGT

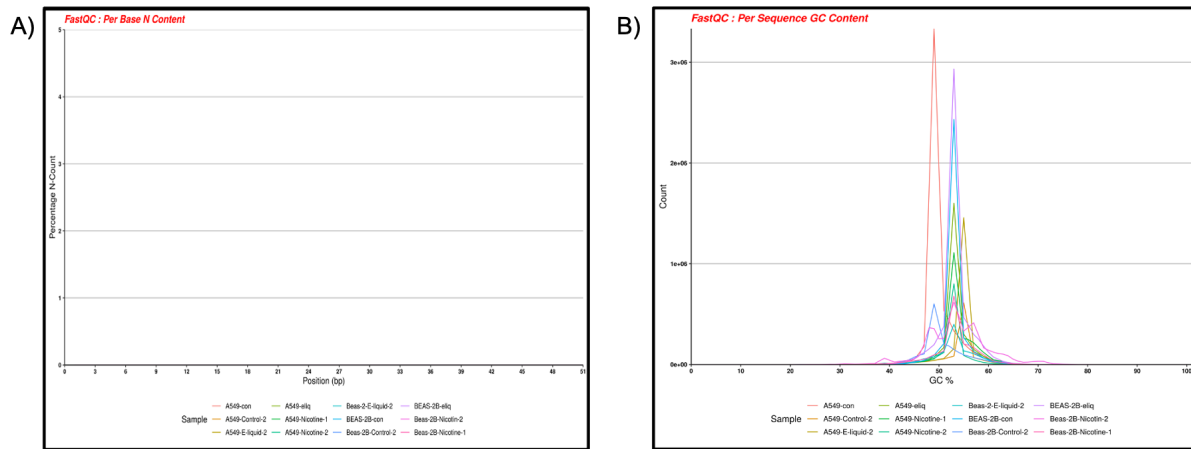


Figure A.2: Per Base N content plot A) and Per Sequence GC content plot B) obtained from NGS data analysis: Plot A) shows the percentage of bases at each position or bin with no base call, “N” and plot B) shows GC content of the data analysed.

The Per Base N content shows the percentage of bases at each position or bin with no base call, “N”. The plot showed that there was no rise in the curve. This indicates that there was no problem occurred during the sequence run as shown in **Error! Reference source not found.2 A)**.

The subsequent QC step was Per Sequence GC Content, which measures the GC content across the length of each sequence and compares the normal distribution of GC content. The miRNA GC content is expected to be 50% in a normal distribution, which is used to build a reference distribution. GC content indicates that there was no contamination of the library as shown in **Error! Reference source not found.2 B)**.

Further, QC for sequence length distribution was performed. This QC shows the distribution of fragment size of the files which were analysed. The plot indicates that there was a variable amount of each different size sequence fragment obtained from each of the samples as shown in **Error! Reference source not found.2**. Later the libraries were trimmed to remove poor quality base calls and the length was made uniform.

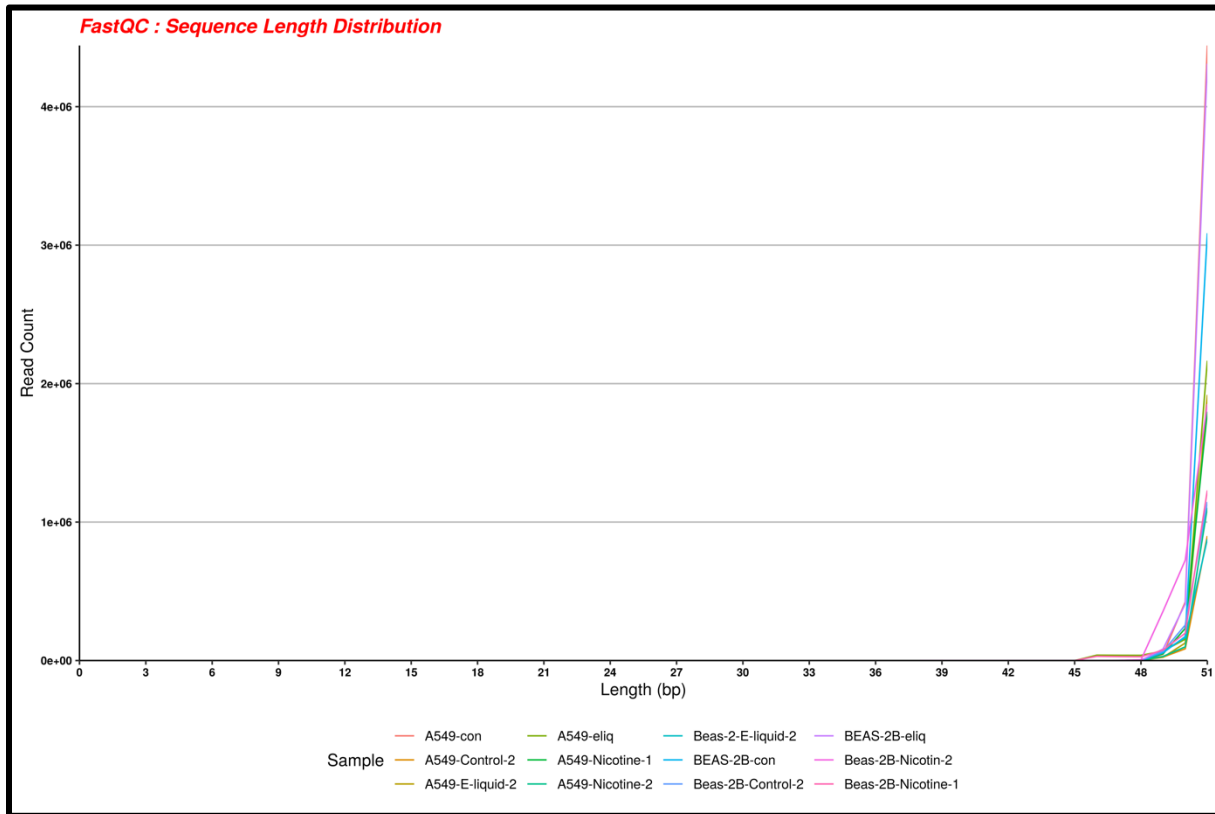


Figure A.3: Sequence Length Distribution plot obtained from NGS data analysis: the graph generated shows the distribution of fragment sizes in the which was analysed.

The sequence data in this study is expected to have a 50 bp single-end sequence as this is a small RNA sequence where miRNA was captured.

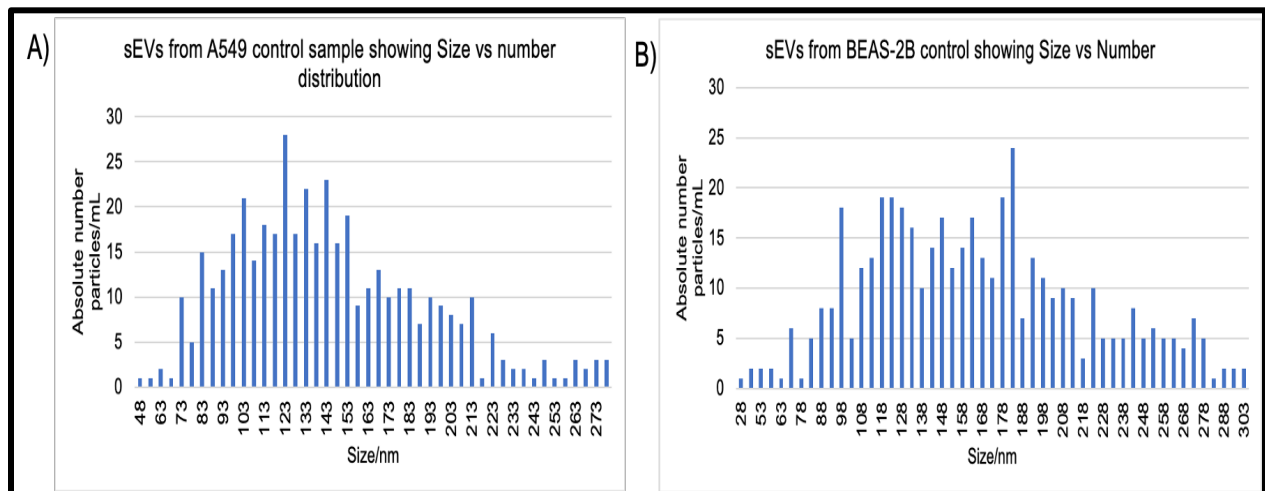


Figure A.4: Size distribution of EV particles measured using NTA: were A) control sEV from A549 and B) is control sEVs from BEAS-2B

A549 control sample	conc. Per/ml	Avg particles/frame	Number of traced particles	% Of particles < 200nm
1	2.7×10^{10}	64	442	94.6
2	8.0×10^9	19	125	82.1
3	5.6×10^9	14	68	64.2
4	7.3×10^9	18	136	81.3
5	6.7×10^9	16	126	74.3
6	7.5×10^9	18	131	78.2

Table A.5 : Characterization of sEVs using NTA: NTA was used to determine the concentration of sEVs along with the percentage of particles which are less than 200 nm were isolated from untreated A549 includes six replicates. These samples were isolated using SEC method and the experiment was performed immediately after isolation.

A549 sample treated with 100 μ M nicotine	conc. Per/ml	Avg particles/frame	Number of traced particles	% Of particles < 200nm
1	8.4×10^9	20	121	58.4
2	1.6×10^{10}	39	252	64.3
3	7.6×10^{10}	18	100	31.1
4	2.6×10^{10}	62	533	54.3
5	1.3×10^{10}	30	202	58.3
6	1.9×10^{10}	46	316	52.1

Table A.6: Characterization of sEVs using NTA: NTA was used to determine the concentration of sEVs along with the percentage of particles which are less than 200 nm were isolated from A549 sample treated with 100 μ M nicotine includes six replicates. These samples were isolated using SEC method and the experiment was performed immediately after isolation.

A549 treated with strawberry flavour E-liquid -100µM nicotine sample	conc. Per/ml	Avg particles/frame	Number of traced particles	% Of particles < 200nm
1	1.6x10 ¹⁰	36	187	60.6
2	1.1x10 ¹⁰	27	126	23.3
3	4.8x10 ⁹	12	23	8.5
4	1.2x10 ⁹	29	144	52.6
5	1.7x10 ¹⁰	41	298	77.1
6	6.4x10 ⁹	15	78	80.1

Table A.7: Characterization of sEVs using NTA: NTA was used to determine the concentration of sEVs along with the percentage of particles which are less than 200 nm were isolated from A549 sample treated with 100 µM strawberry flavour E-liquid with nicotine includes six replicates. These samples were isolated using the SEC method and the experiment was performed immediately after isolation.

Strawberry-no nicotine sample	conc. Per/ml	avg particles/frame	number of traced particles	% of particles <200nm
1	1.2x10 ¹⁰	28	174	63.8
2	1.1x10 ¹⁰	26	159	61.4
3	4.3x10 ¹⁰	103	603	66.6

Table A.8: Characterization of sEVs using NTA: NTA was used to determine the concentration of sEVs along with the percentage of particles which are less than 200 nm were isolated from A549 sample treated with strawberry flavour E-liquid with no nicotine includes three replicates. These samples were isolated using SEC method and the experiment was performed immediately after isolation.

A549 treated with Apple flavour - no nicotine sample	Conc. Per/ml	Avg particles/frame	No. of traced particles	% Of particles <200nm
1	2.4x10 ¹⁰	59	309	76.4
2	2.6x10 ¹⁰	63	441	72.4
3	2.8x10 ¹⁰	67	509	87.5

Table A.9: Characterization of sEVs using NTA: NTA was used to determine the concentration of sEVs along the percentage of particles which are less than 200 nm were isolated from A549 sample treated with apple flavour E-liquid with no nicotine includes three replicates. These samples were isolated using SEC method and the experiment was performed immediately after isolation.

A549 treated with Apple flavour E-liquid -100µM nicotine sample	Conc. Per/ml	Avg particles/frame	Number of traced particles	% Of particles <200nm
1	2.0x10 ¹⁰	48	280	67.8
2	1.4x10 ¹⁰	35	246	67.8
3	3.2x10 ¹⁰	77	516	64.7

Table A.10: Characterization of sEVs using NTA: NTA was used to determine the concentration of sEVs along with the percentage of particles which are less than 200 nm were isolated from A549 sample treated with 100 µM apple flavour E-liquid with nicotine includes three replicates. These samples were isolated using SEC method and the experiment was performed immediately after isolation

BEAS-2B control sample	Conc. Per/ml	Avg particles per frame	No. of traced particles	% Of particles < 200nm
1	6.4x10 ¹⁰	154	990	53.4
2	3.2x10 ¹⁰	78	411	75.3
3	9.7x10 ¹⁰	235	1218	78.8
4	5.0x10 ¹⁰	120	707	52.6
5	8.0x10 ⁹	19	107	63.7
6	3.2x10 ¹⁰	78	462	84.1

Table A.11: Characterization of sEVs using NTA: NTA was used to determine the concentration of sEVs along with the percentage of particles which are less than 200 nm were isolated from untreated BEAS-2B includes six replicates. These samples were isolated using SEC method and the experiment was performed immediately after isolation.

BEAS-2B sample treated with 100µM nicotine	conc. Per/ml	Avg particles per frame	no. of traced particles	% of particles <200nm
1	1.1x10 ¹⁰	26	148	87.1
2	1.6x10 ¹⁰	39	292	36
3	1.9x10 ¹⁰	46	358	50.6
4	1.2x10 ¹⁰	29	191	100
5	9.1x10 ⁹	22	140	77.7
6	5.5x10 ¹⁰	125	524	61.2

Table A.12: Characterization of sEVs using NTA: NTA was used to determine the concentration of sEVs along with the percentage of particles which are less than 200 nm were isolated from BEAS-2B sample treated with 100µM nicotine includes six replicates. These samples were isolated using SEC method and the experiment was performed immediately after isolation.

BEAS-2B treated with strawberry flavour E-liquid - 100mM nicotine sample	conc. Per/ml	Avg particles per frame	no. of traced particles	% of particles <200nm
1	1.2x10 ¹⁰	28	237	53.9
2	1.8x10 ¹⁰	43	244	86.3
3	5.2x10 ⁹	12	65	90.5
4	7.6x10 ¹⁰	184	825	67.2
5	3.8x10 ¹⁰	92	441	11.1
6	2.9x10 ¹¹	700	2171	62.6

Table A.13: Characterization of sEVs using NTA: NTA was used to determine the concentration of sEVs along with the percentage of particles which are less than 200 nm were isolated from BEAS-2B sample treated with 100 µM strawberry flavour E-liquid with nicotine includes six replicates. These samples were isolated using SEC method and the experiment was performed immediately after isolation.

BEAS-2B treated with strawberry flavour E-liquid -no nicotine sample	conc. Per/ml	avg particles per frame	number of traced particles	% Of particles < 200nm
1	8.5x10 ⁹	21	179	90.7
2	2.5x10 ¹⁰	60	337	59.8
3	5.5x10 ¹⁰	134	815	75.7

Table A.14: Characterization of sEVs using NTA: NTA was used to determine the concentration of sEVs along with the percentage of particles which are less than 200 nm were isolated from BEAS-2B sample treated with 100 µM strawberry flavour E-liquid with no nicotine includes three replicates. These samples were isolated using SEC method and the experiment was performed immediately after isolation.

BEAS-2B treated with Apple flavour E-liquid -100mM nicotine sample	conc. Per/ml	Avg particle per frame	number of traced particles	% of particles <200nm
1	1.2x10 ¹⁰	30	177	89.7
2	2.0x10 ¹⁰	47	258	69.4
3	4.7x10 ¹⁰	115	700	87.5

Table A.15: Characterization of sEVs using NTA: NTA was used to determine the concentration of sEVs along with the percentage of particles which are less than 200 nm were isolated from BEAS-2B sample treated with 100 µM apple flavour E-liquid with nicotine includes three replicates. These samples were isolated using SEC method and the experiment was performed immediately after isolation.

BEAS-2B treated with Apple flavour E-liquid -no nicotine sample	Conc. Per/ml	Avg particles per frame	Number of traced particles	% Of particles <200nm
1	2.0x10 ¹⁰	47	380	91.6
2	2.6x10 ¹⁰	62	476	73.4
3	5.9x10 ¹⁰	142	800	69

Table A.16: Characterization of sEVs using NTA: NTA was used to determine the concentration of sEVs along with the percentage of particles which are less than 200 nm were isolated from BEAS-2B sample treated with 100 µM apple flavour E-liquid with no nicotine includes three replicates. These samples were isolated using the SEC method and the experiment was performed immediately after isolation.

CHAPTER 6 : References

- Allen, J. G., Flanigan, S. S., LeBlanc, M., Vallarino, J., MacNaughton, P., Stewart, J. H., & Christiani, D. C. (2016). Flavoring Chemicals in E-Cigarettes: Diacetyl, 2,3-Pentanedione, and Acetoin in a Sample of 51 Products, Including Fruit-, Candy-, and Cocktail-Flavored E-Cigarettes. *Environ Health Perspect*, 124(6), 733-739. <https://doi.org/10.1289/ehp.1510185>
- Altuvia, Y., Landgraf, P., Lithwick, G., Elefant, N., Pfeffer, S., Aravin, A., Brownstein, M. J., Tuschl, T., & Margalit, H. (2005). Clustering and conservation patterns of human microRNAs. *Nucleic Acids Res*, 33(8), 2697-2706. <https://doi.org/10.1093/nar/gki567>
- Andreu, Z., & Yáñez-Mó, M. (2014). Tetraspanins in extracellular vesicle formation and function. *Front Immunol*, 5, 442. <https://doi.org/10.3389/fimmu.2014.00442>
- Armand-Labit, V., & Pradines, A. (2017). Circulating cell-free microRNAs as clinical cancer biomarkers. *Biomol Concepts*, 8(2), 61-81. <https://doi.org/10.1515/bmc-2017-0002>
- Arroyo, J. D., Chevillet, J. R., Kroh, E. M., Ruf, I. K., Pritchard, C. C., Gibson, D. F., Mitchell, P. S., Bennett, C. F., Pogosova-Agadjanyan, E. L., Stirewalt, D. L., Tait, J. F., & Tewari, M. (2011). Argonaute2 complexes carry a population of circulating microRNAs independent of vesicles in human plasma. *Proc Natl Acad Sci U S A*, 108(12), 5003-5008. <https://doi.org/10.1073/pnas.1019055108>
- Assinder, S. J., & Bhoopalan, V. (2017). A Promising Future for Prostate Cancer Diagnostics. *Diagnostics (Basel)*, 7(1). <https://doi.org/10.3390/diagnostics7010006>
- Azevedo, L. C., Janiszewski, M., Pontieri, V., Pedro Mde, A., Bassi, E., Tucci, P. J., & Laurindo, F. R. (2007). Platelet-derived exosomes from septic shock patients induce myocardial dysfunction. *Crit Care*, 11(6), R120. <https://doi.org/10.1186/cc6176>
- Bai, X., Hua, S., Zhang, J., & Xu, S. (2019). The MicroRNA Family Both in Normal Development and in Different Diseases: The miR-17-92 Cluster. *Biomed Res Int*, 2019, 9450240. <https://doi.org/10.1155/2019/9450240>
- Banerjee, A., & Luetlich, K. (2012). MicroRNAs as potential biomarkers of smoking-related diseases. *Biomark Med*, 6(5), 671-684. <https://doi.org/10.2217/bmm.12.50>
- Bartel, D. P. (2004). MicroRNAs: genomics, biogenesis, mechanism, and function. *Cell*, 116(2), 281-297. [https://doi.org/10.1016/s0092-8674\(04\)00045-5](https://doi.org/10.1016/s0092-8674(04)00045-5)

- Becker, A., Thakur, B. K., Weiss, J. M., Kim, H. S., Peinado, H., & Lyden, D. (2016). Extracellular Vesicles in Cancer: Cell-to-Cell Mediators of Metastasis. *Cancer Cell*, 30(6), 836-848. <https://doi.org/10.1016/j.ccell.2016.10.009>
- Bengalli, R., Ferri, E., Labra, M., & Mantecca, P. (2017). Lung Toxicity of Condensed Aerosol from E-CIG Liquids: Influence of the Flavor and the In Vitro Model Used. *Int J Environ Res Public Health*, 14(10). <https://doi.org/10.3390/ijerph14101254>
- Biomarkers and surrogate endpoints: preferred definitions and conceptual framework. (2001). *Clin Pharmacol Ther*, 69(3), 89-95. <https://doi.org/10.1067/mcp.2001.113989>
- Blount, B. C., Karwowski, M. P., Shields, P. G., Morel-Espinosa, M., Valentin-Blasini, L., Gardner, M., Braselton, M., Brosius, C. R., Caron, K. T., Chambers, D., Corstvet, J., Cowan, E., De Jesús, V. R., Espinosa, P., Fernandez, C., Holder, C., Kuklenyik, Z., Kusovschi, J. D., Newman, C., . . . Pirkle, J. L. (2020). Vitamin E Acetate in Bronchoalveolar-Lavage Fluid Associated with EVALI. *N Engl J Med*, 382(8), 697-705. <https://doi.org/10.1056/NEJMoa1916433>
- Bobrie, A., Colombo, M., Krumeich, S., Raposo, G., & Théry, C. (2012). Diverse subpopulations of vesicles secreted by different intracellular mechanisms are present in exosome preparations obtained by differential ultracentrifugation. *J Extracell Vesicles*, 1. <https://doi.org/10.3402/jev.v1i0.18397>
- Braun, T., & Gautel, M. (2011). Transcriptional mechanisms regulating skeletal muscle differentiation, growth and homeostasis. *Nat Rev Mol Cell Biol*, 12(6), 349-361. <https://doi.org/10.1038/nrm3118>
- Briers, N., Briers, T. M., Becker, P. J., & Steyn, M. (2015). Soft tissue thickness values for black and coloured South African children aged 6-13 years. *Forensic Sci Int*, 252, 188.e181-110. <https://doi.org/10.1016/j.forsciint.2015.04.015>
- Burstyn, I. (2014). Peering through the mist: systematic review of what the chemistry of contaminants in electronic cigarettes tells us about health risks. *BMC Public Health*, 14, 18. <https://doi.org/10.1186/1471-2458-14-18>
- Buschow, S. I., Nolte-'t Hoen, E. N., van Niel, G., Pols, M. S., ten Broeke, T., Lauwen, M., Ossendorp, F., Melief, C. J., Raposo, G., Wubbolts, R., Wauben, M. H., & Stoorvogel, W. (2009). MHC II in dendritic cells is targeted to lysosomes or T cell-induced exosomes via distinct multivesicular body pathways. *Traffic*, 10(10), 1528-1542. <https://doi.org/10.1111/j.1600-0854.2009.00963.x>
- Butt, Y. M., Smith, M. L., Tazelaar, H. D., Vaszar, L. T., Swanson, K. L., Cecchini, M. J., Boland, J. M., Bois, M. C., Boyum, J. H., Froemming, A. T., Khor, A., Mira-Avendano, I., Patel, A., & Larsen, B. T. (2019). Pathology of Vaping-Associated Lung Injury. *N Engl J Med*, 381(18), 1780-1781. <https://doi.org/10.1056/NEJMc1913069>

- Caby, M. P., Lankar, D., Vincendeau-Scherrer, C., Raposo, G., & Bonnerot, C. (2005). Exosomal-like vesicles are present in human blood plasma. *Int Immunol*, 17(7), 879-887. <https://doi.org/10.1093/intimm/dxh267>
- Cai, X., Hagedorn, C. H., & Cullen, B. R. (2004). Human microRNAs are processed from capped, polyadenylated transcripts that can also function as mRNAs. *Rna*, 10(12), 1957-1966. <https://doi.org/10.1261/rna.7135204>
- Calin, G. A., & Croce, C. M. (2006). MicroRNA signatures in human cancers. *Nature Reviews Cancer*, 6(11), 857-866. <https://doi.org/10.1038/nrc1997>
- Calin, G. A., Sevignani, C., Dumitru, C. D., Hyslop, T., Noch, E., Yendamuri, S., Shimizu, M., Rattan, S., Bullrich, F., Negrini, M., & Croce, C. M. (2004). Human microRNA genes are frequently located at fragile sites and genomic regions involved in cancers. *Proc Natl Acad Sci U S A*, 101(9), 2999-3004. <https://doi.org/10.1073/pnas.0307323101>
- Catto, J. W., Miah, S., Owen, H. C., Bryant, H., Myers, K., Dudzic, E., Larré, S., Milo, M., Rehman, I., Rosario, D. J., Di Martino, E., Knowles, M. A., Meuth, M., Harris, A. L., & Hamdy, F. C. (2009). Distinct microRNA alterations characterize high- and low-grade bladder cancer. *Cancer Res*, 69(21), 8472-8481. <https://doi.org/10.1158/0008-5472.Can-09-0744>
- Cazzoli, R., Buttitta, F., Di Nicola, M., Malatesta, S., Marchetti, A., Rom, W. N., & Pass, H. I. (2013). microRNAs derived from circulating exosomes as noninvasive biomarkers for screening and diagnosing lung cancer. *J Thorac Oncol*, 8(9), 1156-1162. <https://doi.org/10.1097/JTO.0b013e318299ac32>
- Changeux, J. P. (2010). Nicotine addiction and nicotinic receptors: lessons from genetically modified mice. *Nat Rev Neurosci*, 11(6), 389-401. <https://doi.org/10.1038/nrn2849>
- Chen, B. Y., Sung, C. W., Chen, C., Cheng, C. M., Lin, D. P., Huang, C. T., & Hsu, M. Y. (2019). Advances in exosomes technology. *Clin Chim Acta*, 493, 14-19. <https://doi.org/10.1016/j.cca.2019.02.021>
- Chen, D., Yang, X., Liu, M., Zhang, Z., & Xing, E. (2021). Roles of miRNA dysregulation in the pathogenesis of multiple myeloma. *Cancer Gene Ther*, 28(12), 1256-1268. <https://doi.org/10.1038/s41417-020-00291-4>
- Chen, M., Calin, G. A., & Meng, Q. H. (2014). Circulating microRNAs as Promising Tumor Biomarkers. *Adv Clin Chem*, 67, 189-214. <https://doi.org/10.1016/bs.acc.2014.09.007>
- Chiozzini, C., Ridolfi, B., & Federico, M. (2022). Extracellular Vesicles and Their Use as Vehicles of Immunogens. *Methods Mol Biol*, 2504, 177-198. https://doi.org/10.1007/978-1-0716-2341-1_13

- Chivers, E., Janka, M., Franklin, P., Mullins, B., & Larcombe, A. (2019). Nicotine and other potentially harmful compounds in "nicotine-free" e-cigarette liquids in Australia. *Med J Aust*, 210(3), 127-128. <https://doi.org/10.5694/mja2.12059>
- Cullen, B. R. (2004). Transcription and processing of human microRNA precursors. *Mol Cell*, 16(6), 861-865. <https://doi.org/10.1016/j.molcel.2004.12.002>
- Cvjetkovic, A., Jang, S. C., Konečná, B., Höög, J. L., Sihlbom, C., Lässer, C., & Lötvall, J. (2016). Detailed Analysis of Protein Topology of Extracellular Vesicles-Evidence of Unconventional Membrane Protein Orientation. *Sci Rep*, 6, 36338. <https://doi.org/10.1038/srep36338>
- da Rocha, S. T., Edwards, C. A., Ito, M., Ogata, T., & Ferguson-Smith, A. C. (2008). Genomic imprinting at the mammalian Dlk1-Dio3 domain. *Trends Genet*, 24(6), 306-316. <https://doi.org/10.1016/j.tig.2008.03.011>
- Dasgupta, P., Rizwani, W., Pillai, S., Kinkade, R., Kovacs, M., Rastogi, S., Banerjee, S., Carless, M., Kim, E., Coppola, D., Haura, E., & Chellappan, S. (2009). Nicotine induces cell proliferation, invasion and epithelial-mesenchymal transition in a variety of human cancer cell lines. *Int J Cancer*, 124(1), 36-45. <https://doi.org/10.1002/ijc.23894>
- Davalos, V., & Esteller, M. (2010). MicroRNAs and cancer epigenetics: a macrorevolution. *Curr Opin Oncol*, 22(1), 35-45. <https://doi.org/10.1097/CCO.0b013e328333dccb>
- Davis, R., Rizwani, W., Banerjee, S., Kovacs, M., Haura, E., Coppola, D., & Chellappan, S. (2009). Nicotine promotes tumor growth and metastasis in mouse models of lung cancer. *PLoS One*, 4(10), e7524. <https://doi.org/10.1371/journal.pone.0007524>
- de la Torre Gomez, C., Goreham, R. V., Bech Serra, J. J., Nann, T., & Kussmann, M. (2018). "Exosomics"-A Review of Biophysics, Biology and Biochemistry of Exosomes With a Focus on Human Breast Milk. *Front Genet*, 9, 92. <https://doi.org/10.3389/fgene.2018.00092>
- Defante, A. P., Vreeland, W. N., Benkstein, K. D., & Ripple, D. C. (2018). Using Image Attributes to Assure Accurate Particle Size and Count Using Nanoparticle Tracking Analysis. *J Pharm Sci*, 107(5), 1383-1391. <https://doi.org/10.1016/j.xphs.2017.12.016>
- Doench, J. G., Petersen, C. P., & Sharp, P. A. (2003). siRNAs can function as miRNAs. *Genes Dev*, 17(4), 438-442. <https://doi.org/10.1101/gad.1064703>
- Dong, Z., Li, B., & Wang, X. (2019). MicroRNA-889 plays a suppressive role in cell proliferation and invasion by directly targeting TAB1 in non-small cell lung cancer. *Mol Med Rep*, 20(1), 261-269. <https://doi.org/10.3892/mmr.2019.10245>

- Drazen, J. M., Morrissey, S., & Campion, E. W. (2019). The Dangerous Flavors of E-Cigarettes. *N Engl J Med*, 380(7), 679-680. <https://doi.org/10.1056/NEJMe1900484>
- Du, X., Qi, F., Lu, S., Li, Y., & Han, W. (2018). Nicotine upregulates FGFR3 and RB1 expression and promotes non-small cell lung cancer cell proliferation and epithelial-to-mesenchymal transition via downregulation of miR-99b and miR-192. *Biomed Pharmacother*, 101, 656-662. <https://doi.org/10.1016/j.biopha.2018.02.113>
- Durcin, M., Fleury, A., Taillebois, E., Hilairet, G., Krupova, Z., Henry, C., Truchet, S., Trötz Müller, M., Köfeler, H., Mabileau, G., Hue, O., Andriantsitohaina, R., Martin, P., & Le Lay, S. (2017). Characterisation of adipocyte-derived extracellular vesicle subtypes identifies distinct protein and lipid signatures for large and small extracellular vesicles. *J Extracell Vesicles*, 6(1), 1305677. <https://doi.org/10.1080/20013078.2017.1305677>
- Erku, D. A., Kisely, S., Morphet, K., Steadman, K. J., & Gartner, C. E. (2020). Framing and scientific uncertainty in nicotine vaping product regulation: An examination of competing narratives among health and medical organisations in the UK, Australia and New Zealand. *Int J Drug Policy*, 78, 102699. <https://doi.org/10.1016/j.drugpo.2020.102699>
- Erythropel, H. C., Jabba, S. V., DeWinter, T. M., Mendizabal, M., Anastas, P. T., Jordt, S. E., & Zimmerman, J. B. (2019). Formation of flavorant-propylene Glycol Adducts With Novel Toxicological Properties in Chemically Unstable E-Cigarette Liquids. *Nicotine Tob Res*, 21(9), 1248-1258. <https://doi.org/10.1093/ntr/nty192>
- Etzioni, R., Tsodikov, A., Mariotto, A., Szabo, A., Falcon, S., Wegelin, J., DiTommaso, D., Karnofski, K., Gulati, R., Penson, D. F., & Feuer, E. (2008). Quantifying the role of PSA screening in the US prostate cancer mortality decline. *Cancer Causes Control*, 19(2), 175-181. <https://doi.org/10.1007/s10552-007-9083-8>
- Fan, Q., Yang, L., Zhang, X., Peng, X., Wei, S., Su, D., Zhai, Z., Hua, X., & Li, H. (2018). The emerging role of exosome-derived non-coding RNAs in cancer biology. *Cancer Lett*, 414, 107-115. <https://doi.org/10.1016/j.canlet.2017.10.040>
- Floyd, E. L., Queimado, L., Wang, J., Regens, J. L., & Johnson, D. L. (2018). Electronic cigarette power affects count concentration and particle size distribution of vaping aerosol. *PLoS One*, 13(12), e0210147. <https://doi.org/10.1371/journal.pone.0210147>
- Fortunato, D., Mladenović, D., Criscuoli, M., Loria, F., Veiman, K. L., Zocco, D., Koort, K., & Zarovni, N. (2021). Opportunities and Pitfalls of Fluorescent Labeling Methodologies for Extracellular Vesicle Profiling on High-Resolution Single-Particle Platforms. *Int J Mol Sci*, 22(19). <https://doi.org/10.3390/ijms221910510>

- Freitas, C., Sousa, C., Machado, F., Serino, M., Santos, V., Cruz-Martins, N., Teixeira, A., Cunha, A., Pereira, T., Oliveira, H. P., Costa, J. L., & Hespanhol, V. (2021). The Role of Liquid Biopsy in Early Diagnosis of Lung Cancer. *Front Oncol*, *11*, 634316. <https://doi.org/10.3389/fonc.2021.634316>
- Fu, G., Brkić, J., Hayder, H., & Peng, C. (2013). MicroRNAs in Human Placental Development and Pregnancy Complications. *Int J Mol Sci*, *14*(3), 5519-5544. <https://doi.org/10.3390/ijms14035519>
- Fu, H., Yang, H., Zhang, X., & Xu, W. (2016). The emerging roles of exosomes in tumor-stroma interaction. *J Cancer Res Clin Oncol*, *142*(9), 1897-1907. <https://doi.org/10.1007/s00432-016-2145-0>
- Fuziwara, C. S., & Kimura, E. T. (2014). MicroRNA Deregulation in Anaplastic Thyroid Cancer Biology. *Int J Endocrinol*, *2014*, 743450. <https://doi.org/10.1155/2014/743450>
- Gabriel, E., & Bagaria, S. P. (2018). Assessing the Impact of Circulating Tumor DNA (ctDNA) in Patients With Colorectal Cancer: Separating Fact From Fiction. *Front Oncol*, *8*, 297. <https://doi.org/10.3389/fonc.2018.00297>
- Garcia-Martin, R., Wang, G., Brandão, B. B., Zanotto, T. M., Shah, S., Kumar Patel, S., Schilling, B., & Kahn, C. R. (2022). MicroRNA sequence codes for small extracellular vesicle release and cellular retention. *Nature*, *601*(7893), 446-451. <https://doi.org/10.1038/s41586-021-04234-3>
- Garzon, R., Fabbri, M., Cimmino, A., Calin, G. A., & Croce, C. M. (2006). MicroRNA expression and function in cancer. *Trends Mol Med*, *12*(12), 580-587. <https://doi.org/10.1016/j.molmed.2006.10.006>
- Gelibter, S., Marostica, G., Mandelli, A., Siciliani, S., Podini, P., Finardi, A., & Furlan, R. (2022). The impact of storage on extracellular vesicles: A systematic study. *J Extracell Vesicles*, *11*(2), e12162. <https://doi.org/10.1002/jev2.12162>
- Gezer, U., Özgür, E., Cetinkaya, M., Isin, M., & Dalay, N. (2014). Long non-coding RNAs with low expression levels in cells are enriched in secreted exosomes. *Cell Biol Int*, *38*(9), 1076-1079. <https://doi.org/10.1002/cbin.10301>
- Ghinai, I., Pray, I. W., Navon, L., O'Laughlin, K., Saathoff-Huber, L., Hoots, B., Kimball, A., Tenforde, M. W., Chevinsky, J. R., Layer, M., Ezike, N., Meiman, J., & Layden, J. E. (2019). E-cigarette Product Use, or Vaping, Among Persons with Associated Lung Injury - Illinois and Wisconsin, April-September 2019. *MMWR Morb Mortal Wkly Rep*, *68*(39), 865-869. <https://doi.org/10.15585/mmwr.mm6839e2>

- Glazov, E. A., McWilliam, S., Barris, W. C., & Dalrymple, B. P. (2008). Origin, evolution, and biological role of miRNA cluster in DLK-DIO3 genomic region in placental mammals. *Mol Biol Evol*, 25(5), 939-948. <https://doi.org/10.1093/molbev/msn045>
- Goniewicz, M. L., Knysak, J., Gawron, M., Kosmider, L., Sobczak, A., Kurek, J., Prokopowicz, A., Jablonska-Czapla, M., Rosik-Dulewska, C., Havel, C., Jacob, P., 3rd, & Benowitz, N. (2014). Levels of selected carcinogens and toxicants in vapour from electronic cigarettes. *Tob Control*, 23(2), 133-139. <https://doi.org/10.1136/tobaccocontrol-2012-050859>
- Grana, R., Benowitz, N., & Glantz, S. A. (2014). E-cigarettes: a scientific review. *Circulation*, 129(19), 1972-1986. <https://doi.org/10.1161/circulationaha.114.007667>
- Granados López, A. J., & López, J. A. (2014). Multistep model of cervical cancer: participation of miRNAs and coding genes. *Int J Mol Sci*, 15(9), 15700-15733. <https://doi.org/10.3390/ijms150915700>
- Griffiths-Jones, S., Grocock, R. J., van Dongen, S., Bateman, A., & Enright, A. J. (2006). miRBase: microRNA sequences, targets and gene nomenclature. *Nucleic Acids Res*, 34(Database issue), D140-144. <https://doi.org/10.1093/nar/gkj112>
- Guan, S., Yu, H., Yan, G., Gao, M., Sun, W., & Zhang, X. (2019). Size-dependent sub-proteome analysis of urinary exosomes. *Anal Bioanal Chem*, 411(18), 4141-4149. <https://doi.org/10.1007/s00216-019-01616-5>
- Guo, L. H., Li, H., Wang, F., Yu, J., & He, J. S. (2013). The Tumor Suppressor Roles of miR-433 and miR-127 in Gastric Cancer. *Int J Mol Sci*, 14(7), 14171-14184. <https://doi.org/10.3390/ijms140714171>
- Hajek, P., Phillips-Waller, A., Przulj, D., Pesola, F., Myers Smith, K., Bisal, N., Li, J., Parrott, S., Sasieni, P., Dawkins, L., Ross, L., Goniewicz, M., Wu, Q., & McRobbie, H. J. (2019). A Randomized Trial of E-Cigarettes versus Nicotine-Replacement Therapy. *N Engl J Med*, 380(7), 629-637. <https://doi.org/10.1056/NEJMoa1808779>
- Han, X., Tang, Y., Dai, Y., Hu, S., Zhou, J., Liu, X., Zhu, J., & Wu, Y. (2019). MiR-889 promotes cell growth in human non-small cell lung cancer by regulating KLF9. *Gene*, 699, 94-101. <https://doi.org/10.1016/j.gene.2019.02.077>
- Hanahan, D., & Weinberg, R. A. (2011). Hallmarks of cancer: the next generation. *Cell*, 144(5), 646-674. <https://doi.org/10.1016/j.cell.2011.02.013>
- Hannafon, B. N., Carpenter, K. J., Berry, W. L., Janknecht, R., Dooley, W. C., & Ding, W. Q. (2015). Exosome-mediated microRNA signaling from breast cancer cells is altered by the anti-angiogenesis agent docosahexaenoic acid (DHA). *Mol Cancer*, 14, 133. <https://doi.org/10.1186/s12943-015-0400-7>

- Hayes, D., Jr., Board, A., Calfee, C., Ellington, S., Pollack, L. A., Kathuria, H., Eakin, M. N., Weissman, D. N., Callahan, S. J., Esper, A. M., Crotty Alexander, L. E., Sharma, N. S., Meyer, N. J., Smith, L. S., Novosad, S., Evans, M. E., Goodman, A. B., Click, E. S., Robinson, R. T., . . . Twentyman, E. (2022). Pulmonary and Critical Care Considerations for E-Cigarette, or Vaping, Product Use-Associated Lung Injury. *Chest*. <https://doi.org/10.1016/j.chest.2022.02.039>
- Hecht, S. S. (1999). Tobacco smoke carcinogens and lung cancer. *J Natl Cancer Inst*, 91(14), 1194-1210. <https://doi.org/10.1093/jnci/91.14.1194>
- Henry, N. L., & Hayes, D. F. (2012). Cancer biomarkers. *Mol Oncol*, 6(2), 140-146. <https://doi.org/10.1016/j.molonc.2012.01.010>
- Hermeking, H. (2010). The miR-34 family in cancer and apoptosis. *Cell Death Differ*, 17(2), 193-199. <https://doi.org/10.1038/cdd.2009.56>
- Hesdorffer, C., Derman, D. P., & Bezwoda, W. R. (1984). The value of pleural fluid carcinoembryonic antigen estimation in the diagnosis of malignant tumours of the pleural cavity. *S Afr Med J*, 66(2), 54-56.
- Ho, J. Y., Hsu, R. J., Liu, J. M., Chen, S. C., Liao, G. S., Gao, H. W., & Yu, C. P. (2017). MicroRNA-382-5p aggravates breast cancer progression by regulating the RERG/Ras/ERK signaling axis. *Oncotarget*, 8(14), 22443-22459. <https://doi.org/10.18632/oncotarget.12338>
- Hu, X., Schwarz, J. K., Lewis, J. S., Jr., Huettner, P. C., Rader, J. S., Deasy, J. O., Grigsby, P. W., & Wang, X. (2010). A microRNA expression signature for cervical cancer prognosis. *Cancer Res*, 70(4), 1441-1448. <https://doi.org/10.1158/0008-5472.Can-09-3289>
- Hu, Y., Rao, S. S., Wang, Z. X., Cao, J., Tan, Y. J., Luo, J., Li, H. M., Zhang, W. S., Chen, C. Y., & Xie, H. (2018). Exosomes from human umbilical cord blood accelerate cutaneous wound healing through miR-21-3p-mediated promotion of angiogenesis and fibroblast function. *Theranostics*, 8(1), 169-184. <https://doi.org/10.7150/thno.21234>
- Hua, Y., Larsen, N., Kalyana-Sundaram, S., Kjems, J., Chinnaiyan, A. M., & Peter, M. E. (2013). miRConnect 2.0: identification of oncogenic, antagonistic miRNA families in three human cancers. *BMC Genomics*, 14, 179. <https://doi.org/10.1186/1471-2164-14-179>
- Huda, M. N., Nafiujjaman, M., Deaguero, I. G., Okonkwo, J., Hill, M. L., Kim, T., & Nurunnabi, M. (2021). Potential Use of Exosomes as Diagnostic Biomarkers and in Targeted Drug Delivery: Progress in Clinical and Preclinical Applications. *ACS Biomater Sci Eng*, 7(6), 2106-2149. <https://doi.org/10.1021/acsbiomaterials.1c00217>

- Hukkanen, J., Jacob, P., 3rd, & Benowitz, N. L. (2005). Metabolism and disposition kinetics of nicotine. *Pharmacol Rev*, 57(1), 79-115. <https://doi.org/10.1124/pr.57.1.3>
- Hwang, J. H., Lyes, M., Sladewski, K., Enany, S., McEachern, E., Mathew, D. P., Das, S., Moshensky, A., Bapat, S., Pride, D. T., Ongkeko, W. M., & Crotty Alexander, L. E. (2016). Electronic cigarette inhalation alters innate immunity and airway cytokines while increasing the virulence of colonizing bacteria. *J Mol Med (Berl)*, 94(6), 667-679. <https://doi.org/10.1007/s00109-016-1378-3>
- Jenjaroenpun, P., Kremenska, Y., Nair, V. M., Kremenskoy, M., Joseph, B., & Kurochkin, I. V. (2013). Characterization of RNA in exosomes secreted by human breast cancer cell lines using next-generation sequencing. *PeerJ*, 1, e201. <https://doi.org/10.7717/peerj.201>
- Ji, M., Zhang, Y., Li, N., Wang, C., Xia, R., Zhang, Z., & Wang, S. L. (2017). Nicotine Component of Cigarette Smoke Extract (CSE) Decreases the Cytotoxicity of CSE in BEAS-2B Cells Stably Expressing Human Cytochrome P450 2A13. *Int J Environ Res Public Health*, 14(10). <https://doi.org/10.3390/ijerph14101221>
- Ji, Q., Hao, X., Zhang, M., Tang, W., Yang, M., Li, L., Xiang, D., Desano, J. T., Bommer, G. T., Fan, D., Fearon, E. R., Lawrence, T. S., & Xu, L. (2009). MicroRNA miR-34 inhibits human pancreatic cancer tumor-initiating cells. *PLoS One*, 4(8), e6816. <https://doi.org/10.1371/journal.pone.0006816>
- Jiang, M., Li, X., Quan, X., Li, X., & Zhou, B. (2019). MiR-92a Family: A Novel Diagnostic Biomarker and Potential Therapeutic Target in Human Cancers. *Front Mol Biosci*, 6, 98. <https://doi.org/10.3389/fmolb.2019.00098>
- Jin, X., Chen, Y., Chen, H., Fei, S., Chen, D., Cai, X., Liu, L., Lin, B., Su, H., Zhao, L., Su, M., Pan, H., Shen, L., Xie, D., & Xie, C. (2017). Evaluation of Tumor-Derived Exosomal miRNA as Potential Diagnostic Biomarkers for Early-Stage Non-Small Cell Lung Cancer Using Next-Generation Sequencing. *Clin Cancer Res*, 23(17), 5311-5319. <https://doi.org/10.1158/1078-0432.Ccr-17-0577>
- Jing, H., He, X., & Zheng, J. (2018). Exosomes and regenerative medicine: state of the art and perspectives. *Transl Res*, 196, 1-16. <https://doi.org/10.1016/j.trsl.2018.01.005>
- Johnstone, R. M. (1992). The Jeanne Manery-Fisher Memorial Lecture 1991. Maturation of reticulocytes: formation of exosomes as a mechanism for shedding membrane proteins. *Biochem Cell Biol*, 70(3-4), 179-190. <https://doi.org/10.1139/o92-028>
- Johnstone, R. M., Adam, M., Hammond, J. R., Orr, L., & Turbide, C. (1987). Vesicle formation during reticulocyte maturation. Association of plasma membrane activities with released vesicles (exosomes). *J Biol Chem*, 262(19), 9412-9420.

- Jonas, A. M., & Raj, R. (2020). Vaping-Related Acute Parenchymal Lung Injury: A Systematic Review. *Chest*, 158(4), 1555-1565. <https://doi.org/10.1016/j.chest.2020.03.085>
- Kabekkodu, S. P., Shukla, V., Varghese, V. K., J, D. S., Chakrabarty, S., & Satyamoorthy, K. (2018). Clustered miRNAs and their role in biological functions and diseases. *Biol Rev Camb Philos Soc*, 93(4), 1955-1986. <https://doi.org/10.1111/brv.12428>
- Kalluri, R. (2016). The biology and function of exosomes in cancer. *J Clin Invest*, 126(4), 1208-1215. <https://doi.org/10.1172/jci81135>
- Kamm, R. C., & Smith, A. G. (1972). Nucleic acid concentrations in normal human plasma. *Clin Chem*, 18(6), 519-522.
- Kaur, G., Muthumalage, T., & Rahman, I. (2018). Mechanisms of toxicity and biomarkers of flavoring and flavor enhancing chemicals in emerging tobacco and non-tobacco products. *Toxicol Lett*, 288, 143-155. <https://doi.org/10.1016/j.toxlet.2018.02.025>
- Ke, X., Yuan, Y., Guo, C., Yang, Y., Pu, Q., Hu, X., Tang, K., Luo, X., Jiang, Q., Su, X., Liu, L., Zhu, W., & Wei, Y. (2017). MiR-410 induces stemness by inhibiting Gsk3 β but upregulating β -catenin in non-small cells lung cancer. *Oncotarget*, 8(7), 11356-11371. <https://doi.org/10.18632/oncotarget.14529>
- Ketting, R. F., Fischer, S. E., Bernstein, E., Sijen, T., Hannon, G. J., & Plasterk, R. H. (2001). Dicer functions in RNA interference and in synthesis of small RNA involved in developmental timing in *C. elegans*. *Genes Dev*, 15(20), 2654-2659. <https://doi.org/10.1101/gad.927801>
- Khvorova, A., Reynolds, A., & Jayasena, S. D. (2003). Functional siRNAs and miRNAs exhibit strand bias. *Cell*, 115(2), 209-216. [https://doi.org/10.1016/s0092-8674\(03\)00801-8](https://doi.org/10.1016/s0092-8674(03)00801-8)
- Kim, V. N., & Nam, J. W. (2006). Genomics of microRNA. *Trends Genet*, 22(3), 165-173. <https://doi.org/10.1016/j.tig.2006.01.003>
- Kluiver, J., Poppema, S., de Jong, D., Blokzijl, T., Harms, G., Jacobs, S., Kroesen, B. J., & van den Berg, A. (2005). BIC and miR-155 are highly expressed in Hodgkin, primary mediastinal and diffuse large B cell lymphomas. *J Pathol*, 207(2), 243-249. <https://doi.org/10.1002/path.1825>
- Kmietowicz, Z. (2018). Public Health England insists e-cigarettes are 95% safer than smoking. *Bmj*, 363, k5429. <https://doi.org/10.1136/bmj.k5429>
- Kosaka, N., Iguchi, H., Yoshioka, Y., Takeshita, F., Matsuki, Y., & Ochiya, T. (2010). Secretory mechanisms and intercellular transfer of microRNAs in living cells. *J Biol Chem*, 285(23), 17442-17452. <https://doi.org/10.1074/jbc.M110.107821>

- Kowal, J., Arras, G., Colombo, M., Jouve, M., Morath, J. P., Primdal-Bengtson, B., Dingli, F., Loew, D., Tkach, M., & Théry, C. (2016). Proteomic comparison defines novel markers to characterize heterogeneous populations of extracellular vesicle subtypes. *Proc Natl Acad Sci U S A*, 113(8), E968-977. <https://doi.org/10.1073/pnas.1521230113>
- Kurywchak, P., Tavormina, J., & Kalluri, R. (2018). The emerging roles of exosomes in the modulation of immune responses in cancer. *Genome Med*, 10(1), 23. <https://doi.org/10.1186/s13073-018-0535-4>
- Laddha, S. V., Nayak, S., Paul, D., Reddy, R., Sharma, C., Jha, P., Hariharan, M., Agrawal, A., Chowdhury, S., Sarkar, C., & Mukhopadhyay, A. (2013). Genome-wide analysis reveals downregulation of miR-379/miR-656 cluster in human cancers. *Biol Direct*, 8, 10. <https://doi.org/10.1186/1745-6150-8-10>
- Lai, E. C. (2002). Micro RNAs are complementary to 3' UTR sequence motifs that mediate negative post-transcriptional regulation. *Nat Genet*, 30(4), 363-364. <https://doi.org/10.1038/ng865>
- Lan, H., Lu, H., Wang, X., & Jin, H. (2015). MicroRNAs as potential biomarkers in cancer: opportunities and challenges. *Biomed Res Int*, 2015, 125094. <https://doi.org/10.1155/2015/125094>
- Layden, J. E., Ghinai, I., Pray, I., Kimball, A., Layer, M., Tenforde, M. W., Navon, L., Hoots, B., Salvatore, P. P., Elderbrook, M., Haupt, T., Kanne, J., Patel, M. T., Saathoff-Huber, L., King, B. A., Schier, J. G., Mikosz, C. A., & Meiman, J. (2020). Pulmonary Illness Related to E-Cigarette Use in Illinois and Wisconsin - Final Report. *N Engl J Med*, 382(10), 903-916. <https://doi.org/10.1056/NEJMoa1911614>
- Lee, R. C., Feinbaum, R. L., & Ambros, V. (1993). The *C. elegans* heterochronic gene *lin-4* encodes small RNAs with antisense complementarity to *lin-14*. *Cell*, 75(5), 843-854. [https://doi.org/10.1016/0092-8674\(93\)90529-y](https://doi.org/10.1016/0092-8674(93)90529-y)
- Lee, Y., Ahn, C., Han, J., Choi, H., Kim, J., Yim, J., Lee, J., Provost, P., Rådmark, O., Kim, S., & Kim, V. N. (2003). The nuclear RNase III Drosha initiates microRNA processing. *Nature*, 425(6956), 415-419. <https://doi.org/10.1038/nature01957>
- Lee, Y., Jeon, K., Lee, J. T., Kim, S., & Kim, V. N. (2002). MicroRNA maturation: stepwise processing and subcellular localization. *Embo j*, 21(17), 4663-4670. <https://doi.org/10.1093/emboj/cdf476>
- Lerner, C. A., Sundar, I. K., Watson, R. M., Elder, A., Jones, R., Done, D., Kurtzman, R., Ossip, D. J., Robinson, R., McIntosh, S., & Rahman, I. (2015). Environmental health hazards of e-cigarettes and their components: Oxidants and copper in e-cigarette aerosols. *Environ Pollut*, 198, 100-107. <https://doi.org/10.1016/j.envpol.2014.12.033>

- Lerner, C. A., Sundar, I. K., Yao, H., Gerloff, J., Ossip, D. J., McIntosh, S., Robinson, R., & Rahman, I. (2015). Vapors produced by electronic cigarettes and e-juices with flavorings induce toxicity, oxidative stress, and inflammatory response in lung epithelial cells and in mouse lung. *PLoS One*, *10*(2), e0116732. <https://doi.org/10.1371/journal.pone.0116732>
- Li, C. L., Nie, H., Wang, M., Su, L. P., Li, J. F., Yu, Y. Y., Yan, M., Qu, Q. L., Zhu, Z. G., & Liu, B. Y. (2012). microRNA-155 is downregulated in gastric cancer cells and involved in cell metastasis. *Oncol Rep*, *27*(6), 1960-1966. <https://doi.org/10.3892/or.2012.1719>
- Li, D., Yang, Y., Zhu, G., Liu, X., Zhao, M., Li, X., & Yang, Q. (2015). MicroRNA-410 promotes cell proliferation by targeting BRD7 in non-small cell lung cancer. *FEBS Lett*, *589*(17), 2218-2223. <https://doi.org/10.1016/j.febslet.2015.06.031>
- Li, J., & Liu, C. (2019). Coding or Noncoding, the Converging Concepts of RNAs. *Front Genet*, *10*, 496. <https://doi.org/10.3389/fgene.2019.00496>
- Li, M., Zheng, R., & Yuan, F. L. (2020). MiR-410 affects the proliferation and apoptosis of lung cancer A549 cells through regulation of SOCS3/JAK-STAT signaling pathway. *Eur Rev Med Pharmacol Sci*, *24*(22), 11462. https://doi.org/10.26355/eurrev_202011_23747
- Lin, J., Wang, Y., Zou, Y. Q., Chen, X., Huang, B., Liu, J., Xu, Y. M., Li, J., Zhang, J., Yang, W. M., Min, Q. H., Sun, F., Li, S. Q., Gao, Q. F., & Wang, X. Z. (2016). Differential miRNA expression in pleural effusions derived from extracellular vesicles of patients with lung cancer, pulmonary tuberculosis, or pneumonia. *Tumour Biol*. <https://doi.org/10.1007/s13277-016-5410-6>
- Liu, H. P., Lai, H. M., & Guo, Z. (2020). Prostate cancer early diagnosis: circulating microRNA pairs potentially beyond single microRNAs upon 1231 serum samples. *Brief Bioinform*. <https://doi.org/10.1093/bib/bbaa111>
- Lo Cicero, A., Stahl, P. D., & Raposo, G. (2015). Extracellular vesicles shuffling intercellular messages: for good or for bad. *Curr Opin Cell Biol*, *35*, 69-77. <https://doi.org/10.1016/j.ceb.2015.04.013>
- Lötvall, J., Hill, A. F., Hochberg, F., Buzás, E. I., Di Vizio, D., Gardiner, C., Gho, Y. S., Kurochkin, I. V., Mathivanan, S., Quesenberry, P., Sahoo, S., Tahara, H., Wauben, M. H., Witwer, K. W., & Théry, C. (2014). Minimal experimental requirements for definition of extracellular vesicles and their functions: a position statement from the International Society for Extracellular Vesicles. *J Extracell Vesicles*, *3*, 26913. <https://doi.org/10.3402/jev.v3.26913>

- Luo, R., Liu, H., & Chen, J. (2021). Reduced circulating exosomal miR-382 predicts unfavorable outcome in non-small cell lung cancer. *Int J Clin Exp Pathol*, 14(4), 469-474.
- Mashouri, L., Yousefi, H., Aref, A. R., Ahadi, A. M., Molaei, F., & Alahari, S. K. (2019). Exosomes: composition, biogenesis, and mechanisms in cancer metastasis and drug resistance. *Mol Cancer*, 18(1), 75. <https://doi.org/10.1186/s12943-019-0991-5>
- Masyuk, A. I., Masyuk, T. V., & Larusso, N. F. (2013). Exosomes in the pathogenesis, diagnostics and therapeutics of liver diseases. *J Hepatol*, 59(3), 621-625. <https://doi.org/10.1016/j.jhep.2013.03.028>
- Mathieu, M., Névo, N., Jouve, M., Valenzuela, J. I., Maurin, M., Verweij, F. J., Palmulli, R., Lankar, D., Dingli, F., Loew, D., Rubinstein, E., Boncompain, G., Perez, F., & Théry, C. (2021). Specificities of exosome versus small ectosome secretion revealed by live intracellular tracking of CD63 and CD9. *Nat Commun*, 12(1), 4389. <https://doi.org/10.1038/s41467-021-24384-2>
- McCauley, L., Markin, C., & Hosmer, D. (2012). An unexpected consequence of electronic cigarette use. *Chest*, 141(4), 1110-1113. <https://doi.org/10.1378/chest.11-1334>
- McDonald, B., & Martin-Serrano, J. (2009). No strings attached: the ESCRT machinery in viral budding and cytokinesis. *J Cell Sci*, 122(Pt 13), 2167-2177. <https://doi.org/10.1242/jcs.028308>
- McDonough, S. R., Rahman, I., & Sundar, I. K. (2021). Recent updates on biomarkers of exposure and systemic toxicity in e-cigarette users and EVALI. *Am J Physiol Lung Cell Mol Physiol*, 320(5), L661-L679. <https://doi.org/10.1152/ajplung.00520.2020>
- Meo, S. A., Ansary, M. A., Barayan, F. R., Almusallam, A. S., Almehaid, A. M., Alarifi, N. S., Alsohaibani, T. A., & Zia, I. (2019). Electronic Cigarettes: Impact on Lung Function and Fractional Exhaled Nitric Oxide Among Healthy Adults. *Am J Mens Health*, 13(1), 1557988318806073. <https://doi.org/10.1177/1557988318806073>
- Merritt, W. M., Lin, Y. G., Han, L. Y., Kamat, A. A., Spannuth, W. A., Schmandt, R., Urbauer, D., Pennacchio, L. A., Cheng, J. F., Nick, A. M., Deavers, M. T., Mourad-Zeidan, A., Wang, H., Mueller, P., Lenburg, M. E., Gray, J. W., Mok, S., Birrer, M. J., Lopez-Berestein, G., . . . Sood, A. K. (2008). Dicer, Drosha, and outcomes in patients with ovarian cancer. *N Engl J Med*, 359(25), 2641-2650. <https://doi.org/10.1056/NEJMoa0803785>
- Midekessa, G., Godakumara, K., Dissanayake, K., Hasan, M. M., Reshi, Q. U. A., Rinken, T., & Fazeli, A. (2021). Characterization of Extracellular Vesicles Labelled with a Lipophilic Dye Using Fluorescence Nanoparticle Tracking Analysis. *Membranes (Basel)*, 11(10). <https://doi.org/10.3390/membranes11100779>

- Minciocchi, V. R., Freeman, M. R., & Di Vizio, D. (2015). Extracellular vesicles in cancer: exosomes, microvesicles and the emerging role of large oncosomes. *Semin Cell Dev Biol*, 40, 41-51. <https://doi.org/10.1016/j.semcdb.2015.02.010>
- Mitchell, P., Petfalski, E., Shevchenko, A., Mann, M., & Tollervey, D. (1997). The exosome: a conserved eukaryotic RNA processing complex containing multiple 3'->5' exoribonucleases. *Cell*, 91(4), 457-466. [https://doi.org/10.1016/s0092-8674\(00\)80432-8](https://doi.org/10.1016/s0092-8674(00)80432-8)
- Mitchell, P. S., Parkin, R. K., Kroh, E. M., Fritz, B. R., Wyman, S. K., Pogosova-Agadjanyan, E. L., Peterson, A., Noteboom, J., O'Briant, K. C., Allen, A., Lin, D. W., Urban, N., Drescher, C. W., Knudsen, B. S., Stirewalt, D. L., Gentleman, R., Vessella, R. L., Nelson, P. S., Martin, D. B., & Tewari, M. (2008). Circulating microRNAs as stable blood-based markers for cancer detection. *Proc Natl Acad Sci U S A*, 105(30), 10513-10518. <https://doi.org/10.1073/pnas.0804549105>
- Mittelbrunn, M., Gutiérrez-Vázquez, C., Villarroya-Beltri, C., González, S., Sánchez-Cabo, F., González, M., Bernad, A., & Sánchez-Madrid, F. (2011). Unidirectional transfer of microRNA-loaded exosomes from T cells to antigen-presenting cells. *Nat Commun*, 2, 282. <https://doi.org/10.1038/ncomms1285>
- Muntasell, A., Berger, A. C., & Roche, P. A. (2007). T cell-induced secretion of MHC class II-peptide complexes on B cell exosomes. *Embo j*, 26(19), 4263-4272. <https://doi.org/10.1038/sj.emboj.7601842>
- Muralidhar, B., Winder, D., Murray, M., Palmer, R., Barbosa-Morais, N., Saini, H., Roberts, I., Pett, M., & Coleman, N. (2011). Functional evidence that Drosha overexpression in cervical squamous cell carcinoma affects cell phenotype and microRNA profiles. *J Pathol*, 224(4), 496-507. <https://doi.org/10.1002/path.2898>
- Muthumalage, T., Lucas, J. H., Wang, Q., Lamb, T., McGraw, M. D., & Rahman, I. (2020). Pulmonary Toxicity and Inflammatory Response of E-Cigarette Vape Cartridges Containing Medium-Chain Triglycerides Oil and Vitamin E Acetate: Implications in the Pathogenesis of EVALI. *Toxics*, 8(3). <https://doi.org/10.3390/toxics8030046>
- Nadal, E., Zhong, J., Lin, J., Reddy, R. M., Ramnath, N., Orringer, M. B., Chang, A. C., Beer, D. G., & Chen, G. (2014). A MicroRNA cluster at 14q32 drives aggressive lung adenocarcinoma. *Clin Cancer Res*, 20(12), 3107-3117. <https://doi.org/10.1158/1078-0432.Ccr-13-3348>
- Nieuwland, R., & Sturk, A. (2010). Why do cells release vesicles? *Thromb Res*, 125 Suppl 1, S49-51. <https://doi.org/10.1016/j.thromres.2010.01.037>
- Nilsson, S., Möller, C., Jirström, K., Lee, A., Busch, S., Lamb, R., & Landberg, G. (2012). Downregulation of miR-92a is associated with aggressive breast cancer features

- and increased tumour macrophage infiltration. *PLoS One*, 7(4), e36051. <https://doi.org/10.1371/journal.pone.0036051>
- Ostrowski, M., Carmo, N. B., Krumeich, S., Fanget, I., Raposo, G., Savina, A., Moita, C. F., Schauer, K., Hume, A. N., Freitas, R. P., Goud, B., Benaroch, P., Hacothen, N., Fukuda, M., Desnos, C., Seabra, M. C., Darchen, F., Amigorena, S., Moita, L. F., & Thery, C. (2010). Rab27a and Rab27b control different steps of the exosome secretion pathway. *Nat Cell Biol*, 12(1), 19-30; sup pp 11-13. <https://doi.org/10.1038/ncb2000>
- Pasquinelli, A. E. (2002). MicroRNAs: deviants no longer. *Trends Genet*, 18(4), 171-173. [https://doi.org/10.1016/s0168-9525\(01\)02624-5](https://doi.org/10.1016/s0168-9525(01)02624-5)
- Peck, M. J., Sanders, E. B., Scherer, G., Lüdicke, F., & Weitkunat, R. (2018). Review of biomarkers to assess the effects of switching from cigarettes to modified risk tobacco products. *Biomarkers*, 23(3), 213-244. <https://doi.org/10.1080/1354750x.2017.1419284>
- Perrine, C. G., Pickens, C. M., Boehmer, T. K., King, B. A., Jones, C. M., DeSisto, C. L., Duca, L. M., Lekachvili, A., Kenemer, B., Shamout, M., Landen, M. G., Lynfield, R., Ghinai, I., Heinzerling, A., Lewis, N., Pray, I. W., Tanz, L. J., Patel, A., & Briss, P. A. (2019). Characteristics of a Multistate Outbreak of Lung Injury Associated with E-cigarette Use, or Vaping - United States, 2019. *MMWR Morb Mortal Wkly Rep*, 68(39), 860-864. <https://doi.org/10.15585/mmwr.mm6839e1>
- Poliakov, A., Spilman, M., Dokland, T., Amling, C. L., & Mobley, J. A. (2009). Structural heterogeneity and protein composition of exosome-like vesicles (prostasomes) in human semen. *Prostate*, 69(2), 159-167. <https://doi.org/10.1002/pros.20860>
- Polosa, R., O'Leary, R., Tashkin, D., Emma, R., & Caruso, M. (2019). The effect of e-cigarette aerosol emissions on respiratory health: a narrative review. *Expert Rev Respir Med*, 13(9), 899-915. <https://doi.org/10.1080/17476348.2019.1649146>
- Qin, W., Ren, Q., Liu, T., Huang, Y., & Wang, J. (2013). MicroRNA-155 is a novel suppressor of ovarian cancer-initiating cells that targets CLDN1. *FEBS Lett*, 587(9), 1434-1439. <https://doi.org/10.1016/j.febslet.2013.03.023>
- Raymond, B. H., Collette-Merrill, K., Harrison, R. G., Jarvis, S., & Rasmussen, R. J. (2018). The Nicotine Content of a Sample of E-cigarette Liquid Manufactured in the United States. *J Addict Med*, 12(2), 127-131. <https://doi.org/10.1097/adm.0000000000000376>
- Record, M., Carayon, K., Poirot, M., & Silvente-Poirot, S. (2014). Exosomes as new vesicular lipid transporters involved in cell-cell communication and various pathophysiological processes. *Biochim Biophys Acta*, 1841(1), 108-120. <https://doi.org/10.1016/j.bbaliip.2013.10.004>

- Record, M., Carayon, K., Poirot, M., & Silvente-Poirot, S. (2014). Exosomes as new vesicular lipid transporters involved in cell–cell communication and various pathophysiologicals. *Biochimica et Biophysica Acta (BBA) - Molecular and Cell Biology of Lipids*, 1841(1), 108-120. <https://doi.org/https://doi.org/10.1016/j.bbalip.2013.10.004>
- Relita Mendonca, R., Narayanan, V. A., Sandeep, D. S., Ruman, A., & Charyulu, R. N. (2019). Regulating E-cigarettes in India: A conundrum for the global giant in tobacco production. *Indian J Tuberc*, 66(2), 288-293. <https://doi.org/10.1016/j.ijtb.2019.02.014>
- Ren, L., Yang, C., Dou, Y., Zhan, R., Sun, Y., & Yu, Y. (2017). MiR-541-5p regulates lung fibrosis by targeting cyclic nucleotide phosphodiesterase 1A. *Exp Lung Res*, 43(6-7), 249-258. <https://doi.org/10.1080/01902148.2017.1349210>
- Ren, Y., Zhang, H., & Jiang, P. (2018). MicroRNA-382 inhibits cell growth and migration in colorectal cancer by targeting SP1. *Biol Res*, 51(1), 51. <https://doi.org/10.1186/s40659-018-0200-9>
- Ried, K., Eng, P., & Sali, A. (2017). Screening for Circulating Tumour Cells Allows Early Detection of Cancer and Monitoring of Treatment Effectiveness: An Observational Study. *Asian Pac J Cancer Prev*, 18(8), 2275-2285. <https://doi.org/10.22034/apjcp.2017.18.8.2275>
- Rijavec, E., Coco, S., Genova, C., Rossi, G., Longo, L., & Grossi, F. (2019). Liquid Biopsy in Non-Small Cell Lung Cancer: Highlights and Challenges. *Cancers (Basel)*, 12(1). <https://doi.org/10.3390/cancers12010017>
- Rikkert, L. G., Nieuwland, R., Terstappen, L., & Coumans, F. A. W. (2019). Quality of extracellular vesicle images by transmission electron microscopy is operator and protocol dependent. *J Extracell Vesicles*, 8(1), 1555419. <https://doi.org/10.1080/20013078.2018.1555419>
- Rolfo, C., Castiglia, M., Hong, D., Alessandro, R., Mertens, I., Baggerman, G., Zwaenepoel, K., Gil-Bazo, I., Passiglia, F., Carreca, A. P., Taverna, S., Vento, R., Santini, D., Peeters, M., Russo, A., & Pauwels, P. (2014). Liquid biopsies in lung cancer: the new ambrosia of researchers. *Biochim Biophys Acta*, 1846(2), 539-546. <https://doi.org/10.1016/j.bbcan.2014.10.001>
- Roush, S., & Slack, F. J. (2008). The let-7 family of microRNAs. *Trends Cell Biol*, 18(10), 505-516. <https://doi.org/10.1016/j.tcb.2008.07.007>
- Rowell, T. R., Reeber, S. L., Lee, S. L., Harris, R. A., Nethery, R. C., Herring, A. H., Glish, G. L., & Tarran, R. (2017). Flavored e-cigarette liquids reduce proliferation and viability in the CALU3 airway epithelial cell line. *Am J Physiol Lung Cell Mol Physiol*, 313(1), L52-L66. <https://doi.org/10.1152/ajplung.00392.2016>

- Ryu, J. K., Hong, S. M., Karikari, C. A., Hruban, R. H., Goggins, M. G., & Maitra, A. (2010). Aberrant MicroRNA-155 expression is an early event in the multistep progression of pancreatic adenocarcinoma. *Pancreatology*, 10(1), 66-73. <https://doi.org/10.1159/000231984>
- Schweitzer, K. S., Chen, S. X., Law, S., Van Demark, M., Poirier, C., Justice, M. J., Hubbard, W. C., Kim, E. S., Lai, X., Wang, M., Kranz, W. D., Carroll, C. J., Ray, B. D., Bittman, R., Goodpaster, J., & Petrache, I. (2015). Endothelial disruptive proinflammatory effects of nicotine and e-cigarette vapor exposures. *Am J Physiol Lung Cell Mol Physiol*, 309(2), L175-187. <https://doi.org/10.1152/ajplung.00411.2014>
- Seitz, H., Royo, H., Bortolin, M. L., Lin, S. P., Ferguson-Smith, A. C., & Cavallé, J. (2004). A large imprinted microRNA gene cluster at the mouse Dlk1-Gtl2 domain. *Genome Res*, 14(9), 1741-1748. <https://doi.org/10.1101/gr.2743304>
- Seo, A. N., Jung, Y., Jang, H., Lee, E., Bae, H. I., Son, T., Kwon, O., Chung, H. Y., Yu, W., & Lee, Y. M. (2019). Clinical significance and prognostic role of hypoxia-induced microRNA 382 in gastric adenocarcinoma. *PLoS One*, 14(10), e0223608. <https://doi.org/10.1371/journal.pone.0223608>
- Shi, Y., & Liu, Z. (2020). Serum miR-92a-1 is a novel diagnostic biomarker for colorectal cancer. *J Cell Mol Med*, 24(15), 8363-8367. <https://doi.org/10.1111/jcmm.15282>
- Shushkova, N. A., Vavilov, N. E., Novikova, S. E., Farafonova, T. E., Tikhonova, O. V., Liao, P. C., & Zgoda, V. G. (2018). [Quantitative proteomics of human blood exosomes]. *Biomed Khim*, 64(6), 496-504. <https://doi.org/10.18097/pbmc20186406496> (Kolichestvennyĭ proteomnyĭ analiz ékzosom krovi cheloveka.)
- Silva, D., Cáceres, M., Arancibia, R., Martínez, C., Martínez, J., & Smith, P. C. (2012). Effects of cigarette smoke and nicotine on cell viability, migration and myofibroblastic differentiation. *J Periodontal Res*, 47(5), 599-607. <https://doi.org/10.1111/j.1600-0765.2012.01472.x>
- Simhadri, V. R., Reiners, K. S., Hansen, H. P., Topolar, D., Simhadri, V. L., Nohroudi, K., Kufer, T. A., Engert, A., & Pogge von Strandmann, E. (2008). Dendritic cells release HLA-B-associated transcript-3 positive exosomes to regulate natural killer function. *PLoS One*, 3(10), e3377. <https://doi.org/10.1371/journal.pone.0003377>
- Singh, K. P., Lawyer, G., Muthumalage, T., Maremanda, K. P., Khan, N. A., McDonough, S. R., Ye, D., McIntosh, S., & Rahman, I. (2019). Systemic biomarkers in electronic cigarette users: implications for noninvasive assessment of vaping-associated pulmonary injuries. *ERJ Open Res*, 5(4). <https://doi.org/10.1183/23120541.00182-2019>

- Singh, S., Pillai, S., & Chellappan, S. (2011). Nicotinic acetylcholine receptor signaling in tumor growth and metastasis. *J Oncol*, 2011, 456743. <https://doi.org/10.1155/2011/456743>
- Smolarz, M., Pietrowska, M., Matysiak, N., Mielanczyk, L., & Widlak, P. (2019). Proteome Profiling of Exosomes Purified from a Small Amount of Human Serum: The Problem of Co-Purified Serum Components. *Proteomes*, 7(2). <https://doi.org/10.3390/proteomes7020018>
- Soares Martins, T., Catita, J., Martins Rosa, I., O, A. B. d. C. E. S., & Henriques, A. G. (2018). Exosome isolation from distinct biofluids using precipitation and column-based approaches. *PLoS One*, 13(6), e0198820. <https://doi.org/10.1371/journal.pone.0198820>
- Soma, T., Kaganoi, J., Kawabe, A., Kondo, K., Imamura, M., & Shimada, Y. (2006). Nicotine induces the fragile histidine triad methylation in human esophageal squamous epithelial cells. *Int J Cancer*, 119(5), 1023-1027. <https://doi.org/10.1002/ijc.21948>
- Sommerfeld, C. G., Weiner, D. J., Nowalk, A., & Larkin, A. (2018). Hypersensitivity Pneumonitis and Acute Respiratory Distress Syndrome From E-Cigarette Use. *Pediatrics*, 141(6). <https://doi.org/10.1542/peds.2016-3927>
- Sork, H., Corso, G., Krjutskov, K., Johansson, H. J., Nordin, J. Z., Wiklander, O. P. B., Lee, Y. X. F., Westholm, J. O., Lehtiö, J., Wood, M. J. A., Mäger, I., & El Andaloussi, S. (2018). Heterogeneity and interplay of the extracellular vesicle small RNA transcriptome and proteome. *Sci Rep*, 8(1), 10813. <https://doi.org/10.1038/s41598-018-28485-9>
- Souza, M. F., Kuasne, H., Barros-Filho, M. C., Cilião, H. L., Marchi, F. A., Fuganti, P. E., Paschoal, A. R., Rogatto, S. R., & Cólus, I. M. S. (2017). Circulating mRNAs and miRNAs as candidate markers for the diagnosis and prognosis of prostate cancer. *PLoS One*, 12(9), e0184094. <https://doi.org/10.1371/journal.pone.0184094>
- Šponer, J. E., Šponer, J., & Mauro, E. D. (2017). New evolutionary insights into the non-enzymatic origin of RNA oligomers. *Wiley Interdiscip Rev RNA*, 8(3). <https://doi.org/10.1002/wrna.1400>
- Stiegelbauer, V., Perakis, S., Deutsch, A., Ling, H., Gerger, A., & Pichler, M. (2014). MicroRNAs as novel predictive biomarkers and therapeutic targets in colorectal cancer. *World J Gastroenterol*, 20(33), 11727-11735. <https://doi.org/10.3748/wjg.v20.i33.11727>
- Sun, Z., Yang, S., Zhou, Q., Wang, G., Song, J., Li, Z., Zhang, Z., Xu, J., Xia, K., Chang, Y., Liu, J., & Yuan, W. (2018). Emerging role of exosome-derived long non-coding

- RNAs in tumor microenvironment. *Mol Cancer*, 17(1), 82. <https://doi.org/10.1186/s12943-018-0831-z>
- Sung, H., Ferlay, J., Siegel, R. L., Laversanne, M., Soerjomataram, I., Jemal, A., & Bray, F. (2021). Global Cancer Statistics 2020: GLOBOCAN Estimates of Incidence and Mortality Worldwide for 36 Cancers in 185 Countries. *CA Cancer J Clin*, 71(3), 209-249. <https://doi.org/10.3322/caac.21660>
- Taverna, S., Giallombardo, M., Gil-Bazo, I., Carreca, A. P., Castiglia, M., Chacártegui, J., Araujo, A., Alessandro, R., Pauwels, P., Peeters, M., & Rolfo, C. (2016). Exosomes isolation and characterization in serum is feasible in non-small cell lung cancer patients: critical analysis of evidence and potential role in clinical practice. *Oncotarget*, 7(19), 28748-28760. <https://doi.org/10.18632/oncotarget.7638>
- Taylor, D. D., & Gercel-Taylor, C. (2008). MicroRNA signatures of tumor-derived exosomes as diagnostic biomarkers of ovarian cancer. *Gynecol Oncol*, 110(1), 13-21. <https://doi.org/10.1016/j.ygyno.2008.04.033>
- Tchernitsa, O., Kasajima, A., Schäfer, R., Kuban, R. J., Ungethüm, U., Györffy, B., Neumann, U., Simon, E., Weichert, W., Ebert, M. P., & Röcken, C. (2010). Systematic evaluation of the miRNA-ome and its downstream effects on mRNA expression identifies gastric cancer progression. *J Pathol*, 222(3), 310-319. <https://doi.org/10.1002/path.2759>
- Théry, C., Witwer, K. W., Aikawa, E., Alcaraz, M. J., Anderson, J. D., Andriantsitohaina, R., Antoniou, A., Arab, T., Archer, F., Atkin-Smith, G. K., Ayre, D. C., Bach, J. M., Bachurski, D., Baharvand, H., Balaj, L., Baldacchino, S., Bauer, N. N., Baxter, A. A., Bebawy, M., . . . Zuba-Surma, E. K. (2018). Minimal information for studies of extracellular vesicles 2018 (MISEV2018): a position statement of the International Society for Extracellular Vesicles and update of the MISEV2014 guidelines. *J Extracell Vesicles*, 7(1), 1535750. <https://doi.org/10.1080/20013078.2018.1535750>
- Théry, C., Zitvogel, L., & Amigorena, S. (2002). Exosomes: composition, biogenesis and function. *Nat Rev Immunol*, 2(8), 569-579. <https://doi.org/10.1038/nri855>
- Thiri6n-Romero, I., P6rez-Padilla, R., Zabert, G., & Barrientos-Guti6rrez, I. (2019). RESPIRATORY IMPACT OF ELECTRONIC CIGARETTES AND "LOW-RISK" TOBACCO. *Rev Invest Clin*, 71(1), 17-27. <https://doi.org/10.24875/ric.18002616>
- Tom6skov6, E., & Vorel, F. (2010). Some possibilities in the diagnosis of early acute ischaemic changes in the heart muscle in sudden death. *Soud Lek*, 55(3), 32-35.
- Tovar-Camargo, O. A., Toden, S., & Goel, A. (2016). Exosomal microRNA Biomarkers: Emerging Frontiers in Colorectal and Other Human Cancers. *Expert Review of*

- Tsai, J. R., Chong, I. W., Chen, C. C., Lin, S. R., Sheu, C. C., & Hwang, J. J. (2006). Mitogen-activated protein kinase pathway was significantly activated in human bronchial epithelial cells by nicotine. *DNA Cell Biol*, 25(5), 312-322. <https://doi.org/10.1089/dna.2006.25.312>
- Tsang, E. K., Abell, N. S., Li, X., Anaya, V., Karczewski, K. J., Knowles, D. A., Sierra, R. G., Smith, K. S., & Montgomery, S. B. (2017). Small RNA Sequencing in Cells and Exosomes Identifies eQTLs and 14q32 as a Region of Active Export. *G3 (Bethesda)*, 7(1), 31-39. <https://doi.org/10.1534/g3.116.036137>
- Tüfekci, K. U., Oner, M. G., Meuwissen, R. L., & Genç, S. (2014). The role of microRNAs in human diseases. *Methods Mol Biol*, 1107, 33-50. https://doi.org/10.1007/978-1-62703-748-8_3
- Turchinovich, A., Weiz, L., & Burwinkel, B. (2012). Extracellular miRNAs: the mystery of their origin and function. *Trends Biochem Sci*, 37(11), 460-465. <https://doi.org/10.1016/j.tibs.2012.08.003>
- Tutka, P., Mosiewicz, J., & Wielosz, M. (2005). Pharmacokinetics and metabolism of nicotine. *Pharmacol Rep*, 57(2), 143-153.
- Vader, P., Mol, E. A., Pasterkamp, G., & Schiffelers, R. M. (2016). Extracellular vesicles for drug delivery. *Adv Drug Deliv Rev*, 106(Pt A), 148-156. <https://doi.org/10.1016/j.addr.2016.02.006>
- Valadi, H., Ekström, K., Bossios, A., Sjöstrand, M., Lee, J. J., & Lötvall, J. O. (2007). Exosome-mediated transfer of mRNAs and microRNAs is a novel mechanism of genetic exchange between cells. *Nat Cell Biol*, 9(6), 654-659. <https://doi.org/10.1038/ncb1596>
- Valadi, H., Ekström, K., Bossios, A., Sjöstrand, M., Lee, J. J., & Lötvall, J. O. (2007). Exosome-mediated transfer of mRNAs and microRNAs is a novel mechanism of genetic exchange between cells. *Nature Cell Biology*, 9(6), 654-659. <https://doi.org/10.1038/ncb1596>
- Valpione, S., Gremel, G., Mundra, P., Middlehurst, P., Galvani, E., Girotti, M. R., Lee, R. J., Garner, G., Dhomen, N., Lorigan, P. C., & Marais, R. (2018). Plasma total cell-free DNA (cfDNA) is a surrogate biomarker for tumour burden and a prognostic biomarker for survival in metastatic melanoma patients. *Eur J Cancer*, 88, 1-9. <https://doi.org/10.1016/j.ejca.2017.10.029>
- van Niel, G., Charrin, S., Simoes, S., Romao, M., Rochin, L., Saftig, P., Marks, M. S., Rubinstein, E., & Raposo, G. (2011). The tetraspanin CD63 regulates ESCRT-

- independent and -dependent endosomal sorting during melanogenesis. *Dev Cell*, 21(4), 708-721. <https://doi.org/10.1016/j.devcel.2011.08.019>
- van Niel, G., D'Angelo, G., & Raposo, G. (2018). Shedding light on the cell biology of extracellular vesicles. *Nat Rev Mol Cell Biol*, 19(4), 213-228. <https://doi.org/10.1038/nrm.2017.125>
- Vella, L. J., Sharples, R. A., Nisbet, R. M., Cappai, R., & Hill, A. F. (2008). The role of exosomes in the processing of proteins associated with neurodegenerative diseases. *Eur Biophys J*, 37(3), 323-332. <https://doi.org/10.1007/s00249-007-0246-z>
- Vickers, K. C., Palmisano, B. T., Shoucri, B. M., Shamburek, R. D., & Remaley, A. T. (2011). MicroRNAs are transported in plasma and delivered to recipient cells by high-density lipoproteins. *Nat Cell Biol*, 13(4), 423-433. <https://doi.org/10.1038/ncb2210>
- Villarroya-Beltri, C., Baixauli, F., Gutiérrez-Vázquez, C., Sánchez-Madrid, F., & Mittelbrunn, M. (2014). Sorting it out: regulation of exosome loading. *Semin Cancer Biol*, 28, 3-13. <https://doi.org/10.1016/j.semcancer.2014.04.009>
- Viswam, D., Trotter, S., Burge, P. S., & Walters, G. I. (2018). Respiratory failure caused by lipoid pneumonia from vaping e-cigarettes. *BMJ Case Rep*, 2018. <https://doi.org/10.1136/bcr-2018-224350>
- Walsh, E. J., & McGee, J. (1988). Rhythmic discharge properties of caudal cochlear nucleus neurons during postnatal development in cats. *Hear Res*, 36(2-3), 233-247. [https://doi.org/10.1016/0378-5955\(88\)90065-2](https://doi.org/10.1016/0378-5955(88)90065-2)
- Wang, H., Peng, R., Wang, J., Qin, Z., & Xue, L. (2018). Circulating microRNAs as potential cancer biomarkers: the advantage and disadvantage. *Clin Epigenetics*, 10, 59. <https://doi.org/10.1186/s13148-018-0492-1>
- Wang, J., Chen, J., & Sen, S. (2016). MicroRNA as Biomarkers and Diagnostics. *J Cell Physiol*, 231(1), 25-30. <https://doi.org/10.1002/jcp.25056>
- Wang, J., Sun, X., Zhao, J., Yang, Y., Cai, X., Xu, J., & Cao, P. (2017). Exosomes: A Novel Strategy for Treatment and Prevention of Diseases. *Front Pharmacol*, 8, 300. <https://doi.org/10.3389/fphar.2017.00300>
- Webber, J., & Clayton, A. (2013). How pure are your vesicles? *J Extracell Vesicles*, 2. <https://doi.org/10.3402/jev.v2i0.19861>
- Weber, J. A., Baxter, D. H., Zhang, S., Huang, D. Y., Huang, K. H., Lee, M. J., Galas, D. J., & Wang, K. (2010). The microRNA spectrum in 12 body fluids. *Clin Chem*, 56(11), 1733-1741. <https://doi.org/10.1373/clinchem.2010.147405>

- Ween, M. P., Hamon, R., Macowan, M. G., Thredgold, L., Reynolds, P. N., & Hodge, S. J. (2020). Effects of E-cigarette E-liquid components on bronchial epithelial cells: Demonstration of dysfunctional efferocytosis. *Respirology*, 25(6), 620-628. <https://doi.org/10.1111/resp.13696>
- Weickmann, J. L., & Glitz, D. G. (1982). Human ribonucleases. Quantitation of pancreatic-like enzymes in serum, urine, and organ preparations. *J Biol Chem*, 257(15), 8705-8710.
- Williams, M., Villarreal, A., Bozhilov, K., Lin, S., & Talbot, P. (2013). Metal and silicate particles including nanoparticles are present in electronic cigarette cartomizer fluid and aerosol. *PLoS One*, 8(3), e57987. <https://doi.org/10.1371/journal.pone.0057987>
- Willms, E., Johansson, H. J., Mäger, I., Lee, Y., Blomberg, K. E., Sadik, M., Alaarg, A., Smith, C. I., Lehtiö, J., El Andaloussi, S., Wood, M. J., & Vader, P. (2016). Cells release subpopulations of exosomes with distinct molecular and biological properties. *Sci Rep*, 6, 22519. <https://doi.org/10.1038/srep22519>
- Winter, J. (2015). MicroRNAs of the miR379-410 cluster: New players in embryonic neurogenesis and regulators of neuronal function. *Neurogenesis (Austin)*, 2(1), e1004970. <https://doi.org/10.1080/23262133.2015.1004970>
- Witwer, K. W., Buzás, E. I., Bemis, L. T., Bora, A., Lässer, C., Lötvall, J., Nolte-t Hoen, E. N., Piper, M. G., Sivaraman, S., Skog, J., Théry, C., Wauben, M. H., & Hochberg, F. (2013). Standardization of sample collection, isolation and analysis methods in extracellular vesicle research. *J Extracell Vesicles*, 2. <https://doi.org/10.3402/jev.v2i0.20360>
- Witwer, K. W., Buzás, E. I., Bemis, L. T., Bora, A., Lässer, C., Lötvall, J., Nolte-t Hoen, E. N., Piper, M. G., Sivaraman, S., Skog, J., Théry, C., Wauben, M. H., & Hochberg, F. (2013). Standardization of sample collection, isolation and analysis methods in extracellular vesicle research. *J Extracell Vesicles*, 2, 10.3402/jev.v3402i3400.20360. <https://doi.org/10.3402/jev.v2i0.20360>
- Witwer, K. W., Goberdhan, D. C., O'Driscoll, L., Théry, C., Welsh, J. A., Blenkiron, C., Buzás, E. I., Di Vizio, D., Erdbrügger, U., Falcón-Pérez, J. M., Fu, Q. L., Hill, A. F., Lenassi, M., Lötvall, J., Nieuwland, R., Ochiya, T., Rome, S., Sahoo, S., & Zheng, L. (2021). Updating MISEV: Evolving the minimal requirements for studies of extracellular vesicles. *J Extracell Vesicles*, 10(14), e12182. <https://doi.org/10.1002/jev2.12182>
- Wu, Q., Jiang, D., Minor, M., & Chu, H. W. (2014). Electronic cigarette liquid increases inflammation and virus infection in primary human airway epithelial cells. *PLoS One*, 9(9), e108342. <https://doi.org/10.1371/journal.pone.0108342>

- Wu, S., Huang, S., Ding, J., Zhao, Y., Liang, L., Liu, T., Zhan, R., & He, X. (2010). Multiple microRNAs modulate p21Cip1/Waf1 expression by directly targeting its 3' untranslated region. *Oncogene*, 29(15), 2302-2308. <https://doi.org/10.1038/onc.2010.34>
- Yang, M., Chen, J., Su, F., Yu, B., Su, F., Lin, L., Liu, Y., Huang, J. D., & Song, E. (2011). Microvesicles secreted by macrophages shuttle invasion-potentiating microRNAs into breast cancer cells. *Mol Cancer*, 10, 117. <https://doi.org/10.1186/1476-4598-10-117>
- Yang, Z., Tsuchiya, H., Zhang, Y., Hartnett, M. E., & Wang, L. (2013). MicroRNA-433 inhibits liver cancer cell migration by repressing the protein expression and function of cAMP response element-binding protein. *J Biol Chem*, 288(40), 28893-28899. <https://doi.org/10.1074/jbc.M113.502682>
- Ye, Y. N., Liu, E. S., Shin, V. Y., Wu, W. K., Luo, J. C., & Cho, C. H. (2004). Nicotine promoted colon cancer growth via epidermal growth factor receptor, c-Src, and 5-lipoxygenase-mediated signal pathway. *J Pharmacol Exp Ther*, 308(1), 66-72. <https://doi.org/10.1124/jpet.103.058321>
- Yoshioka, Y., Konishi, Y., Kosaka, N., Katsuda, T., Kato, T., & Ochiya, T. (2013). Comparative marker analysis of extracellular vesicles in different human cancer types. *J Extracell Vesicles*, 2. <https://doi.org/10.3402/jev.v2i0.20424>
- Yuan, Y., Liao, H., Pu, Q., Ke, X., Hu, X., Ma, Y., Luo, X., Jiang, Q., Gong, Y., Wu, M., Liu, L., & Zhu, W. (2020). miR-410 induces both epithelial-mesenchymal transition and radioresistance through activation of the PI3K/mTOR pathway in non-small cell lung cancer. *Signal Transduct Target Ther*, 5(1), 85. <https://doi.org/10.1038/s41392-020-0182-2>
- Zanetti, F., Sewer, A., Titz, B., Schlage, W. K., Iskandar, A. R., Kondylis, A., Leroy, P., Guedj, E., Trivedi, K., Elamin, A., Martin, F., Frentzel, S., Ivanov, N. V., Peitsch, M. C., & Hoeng, J. (2019). Assessment of a 72-hour repeated exposure to Swedish snus extract and total particulate matter from 3R4F cigarette smoke on gingival organotypic cultures. *Food Chem Toxicol*, 125, 252-270. <https://doi.org/10.1016/j.fct.2018.12.056>
- Zhang, H. D., Jiang, L. H., Sun, D. W., Hou, J. C., & Ji, Z. L. (2018). CircRNA: a novel type of biomarker for cancer. *Breast Cancer*, 25(1), 1-7. <https://doi.org/10.1007/s12282-017-0793-9>
- Zhang, X., Ke, X., Pu, Q., Yuan, Y., Yang, W., Luo, X., Jiang, Q., Hu, X., Gong, Y., Tang, K., Su, X., Liu, L., Zhu, W., & Wei, Y. (2016). MicroRNA-410 acts as oncogene in NSCLC through downregulating SLC34A2 via activating Wnt/ β -catenin pathway. *Oncotarget*, 7(12), 14569-14585. <https://doi.org/10.18632/oncotarget.7538>

- Zhang, X., Li, Y., Qi, P., & Ma, Z. (2018). Biology of MiR-17-92 Cluster and Its Progress in Lung Cancer. *Int J Med Sci*, 15(13), 1443-1448. <https://doi.org/10.7150/ijms.27341>
- Zhao, D., Aravindakshan, A., Hilpert, M., Olmedo, P., Rule, A. M., Navas-Acien, A., & Aherrera, A. (2020). Metal/Metalloid Levels in Electronic Cigarette Liquids, Aerosols, and Human Biosamples: A Systematic Review. *Environ Health Perspect*, 128(3), 36001. <https://doi.org/10.1289/ehp5686>
- Zhou, B., Song, J., Han, T., Huang, M., Jiang, H., Qiao, H., Shi, J., & Wang, Y. (2016). MiR-382 inhibits cell growth and invasion by targeting NR2F2 in colorectal cancer. *Mol Carcinog*, 55(12), 2260-2267. <https://doi.org/10.1002/mc.22466>
- Zhou, G. H., Lu, Y. Y., Xie, J. L., Gao, Z. K., Wu, X. B., Yao, W. S., & Gu, W. G. (2019). Overexpression of miR-758 inhibited proliferation, migration, invasion, and promoted apoptosis of non-small cell lung cancer cells by negatively regulating HMGB. *Biosci Rep*, 39(1). <https://doi.org/10.1042/bsr20180855>
- Zhou, W., Fong, M. Y., Min, Y., Somlo, G., Liu, L., Palomares, M. R., Yu, Y., Chow, A., O'Connor, S. T., Chin, A. R., Yen, Y., Wang, Y., Marcusson, E. G., Chu, P., Wu, J., Wu, X., Li, A. X., Li, Z., Gao, H., . . . Wang, S. E. (2014). Cancer-secreted miR-105 destroys vascular endothelial barriers to promote metastasis. *Cancer Cell*, 25(4), 501-515. <https://doi.org/10.1016/j.ccr.2014.03.007>
- Zhou, X., Wen, W., Shan, X., Zhu, W., Xu, J., Guo, R., Cheng, W., Wang, F., Qi, L. W., Chen, Y., Huang, Z., Wang, T., Zhu, D., Liu, P., & Shu, Y. (2017). A six-microRNA panel in plasma was identified as a potential biomarker for lung adenocarcinoma diagnosis. *Oncotarget*, 8(4), 6513-6525. <https://doi.org/10.18632/oncotarget.14311>
- Zhu, S. H., Sun, J. Y., Bonnevie, E., Cummins, S. E., Gamst, A., Yin, L., & Lee, M. (2014). Four hundred and sixty brands of e-cigarettes and counting: implications for product regulation. *Tob Control*, 23 Suppl 3(Suppl 3), iii3-9. <https://doi.org/10.1136/tobaccocontrol-2014-051670>
- Zou, W., Zou, Y., Zhao, Z., Li, B., & Ran, P. (2013). Nicotine-induced epithelial-mesenchymal transition via Wnt/ β -catenin signaling in human airway epithelial cells. *Am J Physiol Lung Cell Mol Physiol*, 304(4), L199-209. <https://doi.org/10.1152/ajplung.00094.2012>